Chapter-3

Chapter-3a

Synthesis of proline-sulphonamide derivatives of chromene-2-ones as anticancer and antidiabetic agents

3a.1 Introduction

Sulphonamide derivative are one of the important class of molecules with various biological applications. Sulphonamide derivatives are known for its antimicrobial, carbonic anhydrase, antitumor and antidiabetic activities [1-3]. Various sulphonamide derivatives **1-8** having antidiabetic and anticancer activities are shown in (**Fig-3a.1**). Compound **1** (**Fig-3a.1**) studied for histone deacetylase (HDAC) inhibitors that can induce hyperacetylation of histones in human cancer cells, which blocks the cell cycle and induce apoptosis in human cancer cells but not in normal cells [4-5]. Indisulam **4** (**Fig-3a.1**) is a novel sulphonamide anticancer agent in clinical development for treatment of solid tumour, which includes renal, breast and colorectal cancer. [6-7]. Dipeptidyl peptidase IV (DPP-IV E.C.3.3.145, CD 26) is a serine protease enzyme formed in various tissues and body fluids of mammals. It plays important roles in variety of disease like autoimmune disease, AIDS and melanoma. DPP-IV is associated with glucose metabolism, immune regulation, signal transduction, apoptosis and regulating cancer. Compounds **6-8** (**Fig-3a.1**) have been reported as potent DPP-IV inhibitors [8-10].

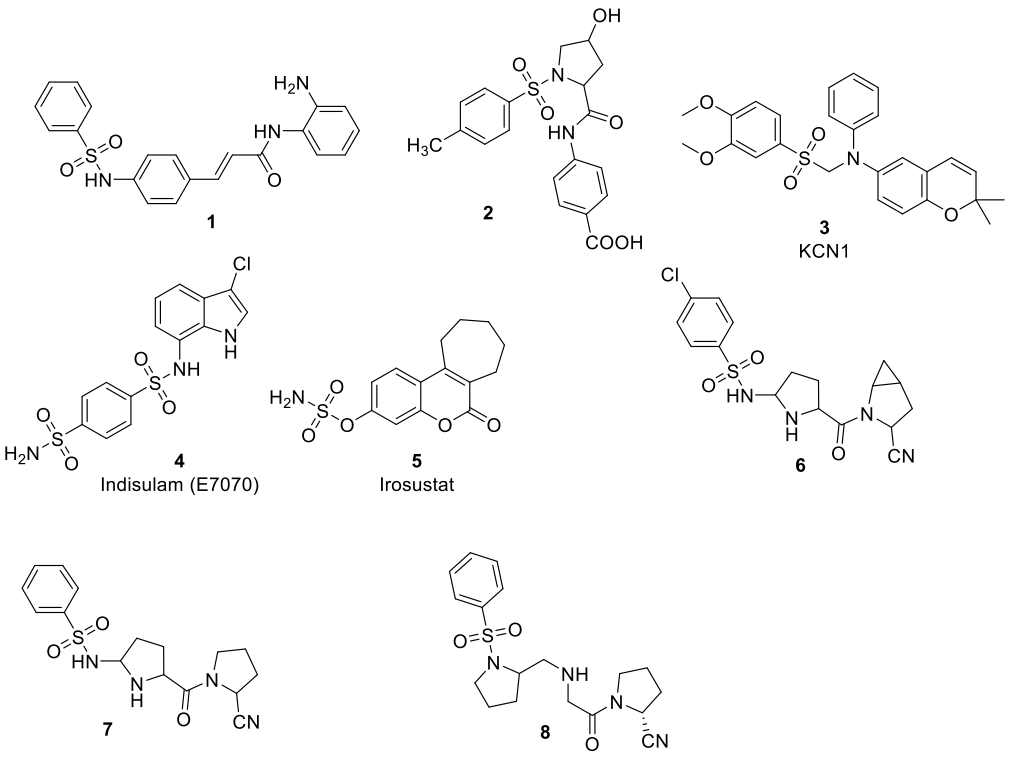

Figure-3a.1 Sulphonamide derivatives **1-8** with anticancer and antidiabetic activity

Sitagliptin was first DPP-IV inhibitor granted by US-FDA for treating type-2 diabetes followed by vildagliptin and saxagliptin [11]. Thus many DPP-4 inhibitors have 5-membered heterocyclic rings that mimic proline. The pharmacophore which may be attributed to the activity of these drugs is due to five membered pyrrolidine ring, or cyanopyrrolidine, amide linker and stearic bulk [12]. Metformin is one of the most widely prescribed drugs for the treatment for type-2 diabetes and also used in cardiovascular disease prevention [13]. Epidemiological observations have suggested that the use of metformin in diabetes mellitus patients is correlated with a reduction in cancer incidence [14]. In previous work from our group, we did several modifications on chromen-2-one to get potent anticancer and antidiabetic activities [15-18].

In present work we have designed and synthesized novel chromen-2-one-proline sulphonamide hybrids with the objective of getting potent anticancer agent and antidiabetic activity which can have binary application. All the compounds were screened for their *In Vitro* anticancer activity using 3-(4,5-dimethylthiazol-2-yl)-2,5-diphenyltetrazolium bromide dye (MTT) assay and antidiabetic activity as dipeptidyl peptidase IV (DPP-IV) inhibition assay.

3a.2 Results and Discussion

3a.2.1 Chemistry

In search of some novel compounds with potent anticancer activity and antidiabetic activity, we have synthesized compounds **16a-c** from 7-amino-4-methyl chromen-2-one **12** (**Scheme-1**). Compound **12** was synthesized in three steps starting with carbamate protected 3-aminophenol **10**, which on Pechmann reaction with ethyl acetoacetate in 70% ethanolic sulphuric acid gave 7-carboethoxy amino chromen-2-one **11** followed by deprotection in sulphuric acid/acetic acid (1:1) to give 7-amino-4-methyl chromen-2-one **12**. (L)-N-Boc-proline **13** was first stirred with ethyl chloroformate in tetrahydrofuran (THF) at 0-5 ^{0}C followed by dropwise addition of solution of compound **12** and triethylamine (TEA) in THF, which further refluxed for 8 hours to give compound **14**. Deprotection of Boc group in compound **14** was carried out using trifluoroacetic acid (TFA) to give compound **15**. Compound **15** was reacted with different benzene sulphonyl chloride derivatives at room temperature using $NaHCO_3$ in DCM:water (1:1) gave compounds **16a-c** (**Scheme-1**).

^{1}H-NMR spectrum of compound **14** showed peak at δ 1.53 ppm for nine protons of three methyl groups of Boc. Proline protons were observed in region from δ 1.92-4.55 and methyl

protons of chromen-2-one at δ 2.27. Aromatic protons were observed in region from δ 6.03-7.70 and amide proton was observed at 10.04 ppm (**Fig-3a.3.2**). ^{13}C-NMR spectrum of compound **14** showed peaks in region from 18.41-80.95 for aliphatic carbons of methyl, Boc group and proline moiety (**Fig-3a.3.3**), while aromatic carbons were observed from δ 106.84-155.78 ppm and carbonyl carbons of amide and lactone ring of chromen-2-one at 161.17 and 171.36 ppm respectively.

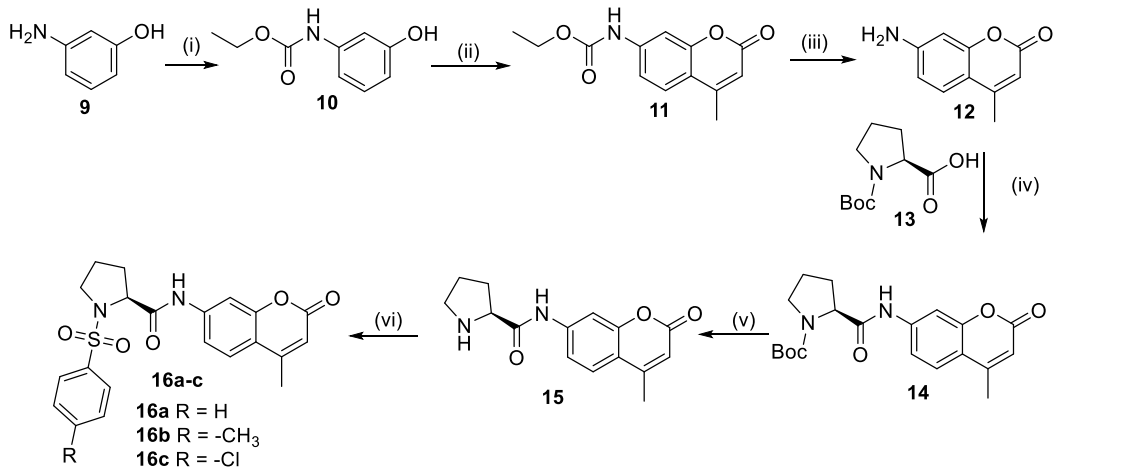

Reagents and conditions: (i) CH_3CH_2OCOCl, ethyl acetate, rt; (ii) CH_3COCH_2COOEt , H_2SO_4:C_2H_5OH (3:7), rt; (iii) H_2SO_4:CH_3COOH (1:1), reflux; (iv) (a) THF, CH_3CH_2OCOCl (0-5 C) 10 mins (b) Boc proline, THF, TEA reflux 8h. (v) TFA, DCM, rt; (vi) $NaHCO_3$, benzeneulphonyl chloride, DCM:Water(1:1), rt.

Scheme-1 Synthesis of 7-Amino-4-methylchromen-2-one derivatives **16a-c**.

The proton NMR of Boc-deprotected compound **15** (**Fig-3a.4.2**) exhibited different peaks at δ 1.77-2.81 ppm for aliphatic protons of proline, -NH proton as broad singlet around δ 2.12 ppm, methyl group of chromen-2-one at δ 2.41 ppm. Protons of proline next to nitrogen were observed at δ 2.98-3.08, 3.01-3.14 and 3.91 ppm. Aromatic protons of chromen-2-one ring were observed in the region of δ 7.51-7.64 ppm and amide proton at δ 10.05 ppm. In ^{13}C-NMR spectrum of compound **15** (**Fig-3a.4.3**) showed peaks at δ 18.67-61.02 ppm for carbons of methyl group and proline ring, peaks at δ 106.66- 154.32 ppm for aromatic carbons and peak at δ 161.24 ppm for amide carbonyl carbon and 174.08 ppm for carbonyl carbon of lactone ring. In IR spectrum of compound **15** (**Fig-3a.4.1**) showed bands at 3304-3082 cm^{-1} is for N-H and C-H stretching, bands at 1724 cm^{-1} and 1679 cm^{-1} corresponds to lactone carbonyl and amide carbonyl functional groups respectively.

The structures of compounds **16a-c** were confirmed by its IR, ^{1}H-NMR, ^{13}C-NMR and ESI-MS analyses. ^{1}H-NMR of compound **16c** (**Fig-3a.7.2**) exhibited singlet for three protons at δ

1.62 for methyl protons. Peaks from δ 1.67-4.28 indicated all pyrrolidine ring protons. Singlet at δ 6.23 for one proton indicated 3rd position proton of lactone ring, all other aromatic protons appeared in between δ 7.43-7.85 range. Singlet at δ 9.02 for one proton indicated –NH proton. ^{13}C-NMR (**Fig-3a.7.3**) of compound **16c** showed five peaks from δ 18.65-63.03 indicated all aliphatic five carbons (one methyl carbon and 4 pyrrolidine ring carbons). All aromatic carbons were observed in the range of 107.55-154.28 ppm. Amide carbonyl carbon observed at 161.04 ppm while lactone carbonyl carbon observed at δ 169.09 ppm. IR spectrum of compound **16c** (**Fig-3a.7.1**) showed one band at 3338 cm^{-1} for –NH stretching vibrations and two bands at 1716 and 1695 cm^{-1} are observed for lactone carbonyl stretching and amide carbonyl stretching frequency respectively. Sulphonamide group showed band at 1226-1201 cm^{-1}. Mass spectrum of compound **16c** (**Fig-3a.7.4**) showed $[M+H]^+$ peak at 477.

X-ray single crystal study

Single crystal was developed by slow evaporation technique using mixture of pet.ether and ethyl acetate solvent. The structure of **16c** was also confirmed by its X-ray single crystal analysis (CCDC number 1876142) which is shown in (**Fig-3a.2**) and its data is given in **Table-3a.1**.

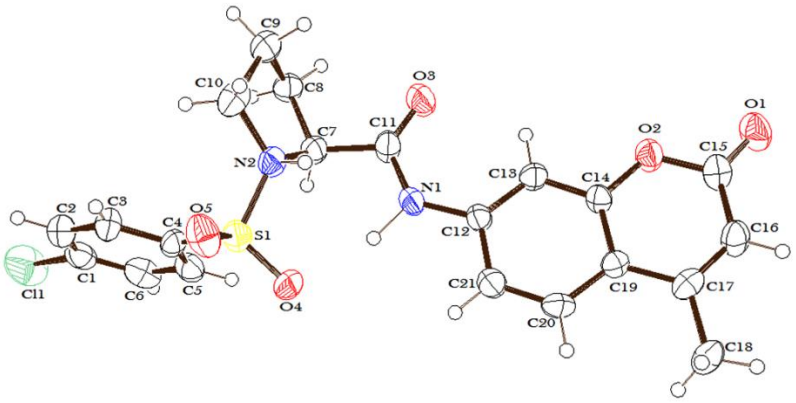

Figure-3a.2 ORTEP diagram of compound 16c.

Table-3a.1 Crystal data and structure refinement of compound 16c (CCDC NO: 1876142)

Empirical formula	$C_{21}H_{20}ClN_2O_5S$		μ/mm^{-1}	0.329
Formula weight	447.90		F(000)	932.0
Temperature/K	293		Crystal size/mm^3	0.8 × 0.4 × 0.2
Crystal system	Orthorhombic		Radiation	MoKα (λ = 0.71073)
Space group	$P2_122$		2Θ range for data collection/°	6.56 to 57.76
a/Å	37.598(4)		Index ranges	-49 ≤ h ≤ 46, -9 ≤ k ≤ 9, -8 ≤ l ≤ 9
b/Å	7.5537(9)		Reflections collected	12640
c/Å	7.1384(7)		Independent reflections	4568 [R_{int} = 0.0788, R_{sigma} = 0.1044]
α/°	90.00		Data/restraints/parameters	4568/0/276
β/°	90.00		Goodness-of-fit on F^2	1.072
γ/°	90.00		Final R indexes [I>=2σ (I)]	R_1 = 0.0793, wR_2 = 0.1503
Volume/$Å^3$	2027.3(4)		Final R indexes [all data]	R_1 = 0.1459, wR_2 = 0.1826
Z	4		Largest diff. peak/hole / e $Å^{-3}$	0.30/-0.29
$\rho_{calc}g/cm^3$	1.467		Flack parameter	0.15(16)

Figure-3a.3.1 IR spectrum of tert-butyl 2-((4-methyl-2-oxo-2H-chromen-7-yl)carbamoyl)pyrrolidine-1-carboxylate (**14**)

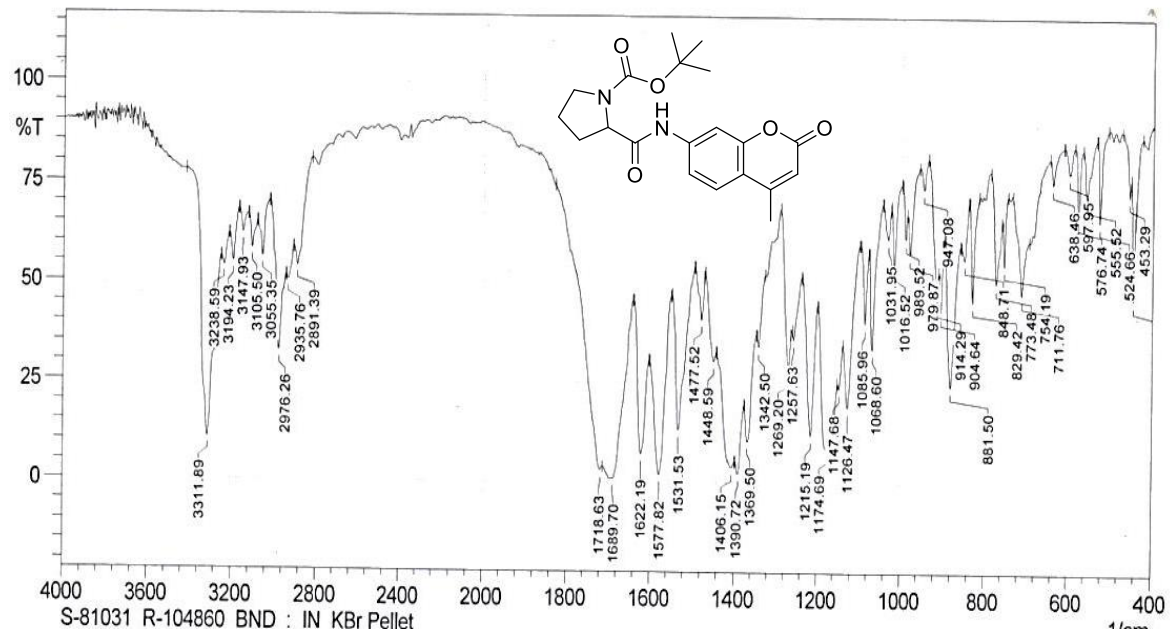

Figure-3a.3.2 ^{1}H-NMR spectrum of tert-butyl 2-((4-methyl-2-oxo-2H-chromen-7-yl)carbamoyl)pyrrolidine-1-carboxylate (**14**) in $CDCl_3$

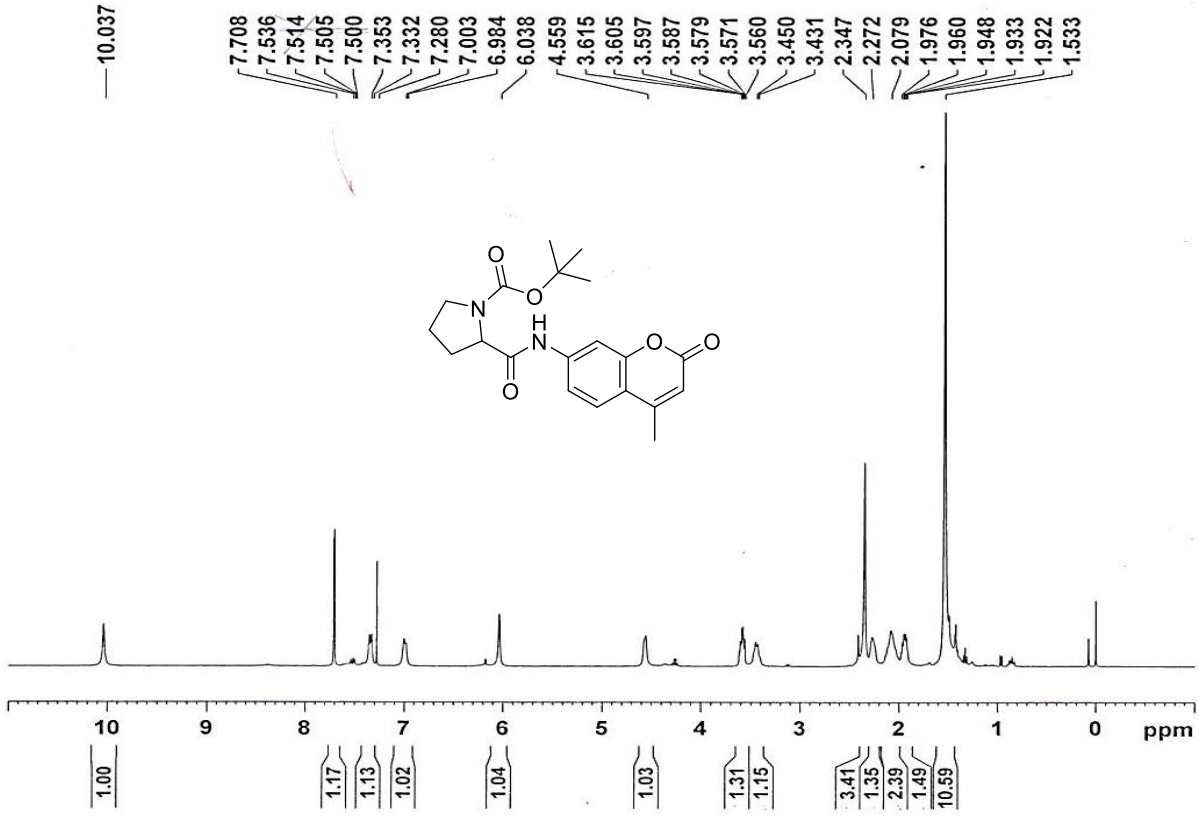

Figure-3a.3.3 ^{13}C-NMR spectrum of tert-butyl 2-((4-methyl-2-oxo-2H-chromen-7-yl)carbamoyl) pyrrolidine-1-carboxylate (**14**) in $CDCl_3$

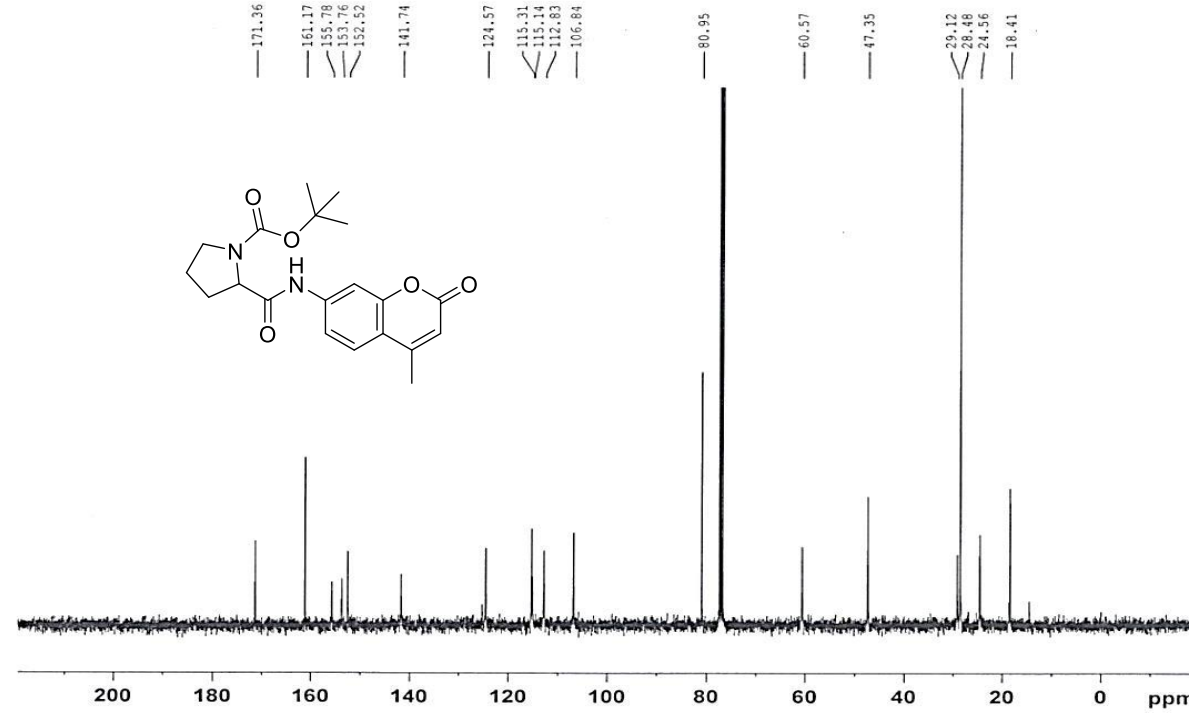

Figure-3a.3.4 ESI-MS spectrum of tert-butyl 2-((4-methyl-2-oxo-2H-chromen-7-yl) carbamoyl) pyrrolidine-1-carboxylate (**14**) M+H peak at 273.10

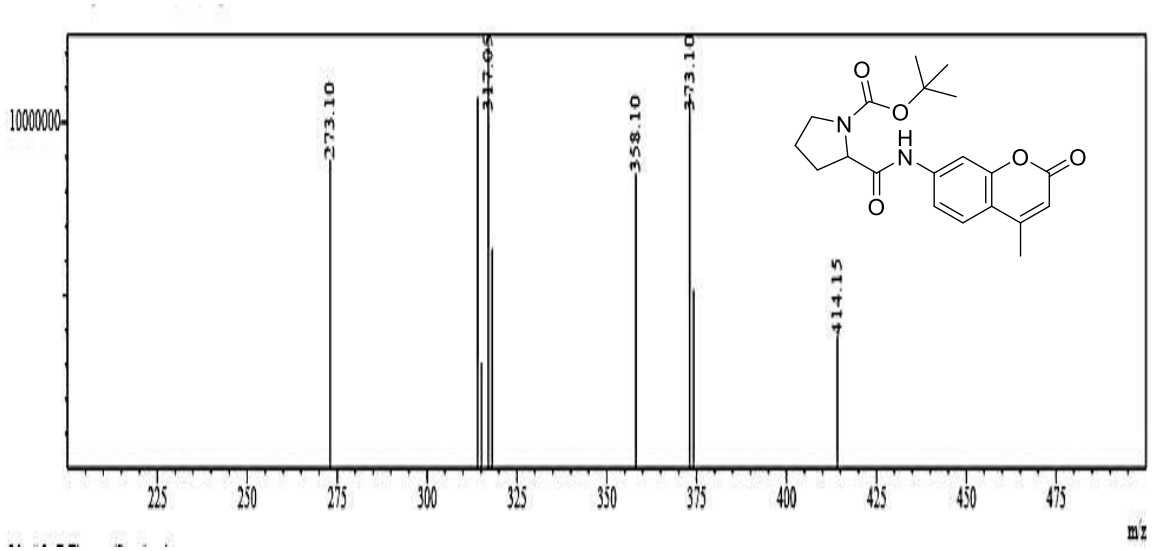

Figure-3a.4.1 IR spectrum of N-(4-methyl-2-oxo-2H-chromen-7-yl)pyrrolidine-2-carboxamide (**15**)

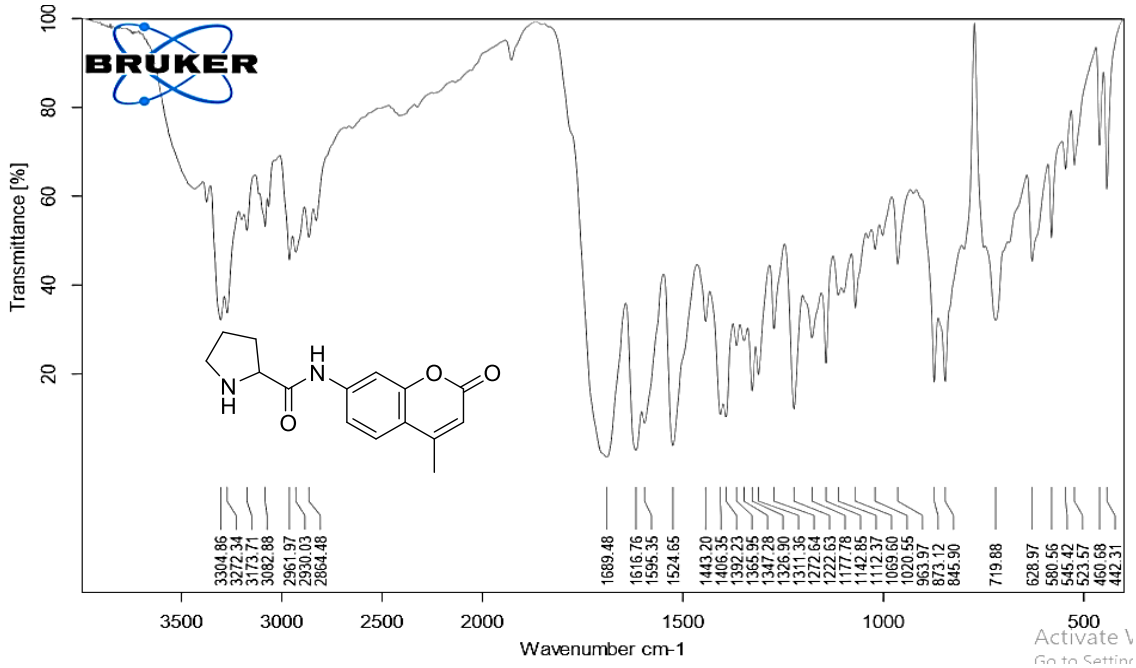

Figure-3a.4.2 ^{1}H-NMR spectrum of N-(4-methyl-2-oxo-2H-chromen-7-yl)pyrrolidine-2-carboxamide (**15**) in $CDCl_3$

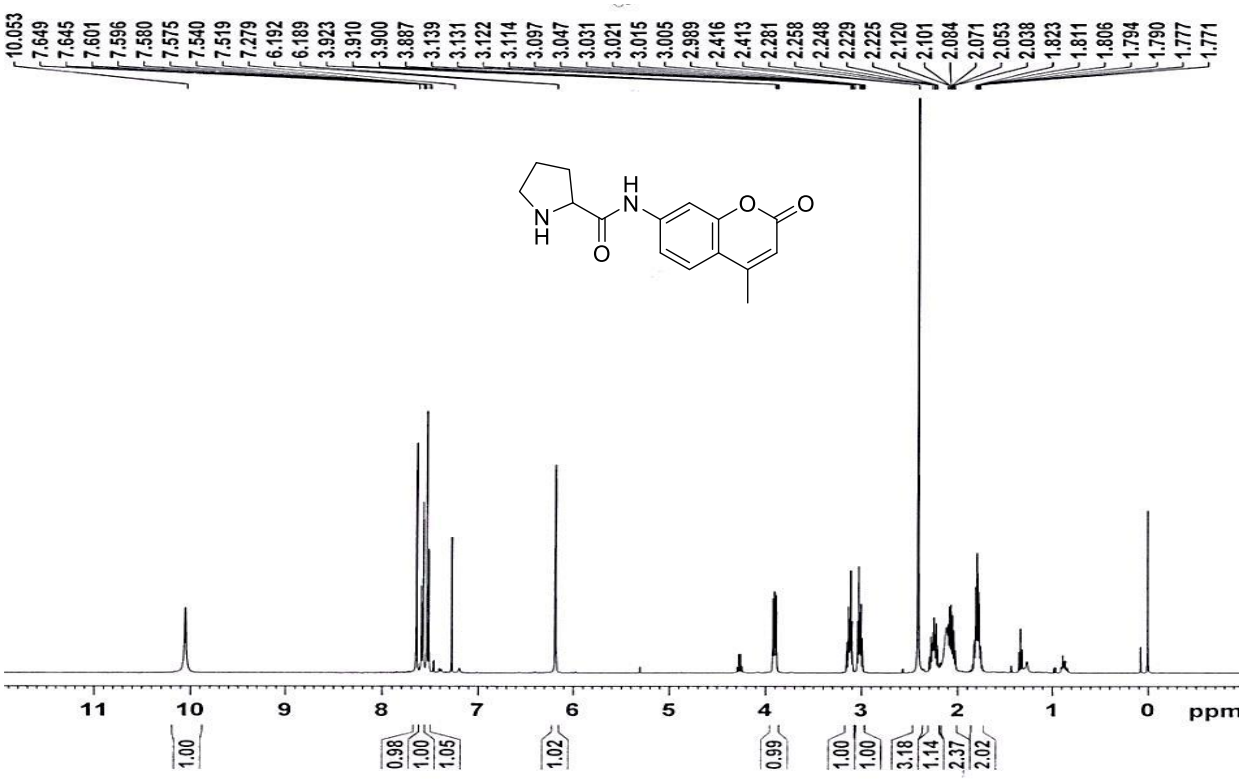

Figure-3a.4.3 ^{13}C-NMR spectrum of N-(4-methyl-2-oxo-2H-chromen-7-yl) pyrrolidine-2-carboxamide (**15**) in $CDCl_3$

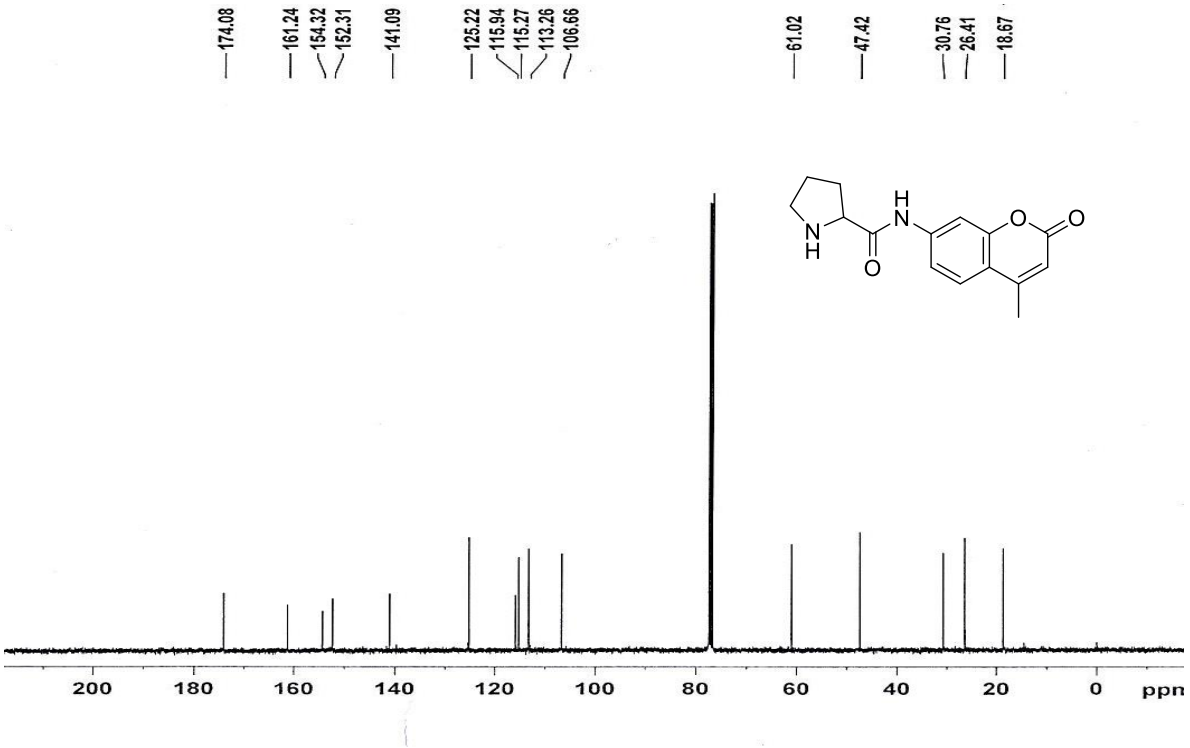

Figure-3a.5.1 IR spectrum of N-(4-methyl-2-oxo-2H-chromen-7-yl)-1-(phenylsulfonyl) pyrrolidine-2-carboxamide (**16a**)

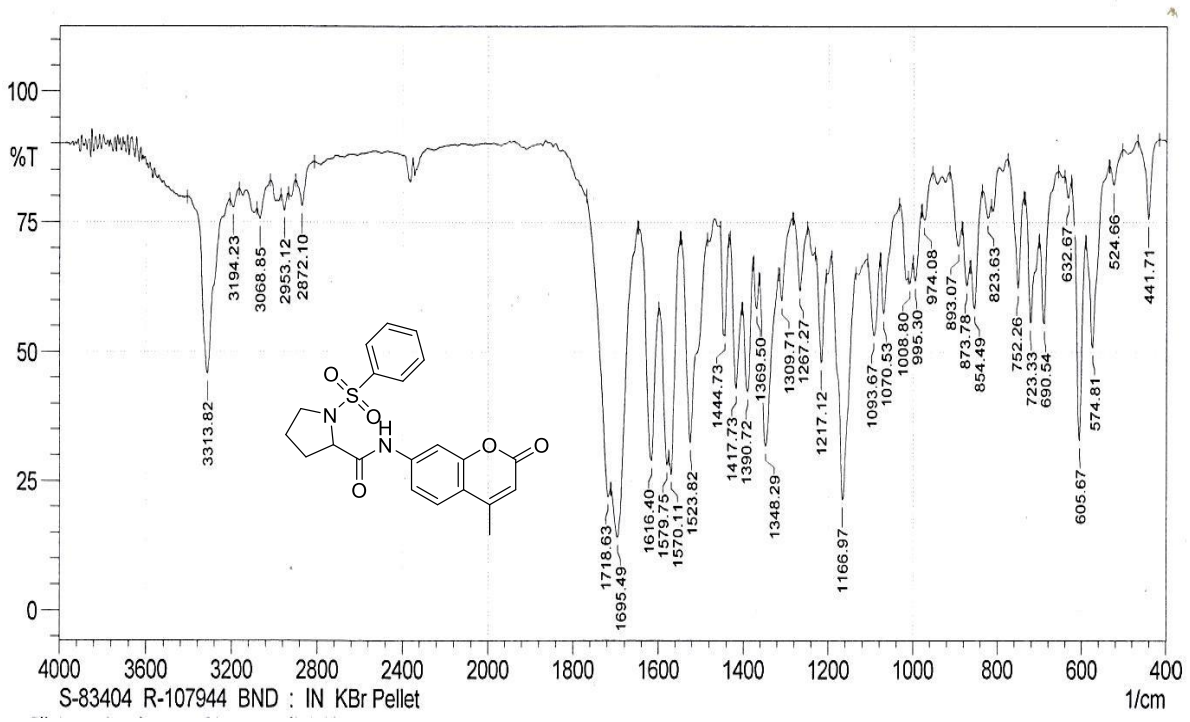

Figure-3a.5.2 ^{1}H-NMR spectrum of N-(4-methyl-2-oxo-2H-chromen-7-yl)-1-(phenylsulfonyl) pyrrolidine-2-carboxamide (**16a**) in $CDCl_3$

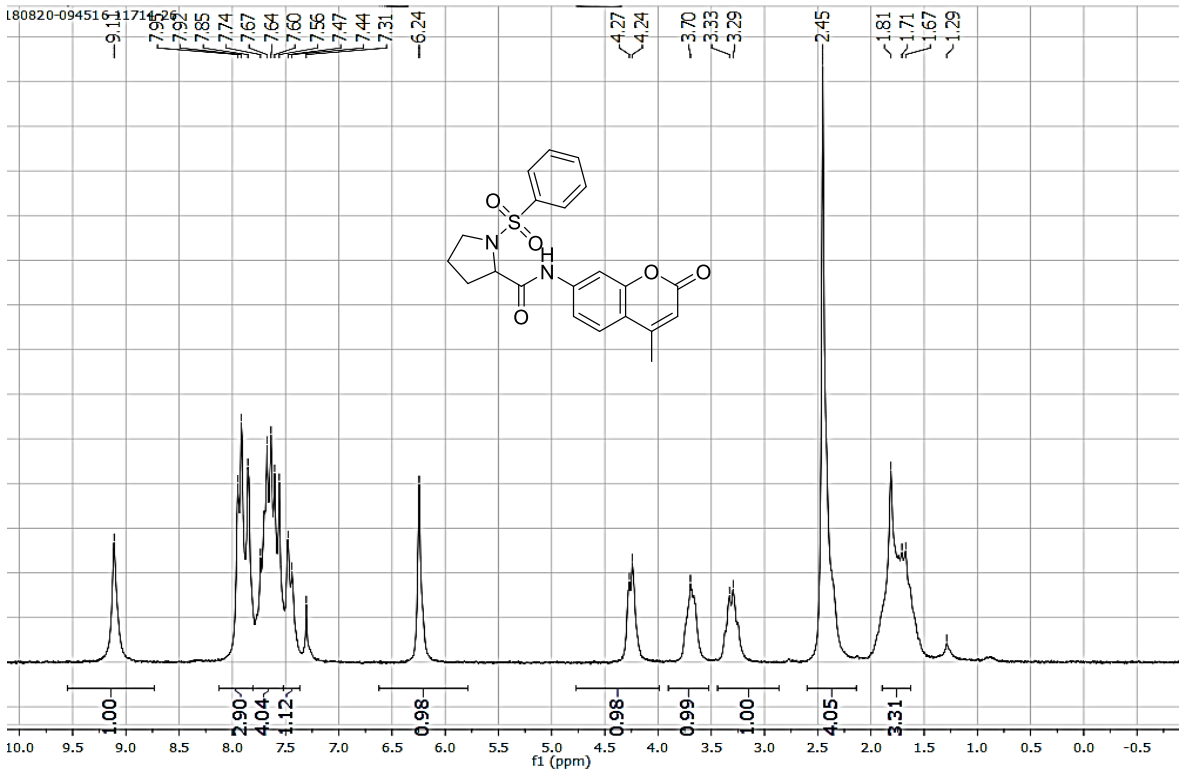

Figure-3a.5.3 ^{13}C-NMR spectrum of N-(4-methyl-2-oxo-2H-chromen-7-yl)-1-(phenylsulfonyl) pyrrolidine-2-carboxamide (**16a**) in $CDCl_3$

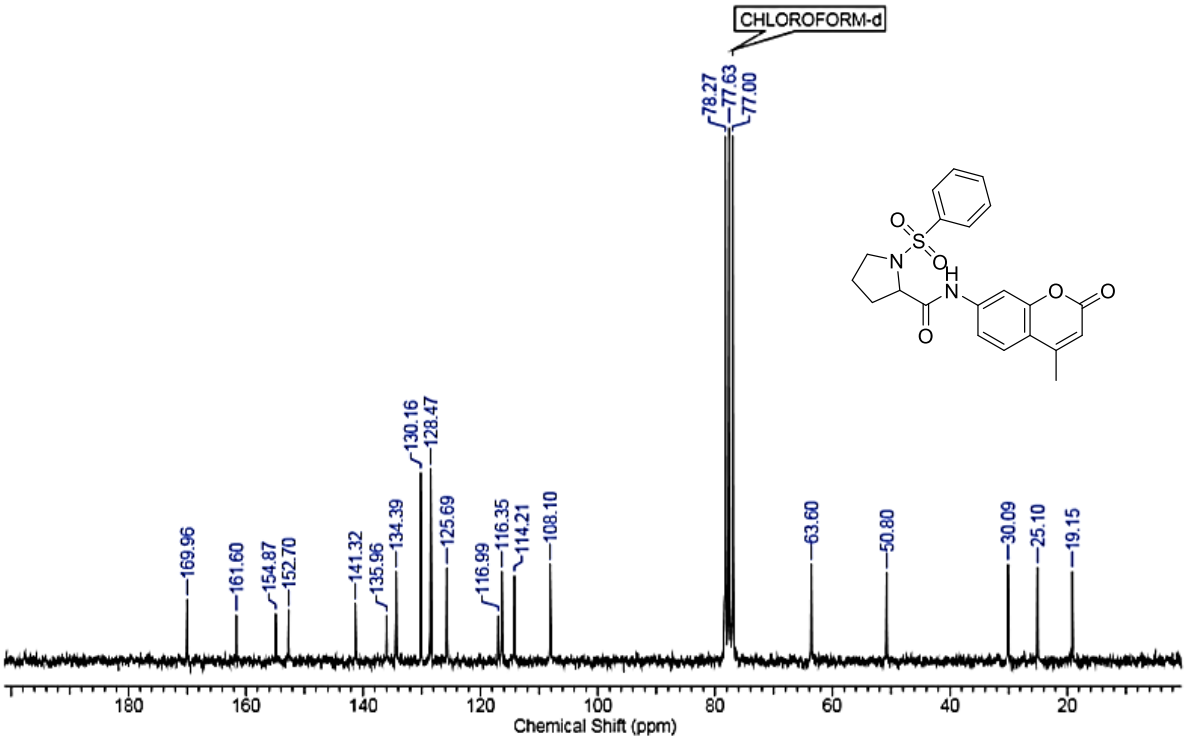

Figure-3a.5.4 ESI-MS spectrum of N-(4-methyl-2-oxo-2H-chromen-7-yl)-1-(phenylsulfonyl) pyrrolidine-2-carboxamide (**16a**) M+H peak at 413.05

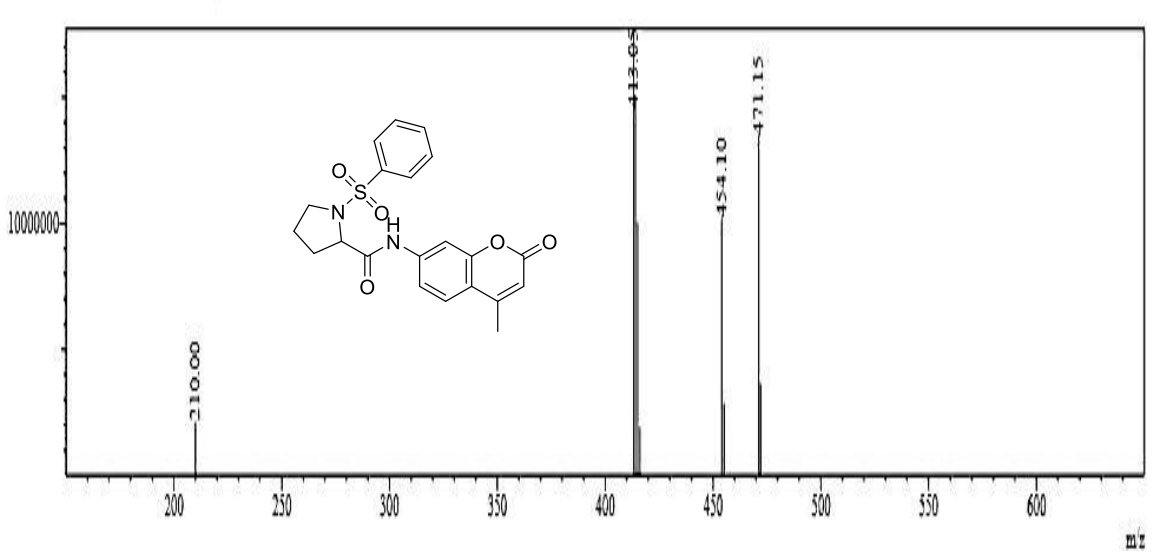

Figure-3a.6.1 IR spectrum of N-(4-methyl-2-oxo-2H-chromen-7-yl)-1-tosylpyrrolidine-2-carboxamide (**16b**)

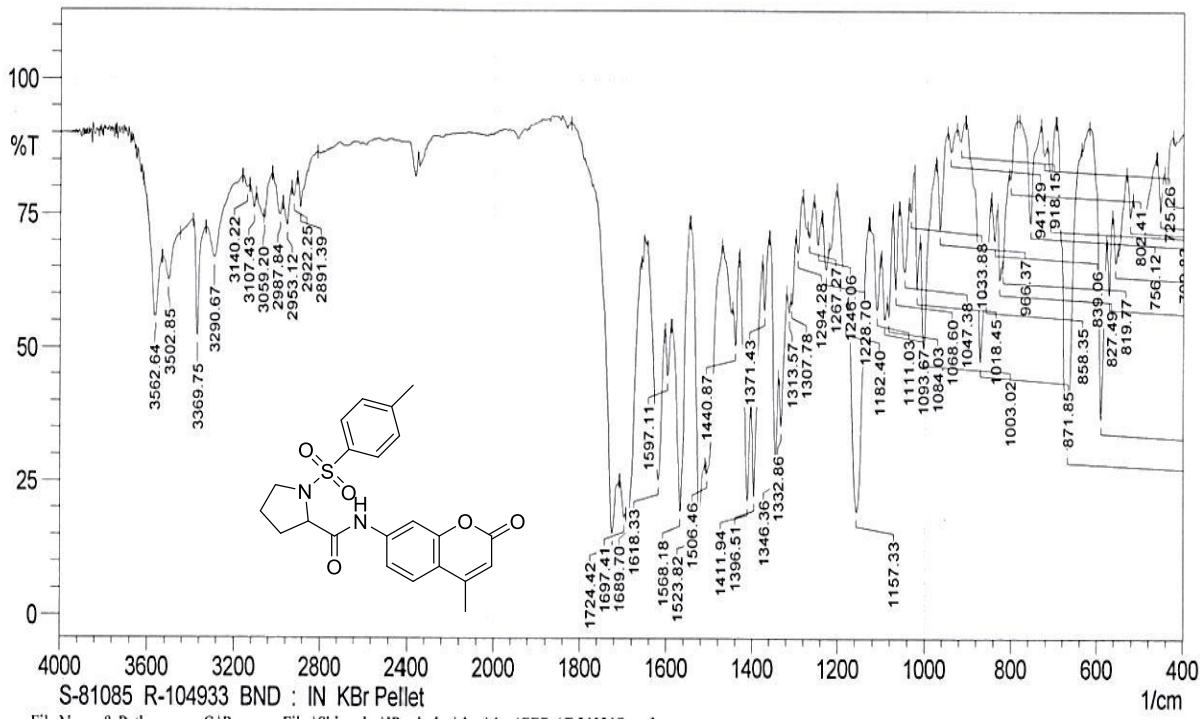

Figure-3a.6.2 ^{1}H-NMR spectrum of N-(4-methyl-2-oxo-2H-chromen-7-yl)-1-tosylpyrrolidine-2-carboxamide (**16b**) in $CDCl_3$

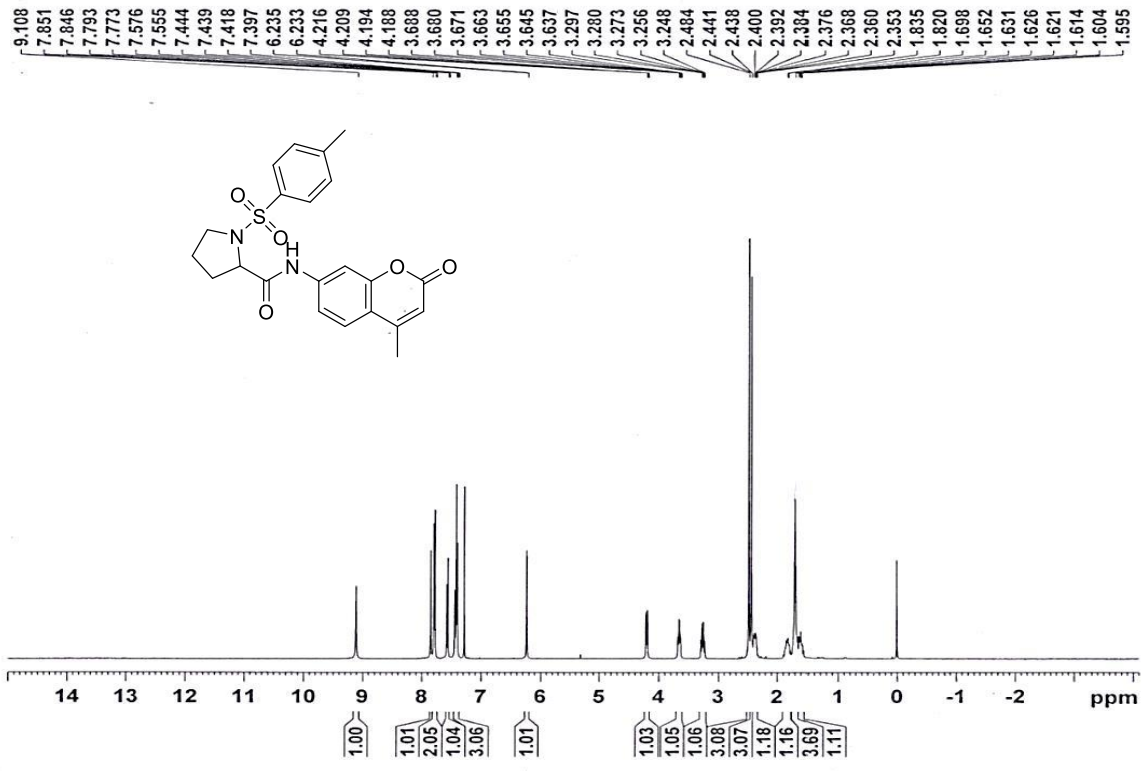

Figure-3a.6.3 ^{13}C-NMR spectrum of N-(4-methyl-2-oxo-2H-chromen-7-yl)-1-tosylpyrrolidine-2-carboxamide (**16b**) in $CDCl_3$

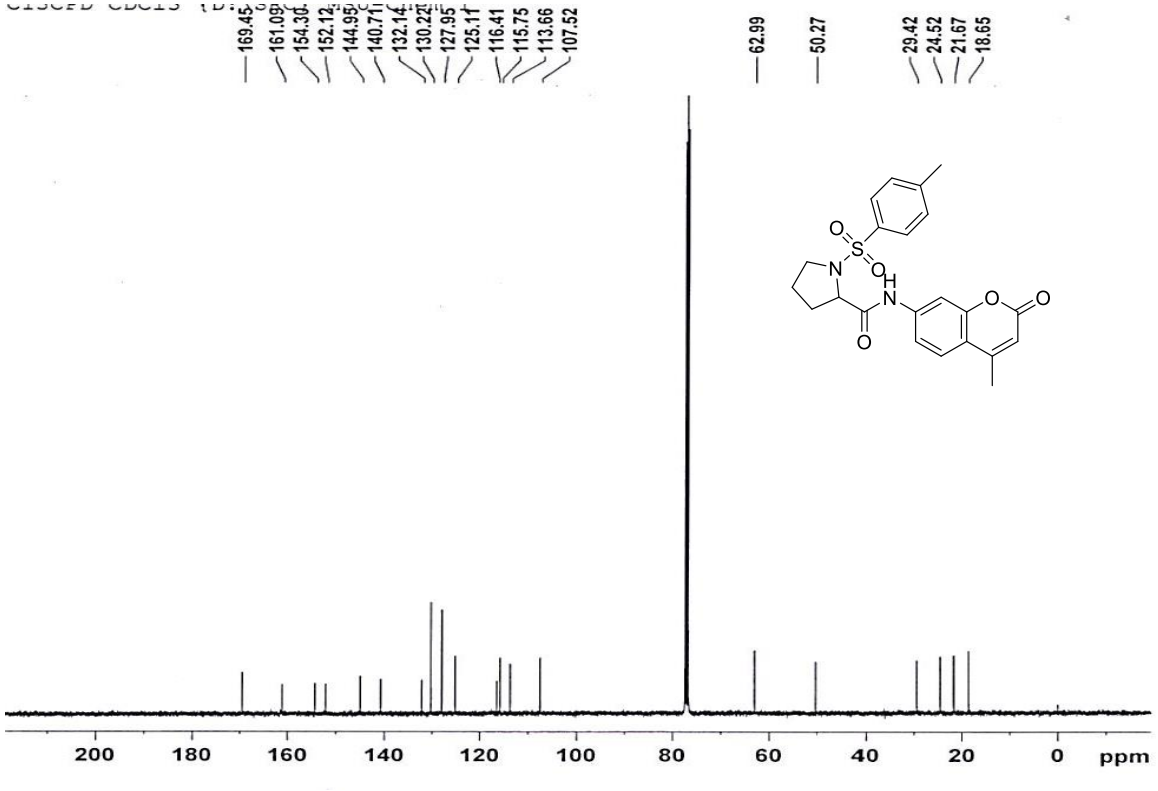

Figure-3a.6.4 ESI-MS spectrum of N-(4-methyl-2-oxo-2H-chromen-7-yl)-1-tosylpyrrolidine-2-carboxamide (**16b**) M+H peak at 427.10

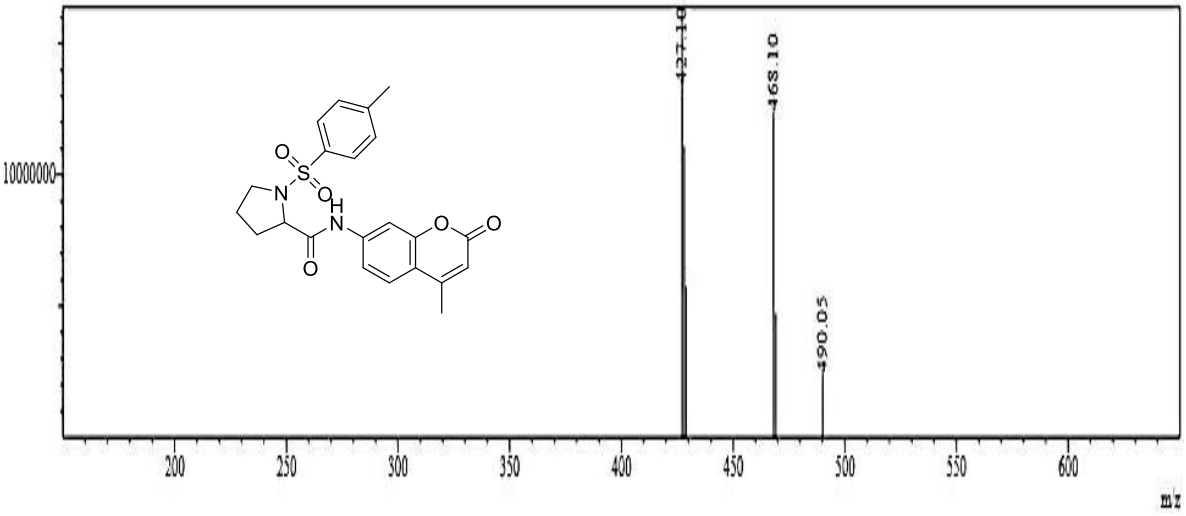

Figure-3a.7.1 IR of 1-((4-chlorophenyl)sulfonyl)-N-(4-methyl-2-oxo-2H-chromen-7-yl) pyrrolidine-2-carboxamide (**16c**)

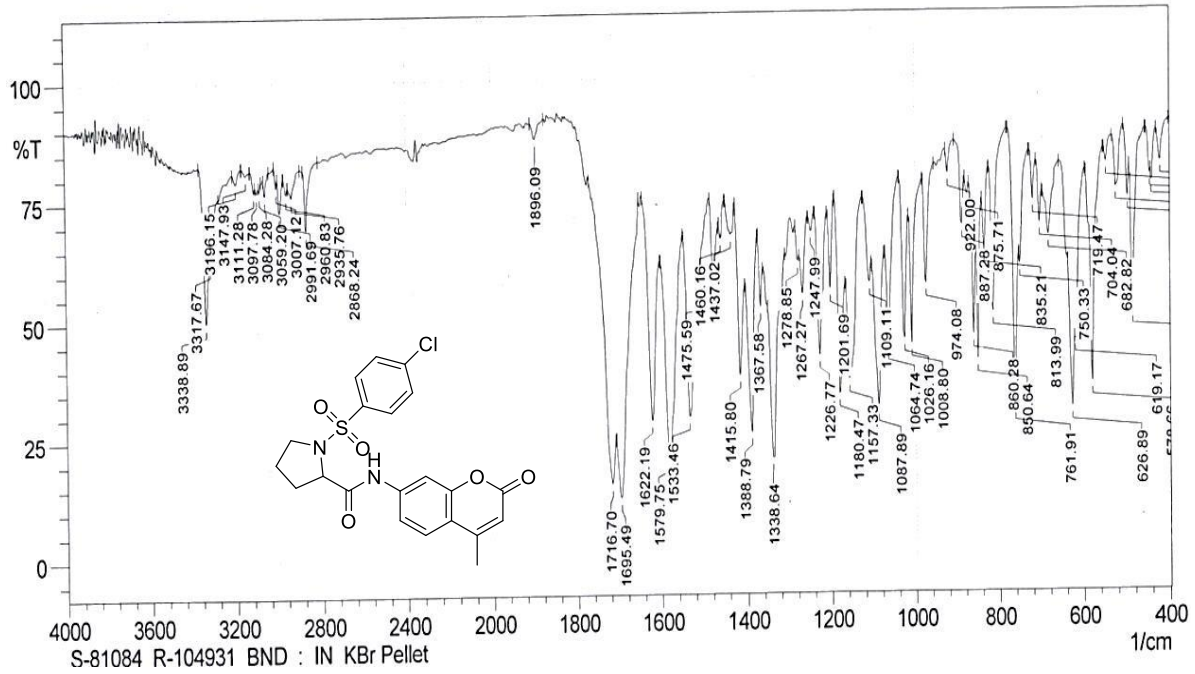

Figure-3a.7.2 ^{1}H-NMR of 1-((4-chlorophenyl)sulfonyl)-N-(4-methyl-2-oxo-2H-chromen-7-yl) pyrrolidine-2-carboxamide (**16c**) in $CDCl_3$

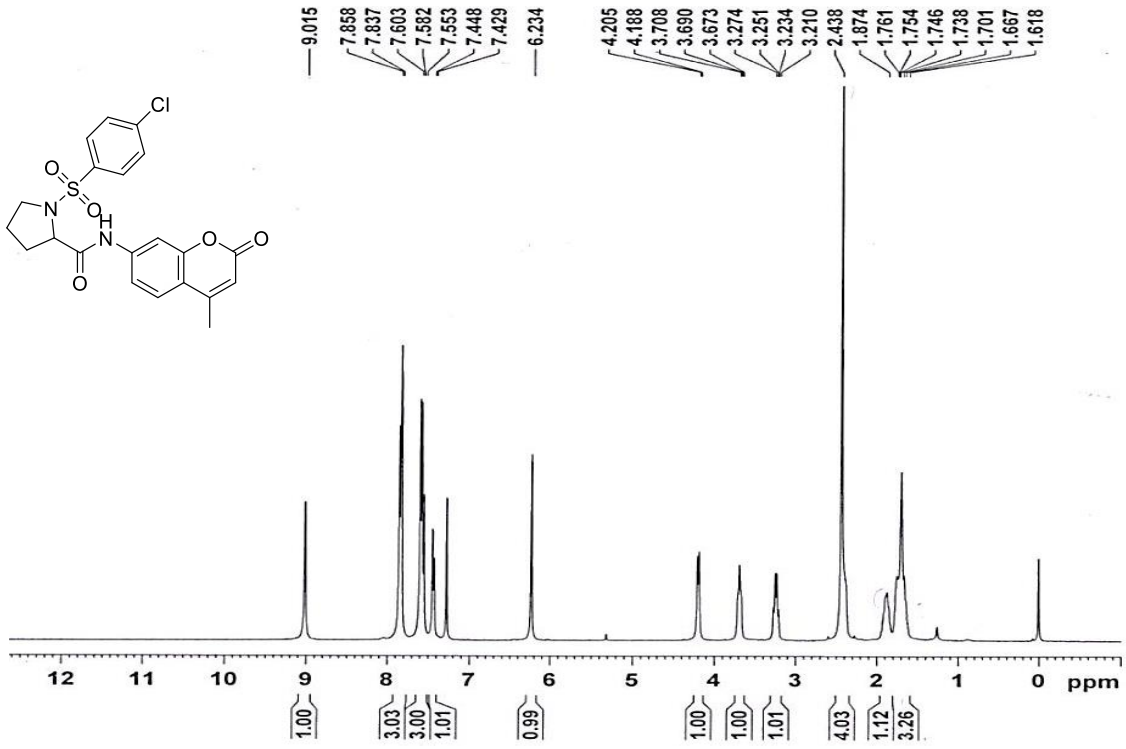

Figure-3a.7.3 ^{13}C-NMR of 1-((4-chlorophenyl)sulfonyl)-N-(4-methyl-2-oxo-2H-chromen-7-yl) pyrrolidine-2-carboxamide (**16c**) in $CDCl_3$

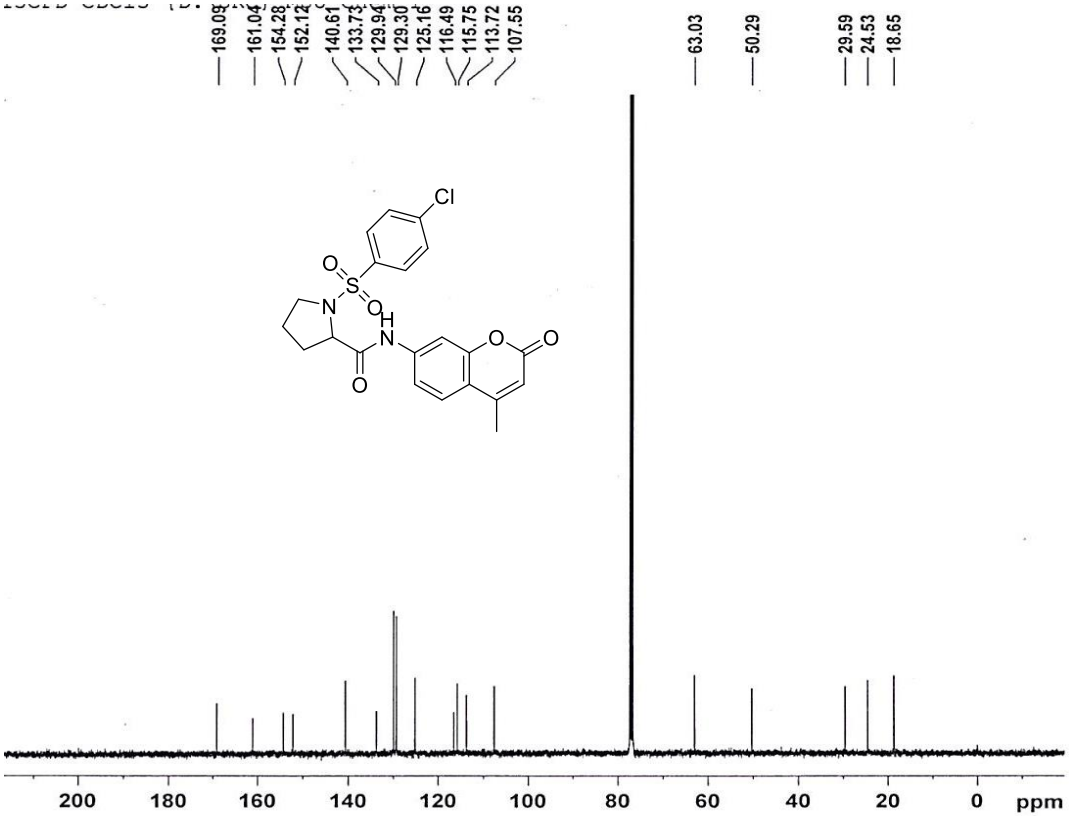

Figure-3a.7.4 ESI-MS spectrum of 1-((4-chlorophenyl)sulfonyl)-N-(4-methyl-2-oxo-2H-chromen-7-yl) pyrrolidine-2-carboxamide (**16c**) M+H peak at 447.00

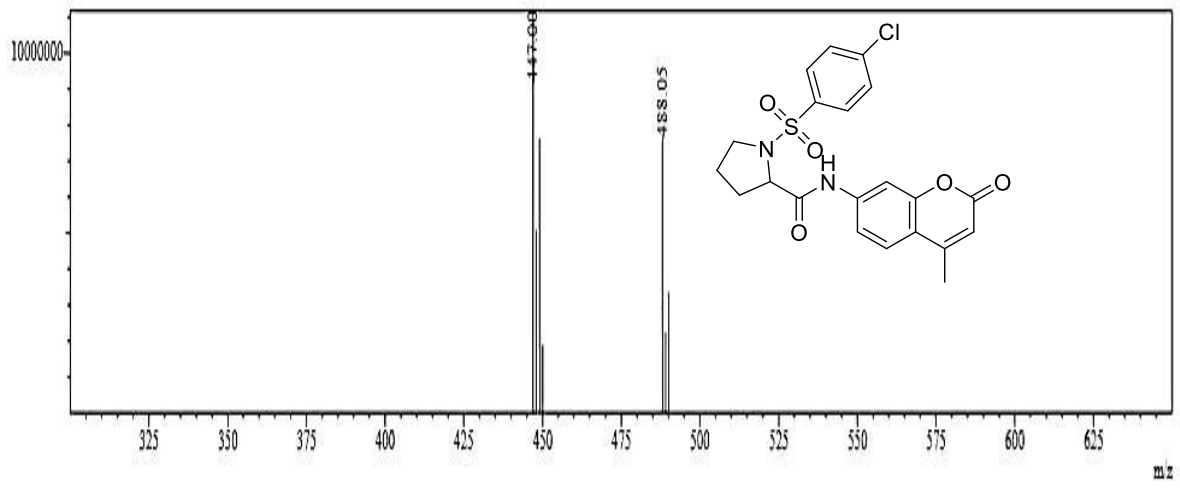

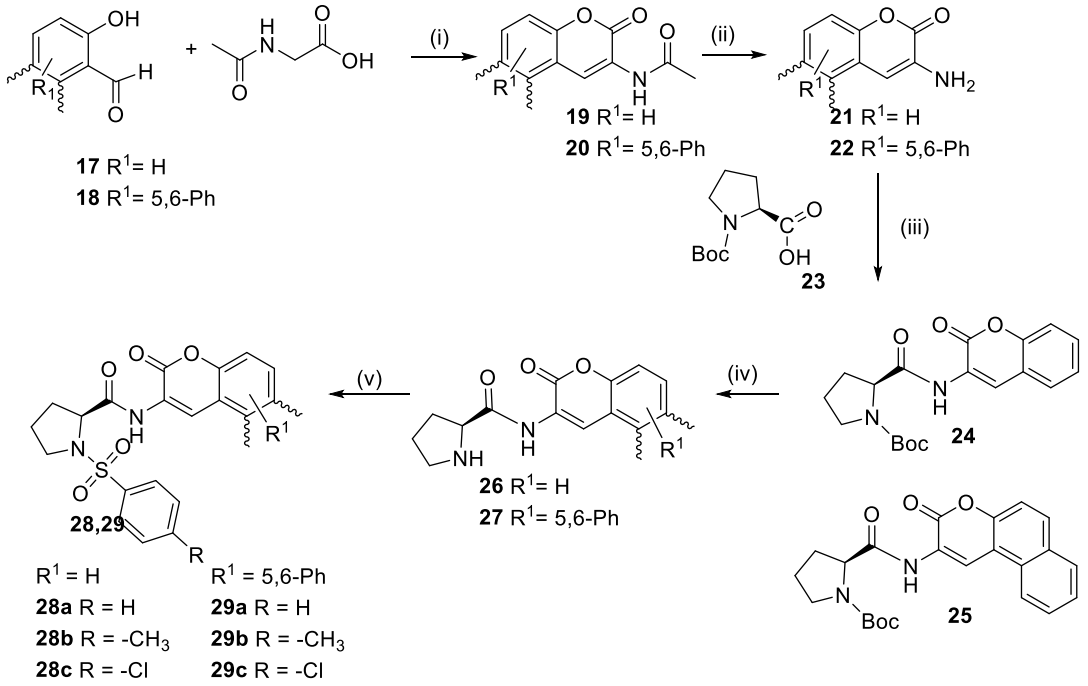

Reagents and conditions: (i)NaOAc, Ac_2O, reflux, 4h;(ii) Conc HCl : EtOH (7:3), reflux;(iii) (a) THF, CH_3CH_2OCOCl (0-5 C) 10 mins (b) Boc proline, THF, TEA reflux 8h; (iv) TFA, DCM; (v) $NaHCO_3$, benzenesulphonyl chloride, DCM:Water(1:1).

Scheme-2 Synthesis of 3-Amino chromen-2-one derivatives **28a-c** and **29a-c**.

Similar set of proline sulphonamide hybrid compounds **28a-c** and **29a-c** were synthesized from 3-amino chromen-2-one **21-22** (**Scheme-2**). 3-Amino chromen-2-one **21-22** were synthesized using Perkin reaction of 2-hydroxy benzaldehyde **17** or 2-hydroxy naphthaldehyde **18** with N-acetyl glycine in presence of sodium acetate and acetic anhydride to give 3-acetamido chromen-2-one derivatives **19** and **20** respectively, followed by hydrolysis of acetyl group using ethanol: conc. HCl (7:3) to yield compounds 3-amino-2H-chromen-2-one (**21**) and 2-amino-3H-benzo[f]chromen-3-one (**22**) respectively. Compounds **28a-c** and **29a-c** were synthesized from compounds **21** and **22** using similar set of reaction conditions as discussed for synthesis of 7-amino chromen-2-one derivatives **16a-c** from compound **15**. All compounds **28a-c** and **29a-c** were well characterized using spectral techniques such as ^{1}H-NMR, ^{13}C-NMR, IR and ESI-MS.

The ^{1}H-NMR (**Fig-3a.15.3**) spectrum of compound **28c** showed multiplet from δ 1.81-1.91 for three protons, singlet at δ 2.27 for one proton, multiplet from δ 3.26-3.32 for one proton, singlet at δ 3.61 for one proton and doublet at δ 4.31 for one proton indicated proline ring protons. Aromatic protons were observed in the region from δ 7.29- 8.68 ppm and sharp

singlet for amide proton at δ 9.30 distinctively. ^{13}C-NMR of compound **28c** (**Fig-3a.15.3**) showed proline ring carbons at δ 24.69, 30.54, 49.89, 62.75, aromatic region carbons from δ 116.45 to 150. Carbonyl carbon of amide and lactone were observed at δ 158.41 and δ 170.60 ppm respectively. In IR spectrum of compound **28c** (**Fig-3a.15.1**) bands for N-H and C-H stretching were observed at 3311 and 3093 cm^{-1}, carbonyl stretching for lactone at 1722 cm^{-1} and amide at 1693 cm^{-1} respectively. The ESI-MS (**Fig-3a.15.4**) spectrum showed peak at 433.00 for $[M+H]^+$ which confirms the formation of desired compound **28c**.

X-ray single crystal study

Single crystal was developed by slow evaporation technique using mixture of pet.ether and ethyl acetate solvent. X-ray single crystal of compound **29a** has confirmed the structure of it (**Fig-3a.8**). The data is given in **Table-3a.2** (CCDC: 1876145)

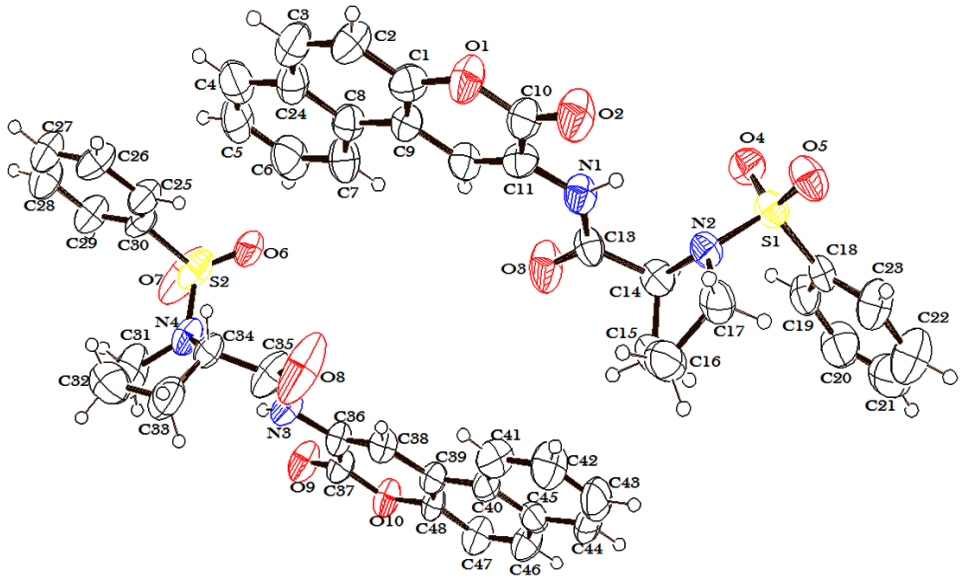

Figure-3a.8 ORTEP diagram of compound **29a**

Table 3a.2: Crystal data and structure refinement for compound **29a** with (CCDC NO: 1876145)

Empirical formula	$C_{24}H_{20}N_2O_5S$		μ/mm^{-1}	0.190
Formula weight	448.50		F(000)	468.5
Temperature/K	293		Crystal size/mm^3	0.4 × 0.2 × 0.1
Crystal system	Triclinic		Radiation	Mo Kα (λ = 0.71073)
Space group	P1		2Θ range for data collection/°	5.86 to 52.74
a/Å	7.5147(4)		Index ranges	-10 ≤ h ≤ 10, -11 ≤ k ≤ 11, -23 ≤ l ≤ 23
b/Å	8.2722(8)		Reflections collected	23044
c/Å	17.7350(14)		Independent reflections	8738 [R_{int} = 0.1030, R_{sigma} = 0.1943]
α/°	80.546(8)		Data/restraints/parameters	8738/3/577
β/°	81.431(6)		Goodness-of-fit on F^2	0.976
γ/°	87.796(6)		Final R indexes [I>=2σ (I)]	R_1 = 0.0872, wR_2 = 0.1721
Volume/$Å^3$	1075.24(15)		Final R indexes [all data]	R_1 = 0.2221, wR_2 = 0.2441
Z	2		Largest diff. peak/hole / e $Å^{-3}$	1.30/-0.51
$\rho_{calc}g/cm^3$	1.3852		Flack parameter	-0.00(14)

Figure-3a.9.1 IR spectrum of tert-butyl 2-((2-oxo-2H-chromen-3-yl)carbamoyl) pyrrolidine-1-carboxylate (**24**)

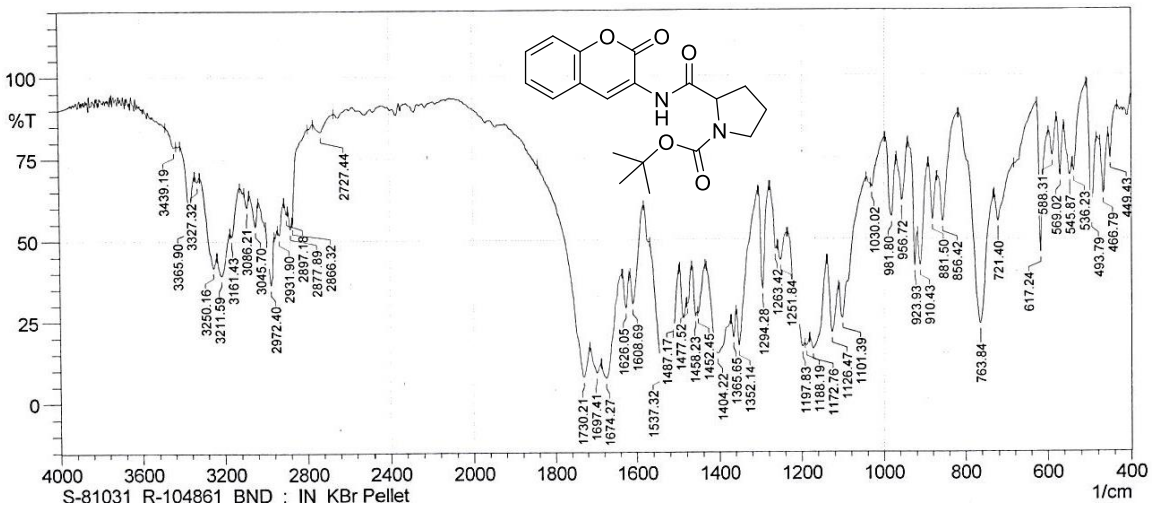

Figure-3a.9.2 ^{1}H-NMR spectrum of tert-butyl 2-((2-oxo-2H-chromen-3-yl)carbamoyl) pyrrolidine-1-carboxylate (**24**) in $CDCl_3$

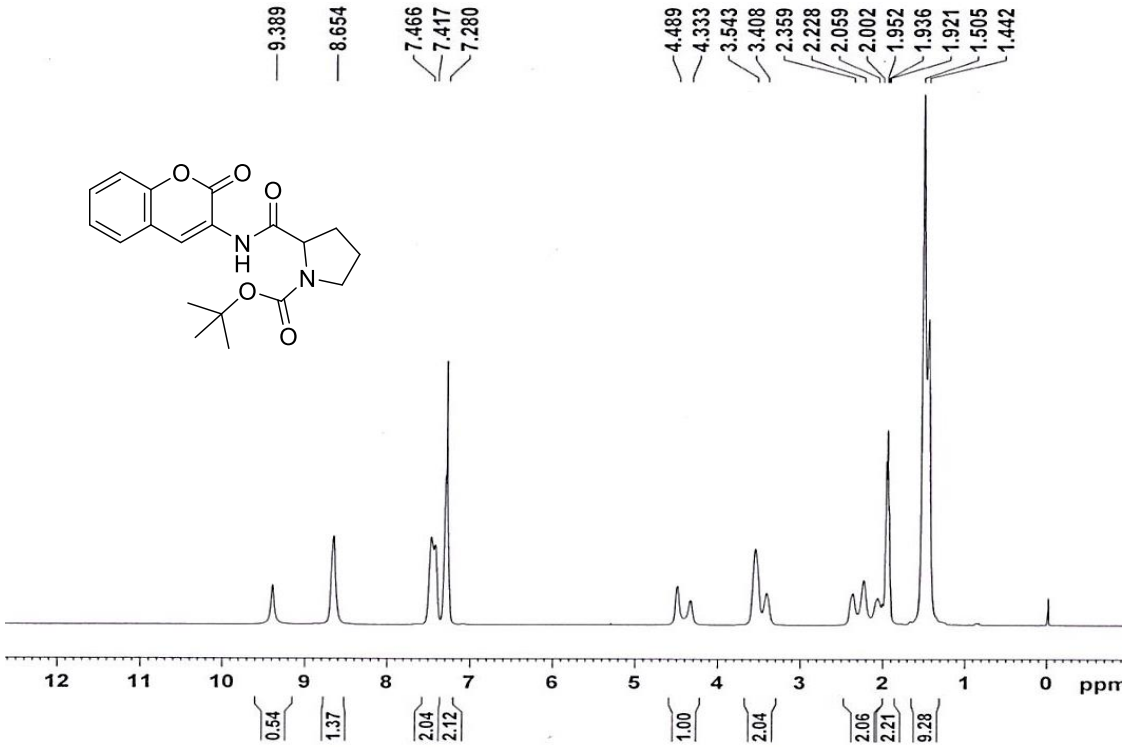

Figure-3a.9.3 ^{13}C-NMR spectrum of tert-butyl 2-((2-oxo-2H-chromen-3-yl) carbamoyl)pyrrolidine-1-carboxylate (**24**) in $CDCl_3$

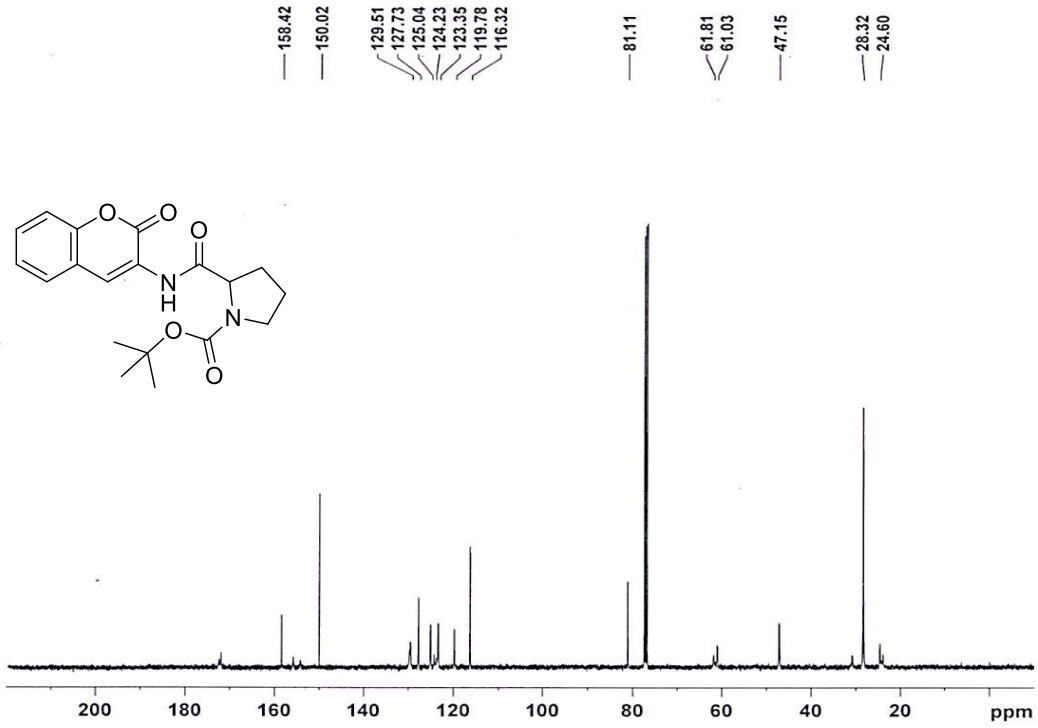

Figure-3a.9.4 ESI-MS spectrum of tert-butyl 2-((2-oxo-2H-chromen-3-yl)carbamoyl) pyrrolidine-1-carboxylate (**24**) M+H peak at 359.10

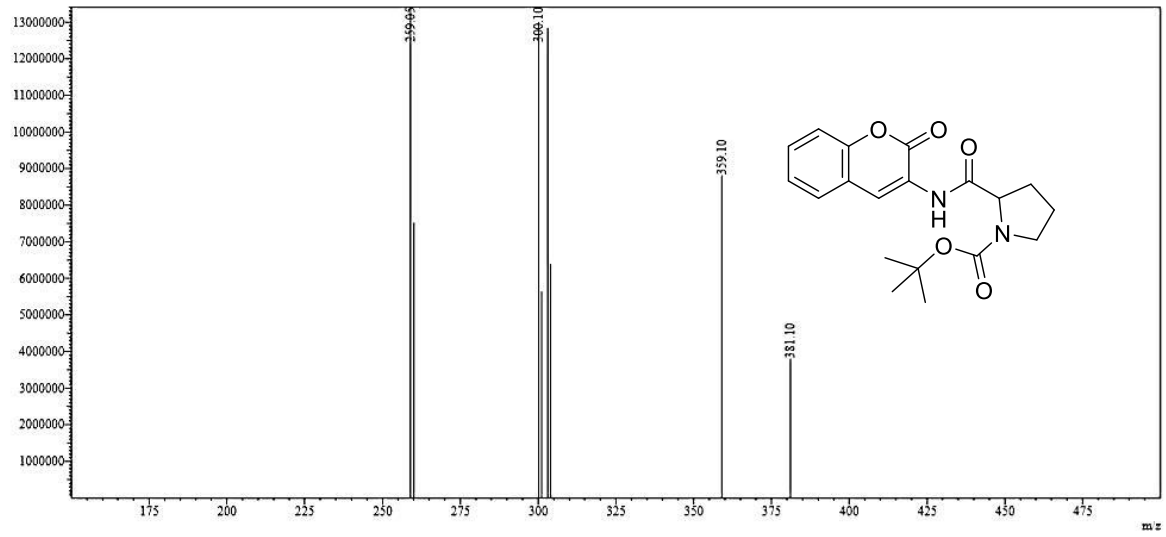

Figure-3a.10.1 IR spectrum of tert-butyl 2-((3-oxo-3H-benzo[f]chromen-2-yl) carbamoyl)pyrrolidine-1-carboxylate (**25**)

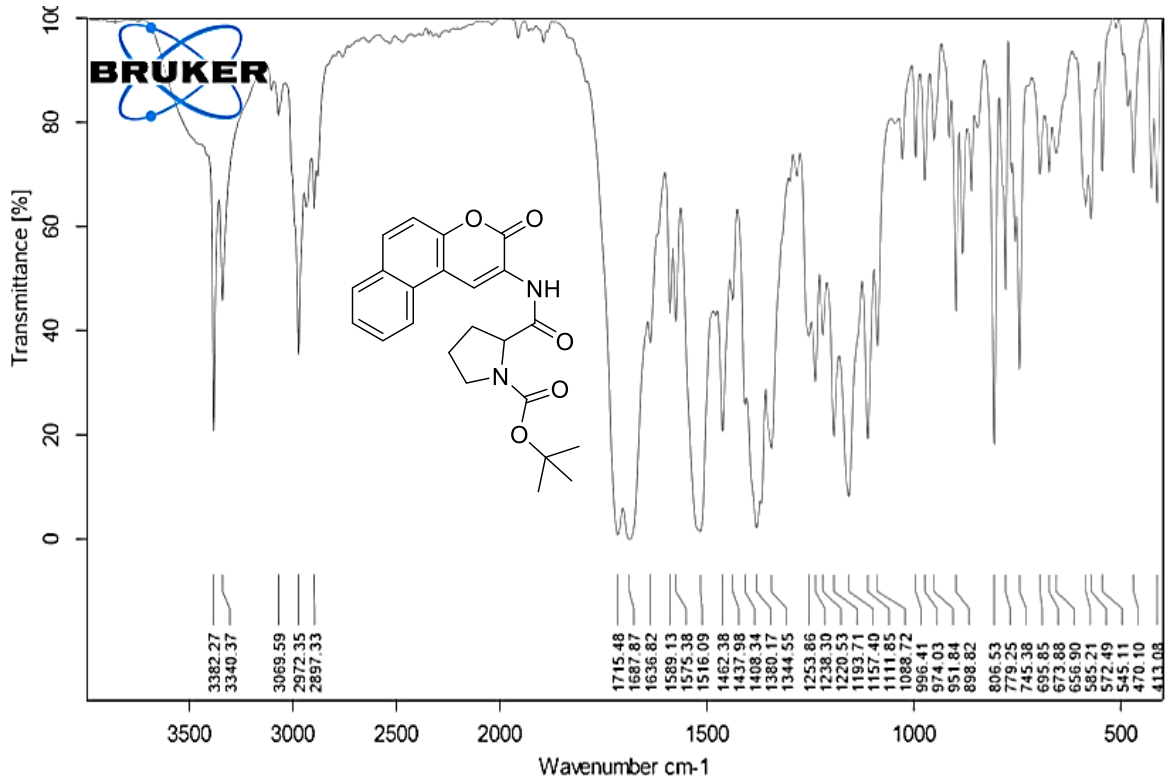

Figure-3a.10.2 ^{1}H-NMR spectrum of tert-butyl 2-((3-oxo-3H-benzo[f]chromen-2-yl) carbamoyl)pyrrolidine-1-carboxylate (**25**) in $CDCl_3$

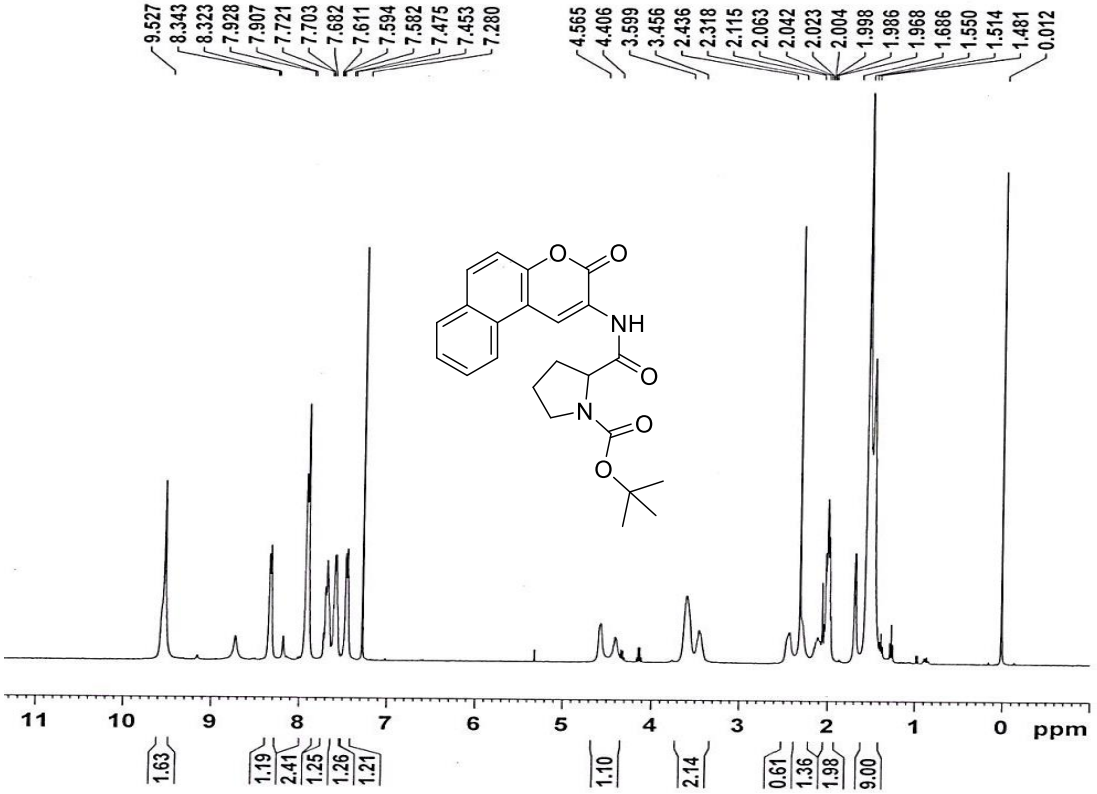

Figure-3a.10.3 ^{13}C-NMR spectrum of tert-butyl 2-((3-oxo-3H-benzo[f]chromen-2-yl)carbamoyl)pyrrolidine-1-carboxylate (**25**) in $CDCl_3$

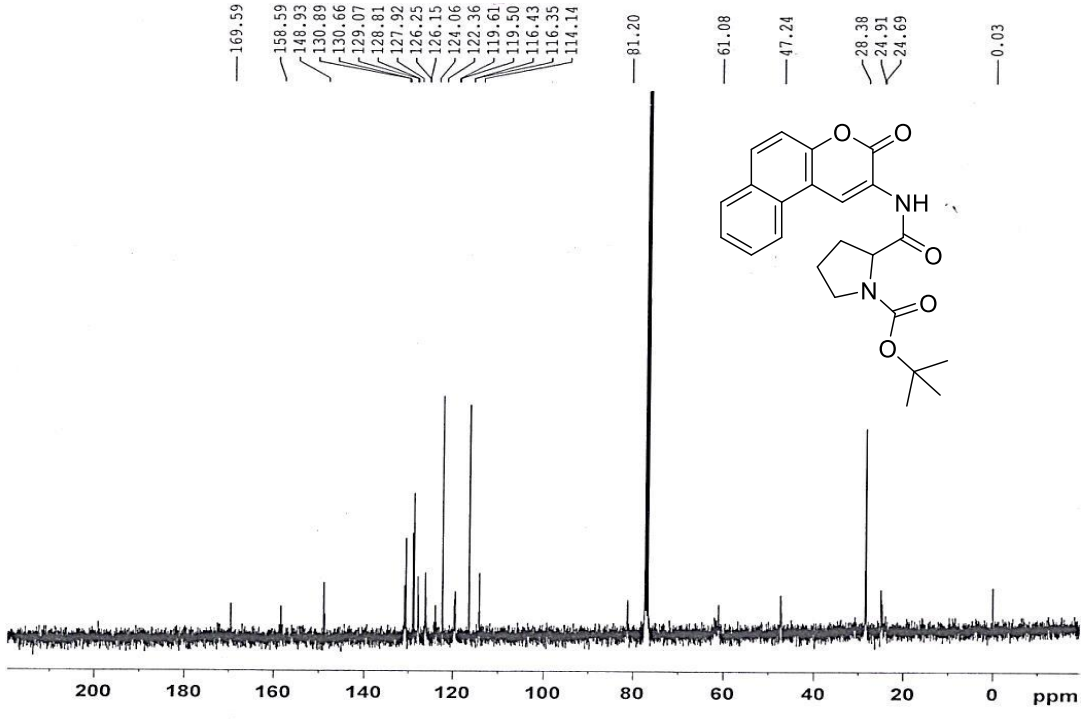

Figure-3a.11.1 IR spectrum of N-(2-Oxo-2H-chromen-3-yl)pyrrolidine-2-carboxamide (**26**)

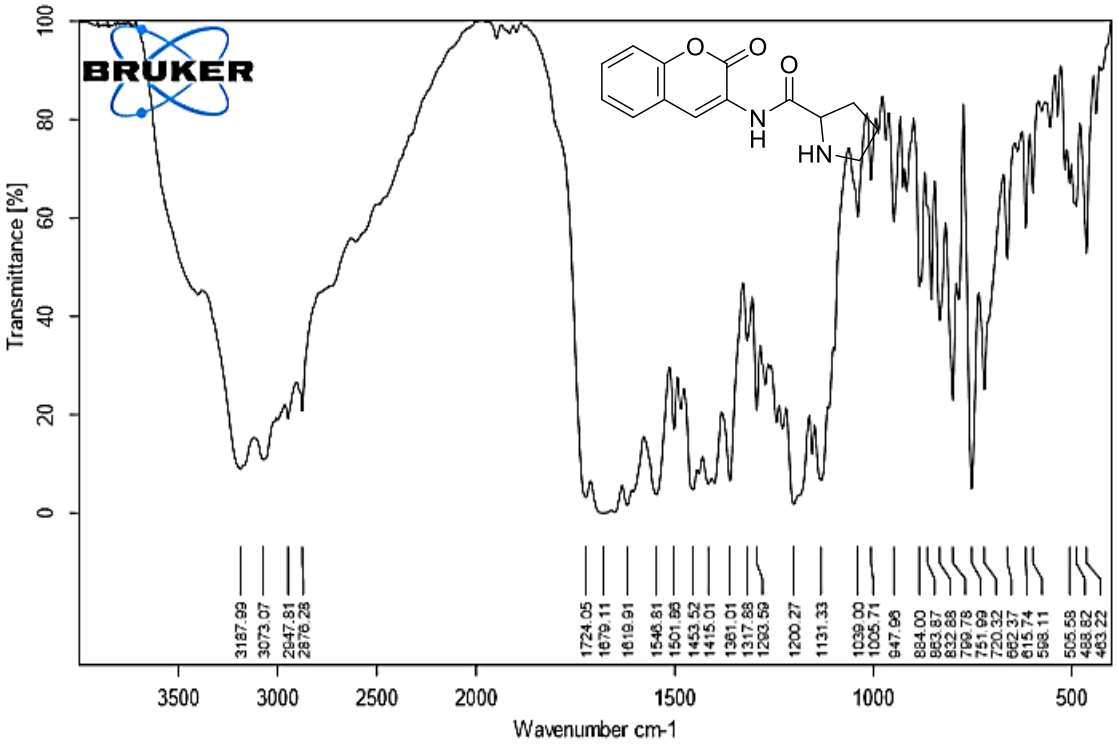

Figure-3a.11.2 ^{1}H-NMR spectrum of N-(2-Oxo-2H-chromen-3-yl)pyrrolidine-2-carboxamide (**26**) in $CDCl_3$

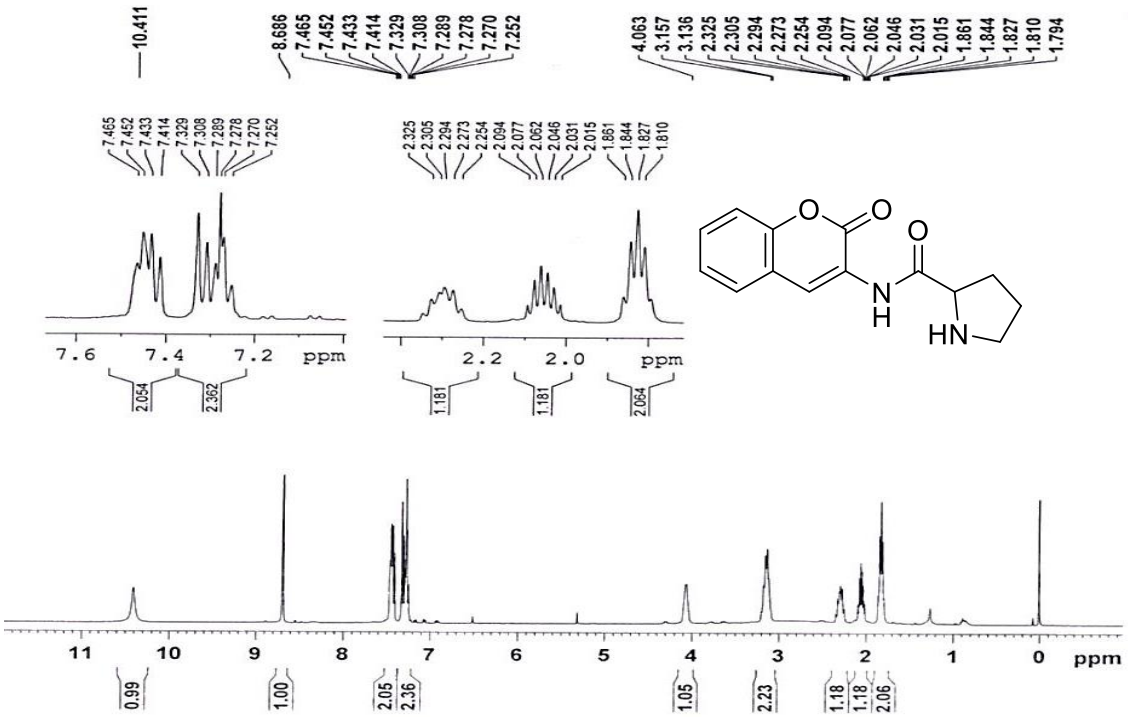

Figure-3a.11.3 ^{13}C-NMR spectrum of N-(2-Oxo-2H-chromen-3-yl)pyrrolidine-2-carboxamide (**26**) in $CDCl_3$

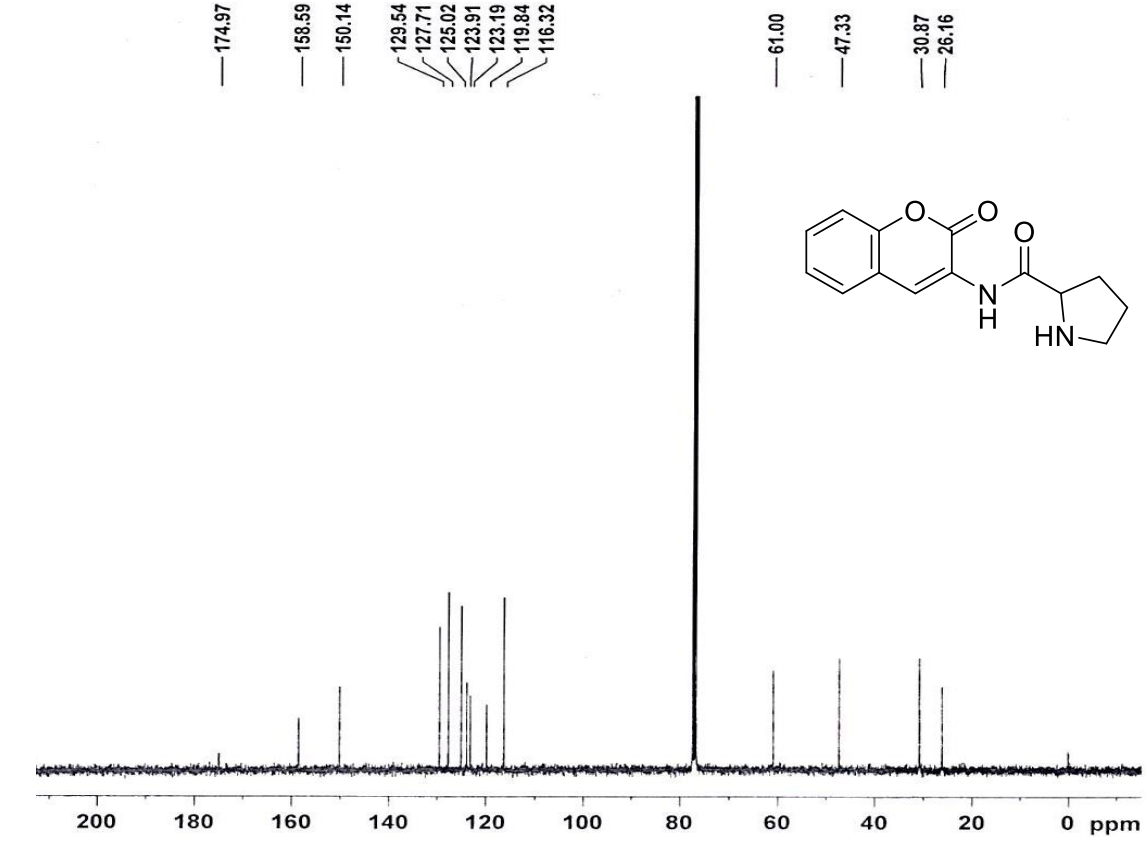

Figure-3a.12.1 IR spectrum of N-(3-Oxo-3H-benzo[f]chromen-2-yl)pyrrolidine-2-carboxamide (**27**)

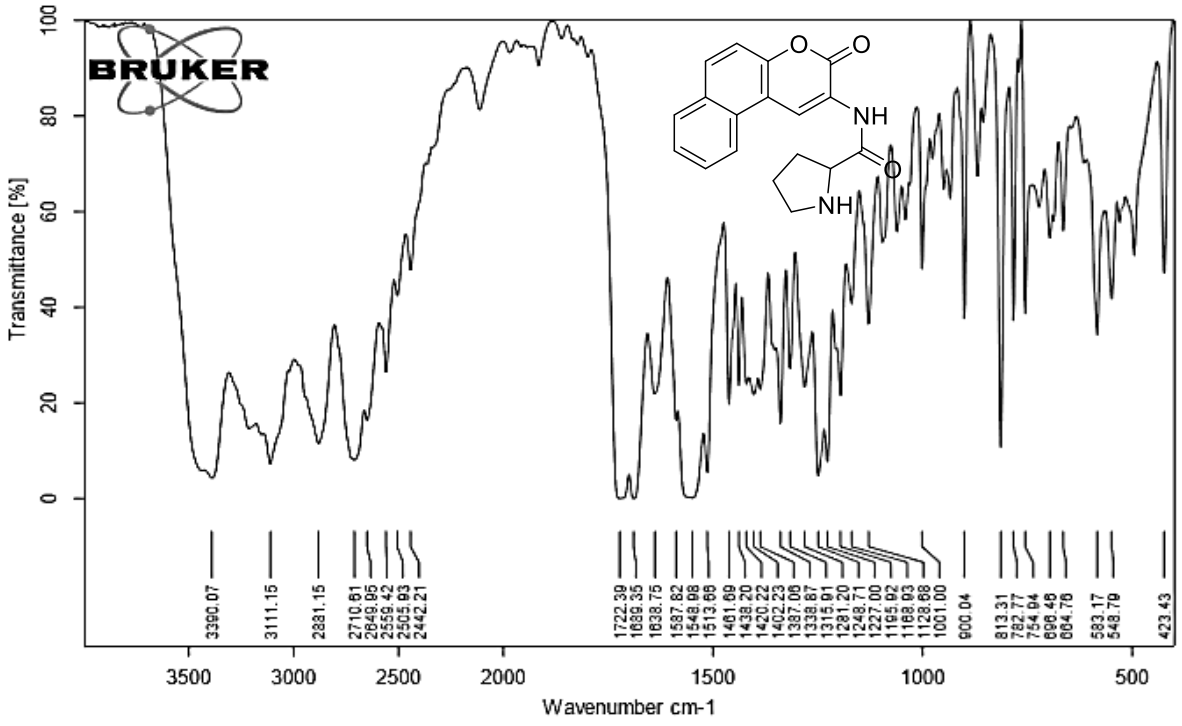

Figure-3a.12.2 ^{1}H-NMR spectrum of N-(3-Oxo-3H-benzo[f]chromen-2-yl) pyrrolidine-2-carboxamide **(27)** in $CDCl_3$

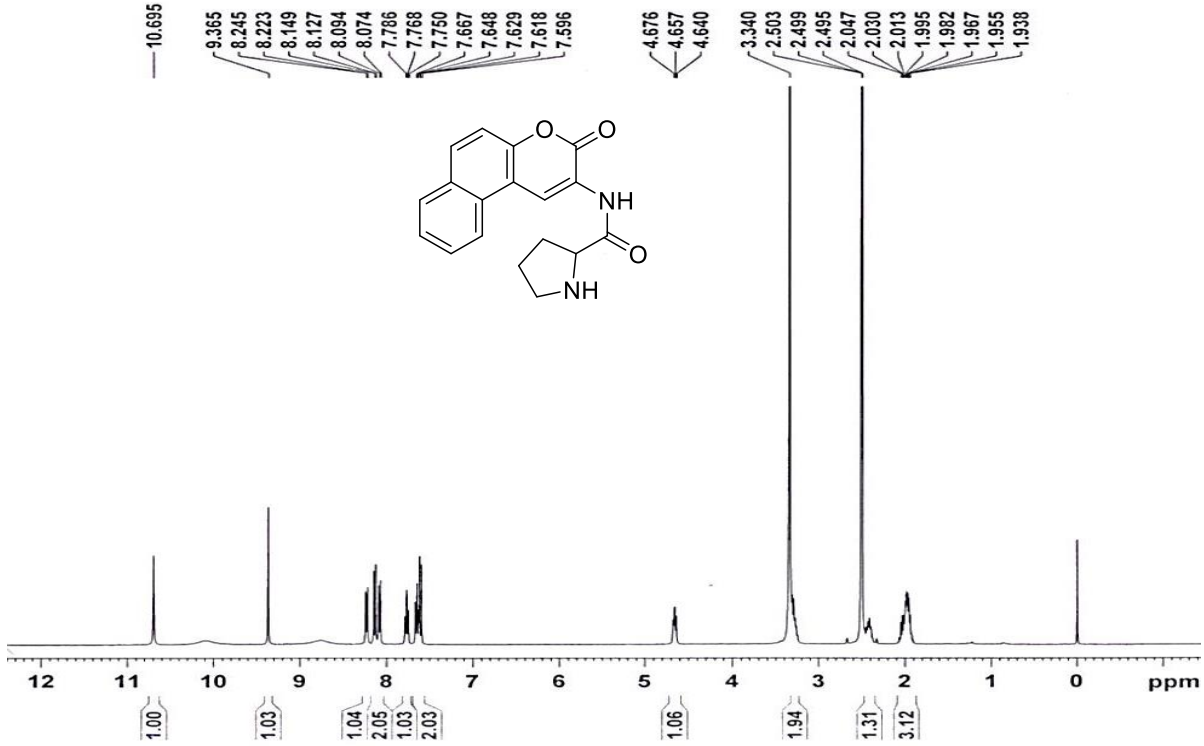

Figure-3a.12.3 ^{13}C-NMR spectrum of N-(3-Oxo-3H-benzo[f]chromen-2-yl) pyrrolidine-2-carboxamide (**27**) in $CDCl_3$

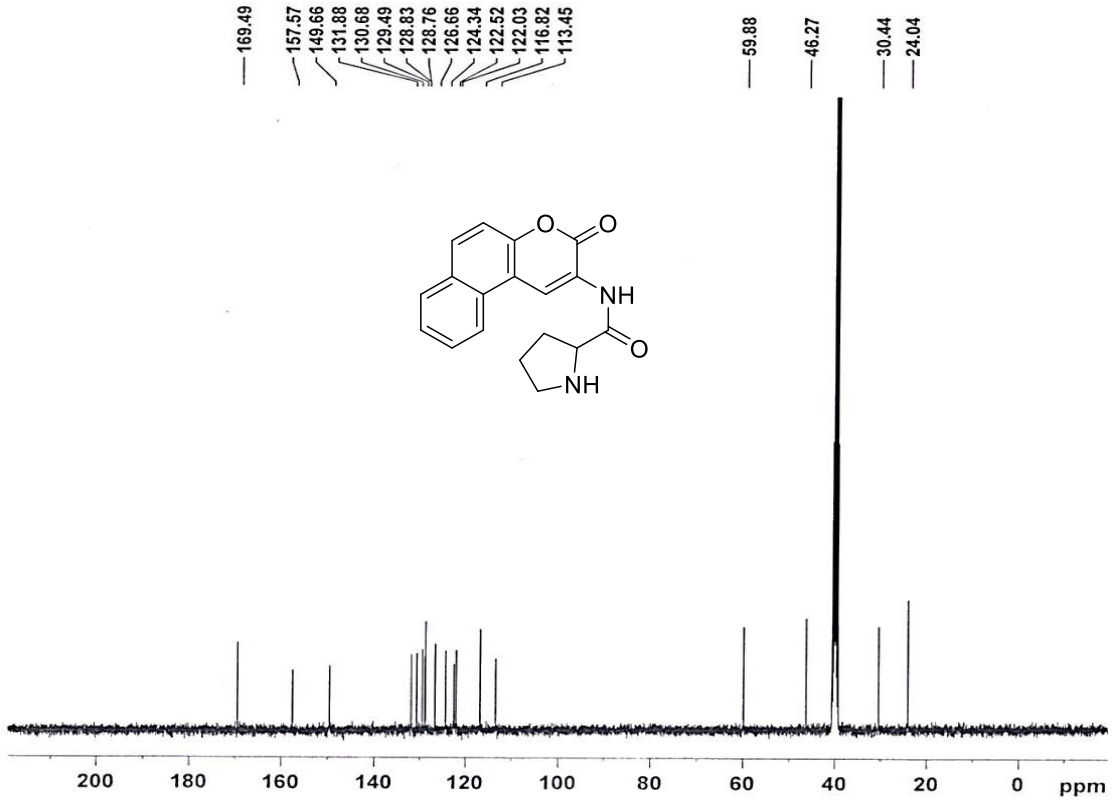

Figure-3a.13.1 IR spectrum of N-(2-oxo-2H-chromen-3-yl)-1-(phenylsulfonyl) pyrrolidine-2-carboxamide (**28a**)

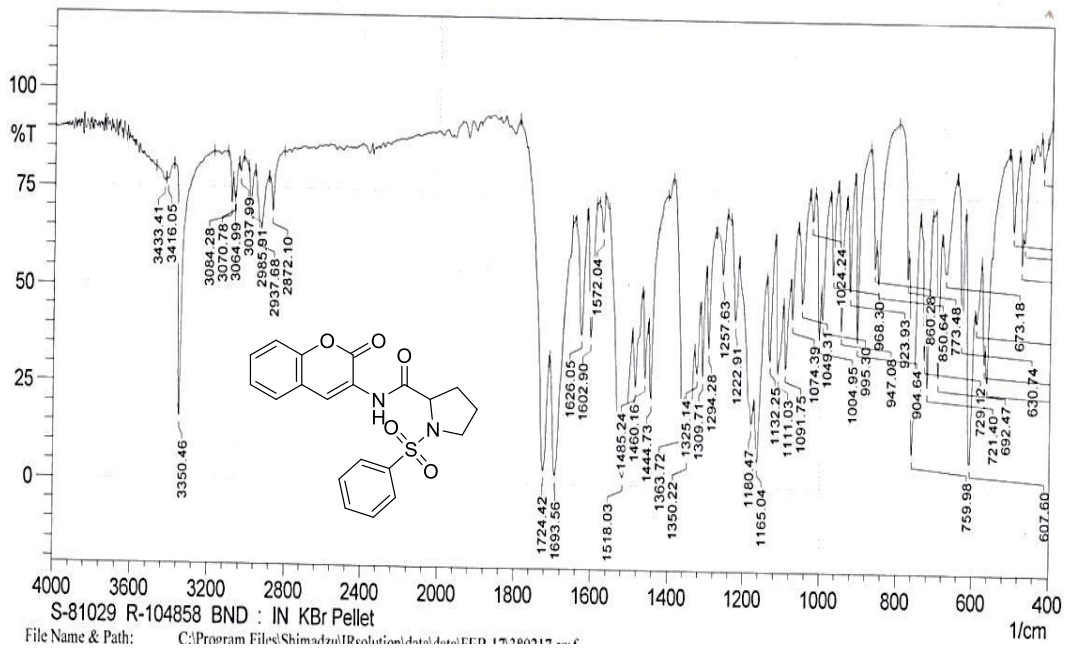

Figure-3a.13.2 ^{1}H-NMR spectrum of N-(2-oxo-2H-chromen-3-yl)-1-(phenylsulfonyl) pyrrolidine-2-carboxamide (**28a**) in $CDCl_3$

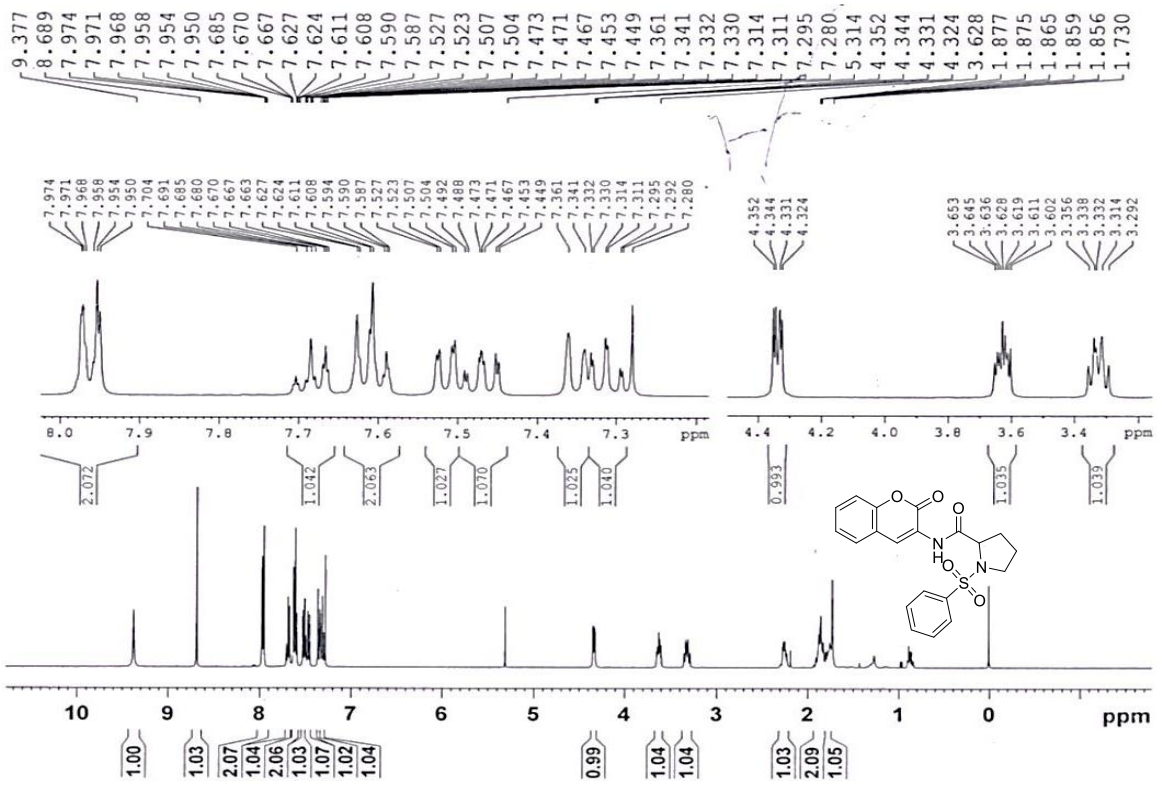

Figure-3a.13.3 ^{13}C-NMR spectrum of N-(2-oxo-2H-chromen-3-yl)-1-(phenylsulfonyl) pyrrolidine-2-carboxamide (**28a**) in $CDCl_3$

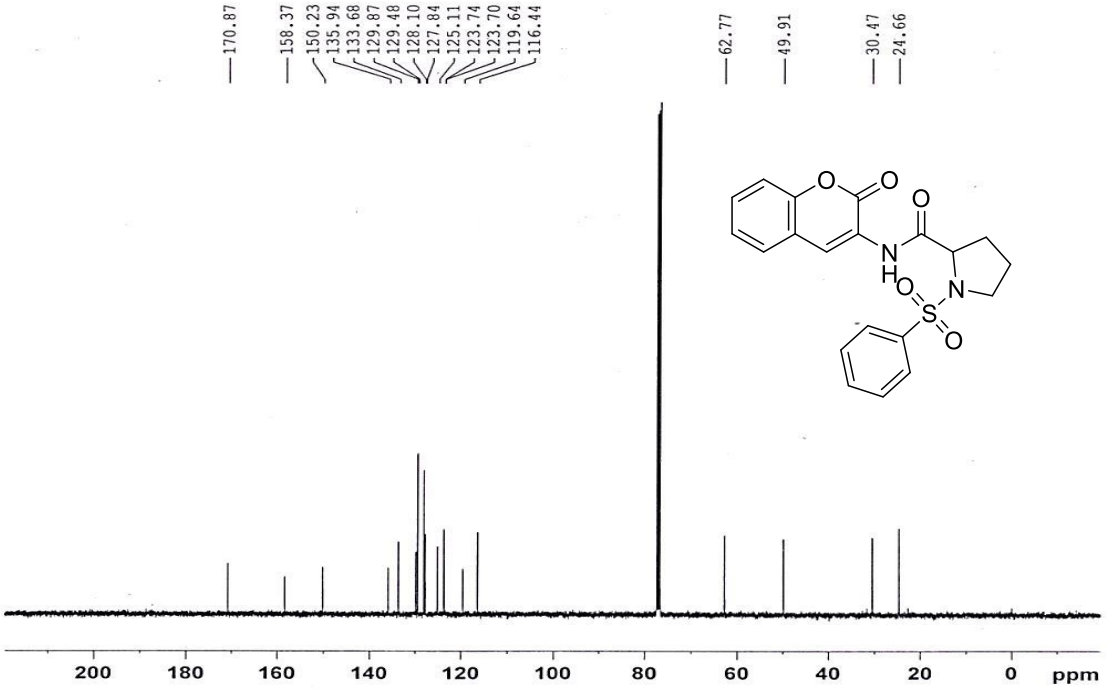

Figure-3a.13.4 ESI-MS spectrum of N-(2-oxo-2H-chromen-3-yl)-1-(phenylsulfonyl) pyrrolidine-2-carboxamide (**28a**) M+H peak at 399.05

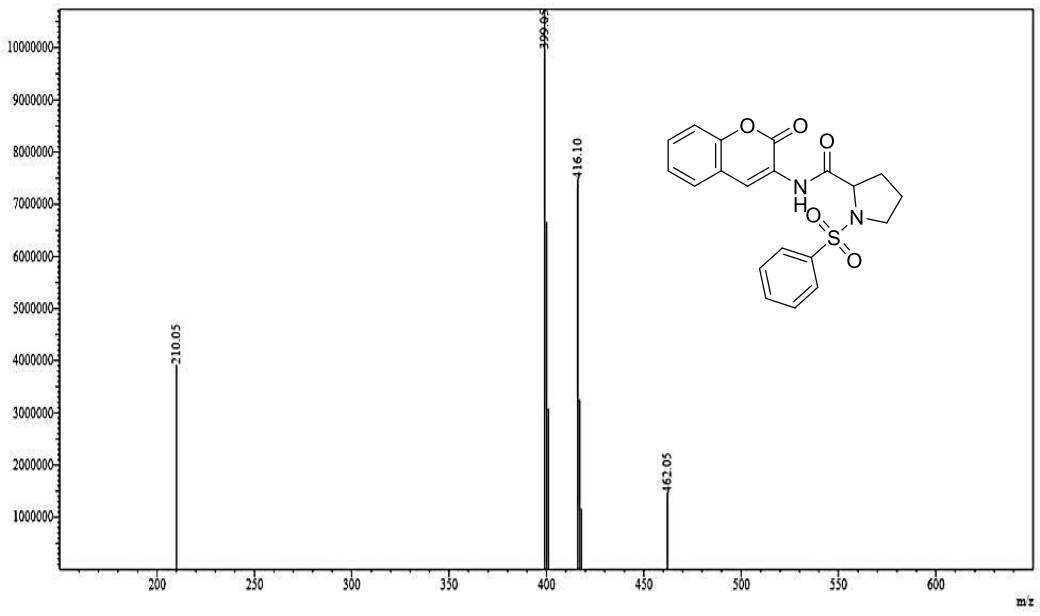

Figure-3a.14.1 IR spectrum of N-(2-oxo-2H-chromen-3-yl)-1-tosylpyrrolidine-2-carboxamide (**28b**)

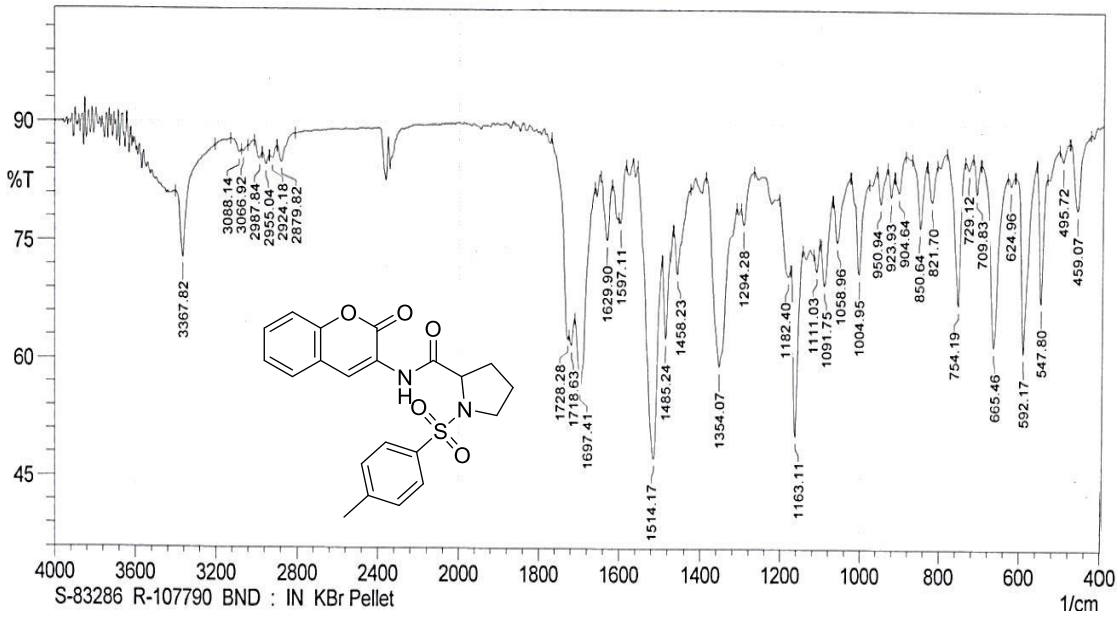

Figure-3a.14.2 ^{1}H-NMR spectrum of N-(2-oxo-2H-chromen-3-yl)-1-tosylpyrrolidine-2-carboxamide (**28b**)

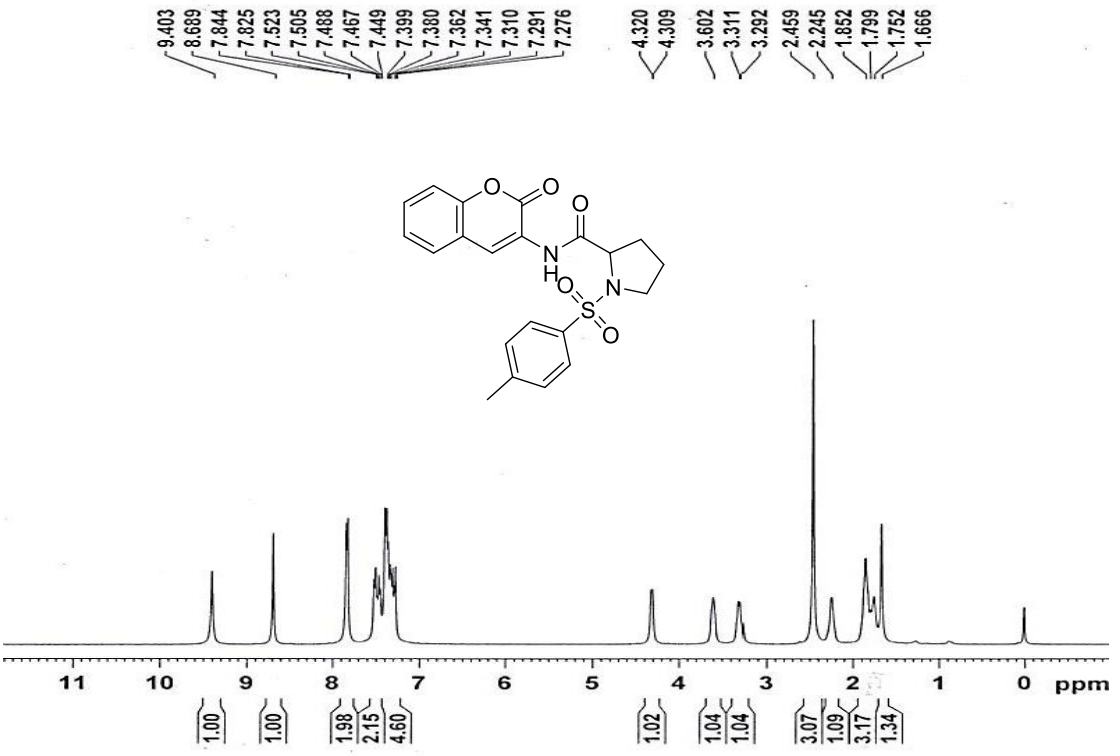

Figure-3a.14.3 ^{13}C-NMR spectrum of N-(2-oxo-2H-chromen-3-yl)-1-tosylpyrrolidine-2-carboxamide (**28b**) in $CDCl_3$

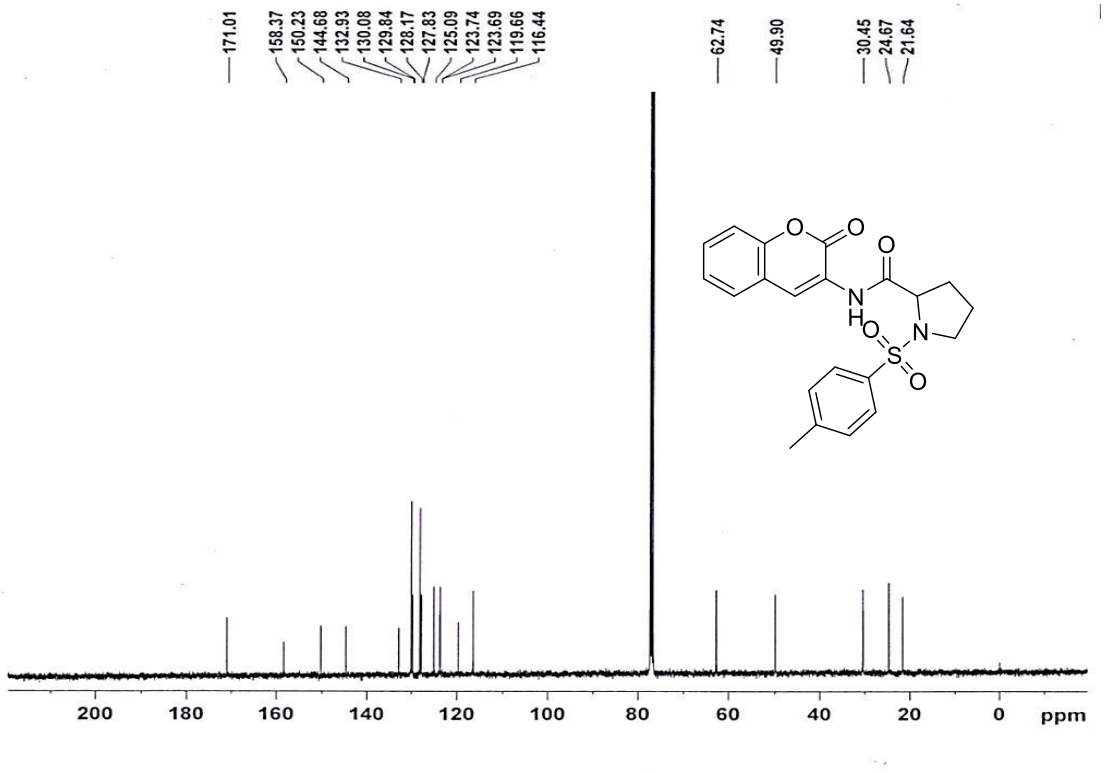

Figure-3a.14.4 ESI-MS spectrum of N-(2-oxo-2H-chromen-3-yl)-1-tosylpyrrolidine-2-carboxamide (**28b**) M+H peak at 413.05

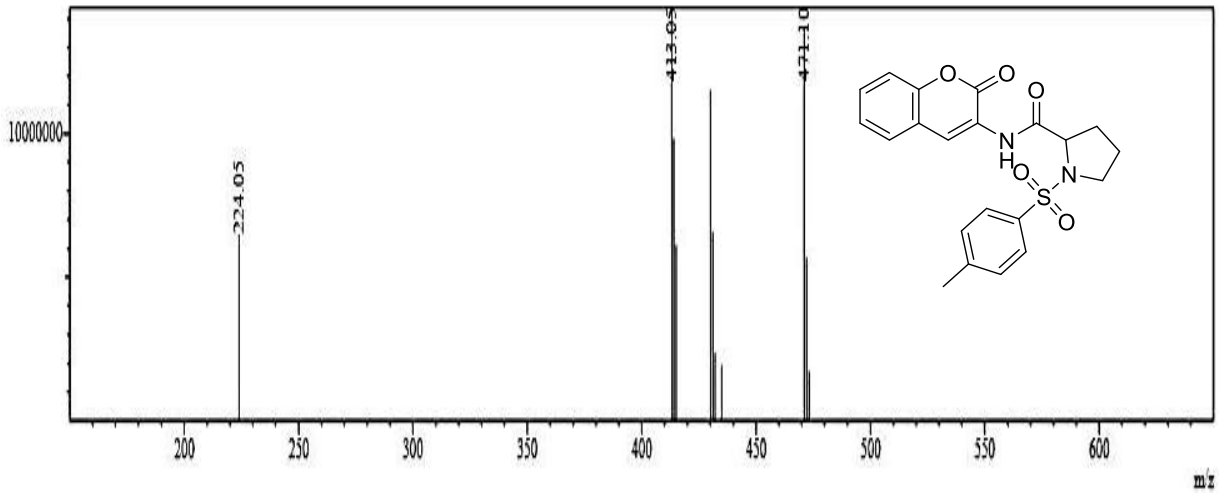

Figure-3a.15.1 IR spectrum of 1-((4-chlorophenyl)sulfonyl)-N-(2-oxo-2H-chromen-3-yl) pyrrolidine-2-carboxamide (**28c**)

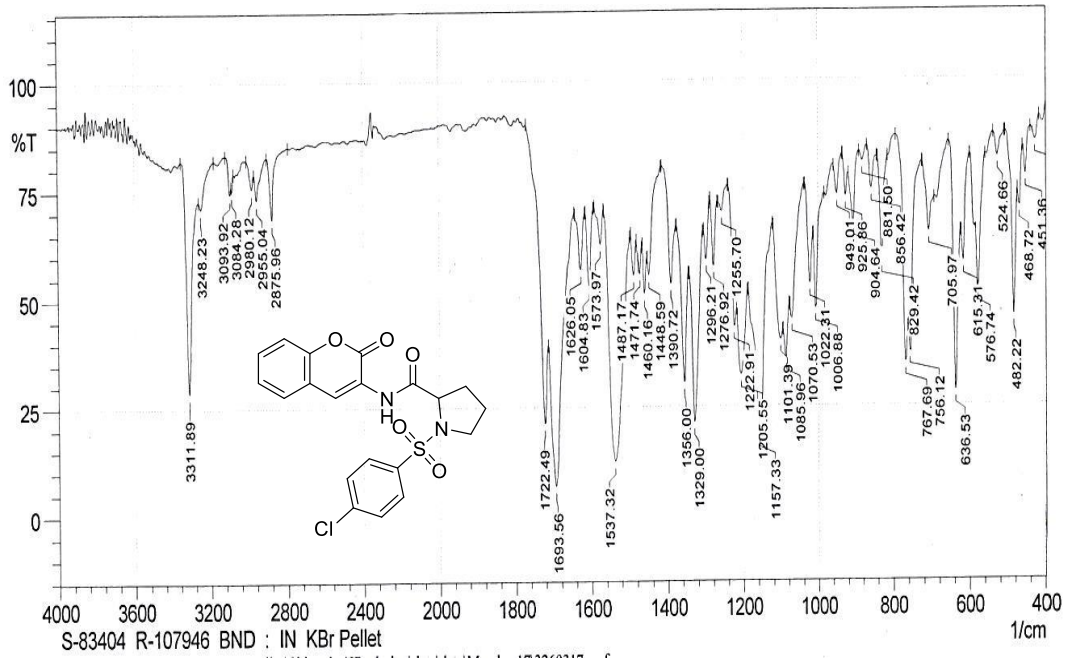

Figure-3a.15.2 ^{1}H-NMR spectrum of 1-((4-chlorophenyl)sulfonyl)-N-(2-oxo-2H-chromen-3-yl) pyrrolidine-2-carboxamide (**28c**) in $CDCl_3$

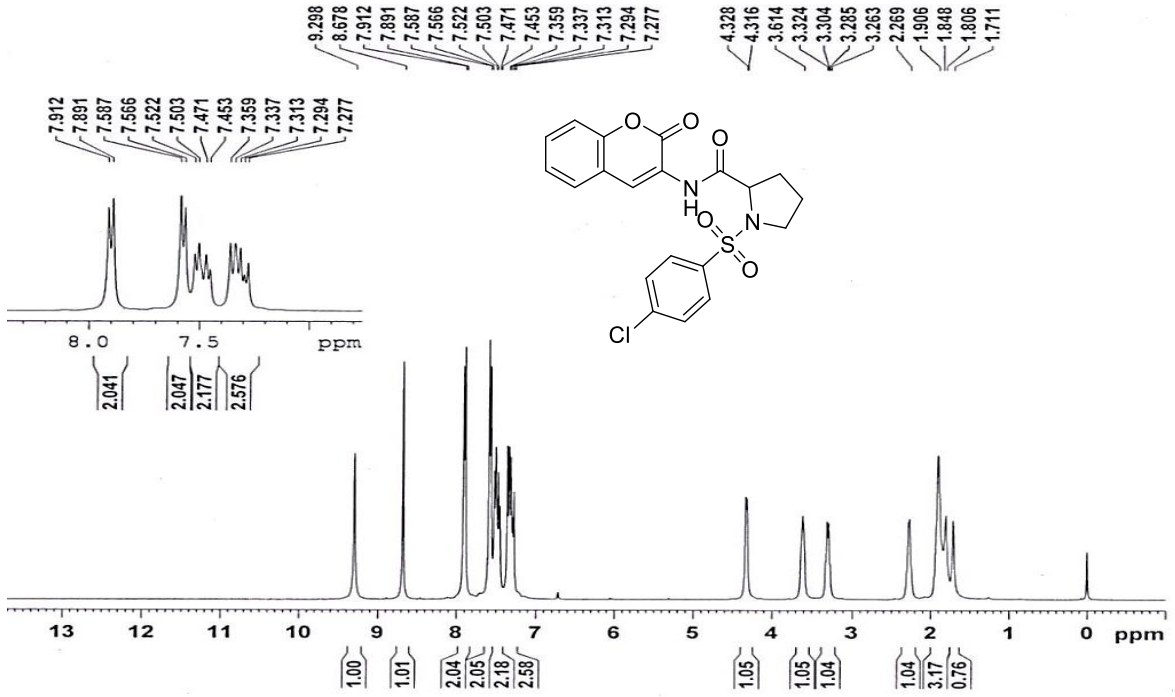

Figure-3a.15.3 ^{13}C-NMR spectrum of 1-((4-chlorophenyl)sulfonyl)-N-(2-oxo-2H-chromen-3-yl) pyrrolidine-2-carboxamide (**28c**) in $CDCl_3$

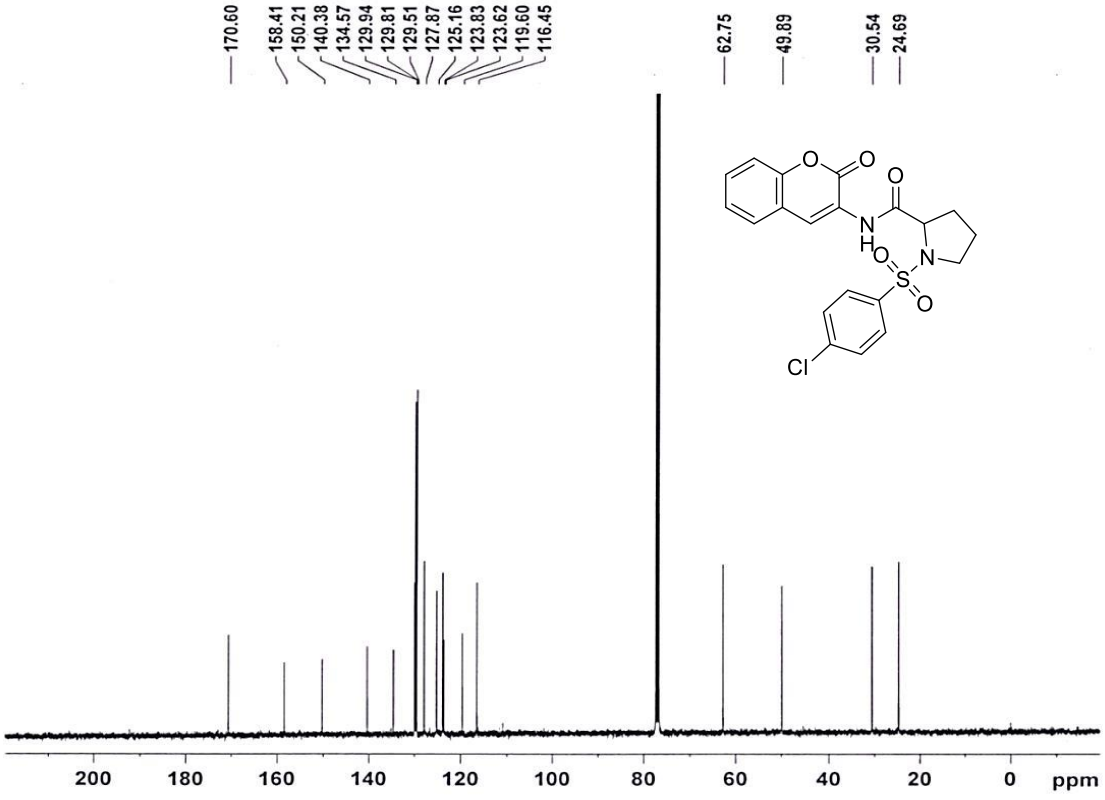

Figure-3a.15.4 ESI-MS spectrum of 1-((4-chlorophenyl)sulfonyl)-N-(2-oxo-2H-chromen-3-yl) pyrrolidine-2-carboxamide (**28c**) M+H peak at 433.00

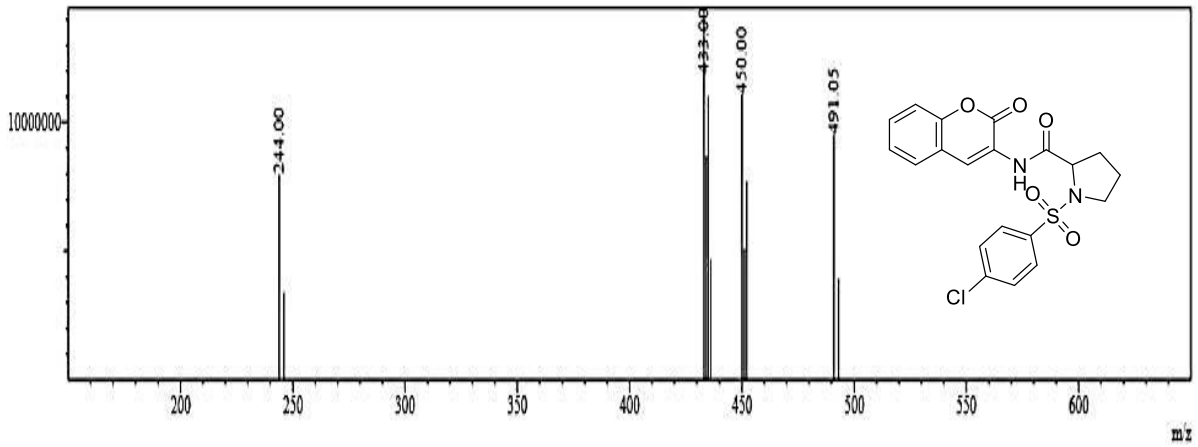

Figure-3a.16.1 IR spectrum of N-(3-oxo-3H-benzo[f]chromen-2-yl)-1-(phenylsulfonyl)pyrrolidine-2-carboxamide (**29a**)

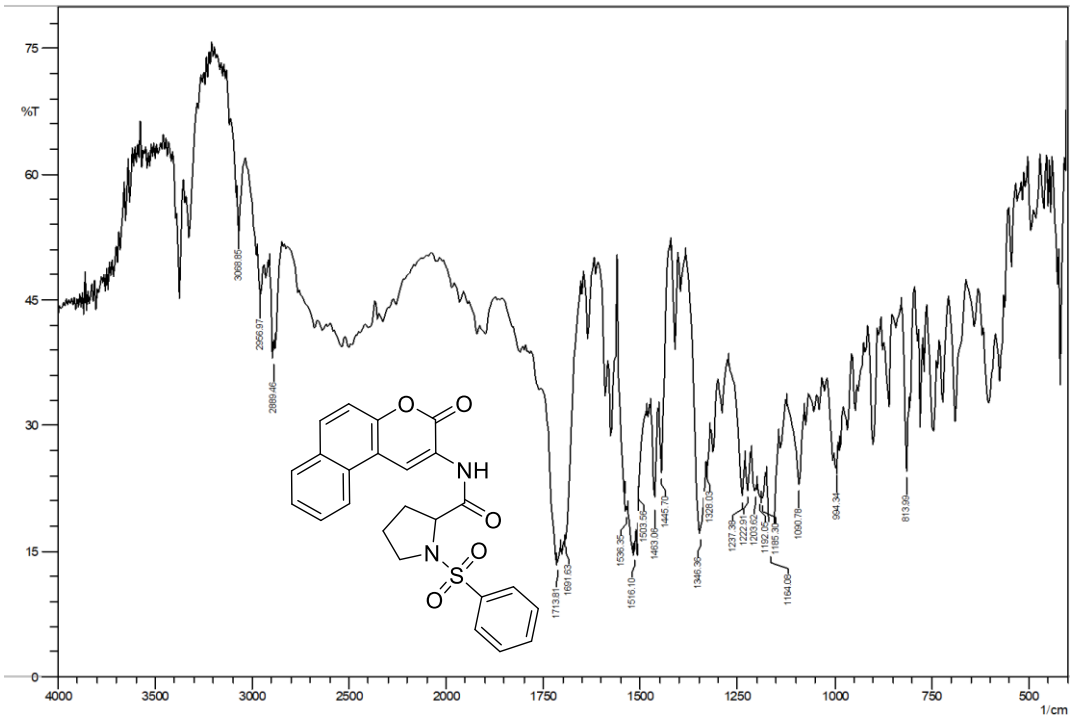

Figure-3a.16.2 ^{1}H-NMR spectrum of N-(3-oxo-3H-benzo[f]chromen-2-yl)-1-(phenylsulfonyl) pyrrolidine-2-carboxamide **(29a)** in $CDCl_3$

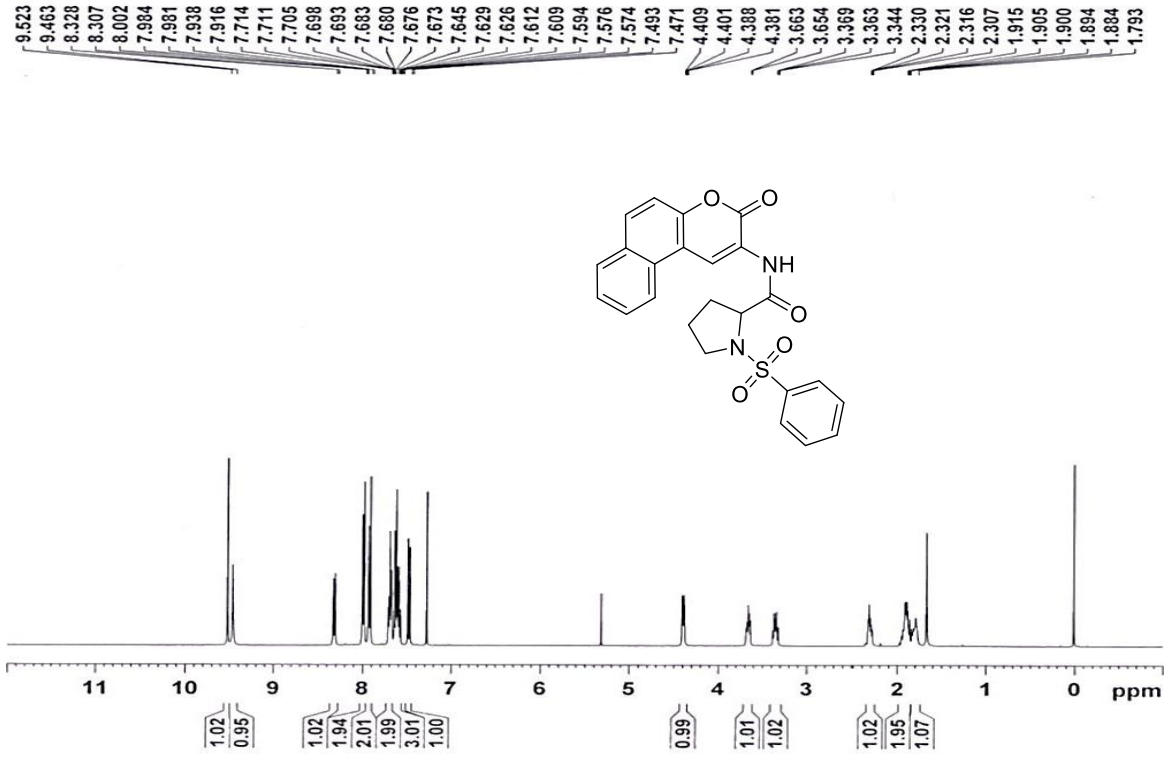

Figure-3a.16.3 ^{13}C-NMR spectrum of N-(3-oxo-3H-benzo[f]chromen-2-yl)-1-(phenylsulfonyl) pyrrolidine-2-carboxamide (**29a**) in $CDCl_3$

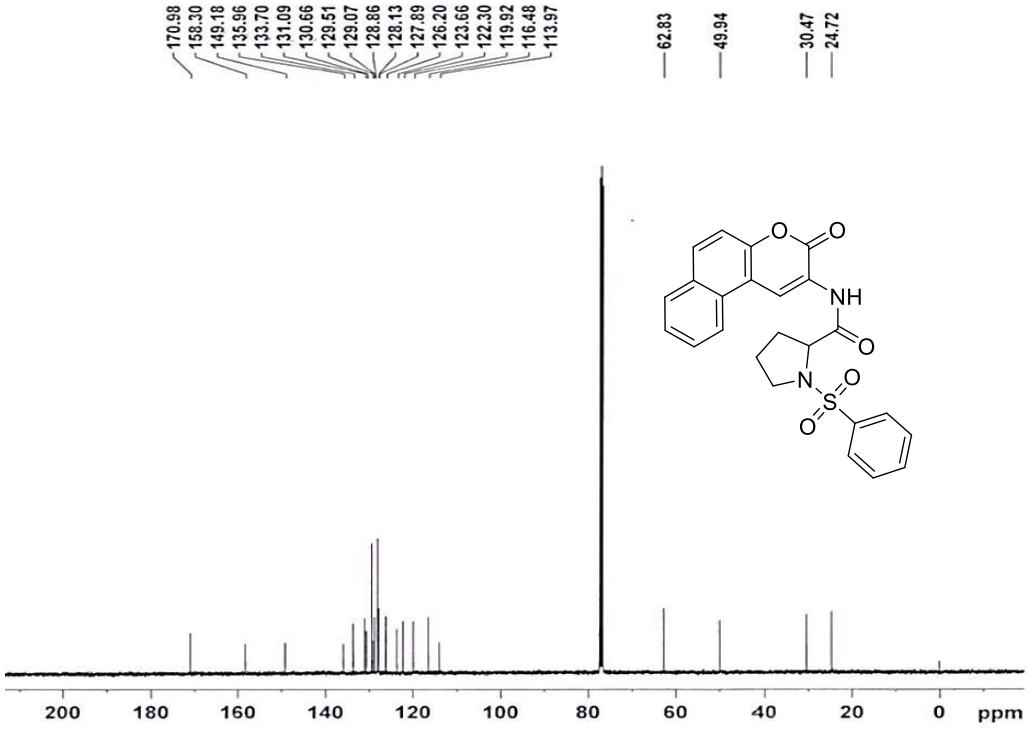

Figure-3a.16.4 ESI-MS spectrum of N-(3-oxo-3H-benzo[f]chromen-2-yl)-1-(phenylsulfonyl) pyrrolidine-2-carboxamide (**29a**) M+H peak at 449.10

Figure-3a.17.1 IR spectrum of N-(3-oxo-3H-benzo[f]chromen-2-yl)-1-tosylpyrrolidine-2-carboxamide (**29b**)

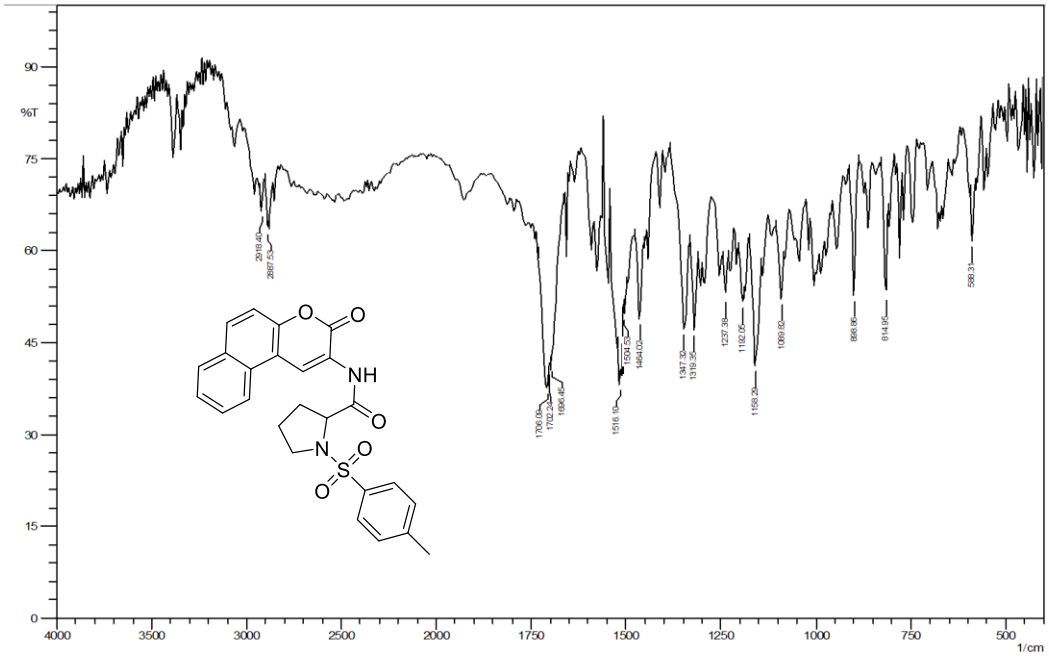

Figure-3a.17.2 ^{1}H-NMR spectrum of N-(3-oxo-3H-benzo[f]chromen-2-yl)-1-tosylpyrrolidine-2-carboxamide (**29b**) in $CDCl_3$

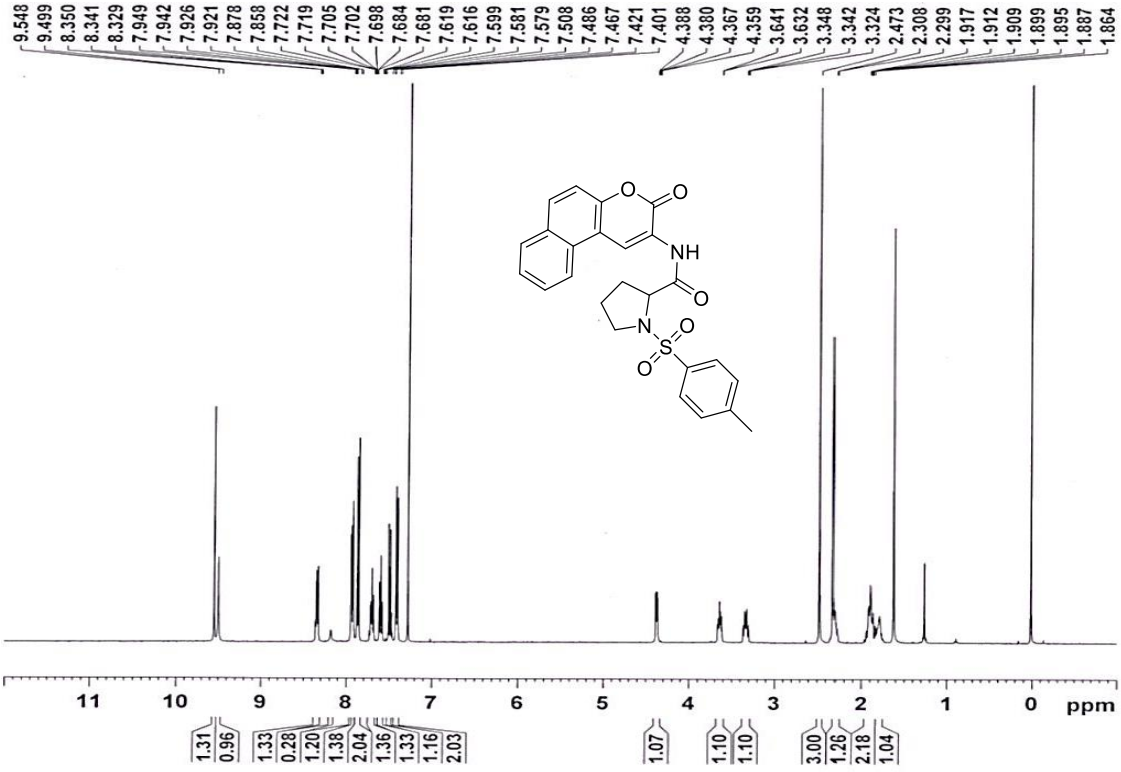

Figure-3a.17.3 ^{13}C-NMR spectrum of N-(3-oxo-3H-benzo[f]chromen-2-yl)-1-tosylpyrrolidine-2-carboxamide (**29b**) in $CDCl_3$

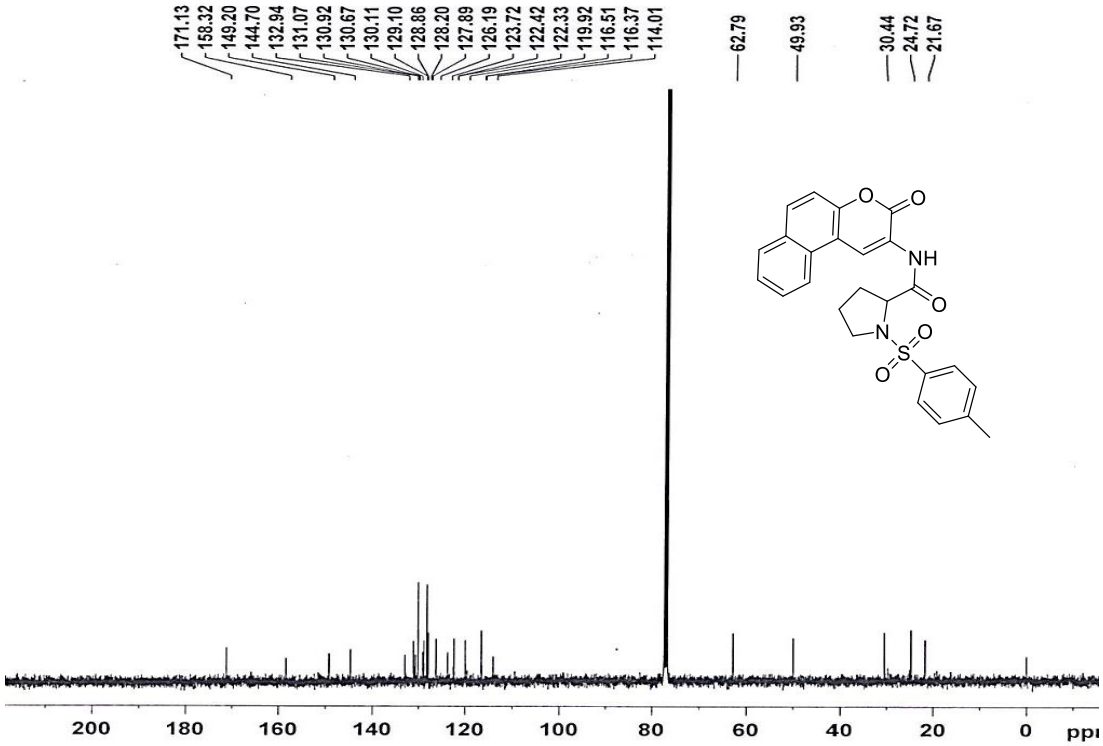

Figure-3a.17.4 ESI-MS spectrum of N-(3-oxo-3H-benzo[f]chromen-2-yl)-1-tosylpyrrolidine-2-carboxamide (**29b**) M+H peak at 463.13

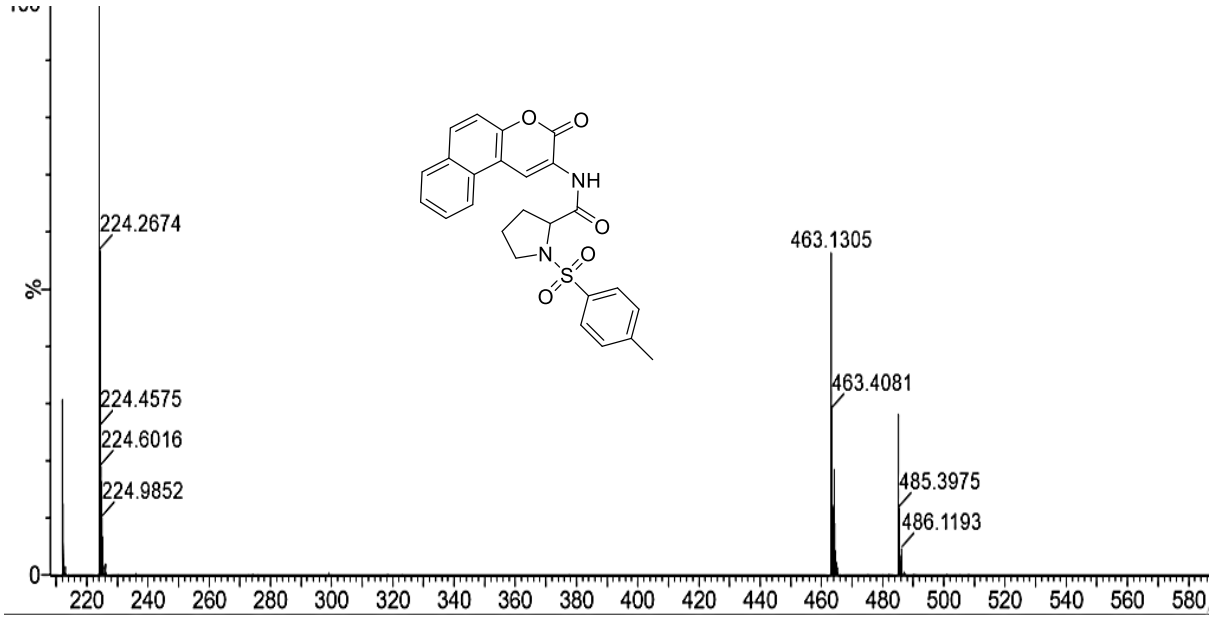

Figure-3a.18.1 IR spectrum of 1-((4-chlorophenyl)sulfonyl)-N-(3-oxo-3H-benzo[f]chromen-2-yl)pyrrolidine-2-carboxamide (**29c**)

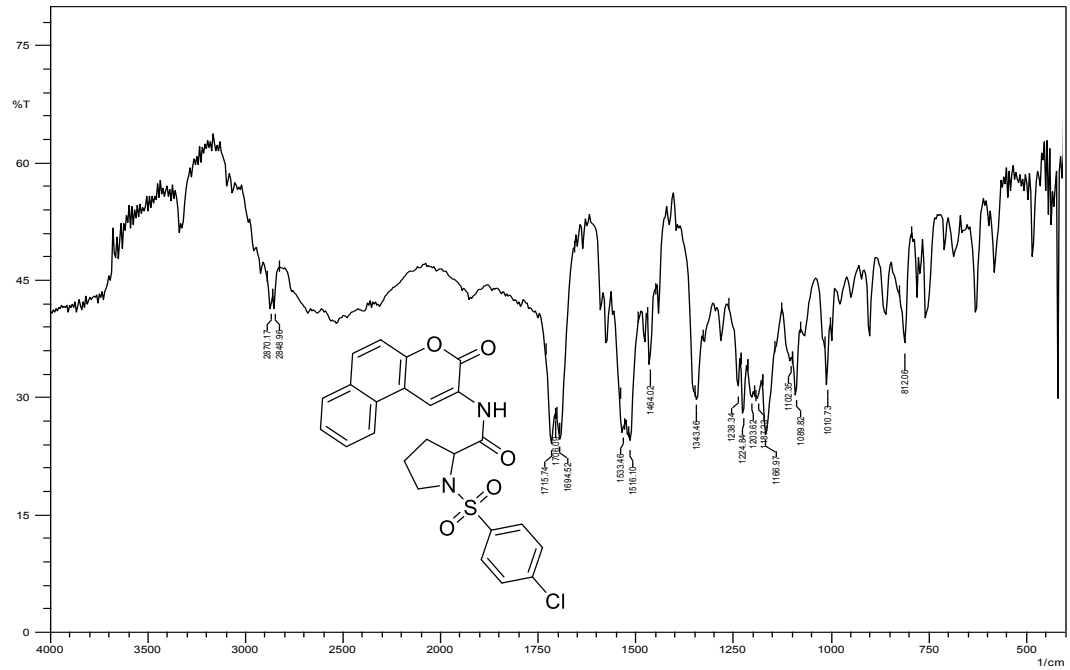

Figure-3a.18.2 ^{1}H-NMR spectrum of 1-((4-chlorophenyl)sulfonyl)-N-(3-oxo-3H-benzo[f]chromen-2-yl)pyrrolidine-2-carboxamide (**29c**) in $CDCl_3$

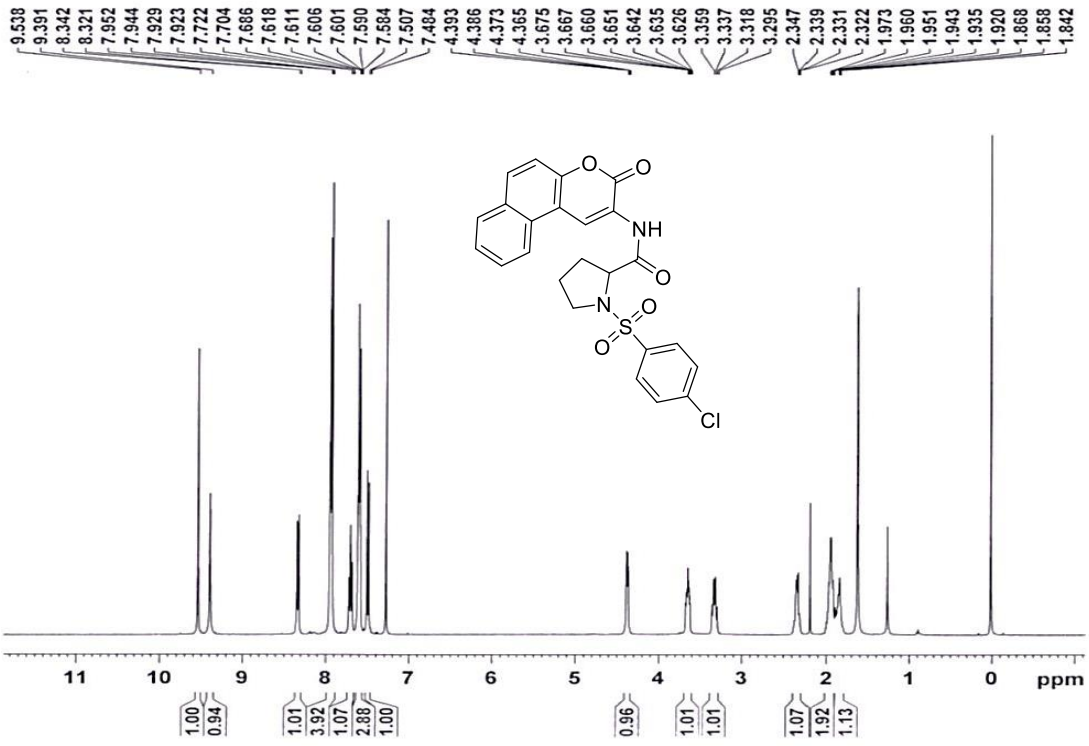

Figure-3a.18.3 ^{13}C-NMR spectrum of 1-((4-chlorophenyl)sulfonyl)-N-(3-oxo-3H-benzo[f]chromen-2-yl)pyrrolidine-2-carboxamide (**29c**) in $CDCl_3$

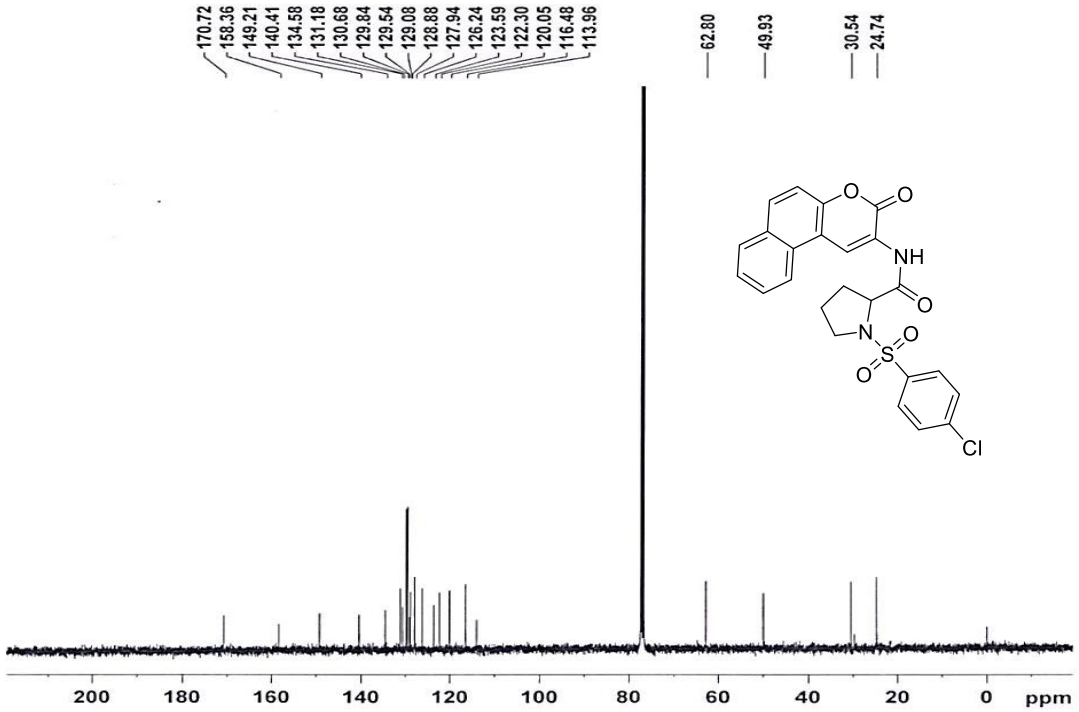

Figure-3a.18.4 ESI-MS spectrum of 1-((4-chlorophenyl)sulfonyl)-N-(3-oxo-3H-benzo[f]chromen-2-yl)pyrrolidine-2-carboxamide (**29c**) M+H peak at 483.06

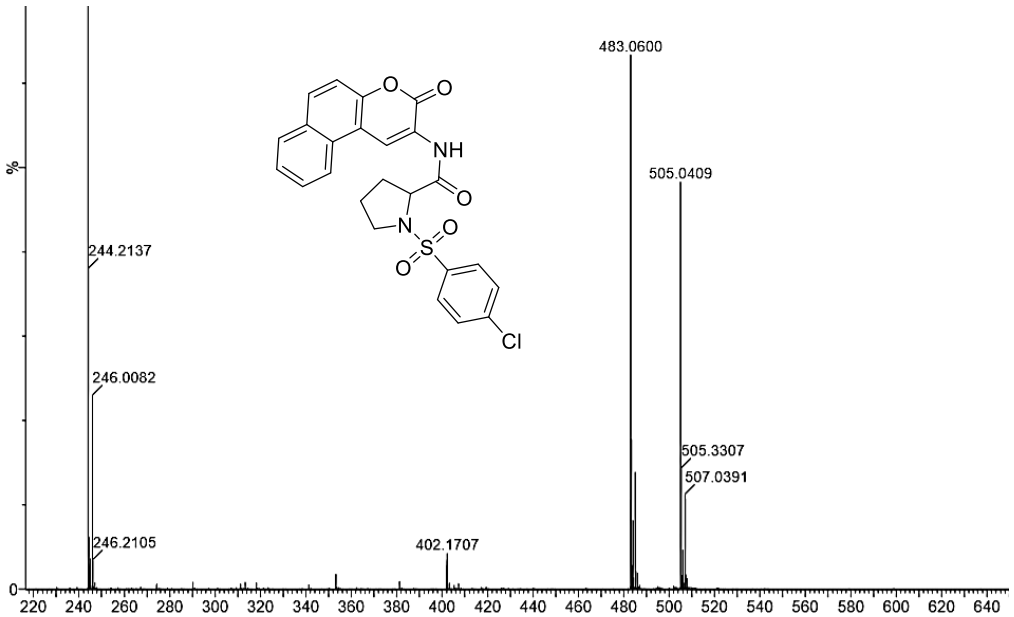

3a.2.2 Biological Evaluation

3a.2.2.1 Anticancer activity

Chromen-2-one-proline sulphonamide hybrids **16a-c**, **28a-c** and **29a-c** were synthesized from 7-amino-4-methyl chromen-2-one and 3-amino chromen-2-one. All compounds **16a-c**, **28a-c** and **29a-c** were screened initially for their anticancer activity using MTT assay against A549 (Lungs cancer cell line), MCF-7 (Breast cancer cell line) and compared with 5-fluorouracil as shown in **Table-3a.3**. Anticancer activity of chromen-2-one-proline sulphonamide hybrids were also compared with their precursor chromen-2-one -proline derivatives **15** and **26-27**.

Structure activity relationship (SAR) for anticancer activity

Compound **15** with proline linked to 7-amino-4-methyl chromen-2-one, showed good activity against both A549 and MCF7 cancer cell line with IC_{50} values 2.34 μM and 5.42 μM (**Table-3a.3**). Compound **16a** with benzene sulphonamide group, showed drop in activity against A549 cell line, while showed good activity in MCF7 cell line with IC_{50} value of 2.58 μM. Methyl substitution on benzene ring at para to sulphonamide group in compound **16b** resulted in loss of activity against A549 cell line, but showed excellent activity with IC_{50} 1.07 μM against MCF7 cell line (**Table-3a.3**). Compound **16c** with 4-chlorobenzene sulphonamide, showed moderate activity against both tested cell lines.

3-Aminochromen-2-one-proline hybrid compound **26** showed moderate activity against both the tested cell lines. While benzene sulphonamide derivative **28a** showed relatively good activity compared to compound **26** against both tested cell lines. Compound **28b** showed moderate activity against MCF7 cell line and lost the activity against A549 cell line (**Table-3a.3**). However, 4-chlorobenzene sulphonamide compound **28c** exhibited good activity with IC_{50} value of 7.39 μM and 3.81 μM against A549 and MCF7 cell lines respectively. Compound **27** with extension of aromatic ring on amino chromen-2-one part as compared to compound **26**, showed good activity against A549 cell line with IC_{50} value of 3.75 μM and moderate activity against MCF7 cancer cell line (**Table-3a.3**). Interestingly, conversion of compound **27** to substituted benzene sulphonamide derivatives **29a-c** resulted in loss of activity against both tested cancer cell lines.

Table-3a.3 Anticancer activity against A549 (Lungs cancer cell line), MCF-7 (Breast cancer cell line) for chromen-2-one-proline sulphonamide hybrid derivatives

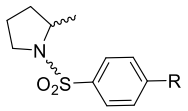

Compound	R	IC_{50} in μM [a]	
		A549	MCF-7
15		2.34	5.42
16a	H	18.09	2.58
16b	$-CH_3$	27.54	1.07
16c	-Cl	27.32	7.05
26		12.40	17.14
28a	H	9.34	4.39
28b	$-CH_3$	N.A	7.759
28c	-Cl	7.39	3.81
27		3.75	11.74
29a	H	19.95	22.94
29b	$-CH_3$	11.95	7.37
29c	-Cl	23.09	50.99
Fluorouracil		11.13	45.04

[a]IC_{50} values were determined based on MTT assay using GraphPad Prism software. NA = Not active

3a.2.2.2 DPP-IV inhibition activity

Recently, chromen-2-one containing compounds have been reported with very good DPP-IV inhibition activity [19-20]. Interestingly, position of attachment with chromen-2-one moiety and type of attachment showed drastic effect on DPP-IV inhibition activity of chromen-2-one containing compounds. Proline containing derivatives as substrate like inhibitors are known and reported with excellent DPP-IV inhibition activity. As these compounds **16a-c**, **28a-c** and **29a-c** are hybrid of chromene-proline and sulphonamide, they were also selected to screen for their initial DPP-IV inhibition activity at three different concentrations of 25, 50 and 100 μM and compared with Vildagliptin (**Table-3a.4**)

Compound with 7-amino-4-methyl chromen-2-one with proline sulphonamide **16a** showed poor activity with 19.36 % DPP-IV inhibition at 100 μM concentration, substituting methyl group on para position of benzene ring of sulphonamide resulted in compound **16b** with decrease in activity with 13.96% DPP-IV inhibition at 100 μM. Change of methyl group by chloro resulted in compound **16c** slightly increase in DPP4 inhibition of 20.76% in 100 μM concentration.

Table-3a.4 DPP-IV inhibition activity of amino chromen-2-one-proline sulphonamide derivatives **16a-c**, **28a-c** and **29a-c**.

Compounds	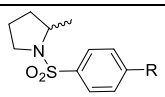	% DPP-4 enzyme inhibition activity[a]		
		25 μM	50 μM	100 μM
16a	H	11.11	16.29	19.36
16b	$-CH_3$	5.05	7.54	13.96
16c	-Cl	10.90	17.08	20.76
28a	H	9.87	13.60	20.17
28b	$-CH_3$	13.76	19.36	20.73
28c	-Cl	13.04	18.67	22.00
29a	H	7.06	10.44	14.32
29b	$-CH_3$	9.12	12.90	16.02
29c	-Cl	11.68	15.31	19.79
Vildagliptin		56.3 % at 0.1μM		

[a]DPP-IV inhibitory activity determined by fluorescence-based assay was measured using Spectra Max fluorometer (Molecular Devices, CA). Values of % inhibition are mean of three independent determinations at 25, 50 and 100 μM concentrations of the test samples.

Change of attachment of proline-sulphonamide moiety with chromen-2-one from 7th positions to 3rd position did not show much change in DPP-IV inhibition activity for compounds **28a-c**. 3-Amino chromen-2-one analogues of proline-sulphonamide derivatives compound **28a** showed poor activity with 20.17% inhibition at 100 μM concentration. Compound **28b** with para-methyl and **28c** with para-chloro on benzene sulphonamide showed moderate DPP4 inhibition at 100 μM.

Further, extension of aromatic ring on 3-amino chromen-2-one resulted in compound **29a-c** with 3-aminobenzo chromen-2-one proline-sulphonamide derivatives**.** Compounds **29a-c** were also showed similar trend of inhibitions with moderate activity at all three tested concentrations. All synthesized compounds were compared with standard drug vildagliptin with 56.3% inhibition at 0.1 μM concentration.

3a.3 Conclusion

In this work, novel amino chromen-2-one-proline sulfonamide hybrids were synthesized and their *In-Vitro* anticancer activity and DPP-IV inhibition activity were evaluated. For benzene sulphonamide derivatives we have selected three different benzene sulphonyl chlorides. One with electron withdrawing group, one without any substitution and one with electron releasing group. Among the tested compounds almost all compounds showed moderate activity in A549 cell line and excellent activity in MCF7 cancer cell line.

It is observed that when methyl substitution on phenyl ring of benzene sulphonamide was there, the IC_{50} values for MCF-7 cell line was excellent as observed in **16b**, **28b** and **29b**. Compounds were also screened for their DPP-IV inhibition activity, Compounds **16a-c, 28a-c** and **29a-c** were found to be inactive. The active compounds could be considered as useful templates for further development to obtain more potent anticancer agents.

3a.4 Experimental

3a.4.1 Chemistry

Reagent grade chemicals and solvents were purchased from commercial supplier and used after purification. TLC was performed on silica gel F254 plates (Merck). Merck silica gel (60-120 mesh) was used for column chromatographic purification. Melting points are uncorrected and were measured in open capillary tubes, using a Rolex melting point apparatus. IR spectra were recorded as KBr pellets on Perkin Elmer RX 1 spectrometer. ^{1}H-NMR and ^{13}C-NMR spectral data were recorded on Advance Bruker 400 spectrometer (400 MHz) with $CDCl_3$ or DMSO-d_6 as solvent and TMS as internal standard and *J* values are in Hz. Mass spectra were determined by ESI-MS, using a Shimadzu LCMS 2020 apparatus. 2,4-dihydroxy benzaldehyde was prepared from resorcinol using $POCl_3$ and DMF.

Synthesis of ethyl (3-hydroxyphenyl)carbamate (10)

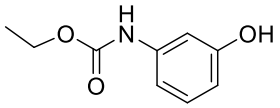

Ethyl chloroformate (1.0 mmol) was added in one portion to a stirred suspension of *m*-aminophenol **9** (1.0 mmol) in ethyl acetate (20 mL). A white precipitate formed immediately. The reaction mixture was stirred for 3 h at room temperature. The amine hydrochloride precipitated out was removed by filtration, washed with ethyl acetate (5 mL) and filtrate was concentrated under reduced pressure to give colourless crystals of ethyl (3-hydroxyphenyl) carbamate **10**. (M.P= 92-94 ^{o}C, Yield = 85%)

Synthesis of ethyl (4-methyl-2-oxo-2H-chromen-7-yl)carbamate (11)

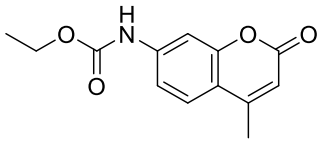

A solution of ethyl (3-hydroxyphenyl) carbamate **10** (1 mmol) and ethyl acetoacetate (1.2 eq) suspended in 20 mL of 70% ethanolic H_2SO_4 and stirred at room temperature for 4-6 h. The product formation was monitored by TLC. On completion of the reaction, the solution was poured into ice cold water (100 mL) to give a brown crystalline solid. The solid was filtered washed with water and recrystallized from ethanol to give compound **11**. (M.P= 188-190 ^{o}C, Yield = 55 %)

Synthesis of 7-amino 4-methyl chromen-2-one (12)

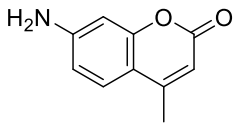

Ethyl (4-methyl-2-oxo-2H-chromen-7-yl) carbamate **11** was refluxed in a mixture of conc. H_2SO_4 and glacial acetic acid (1:1) for 4 h. The completion of reaction was checked by using TLC. After completion of reaction, the mixture was cooled to room temperature to give yellow precipitate. Resulting mixture was poured into ice cold water (100 mL) and neutralized with 50% NaOH solution to give white solid. The solid obtained was filtered, washed with water, dried and recrystallized from ethanol to give compound 7-amino 4-methyl chromen-2-one **12**. (M.P= 212-214 ^oC, Yield = 42%)

General procedure for synthesis of N-(2-oxo-2H-chromen-3-yl)acetamide (19-20)

To stirred solution of salicylaldehyde **17/**beta-hydroxy naphthaldehyde **18** (1.0 mmol) in acetic anhydride (5.0 mmol) N-acetylglycine (1.0 mmol) and sodium acetate (4.0 mmol) were added and mixture was refluxed at 100-110 ^oC for 4 h. After completion of reaction on TLC, reaction mass was poured into ice cold water to give solid. The solid was filtered, washed with ethyl acetate (10 mL), dried and recrystallized using ethanol to give compound **19/20** as light yellow solid. (M.P of compound **19**= 218-220 ^oC, compound **20**= 288-290 ^oC, Yield = 64%)

General procedure for synthesis of 3-amino chromen-2-one (21/22)

Compound **19/20** (10.0 mmol) was refluxed with ethanolic:HCl (7:3) (100 mL) for 3-4 h. The completion of reaction was checked by TLC. After completion of reaction, reaction mixture was poured into ice cold water to give solid and neutralized with saturated $NaHCO_3$ solution. The solid was filtered, washed with water, dried and recrystallized from ethanol to give compound **21/22** as light brown crystals. (M.P of compound **21**= 138-140 ^oC, compound **22**= 154-156 ^oC, Yields = 52%).

General procedure for preparation of tert-butyl 2-((4-methyl-2-oxo-2H-chromen-7-yl)carbamoyl)pyrrolidine-1-carboxylate

To an ice cold solution of ethyl chloroformate (2.55 mmol) in THF, the mixture of N-Boc proline **13** (1.5 mmol) and triethylamine (1.5 mmol) in THF (10 mL) was added dropwise followed by stirring for 10-15 minute. To this mixture, the solution of amino chromen-2-one **12/21/22**(1.5 mmol) and triethylamine (1.5 mmol) in THF (20 mL) was added dropwise over a period of 30 minutes at 0-5 ^oC. The resulting mixture was stirred for another 30 minutes at

0-5 ^{o}C, brought to room temperature and then refluxed for 8 h at 60 ^{o}C. The completion of reaction was monitored by TLC. After completion of reaction, solvents were removed under reduced pressure to give residue. The residue was dissolved in dichloromethane (DCM). The organic layer was washed with water, dil. HCl and sodium bicarbonate. The organic layer was dried over sodium sulphate, and concentrated to give compound. The product was used in next step without any further purification.

tert-Butyl 2-((4-methyl-2-oxo-2H-chromen-7-yl)carbamoyl)pyrrolidine-1-carboxylate (14)

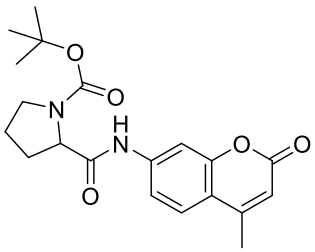

Pale yellow solid, Yield: 78 %; M.P: 165-168 ºC; IR (KBr) 3312 3055, 2976, 2891, 1718, 1689, 1622, 1577, 1531, 1448, 1406, 1390, 1369, 1269, 1215, 1174, 1126, 1068, 1016, 904, 881, 829, 773, 754, 711, 638, 576, 524 cm^{-1}; ^{1}H-NMR(400 MHz, $CDCl_3$): δ 1.53 (s, 9H), 1.92-1.98 (m, 1H), 2.08 (br s, 2H), 2.27 (br s, 1H) 2.34 (s, 3H), 3.43-3.45 (m, 1H), 3.56-3.61 (m, 1H), 4.56 (br s, 1H), 6.03 (s, 1H), 6.99 (d, *J*=7.6 Hz, 1H), 7.33 (d, *J*=8.4 Hz, 1H), 7.70 (s, 1H), 10.04 (s, 1H); ^{13}C-NMR(100 MHz, $CDCl_3$): δ ppm 18.41, 24.56, 28.48, 29.12, 47.35, 60.57, 80.95, 106.84, 112.83, 115.14, 115.31, 124.57, 141.74, 152.52, 153.76, 155.78, 161.17, 171.36; ESI-MS: 373.10 $[M+H]^{+}$.

tert-Butyl 2-((2-oxo-2H-chromen-3-yl)carbamoyl)pyrrolidine-1-carboxylate (24)

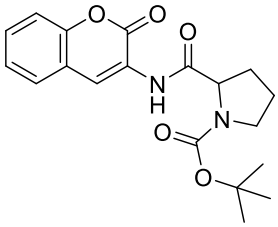

Pale yellow solid, Yield: 81 %; M.P: 138-140 ºC; IR (KBr) 3365, 3250, 3211, 3045, 2972, 2931, 2877, 2866, 1730, 1697, 1674, 1626, 1608, 1537, 1477, 1458, 1452, 1404, 1352, 1294, 1263, 1197, 1188, 1172, 1126, 1101, 1030, 981, 956, 923, 910, 881, 856, 763, 721 cm^{-1}; ^{1}H-NMR(400 MHz, $CDCl_3$): δ 1.50 (s, 9H), 1.95-2.06 (m, 2H), 2.23-2.36 (m, 2H), 3.40-3.54 (m, 2H), 4.33-4.49 (m, 1H), 7.42 (br s, 2H), 7.47 (m, 2H), 8.65 (s, 1H), 9.39 (s, 1H); ^{13}C-NMR (100 MHz, $CDCl_3$): δ ppm 24.60, 28.32, 47.15, 61.03, 61.81, 81.11, 116.32, 119.78, 123.35, 124.23, 125.04, 127.73, 129.51, 150.02, 158.42, 171; ESI-MS: 359.10 $[M+H]^{+}$.

tert-Butyl 2-((3-oxo-3H-benzo[f]chromen-2-yl)carbamoyl)pyrrolidine-1-carboxylate (25)

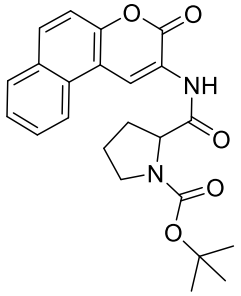

Pale yellow solid, Yield: 76 %; M.P: 192-196 ºC; ; IR (KBr) 3382, 3340, 3069, 2972, 2897, 1715, 1687, 1589, 1575, 1516, 1462, 1437, 1408, 1344, 1253, 1220, 1193, 1111, 1088, 996, 974, 951, 806, 779 cm^{-1}; ^{1}H-NMR(400 MHz, $CDCl_3$): δ 1.55 (s, 9H), 1.68 (s, 2H), 1.97-2.32 (m, 1H), 2.44 (s, 1H), 3.46-3.60 (m, 2H), 4.41-4.56 (m, 1H), 7.46 (d, *J*=8.8 Hz, 1H), 7.58-7.61 (m, 1H), 7.68-7.72 (m, 1H), 7.91 (d, *J*=8.4 Hz, 2H), 8.33 (d, *J*=8.0 Hz, 1H), 9.53 (s, 1H); ^{13}C-NMR(100 MHz, $CDCl_3$): δ ppm 24.69, 24.91, 28.38, 47.24, 61.08, 81.20, 114.14, 116.35, 116.43, 119.50, 119.61, 122.36, 124.06, 126.15, 126.25, 127.92, 128.81, 129.07, 130.66, 130.89, 148.93, 158.59, 169.59.

General procedure for Boc-deprotection

To a solution of compound **14/24/25** (1.0 mmol) into dichloromethane (DCM) (10 mL) was added trifloroacetic acid (TFA) (0.1 mL). The resulting solution was stirred at room temperature for overnight. The completion of reaction was monitored by TLC. After completion of reaction, reaction mixture was concentrated to give residue. The residue was taken in water, neutralized with saturated $NaHCO_3$ solution, and extracted with DCM (3 x 15 mL). The organic layer was dried over anhydrous Na_2SO_4, filtered and concentrated to give compound **15/26/27** as solid. The product was used in next step without any further purification. (Yield= 96-98%)

N-(4-Methyl-2-oxo-2H-chromen-7-yl)pyrrolidine-2-carboxamide (15)

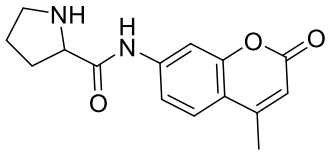

Light pink solid, Yield: 98 %; M.P: 152-154 ºC; IR (KBr) 3304, 3272, 3173, 3082, 2961, 2930, 2864, 1689, 1616, 1595, 1524, 1443, 1392, 1347, 1326, 1272, 1222, 1177, 1112, 1020, 963, 873, 845, 719 cm^{-1}; ^{1}H-NMR(400 MHz, $CDCl_3$): δ 1.77-1.85 (m, 2H), 2.04-2.12 (m, 2H), 2.21-2.28 (m, 1H), 2.41 (d, *J*=1.2 Hz, 3H), 2.99-3.05 (m, 1H), 3.10-3.14 (m, 1H), 3.91 (dd, *J*=9.2, 5.2 Hz, 1H), 6.19 (s, 1H), 7.53 (d, *J*=8.4 Hz, 1H), 7.59 (dd, *J*=8.4, 2.0 Hz, 1H),

7.64 (d, *J*=1.6 Hz, 1H), 10.05 (s,1H); ^{13}C-NMR (100 MHz, $CDCl_3$): δ ppm 18.67, 26.41, 30.76, 47.42, 61.02, 106.66, 113.26, 115.27, 115.94, 125.22, 141.09, 152.31, 154.32, 161.24, 174.08.

N-(2-Oxo-2H-chromen-3-yl)pyrrolidine-2-carboxamide (26)

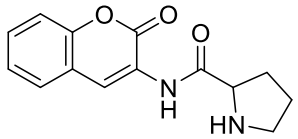

Pale yellow solid, Yield: 96 %; M.P: 145-158 ºC; IR (KBr) 3187, 3073, 2947, 2876, 1724, 1679, 1619, 1546, 1501, 1453, 1415, 1361, 1317, 1293, 1200, 1131, 1039, 1005, 947, 884, 863, 832, 799, 751 cm^{-1}; ^{1}H-NMR(400 MHz, $CDCl_3$): δ 1.79-1.86 (m, 2H), 2.01-2.09 (m, 1H), 2.25-2.33 (m, 1H), 3.13-3.16 (m, 2H), 4.06 (br s, 1H), 7.25-7.33 (m, 2H), 7.41-7.46 (m, 2H), 8.68 (s, 1H), 10.41 (s, 1H); ^{13}C-NMR (100 MHz, CDCl3): δ ppm 26.16, 30.87, 47.33, 61.00, 116.32, 119.84, 123.19, 123.91, 125.02, 127.71, 129.54, 150.14, 158.59, 174.97.

N-(3-Oxo-3H-benzo[f]chromen-2-yl)pyrrolidine-2-carboxamide (27)

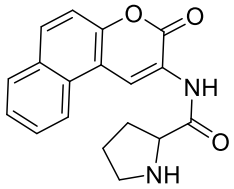

Pale white solid, Yield: 92 %; M.P: 250-255 ºC; IR (KBr) 3390, 3111, 2881, 2710, 2649, 2559, 2505, 2442, 1722, 1689, 1587, 1548, 1513, 1461, 1438, 1420, 1402, 1387, 1338, 1315, 1248, 1227, 1197, 1128, 1101, 900, 813, 782, 754 cm^{-1}; ^{1}H-NMR(400 MHz, $CDCl_3$): δ 1.94-2.05 (m, 3H), 2.49-2.50 (m, 1H), 3.34 (m, 2H), 4.64-4.68 (m, 1H), 7.59-7.67 (m, 2H), 7.76 (t, *J*=7.2 Hz, 1H), 8.08 (d, *J*=8 Hz 1H), 8.13 (d, *J*=8.8 Hz 1H), 8.23 (d, *J*=8.8 Hz 1H), 9.36 (s, 1H), 10.69 (s, 1H); ^{13}C-NMR (100 MHz, $CDCl_3$): δ ppm 24.04, 30.44, 46.27, 59.88, 113.45, 116.82, 122.03, 122.52, 124.34, 126.66, 128.76, 128.83, 129.49, 130.68, 131.88, 149.66, 157.57, 169.49; ESI-MS: 309 $[M+H]^+$.

General procedure for synthesis of benzenesulphonamide derivatives 16a-c, 28a-c and 29a-c

To a solution of compound **15** (1.0 mmol) and sodium bicarbonate (3.0 mmol) in dichloro methane (DCM): Water (1:1) (25 mL) un/substituted benzenesulphonyl chloride (1.1 mmol) was added. The resulting mixture was stirred at room temperature for 18 h. The completion of reaction was monitored by TLC. After completion of the reaction, the reaction mixture was concentrated to give residue. The residue was neutralized with dil HCl, filtered, washed with

water (3 x 5 mL), pet. ether (5 mL) and dried to give compounds **16a-c**. 3-Amino chromen-2-one derivatives **28a-c** and **29a-c** were synthesised using same procedure as used for compound **16a-c**.

N-(4-Methyl-2-oxo-2H-chromen-7-yl)-1-(phenylsulfonyl)pyrrolidine-2-carboxamide (16a)

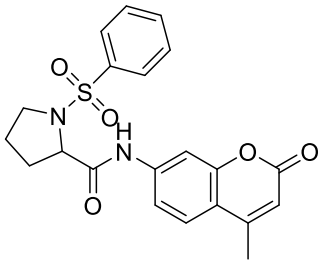

Pale white solid, Yield: 89 %; M.P: 225-228 ºC; IR (KBr) 3313, 3194, 3068, 2953, 2872, 1718, 1695, 1616, 1579, 1570, 1523, 1444, 1417, 1390, 1348, 1309, 1217, 1166, 1093, 1070, 1008, 995, 893, 854, 752, 723 cm^{-1}; ^{1}H-NMR (400 MHz, $CDCl_3$): δ 1.29-1.81 (m, 3H), 2.45 (s, 4H), 3.29-3.33 (m, 1H), 3.70 (s, 1H), 4.24-4.27 (m, 1H), 6.24 (s, 1H), 7.31-7.47 (m, 1H), 7.56-7.74 (m, 4H), 7.85-7.95 (m, 3H), 9.11 (s, 1H); ^{13}C-NMR (100 MHz, $CDCl_3$): δ ppm 19.15, 25.10, 30.09, 50.80, 63.60, 77.00, 78.27, 108.10, 114.21, 116.35, 116.99, 125.69, 128.47, 130.16, 134.39, 135.96, 141.32, 152.70, 154.87,161.60, 169.96; ; Anal. Calc. for $C_{21}H_{20}N_2O_5S$; C, 61.15; H, 4.89; N, 6.79; S, 7.77; ESI-MS: 413.05 $[M+H]^+$.

N-(4-Methyl-2-oxo-2H-chromen-7-yl)-1-tosylpyrrolidine-2-carboxamide (16b)

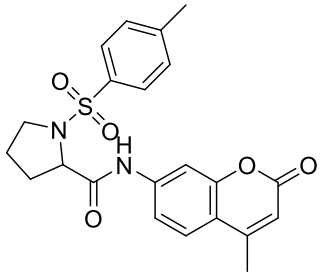

Pale white solid, Yield: 86 %; M.P: 216-220 ºC; IR (KBr) 3562, 3369, 3290, 3140, 3059, 2987, 2953, 2891, 1724, 1697, 1689, 1618, 1597, 1568, 1523, 1506, 1440, 1411, 1396, 1346, 1332, 1313, 1294, 1157, 1182, 1093, 1003, 966, 941, 871, 827, 756, 725 cm^{-1}; ^{1}H-NMR(400 MHz, $CDCl_3$): δ 1.60-1.70 (m, 2H), 1.82-1.84 (m, 1H), 2.35-2.43 (m, 1H), 2.44 (s, 3H), 2.48 (s, 3H), 3.25-3.30 (m, 1H), 3.64-3.69 (m, 1H), 4.20 (dd, *J*=8.8, 2.8 Hz, 1H), 6.24 (s,1H), 7.40-7.44 (m, 3H), 7.56 (d, *J*=8.4 Hz, 1H), 7.78 (d, *J*=8.0 Hz, 2H), 7.84 (d, *J*=2.0 Hz, 1H), 9.11 (s, 1H); ^{13}C-NMR (100 MHz, $CDCl_3$): δ ppm 18.65, 21.67, 24.52, 29.42, 50.27, 62.99, 107.52, 113.66, 115.75, 116.41, 125.11, 127.95, 130.22, 132.14, 140.71, 144.95, 152.12, 154.30, 161.09, 169.45; Anal. Calc. for $C_{22}H_{22}N_2O_5S$; C, 61.96; H, 5.20; N, 6.57; S, 7.52; found: C, 59.90; H, 4.98; N, 6.34; S, 6.48 % ESI-MS: 427.10 $[M+H]^+$.

1-((4-Chlorophenyl)sulfonyl)-N-(4-methyl-2-oxo-2H-chromen-7-yl)pyrrolidine-2-carboxamide (16c)

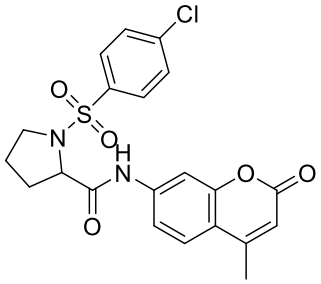

Pale white solid, Yield: 87 %; M.P: -230-234 ºC; IR (KBr) 3338, 3196, 3111, 3059, 2991, 2868, 1716, 1695, 1622, 1579, 1533, 1475, 1460, 1437, 1415, 1388, 1338, 1267, 1226, 1180, 1157, 1087, 1064, 1026, 1008, 974, 922, 850, 860, 761 cm^{-1}; ^{1}H-NMR(400 MHz, $CDCl_3$): δ 1.61-1.76 (m, 2H), 1.87 (br s, 1H) 2.43 (s, 4H), 3.21-3.27 (m, 1H), 3.67-3.71 (m, 1H), 4.19 (d, *J*=6.8 Hz, 1H), 6.23 (s, 1H), 7.44 (d, *J*=7.6 Hz, 1H), 7.55-7.60 (m, 3H), 7.84-7.86 (m, 3H), 9.01 (s, 1H); ^{13}C-NMR (100 MHz, $CDCl_3$): δ ppm 18.65, 24.53, 29.59, 50.29, 63.03, 107.55, 113.72, 115.75, 116.49, 125.16, 129.30, 129.94, 133.73, 140.61, 152.12, 154.28, 161.04, 169.09; Anal. Calc. for $C_{21}H_{19}ClN_2O_5S$; C, 56.44; H, 4.29; N, 6.27; S, 7.17, found: C, 57.00; H, 4.32; N, 6.18; S, 8.30; ESI-MS: 447.00 $[M+H]^+$.

N-(2-Oxo-2H-chromen-3-yl)-1-(phenylsulfonyl)pyrrolidine-2-carboxamide (28a)

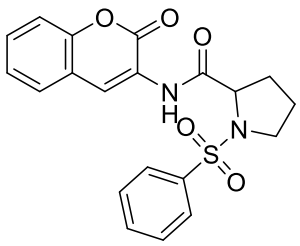

Pale white solid, Yield: 92 %; M.P: 186-188 ºC; IR (KBr) 3350, 3084, 3064, 3037, 2985, 2937, 2872, 1724, 1693, 1626, 1602, 1572, 1518, 1460, 1444, 1363, 1350, 1309, 1294, 1257, 1222, 1180, 1165, 1132, 1111, 1091, 1074, 1049, 1004, 995, 968, 947, 923, 904, 860, 850, 773, 759, 721 cm^{-1}; ^{1}H-NMR(400 MHz, $CDCl_3$): δ 1.73 (m, 1H), 1.86-1.88 (m, 2H), 2.3-2.4 (m,1H), 3.29-3.36 (m, 1H) 3.60-3.65 (m, 1H), 4.34 (dd, *J*=8.4, 3.0 Hz, 1H), 7.29-7.31 (dt, *J*=7.6, 1.2 Hz, 1H), 7.35 (br, d, *J*=8.00 Hz, 1H), 7.45-7.49 (m, 1H), 7.51 (dd, *J*=8, 1.4 Hz, 1H), 7.59-7.63 (m, 2H), 7.67-7.70 (m, 1H), 7.95-7.97 (m, 2H), 8.69 (s, 1H), 9.38 (s, 1H); ^{13}C-NMR (100 MHz, $CDCl_3$): δ ppm 24.66, 30.47, 49.91, 62.77, 116.44, 119.64, 123.70, 123.74, 125.11, 127.84, 128.10, 129.48, 129.87, 133.68, 135.94, 150.23, 158.37, 170.87; Anal. Calc. for $C_{20}H_{18}N_2O_5S$; C, 60.29; H, 4.55; N, 7.03; S, 8.05; found: C, 60.33; H, 4.48; N, 6.98; S, 8.08; ESI-MS: 399.05 $[M+H]^+$.

N-(2-Oxo-2H-chromen-3-yl)-1-tosylpyrrolidine-2-carboxamide (28b)

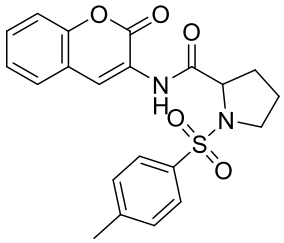

Pale white solid, Yield: 90 %; M.P: 170-172 ºC; IR (KBr) 3367, 3088, 3066, 2955, 2879, 1728, 1718, 1697, 1629, 1597, 1514, 1485, 1458, 1354, 1294, 1163, 1111, 1091, 1058, 1004, 950, 923, 904, 850, 754, 665 cm^{-1}; ^{1}H-NMR(400 MHz, $CDCl_3$): δ 1.66 (br s, 1H), 1.75-1.85 (m, 2H), 2.24 (br s, 1H), 2.46 (s, 3H) 3.29-3.31 (m, 1H), 3.60 (br s, 1H),4.31 (br d, 1H), 7.28-7.40 (m, 4H), 7.45-7.52 (m, 2H), 7.83 (d, *J*=7.6 Hz, 2H), 8.69 (s, 1H), 9.40 (s, 1H); ^{13}C-NMR (100 MHz, $CDCl_3$): δ ppm 21.64, 24.67, 30.45, 49.90, 62.74, 116.44, 119.66, 123.69, 123.74, 125.09, 127.83, 128.17, 129.84, 130.08, 132.93, 144.68, 150.23, 158.37, 171.01; Anal. Calc. for $C_{21}H_{20}N_2O_5S$; C, 61.15; H, 4.89; N, 6.79; S, 7.77, found: C, 61.71; H, 4.91; N, 6.79; S, 7.77; ESI-MS: 413.05 $[M+H]^+$.

1-((4-Chlorophenyl)sulfonyl)-N-(2-oxo-2H-chromen-3-yl)pyrrolidine-2-carboxamide (28c)

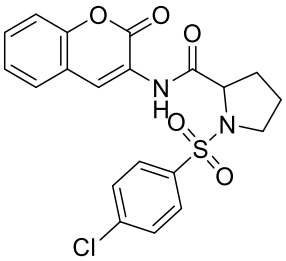

Pale white solid, Yield: 95 %; M.P: 202-206 ºC; IR (KBr) 3311, 3248, 3093, 3084, 2955, 2875, 1722, 1693, 1626, 1604, 1537, 1487, 1460, 1448, 1356, 1329, 1296, 1276, 1222, 1205, 1157, 1101, 1085, 1070, 1022, 1006, 949, 904, 881, 856, 767, 756 cm^{-1}; ^{1}H-NMR(400 MHz, $CDCl_3$): δ 1.71 (s, 1H), 1.81-1.91 (m, 2H), 2.27 (br s, 1H), 3.26-3.32 (m, 1H) 3.61 (br s, 1H), 4.32-4.33 (br d, 1H), 7.29-7.36 (m, 2H), 7.45-7.57 (m, 2H) 7.58 (d, *J*=8.4 Hz, 2H), 7.90 (d, *J*=8.4Hz, 2H), 8.68 (s, 1H), 9.30 (s, 1H); ^{13}C-NMR (100 MHz, $CDCl_3$): δ ppm 24.69, 30.54, 49.89, 62.75, 116.45, 119.60, 123.62, 123.83, 125.16, 127.87, 129.51, 129.81, 129.94, 134.57, 140.38, 150.21, 158.41, 170.60; Anal. Calc. for $C_{20}H_{17}ClN_2O_5S$; C, 55.49; H, 3.96; N, 6.47; S, 7.41; found: C, 55.58; H, 3.89; N, 6.39; S, 7.30; ESI-MS: 433.00 $[M+H]^+$.

N-(3-Oxo-3H-benzo[f]chromen-2-yl)-1-(phenylsulfonyl)pyrrolidine-2-carboxamide (29a)

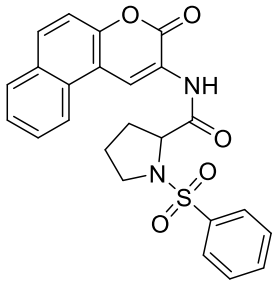

Pale white solid, Yield: 90 %; M.P: 206-208 ºC; IR (KBr) 3068, 2956, 2889, 1713, 1691, 1536, 1516, 1503, 1463, 1445, 1328, 1237, 1222, 1203, 1192, 1164, 1185, 1090, 994, 814 cm^{-1}; ^{1}H-NMR(400 MHz, $CDCl_3$): δ 1.80-1.84 (m, 1H), 1.86-1.95 (m, 2H), 2.29-2.33 (m, 1H), 3.32-3.39 (br m, 1H), 3.64-3.69 (m, 1H), 4.39 (dd, *J*=8.4, 3.2 Hz, 1H), 7.48 (d , *J*=8.8 Hz, 1H), 7.57-7.64 (m, 3H), 7.67-7.71 (m, 2H), 7.92 (d, *J*=8.8 Hz, 2H), 7.98-8.00 (m, 2H), 8.31 (d, *J*=8.4 Hz, 1H), 9.46 (s, 1H), 9.52 (s, 1H); ^{13}C-NMR (100 MHz, $CDCl_3$): δ ppm 24.72, 30.47, 49.94, 62.83, 113.97, 116.48, 119.92, 122.30, 123.66, 126.20, 127.89, 128.13, 128.86, 129.07, 129.51, 130.66, 131.09, 133.70, 135.96, 149.18, 158.30, 170.98; Anal. Calc. for $C_{24}H_{20}N_2O_5S$; C, 64.27; H, 4.50; N, 6.25; S, 7.15; found: C, 64.34; H, 4.47; N, 6.18; S, 7.30; ESI-MS: 449.01 $[M+H]^+$.

N-(3-Oxo-3H-benzo[f]chromen-2-yl)-1-tosylpyrrolidine-2-carboxamide (29b)

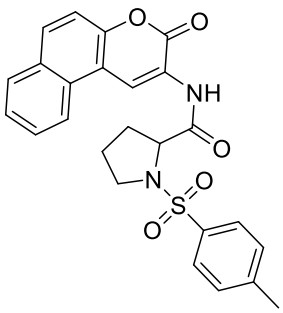

Pale white solid, Yield: 87 %; M.P: 202-206 ºC; IR (KBr) 2918, 2887, 1706, 1702, 1696, 1516, 1504, 1464, 1347, 1319, 1237, 1137, 1192, 1158, 1089, 898, 814 cm^{-1}; ^{1}H-NMR(400 MHz, $CDCl_3$): δ 1.76-1.84 (m, 1H), 1.86-1.94 (m, 2H), 2.29-2.31 (m, 1H), 2.47 (s, 3H), 3.30-3.37 (br m, 1H), 3.62-3.66 (m, 1H), 4.37 (dd, *J*=8.4, 3.2 Hz, 1H), 7.41 (d , *J*=8.0 Hz, 2H), 7.49 (d, *J*=8.8 Hz, 1H), 7.58-7.62 (m, 1H), 7.68-7.72 (m, 1H), 7.87 (d, *J*=8.0 Hz, 2H), 7.92 (d, *J*=2.0 Hz, 1H), 7.94 (d, *J*=2.8 Hz, 1H), 8.33-8.36 (m, 1H), 9.50 (s, 1H), 9.55 (s, 1H); ^{13}C-NMR (100 MHz, $CDCl_3$): δ ppm 21.67, 24.72, 30.44, 49.93, 62.79, 114.01, 116.37, 116.51, 119.92, 122.33, 122.42, 123.72, 126.19, 127.89, 128.20, 128.86, 129.10, 130.11, 130.67, 130.92, 131.07, 132.94, 144.70, 149.20, 158.32, 171.13; Anal. Calc. for $C_{25}H_{22}N_2O_5S$; C,

64.92; H, 4.79; N, 6.06; S, 6.93; found: C, 64.99; H, 4.72; N, 6.12; S, 7.09; ESI-MS: 463.13 $[M+H]^+$.

1-((4-Chlorophenyl)sulfonyl)-N-(3-oxo-3H-benzo[f]chromen-2-yl)pyrrolidine-2-carboxamide (29c)

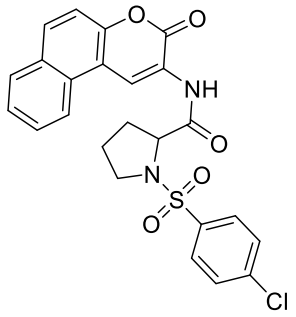

Pale white solid, Yield: 91 %; M.P: 230-234 ºC; IR (KBr) 2870, 2848, 1715, 1706, 1694, 1533, 1516, 1464, 1343, 1238, 1224, 1203, 1187, 1166, 1102, 1089, 1010, 812 cm^{-1}; ^{1}H-NMR(400 MHz, $CDCl_3$): δ 1.81-1.90 (m, 1H), 1.92-2.01 (m, 2H), 2.31-2.35 (m, 1H), 3.30-3.36 (m, 1H), 3.63-3.67 (m, 1H), 4.38 (dd, *J*=8.0, 2.8 Hz, 1H), 7.50 (d , *J*=8.8 Hz, 1H), 7.58-7.62 (m, 3H), 7.70 (t, *J*=7.2 Hz, 1H), 7.92-7.95 (m, 4H), 8.33 (d, *J*=8.4 Hz, 1H), 9.39 (s, 1H), 9.54 (s, 1H); ^{13}C-NMR (100 MHz, $CDCl_3$): δ ppm 24.74, 30.54, 49.93, 62.80, 113.96, 116.48, 120.05, 122.30, 123.59, 126.24, 127.94, 128.88, 129.08, 129.54, 129.84, 130.68, 131.18, 134.58, 140.41, 149.21, 158.36, 170.72; Anal. Calc. for $C_{24}H_{19}ClN_2O_5S$; C, 59.69; H, 3.97; N, 5.80; S, 6.64, found: C, 59.31; H, 3.95; N, 5.75; S, 5.44 %; ESI-MS: 483.06 $[M+H]^+$.

3a.4.2 Materials and Methods for Biological assay

3a.4.2.1: MTT Assay

The compounds were tested for their cytotoxic potential on two types of cancer cells, *viz*., A549 (lung cancer cell-line) and MCF7 (breast cancer cell-line). The MTT assay was used to determine the effect of each compound on the proliferation of cancer cells. Fluorouracil (Neon Laboratory) was used as standard. A549 and MCF7 cultures were purchased from National Centre for Cell Science, Pune, India. All growth media, supplements and reagents were purchased from HiMedia Labs, Mumbai, India. For the assay, cells were seeded at 10^5 cells/ml in a 96-well plate in dulbecco's modified minimum essential medium (DMEM) supplemented with 10% fetal bovine serum (FBS). To each well, test compound was added at six different concentrations of 100μM, 50μM, 10μM, 5μM, 1μM and 0.5μM. Each concentration was tested in triplicates. The cells were incubated with these compounds at 37^{o}C under 5% CO_2 for 48 hours. Following this, 3-[4,5-dimethylthiazol-2-yl]-2,5-diphenyltetrazolium bromide (MTT) was added to each well at a final concentration of

0.5mg/ml. Cells were incubated with this tetrazolium dye for 4 hours. Subsequently, purple crystals of formazan were observed in each well, formed as a metabolic product of MTT. These crystals were dissolved in Isopropanol and the absorbance in each well was recorded at 570nm in a microplate reader (Metertech Sigma360). Absorbance at 570nm directly correlates with cell viability. IC_{50} (μM) values were determined using Graph Pad prism software.

3a.4.2.2: DPP-4 Inhibition assay

In a 96 well clear bottom microtiter plate 25μL of assay buffer (50 mM TrisHCl, 1 mM EDTA, 100 mM NaCl, pH 7.5) was added followed by addition of 15 μL of 20 μU/μL of human recombinant DPP-IV (Prospec; enz-375-b) and 10μL of test compounds diluted at range of concentrations. Finally 50μL of 50μM of GP-AMC substrate (H-Gly-Pro-AMC, Enzo life science; lot no: 01221304) was added to initiate the reaction. Wells without inhibitor but with DPP-IV, assay buffer and substrate were assigned as assay control. The plate was then incubated at 37^{o}C for 30 min in dark. Post incubation fluorescence was measured using a Spectra Max fluorometer (Molecular Devices, Sunnyvale CA) by exciting at 360 nm and emission at 460 nm. The IC_{50} values were determined for test compounds of three independent determinations and calculated using Graph Pad prism software.

Calculation for DPP-IV Inhibitor

DPP-IV inhibition assay was employed for *In-Vitro* biological activity evaluation of synthesized compounds. The percentage DPP-IV inhibition is calculated by the formula (Fluorescence of 100% activity – Fluorescence of test / Fluorescence of 100% activity)*100.

3a.5 References

[1] C. T. Supuran, A. Casini, A. Mastrolorenzo, A. Scozzafava, *Mini-Rev. Med. Chem.*, **2004**, *4*, 625.

[2] F. Abbate, A. Casini, T. Owa, A. Scozzafava, C. T. Supuran, *Bioorg. Med. Chem. Lett.*, **2004**, *14*, 217.

[3] S. S. Abd El-Karim, M. M. Anwar, Y. M. Syam, M. A. Nael, H.F. Ali, M. A. Motaleb, *Bioorg. Chem,*. **2018**, *81*, 481.

[4] G. Bouchain, S. Leit, S. Frechette, A. E. Khalil, R. Lavoie, O. Moradei, S. H. Woo, M. Fournel, P. T. Yan, A. Kalita, M. C. Trachy-Bourget, C. Beaulieu, Z. Li, M. F. Robert, A. R. MacLeod, J. M. Besterman, D. J. Delorme, *Med. Chem.*, **2003**, *46*, 820.

[5] M. Mirian, A. Zarghi, S. Sadeghi, P. Tabaraki, M. Tavallaee, O. Dadrass, H. Sadeghi-aliabadi, *Iran. J. Pharm. Res.,* **2011**, *10,* 741.

[6] J. F.Smyth, S. Aamdal, A. Awada, C. Dittrich, F. Caponigro, P. Schöffski, M. Gore, T. Lesimple, N. Djurasinovic, B. Baron, M. Ravic, P. Fumoleau, C. J. A Punt, *Ann. Oncol.,* **2005**, *16*, 158.

[7] D .C Talbot, V. J. Pawel, E. Cattell, S. M. Yule, C. Johnston, A. S. Zandvliet, A. D. Huitema, C. J. Norbuty, P. Ellis, L. Bosquee, M. Reck, *Clin. Cancer Res.*, **2007**, *13*, 1816.

[8] G. Zhao, P. C. Taunk, D. R. Magnin, L. M. Simpkins, J. A. Robl, A. Wang, J. G Robertson, J. Marcinkeviciene, D. F. Sitkoff, R.A. Parker, M. S. Kirby, *Bioorg. Med. Chem. Lett.,* **2005**, *15*, 3992.

[9] S. Hiroshi, K. Hiroshi, N. Mitsuharu, A. Fumihiko, H. Yoshiharu, *Bioorg. Med. Chem. Lett.,* **2005**, *15*, 2441.

[10] S. Sharma, S. S. Soman, *Synth. Commun.,* **2016**, *46***,** 1307.

[11] C. Shu, H. Ge, M. Song, J Chen, M Zhou, Q Qi, F Wang, X. Ma, X. Yang, G. Zhang, Y. Ding, D. Zhou, P. Peng, C. Shih, J. Xu, F. Wu, *A C S Med. Chem. Lett.*, **2014**, *5*, 921.

[12] I. L. Lu, K. C. Tsai, Y. K. Chiang, W. T. Jiaang, S. H. Wu, N. Mahindroo, C. H. Chien, S. J. Lee, X. Chen, S. Y. Chao, S. Y. Wu*, Eur. J. Med. Chem.,* **2009**, *44*, 2763.

[13] A. Leone, E. Di Gennaro, F. Bruzzese, A. Avallone, A. Budillon, **2014**, New Perspective for an Old Antidiabetic Drug: Metformin as Anticancer Agent. In: V. Zappia, S. Panico, G. Russo, A. Budillon, F. Della Ragione (eds) Advances in Nutrition and Cancer. Cancer Treatment and Research, vol *159* (355-376). Springer, Berlin, Heidelberg

[14] J. M. Evans, L. A. Donnelly, A. M. Emslie-Smith, D. R. Alessi, A. D. Morris, *The BMJ*, **2005**, *330*, 1304.

[15] R. Soni, S.S. Soman, *Bioorg. Chem.*, **2018**, *79*, 277.

[16] R. Sharma, S. S. Soman, *Eur. J. Med. Chem.,* **2015**, *90,* 342.

[17] S. D. Durgapal, R. Soni, S. Umar, B. Suresh, S. S. Soman, *ChemistrySelect*, **2017**, *2*, 147.

[18] S. Karandikar, R. Soni, S. S. Soman, S. Umar, B Suresh, *Synth. Commun.,* **2018**, *48*, 2877.

[19] M. Kawaguchi, T. Okabe, T. Terai, K. Hanaoka, H. Kojima, I. Minegishi, T. Nagano, *Chem. Eur. J.,* **2010**, *16,* 13479.

[20] N. Dietrich, M. Kolibabka, S. Busch, P. Bugert , U. Kaiser , J. Lin, T. Fleming, M. Morcos, T. Klein, A. Schlotterer, H. P. Hammes. The DPP4 Inhibitor Linagliptin Protects from Experimental Diabetic Retinopathy. *PLoS ONE*, **2016**, *11*, e0167853.

Chapter-3b
Synthesis and Cytotoxic studies of Chalcone derivatives of Chromen-2-ones and 3-Aminomethyl pyridine

3b.1 Introduction

Among the current identified anticancer agents, Chalcones have attracted attention because of their promising therapeutic effects, since they are able to target multiple cellular molecules, such as MDM2/p53, tubulin, proteasome, TNF-related apoptosis-inducing ligand (TRIAL)/death receptors and mitochondria-mediated apoptotic pathways, cell cycle and many other [1]. The double bond of the enone system is essential for anticancer activity of chalcone prototypes [2].

α,β-Unsaturated ketones, commonly known as chalcones are important class of natural as well as synthetic products which show variety of biological activities. During last few decades, chalcone derivatives have been reported having potent anticancer activity with low side effects and better solubility for therapeutic applications [3-4]. Simple structural modification in chalcone moiety with heterocycles, polyarene compounds or organometal complexes may lead to new anticancer agents with promising activity [5-6]. Chalcone based small molecules provide advantage over others due to low toxicity and mutagenicity profile. Yu *et al* showed that 4-(dimethylamino)-4-amino chalcone can interact into base pair and created a new method to determine trace amount of DNA [7].

Interestingly, pyridine derivatives have shown very good effect on anticancer activity when substituted at 3rd position as shown in **Fig-3b.1**, Entinostat **1** (MS-275) is in phase II clinical trials for treatment of various types of cancers [8]. Inci Gul *et al* have reported compound **2** as tumor selective cytotoxin containing both chalcone and pyridine moieties in a molecule [9]. Recently, Wang *et al* have reported pyridine containing compound **3** with very good antitumor activity against xenograft A2780 ovarian cancer [10].

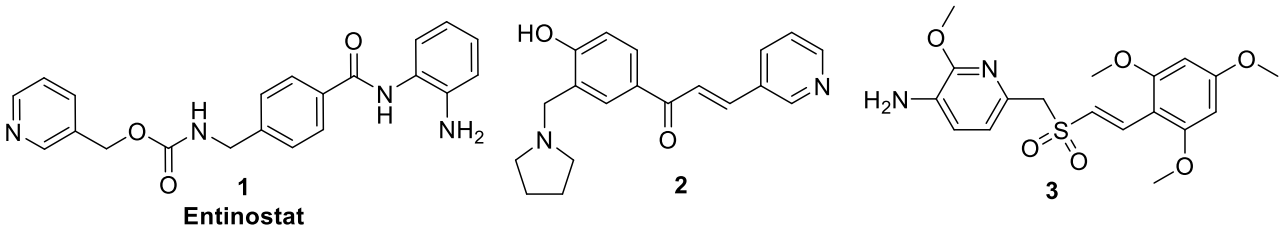

Figure-3b.1 Compounds with anticancer activity.

As a part of our ongoing research on anticancer agents containing chromene derivatives, [11-12] synthesis of compounds **6a-b, 9a-j** and **10c,i** is carried out in this chapter and all the newly synthesized compounds are screened for anticancer activity by MTT assay. Compounds **6a,b** were designed based on 3-aminomethyl pyridine attached to chromen-2-one

moiety. Compounds **9a-j** were designed as chalcone derivatives of 3-aminomethyl pyridine, compounds **10c,i** were designed as 2-aminomethyl pyridine with 4-amino chalcones.

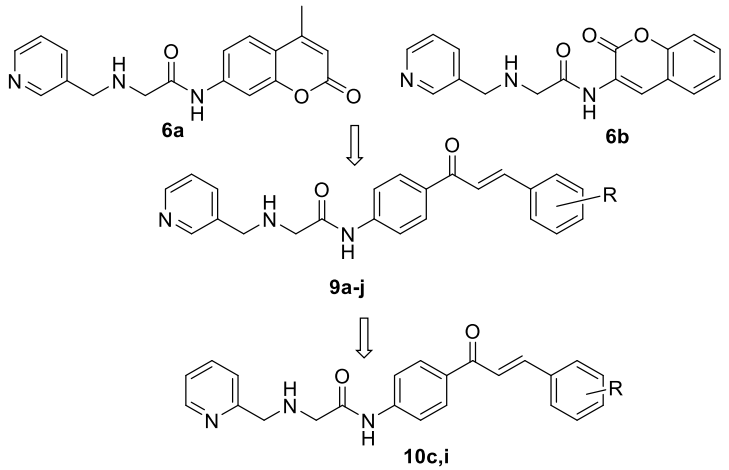

Figure-3b.2 Designing of hybrid chlacones **9a-j** derived from 3-aminomethyl pyridine and 4-amino chalcones.

3b.2 Results and Discussion

3b.2.1 Chemistry

7-amino-4-methyl chromen-2-one and 3-amino chromen-2-one were reacted with bromoacetyl bromide to give compounds **4-5** (**Scheme-1**). Compounds **6a-b** were obtained by reacting chromene derivatives **4** and **5** with 3-aminomethyl pyridine (**Scheme-1**). Compounds **6a-b** were obtained as a solid, 3-aminomethyl pyridine was attached to chromen-2-one moiety at 7th position and 3rd position as shown in **scheme-1** for compounds **6a-b**.

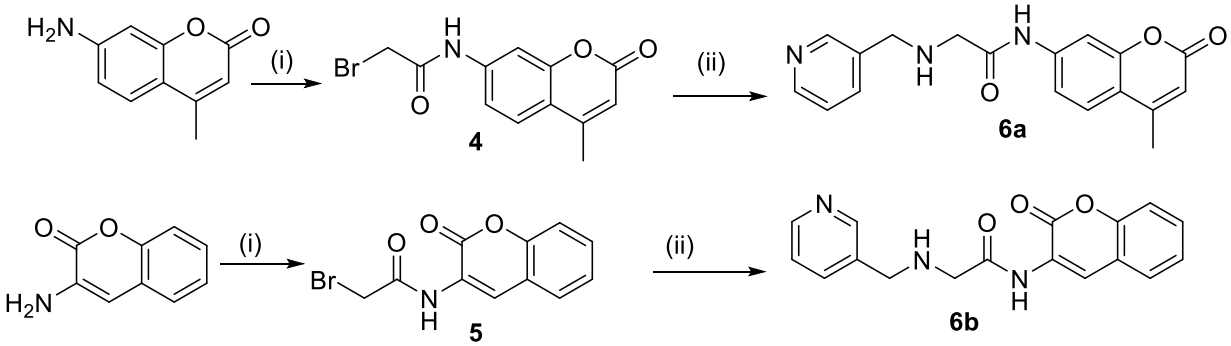

Reagents and Conditions: (i) Bromoacetyl bromide, TEA, DCM, 3-4 h, r.t
(ii) 3-aminomethly pyridine, TEA, DMF, 0-5 ^{o}C, 30 min, r.t 14-16 h.

Scheme-1 Synthesis of compound **6a-b** from 7-amino chromen-2-one and 3-amino chromen-2-one derivative.

The structures of compounds **6a-b** were confirmed by different analytical techniques such as ^{1}H-NMR, ^{13}C-NMR, IR, ESI-MS. In general, the IR spectra of compounds **6a-b** exhibited one

strong band in the range of 3294 cm^{-1} for N-H stretching vibrations and another strong band at 3000 cm^{-1} for C-H Stretching vibrations. (**Fig-3b.3.1)** Carbonyl stretching vibrations of lactone and amide were observed in the range of 1720-1685 cm^{-1}. In the ^{1}H NMR spectrum of **6a (Fig-3b.3.2)** methyl protons on chromene ring were observed at δ 2.41ppm, peak for methylene protons next to amide group was observed at δ ~3.59 while methylene next to pyridine was observed at δ 3.97, 3rd position proton of lactone ring was observed at δ 6.18ppm, aromatic protons were observed in range of 7.25-9.48. The amide N-H proton was observed as a singlet at 10.01 ppm **(Fig-3b.3.2)**. In the ^{13}C NMR spectra of **6a (Fig-3b.3.3)** peak for methyl carbon is observed at δ 18.64, methylene carbon peaks were observed at δ 51.41 and 52.41 ppm, aromatic carbons observed in range of 106-154 ppm, amide carbonyl carbon for compound **6a** was observed at 161 and carbonyl carbon of lactone at 169 ppm. For compound **6b (Fig-3b.4.3)** amide carbonyl carbon was observed at 158ppm and lactone carbonyl carbon was observed at 170ppm. Methyl carbon is absent, rest of the signals were almost same as in **6a**

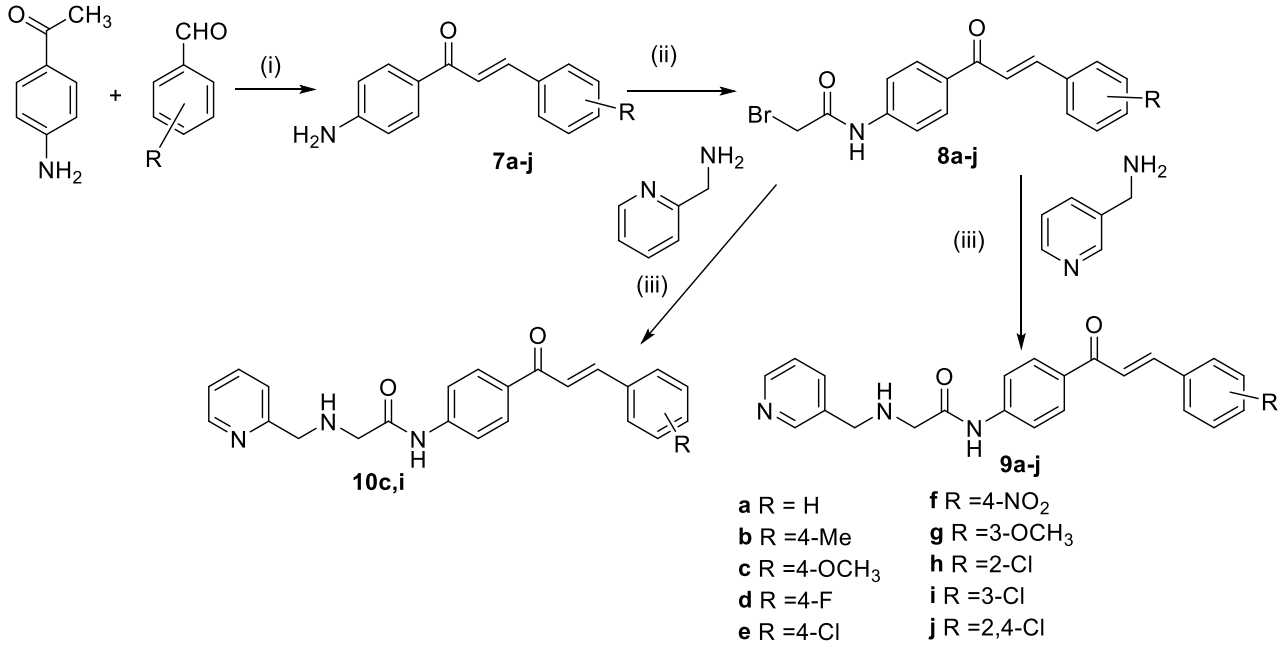

Reagents and Conditions: (i) 40% aq NaOH, ethanol, r.t 5-10 h; (ii) bromoacetyl bromide, TEA, DCM, r.t, 16-18 h; (iii) TEA, DMF, 0-5 oC, 30 min, r.t 14-16 h.

Scheme-2 Synthesis of compound **9a-j, 10c, 10i** with 3-aminomethyl pyridine chalcone derivatives

3-aminomethyl pyridine was linked to 4-amino chalcone derivatives to study the effect of chalcone on activity profile. Compounds **9a-j** were synthesized by the reaction of bromoacetamide derivatives **8** with 3-aminomethyl pyridine (**Scheme-2**). 4-

Aminoacetophenone on reaction with different aldehydes under basic conditions gave 4-amino chalcone derivatives **7** as shown in **scheme 3**. 4-Amino chalcones **7a-j** on reaction with bromoacetyl bromide gave **8a-j**, which on reaction with 3-aminomethyl pyridine gave various derivatives **9a-j** (**Scheme-2**).

The structures of compounds **9a-j** were confirmed by different analytical techniques such as ^{1}H-NMR, ^{13}C-NMR, IR, ESI-MS. The IR spectrum of one of the compound **9a (Fig-3b.5.1)** showed bands at 3327 and 3267 cm^{-1} for N-H stretching vibrations. Bands at 3055 and 2912 cm^{-1} was observed for C-H stretching vibrations. Bands at 1685 and 1649 cm^{-1} indicated carbonyl stretching frequency for lactone carbonyl and amide carbonyl respectively. In ^{1}H NMR spectrum of compound **9a** two singlets are observed at 3.48 and 3.90 ppm for methylene protons. Aromatic and olenific protons are observed from δ 7.30-8.64 ppm. Amide proton was observed at δ 9.41 ppm. In ^{13}C NMR spectrum of compound **9a** peaks at 51.39 and 52.44 ppm were observed for methylene carbons. All aromatic carbons were observed from 118-149 ppm carbonyl carbons of amide and chalcone were observed at δ 169 and 189 ppm respectively. The ESI-MS of compound **9a** showed M+H peak at 372.10 which confirmed formation of product. In general, the IR spectra of compounds **9a-j** exhibited two strong bands in the range of 3333-3236 cm^{-1} and 3290-3169 cm^{-1} for secondary amine and amide N-H stretching vibrations respectively. Carbonyl group of chalcone exhibited stretching frequency in range of 1693-1685 cm^{-1} and that of amide carbonyl in range of 1658-1649 cm^{-1}. In the ^{1}H NMR spectra of **9a-j**, peak for methylene next to amide group was observed in the range of δ ~3.34-4.13 while methylene next to pyridine was observed in range of δ ~3.78-4.50, aromatic protons and chalcone protons observed in range of 6.93-9.11 depending on effect of different substituents on aldehyde. For compounds **9a-j** -NH protons are observed between δ 9.42-11.49 ppm. In the ^{13}C NMR spectra of **9a-j**, two peaks for methylene carbons observed around 46.37-51.51 and 48.03-52.50 ppm, aromatic carbons observed between δ 113-161 ppm, amide carbonyl carbon around δ 164-171 ppm, chalcone carbonyl carbon between δ 187-189 ppm. All compounds **9a-j** were analyzed by ESI-MS analysis to give $[M+H]^{+}$/$[M+Na]^{+}$ peak corresponding to their molecular weight. Chalcone derivatives of active compound **10c** and **10i** were synthesized using 2-Aminomethyl pyridine. All these new chemical entities were subjected to *In-Vitro* studies for anticancer activity by MTT assay method.

Figure-3b.3.1 IR spectrum of N-(4-Methyl-2-oxo-2H-1-benzopyran-7-yl)-2-{[(pyridin-3-yl) methyl] amino}acetamide (**6a**)

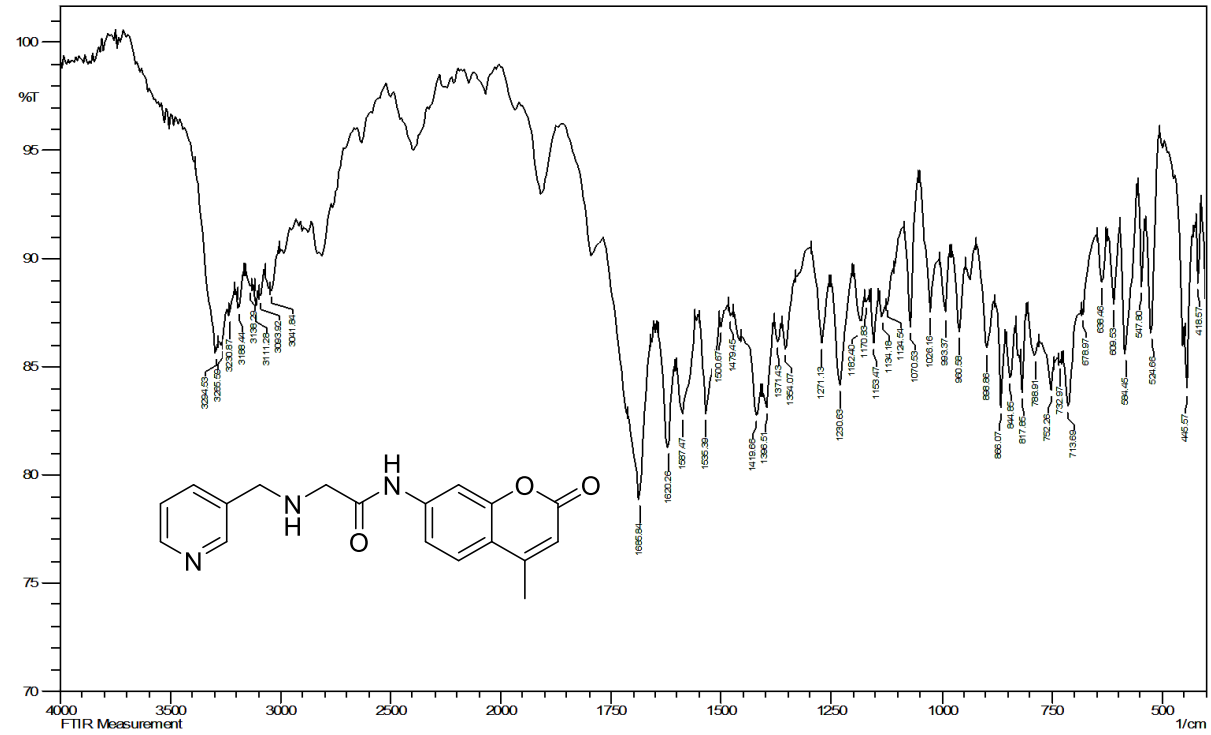

Figure-3b.3.2 ^{1}H-NMR spectrum of N-(4-Methyl-2-oxo-2H-1-benzopyran-7-yl)-2-{[(pyridin-3-yl)methyl] amino}acetamide (**6a**) in $CDCl_3$

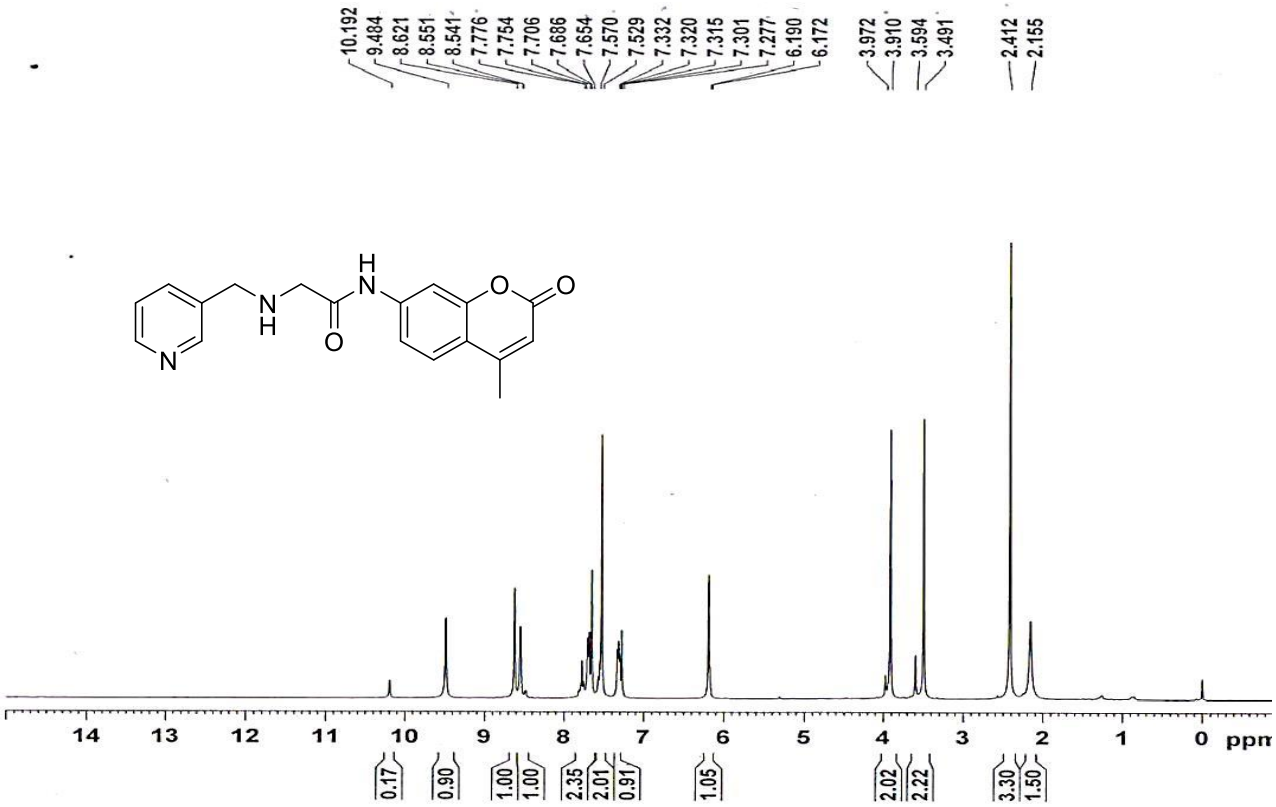

Figure-3b.3.3 ^{13}C-NMR spectrum of N-(4-Methyl-2-oxo-2H-1-benzopyran-7-yl)-2-{[(pyridin-3-yl)methyl]amino}acetamide (**6a**) in $CDCl_3$

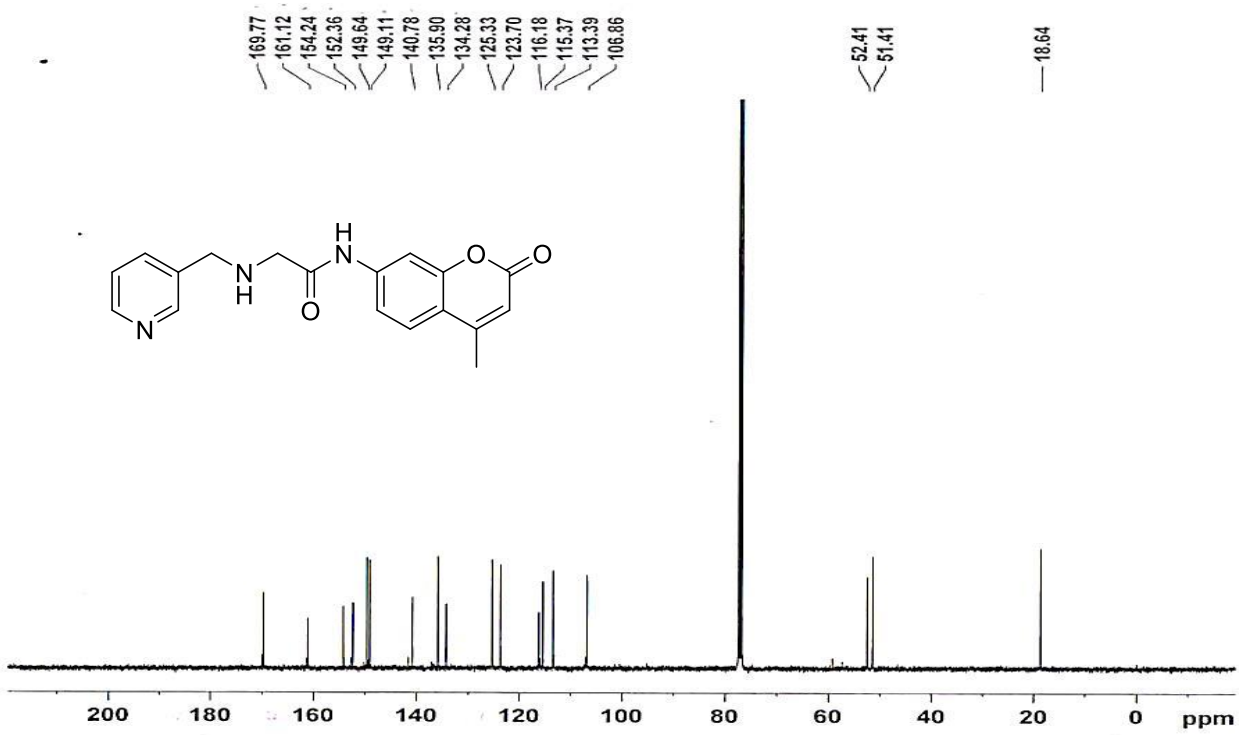

Figure-3b.3.4 ESI-MS spectrum of N-(4-Methyl-2-oxo-2H-1-benzopyran-7-yl)-2-{[(pyridin-3-yl) methyl]amino}acetamide (**6a**) M^+ peak at 323

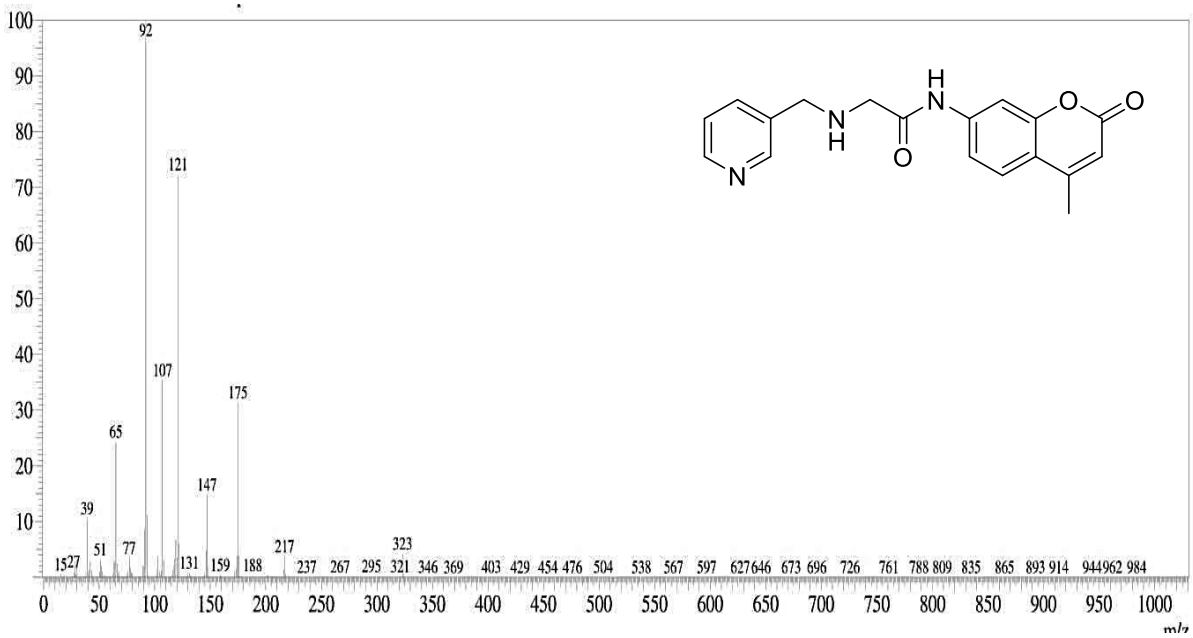

Figure-3b.4.1 IR spectrum of N-(2-Oxo-2H-1-benzopyran-3-yl)-2-{[(pyridin-3-yl)methyl] amino}acetamide (**6b**)

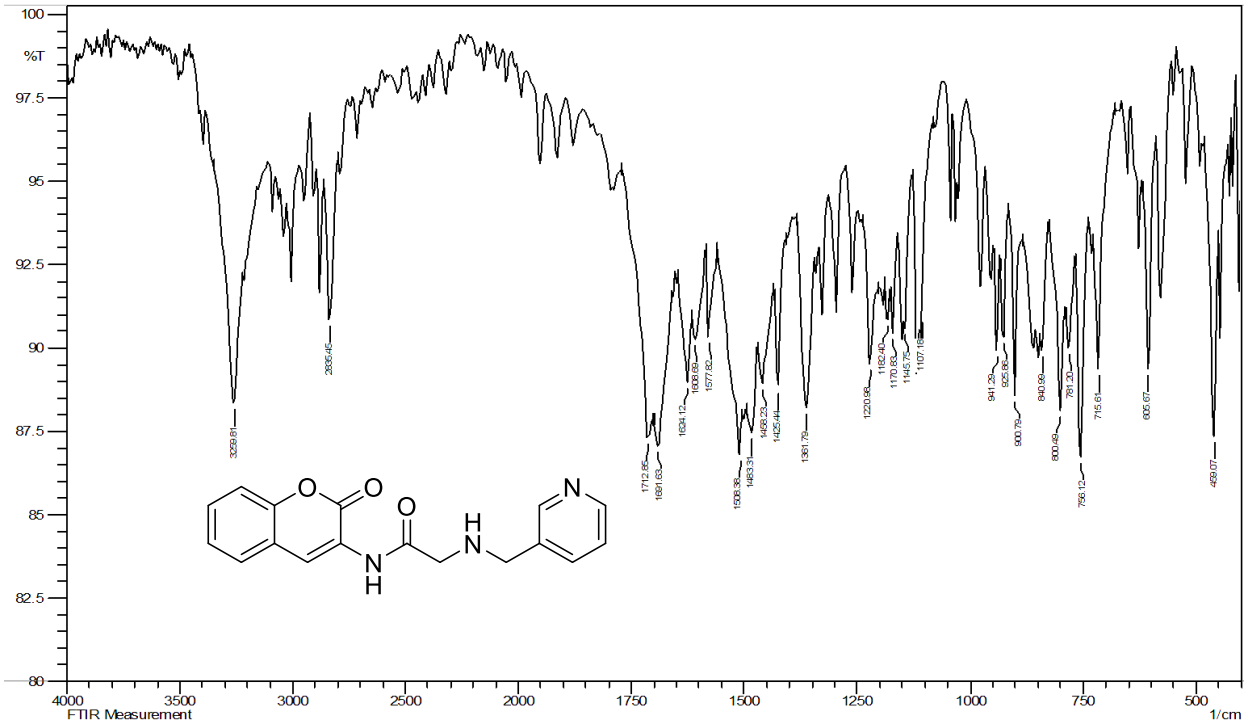

Figure-3b.4.2 ^{1}H-NMR spectrum of N-(2-Oxo-2H-1-benzopyran-3-yl)-2-{[(pyridin-3-yl) methyl]amino}acetamide (**6b**) in $CDCl_3$

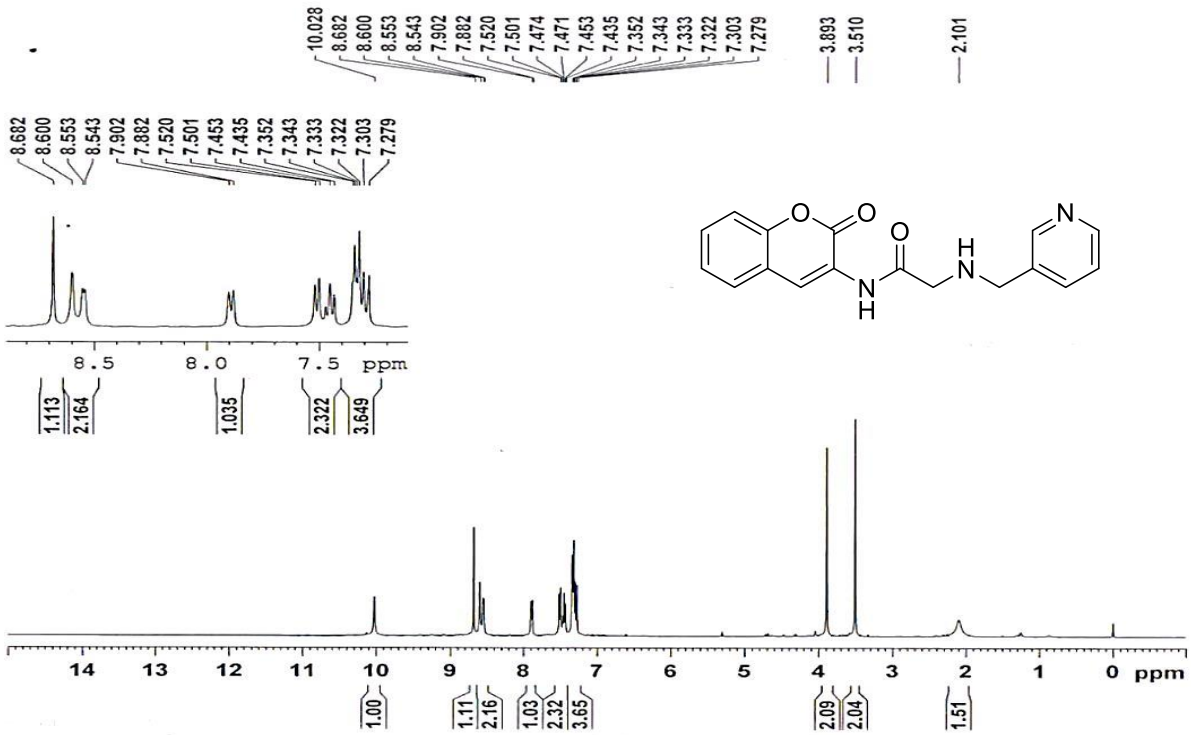

Figure-3b.4.3 ^{13}C-NMR spectrum of N-(2-Oxo-2H-1-benzopyran-3-yl)-2-{[(pyridin-3-yl) methyl]amino}acetamide (**6b**) in $CDCl_3$

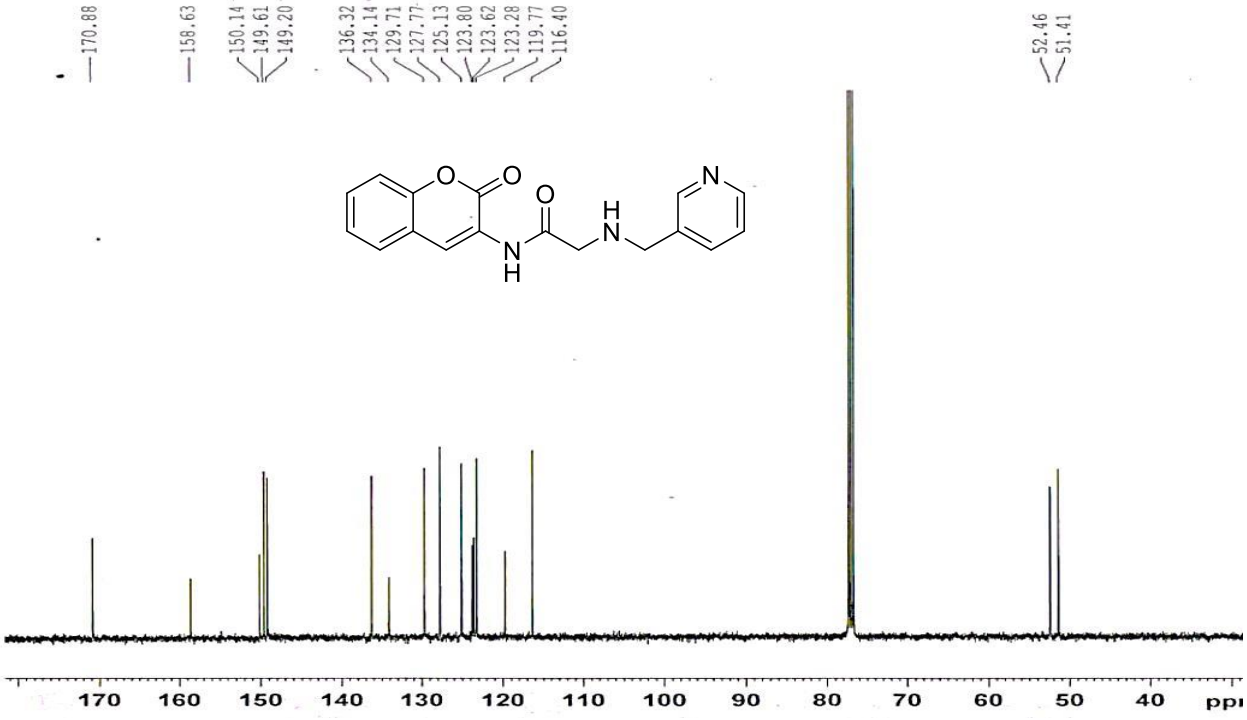

Figure-3b.4.4 ESI-MS spectrum of N-(2-Oxo-2H-1-benzopyran-3-yl)-2-{[(pyridin-3-yl)methyl] amino}acetamide (**6b**) M^+ peak at 309.

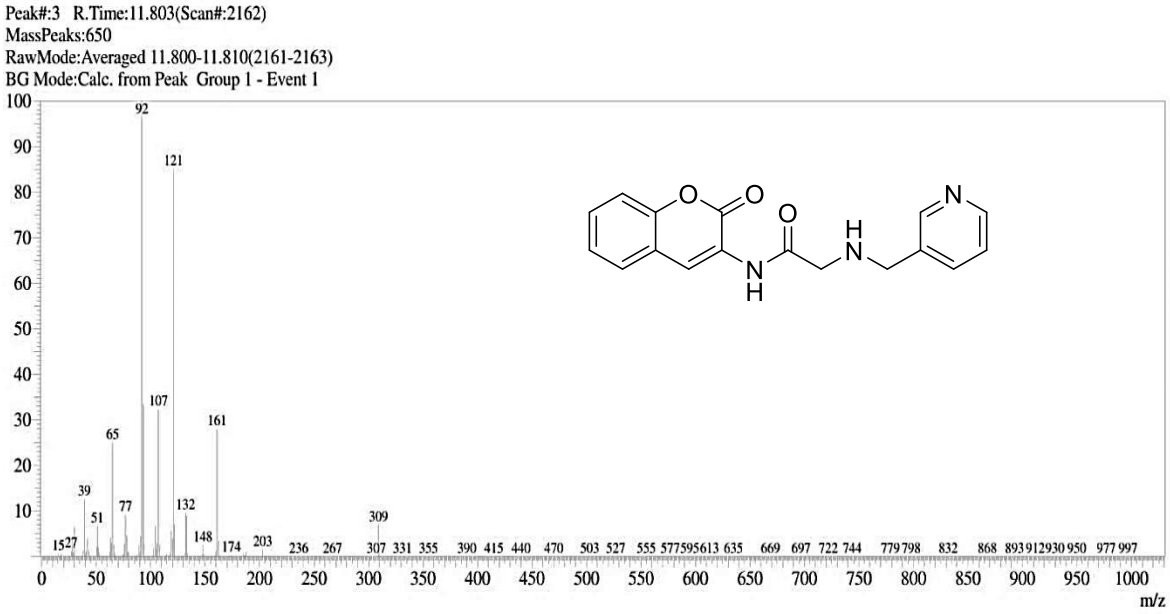

Figure-3b.5.1 IR spectrum of N-{4-[(2E)-3-Phenylprop-2-enoyl]phenyl}-2-{[(pyridin-3-yl) methyl]amino}acetamide (**9a**)

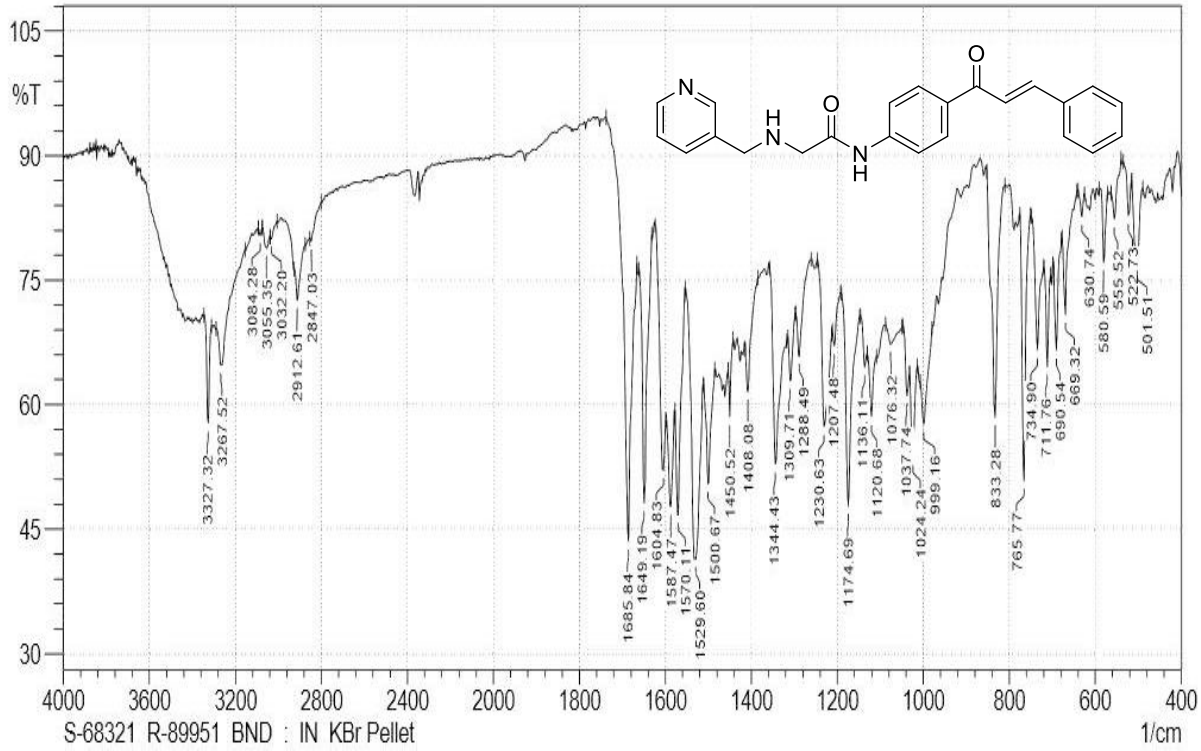

Figure-3b.5.2 ^{1}H-NMR spectrum of N-{4-[(2E)-3-Phenylprop-2-enoyl]phenyl}-2-{[(pyridin-3-yl) methyl]amino}acetamide (**9a**) in $CDCl_3$

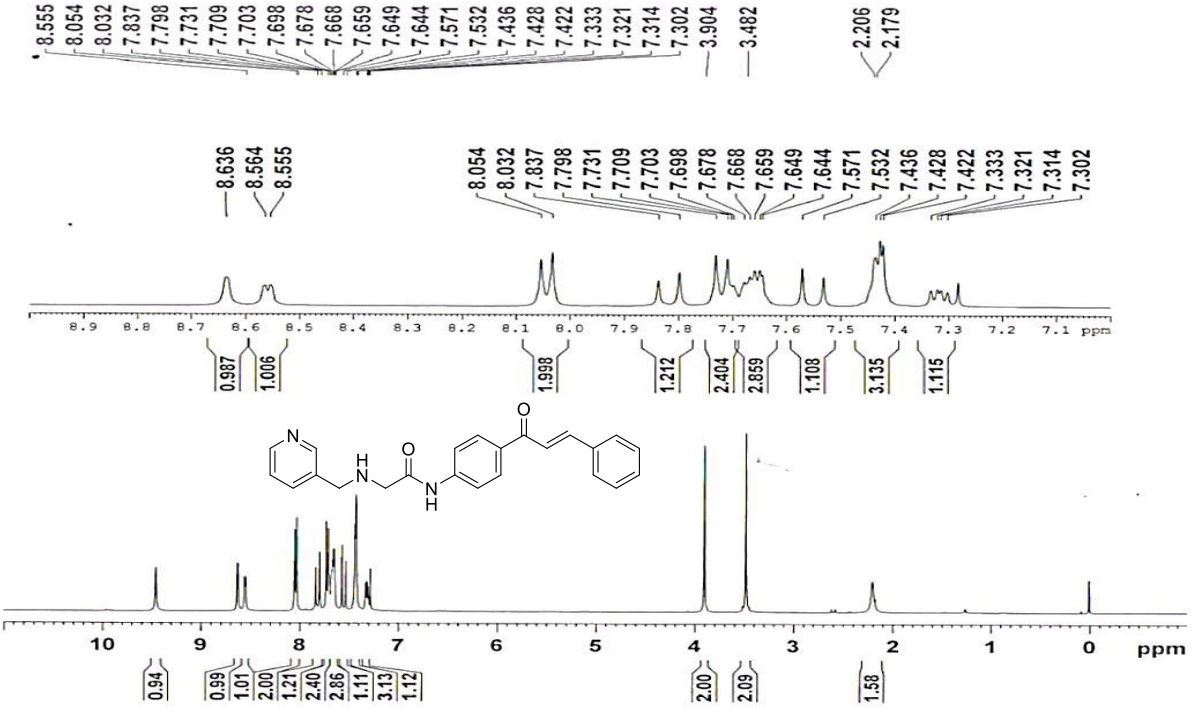

Figure-3b.5.3 ^{13}C-NMR spectrum of N-{4-[(2E)-3-Phenylprop-2-enoyl]phenyl}-2-{[(pyridin-3-yl)methyl]amino}acetamide (**9a**) in $CDCl_3$

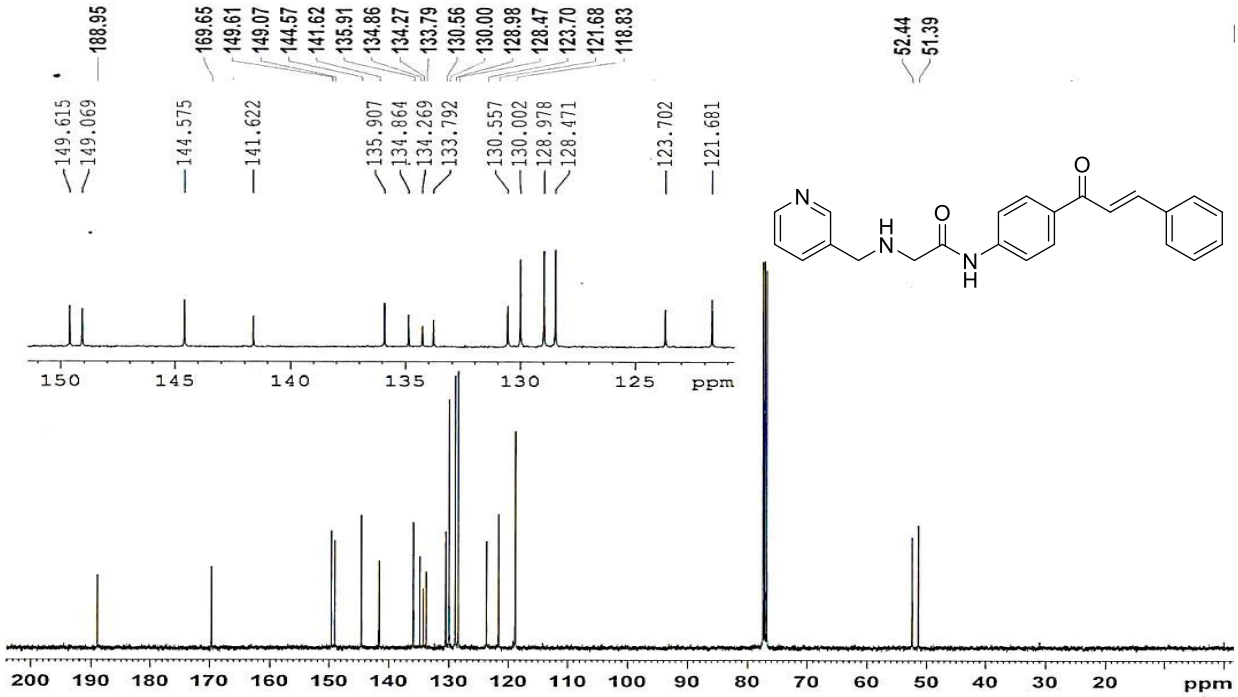

Figure-3b.5.4 ESI-MS spectrum of N-{4-[(2E)-3-Phenylprop-2-enoyl]phenyl}-2-{[(pyridin-3-yl)methyl]amino}acetamide(**9a**) M-H peak at 370.10

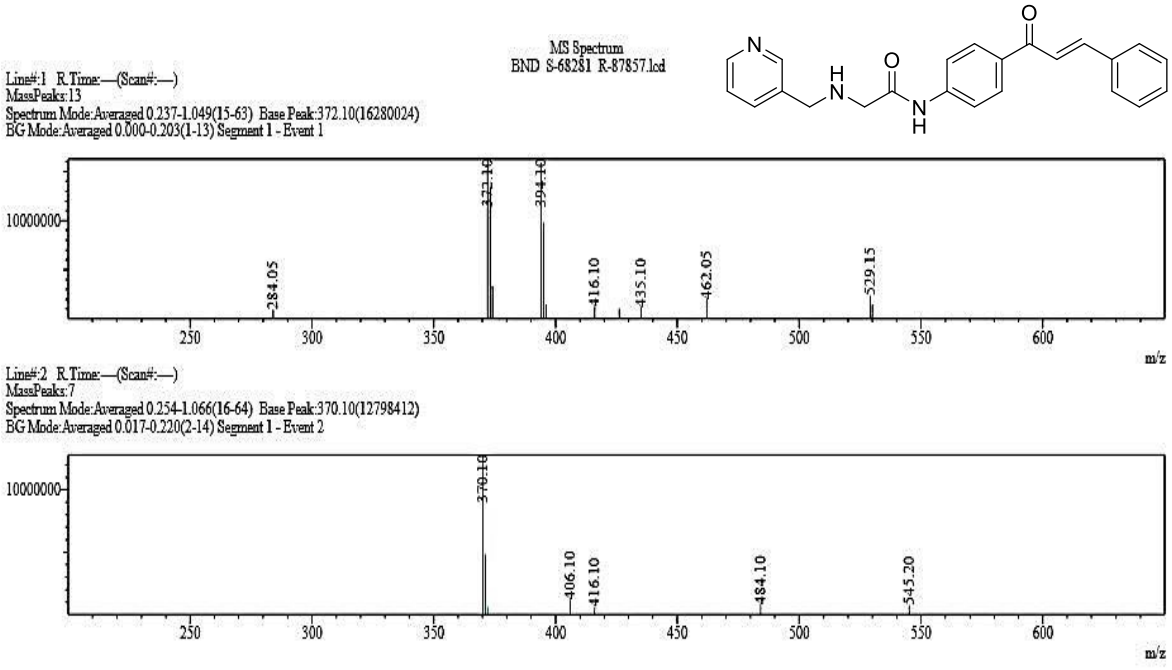

Figure-3b.6.1 IR spectrum of N-{4-[(2E)-3-(4-Methylphenyl)prop-2-enoyl]phenyl}-2-{[(pyridin-3-yl)methyl]amino} acetamide (**9b**)

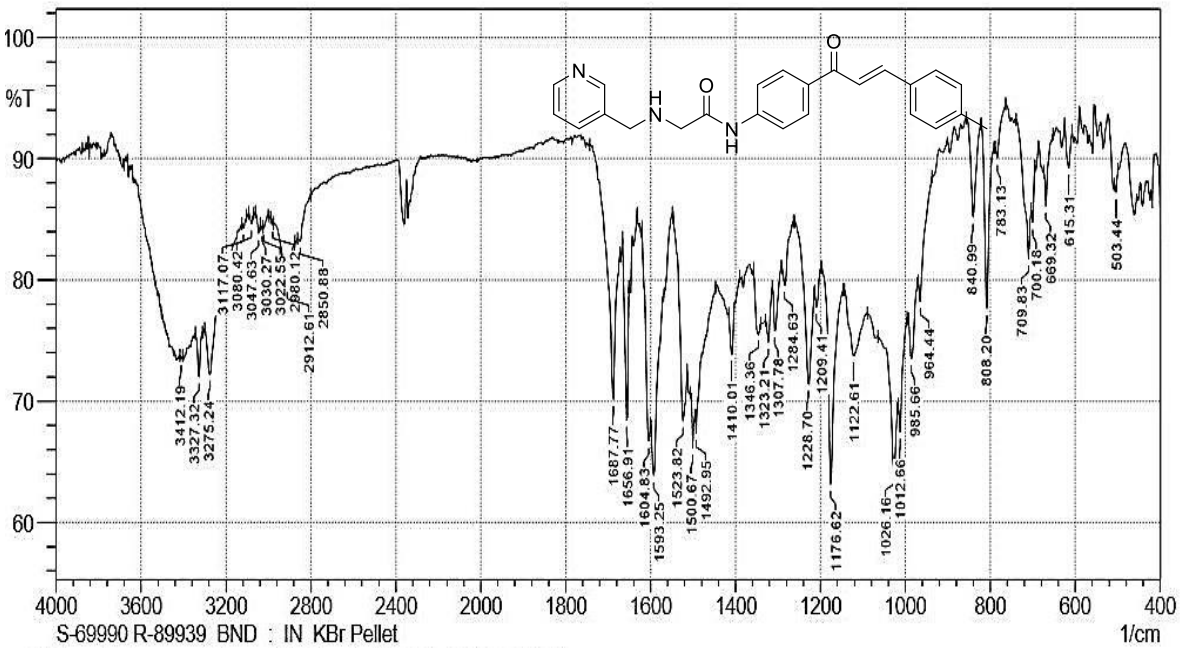

Figure-3b.6.2 ^{1}H-NMR spectrum of N-{4-[(2E)-3-(4-Methylphenyl)prop-2-enoyl]phenyl}-2-{[(pyridin-3-yl)methyl]amino} acetamide (**9b**) in $CDCl_3$

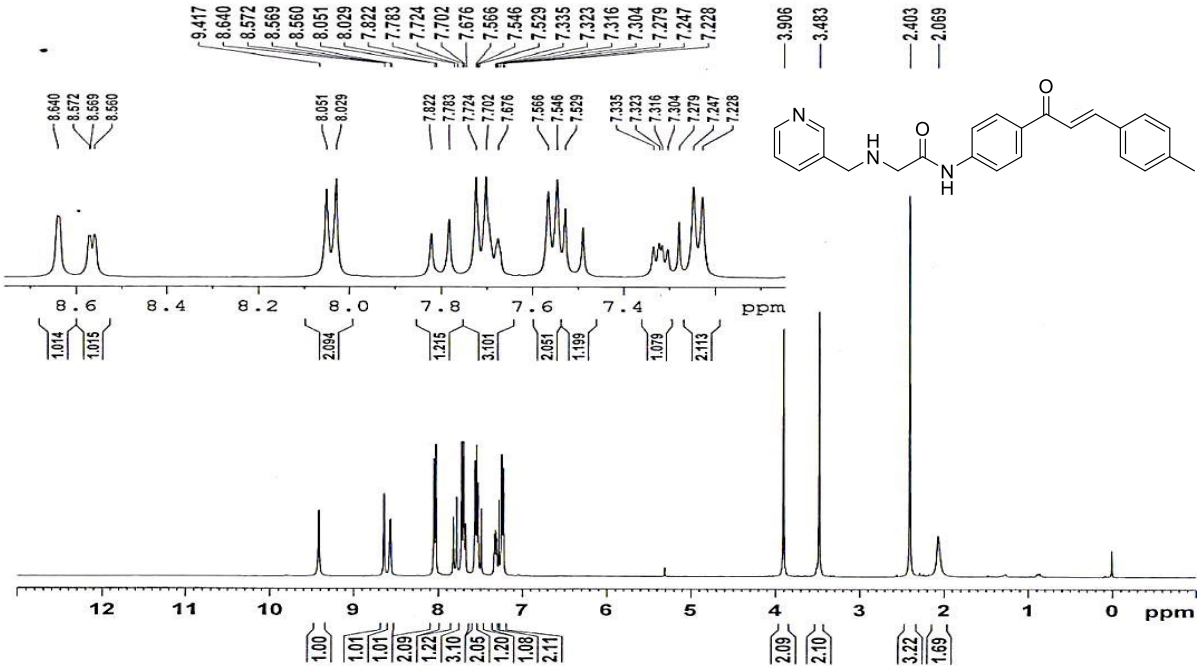

Figure-3b.6.3 ^{13}C-NMR spectrum of N-{4-[(2E)-3-(4-Methylphenyl)prop-2-enoyl]phenyl}-2-{[(pyridin-3-yl)methyl]amino} acetamide (**9b**) in $CDCl_3$

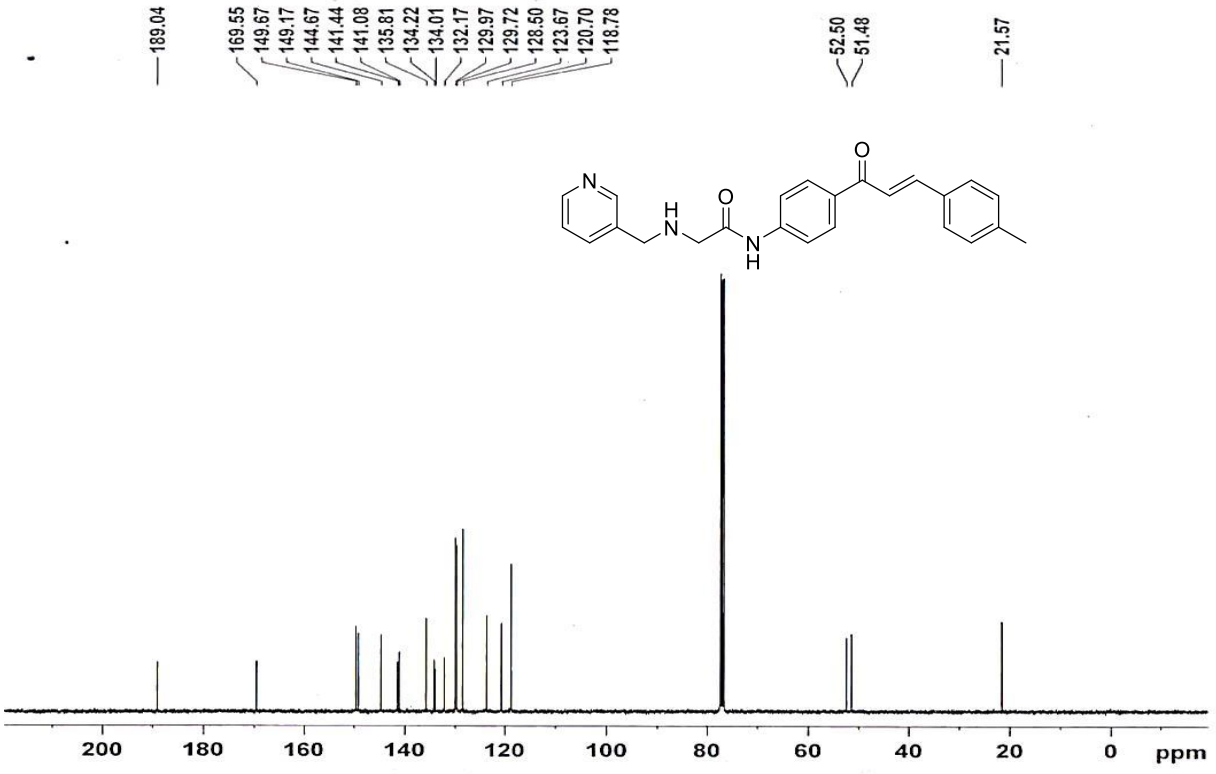

Figure-3b.6.4 ESI-MS spectrum of N-{4-[(2E)-3-(4-Methylphenyl)prop-2-enoyl]phenyl}-2-{[(pyridin-3-yl)methyl]amino} acetamide (**9b**) M-H=384.15

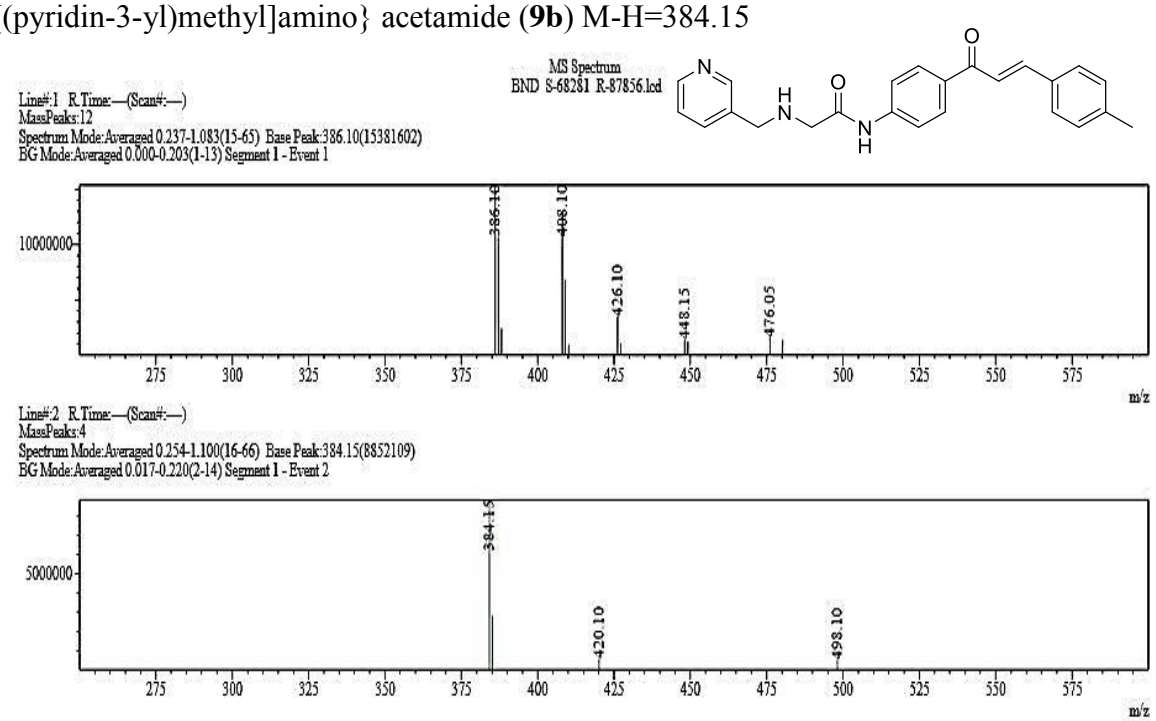

Figure-3b.7.1 IR spectrum of N-{4-[(2E)-3-(4-Methoxyphenyl)prop-2-enoyl]phenyl}-2-{[(pyridin-3-yl)methyl]amino} acetamide (**9c**)

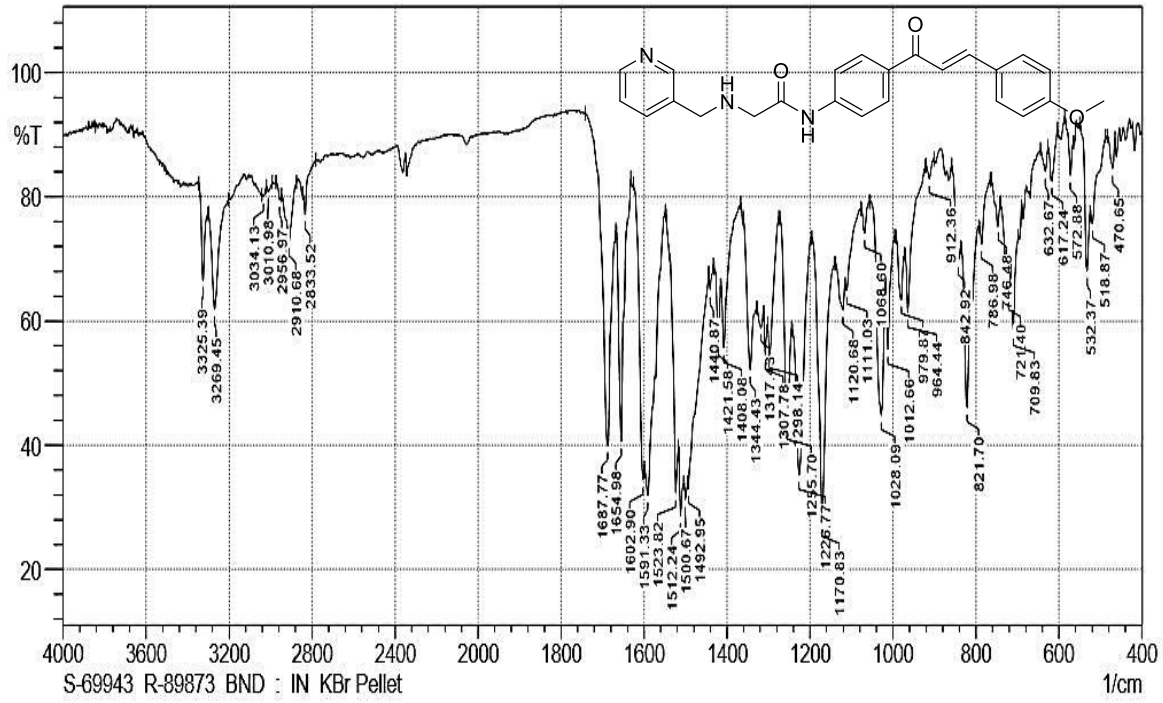

Figure-3b.7.2 ^{1}H-NMR spectrum of N-{4-[(2E)-3-(4-Methoxyphenyl)prop-2-enoyl]phenyl}-2-{[(pyridin-3-yl)methyl]amino} acetamide (**9c**) in $CDCl_3$

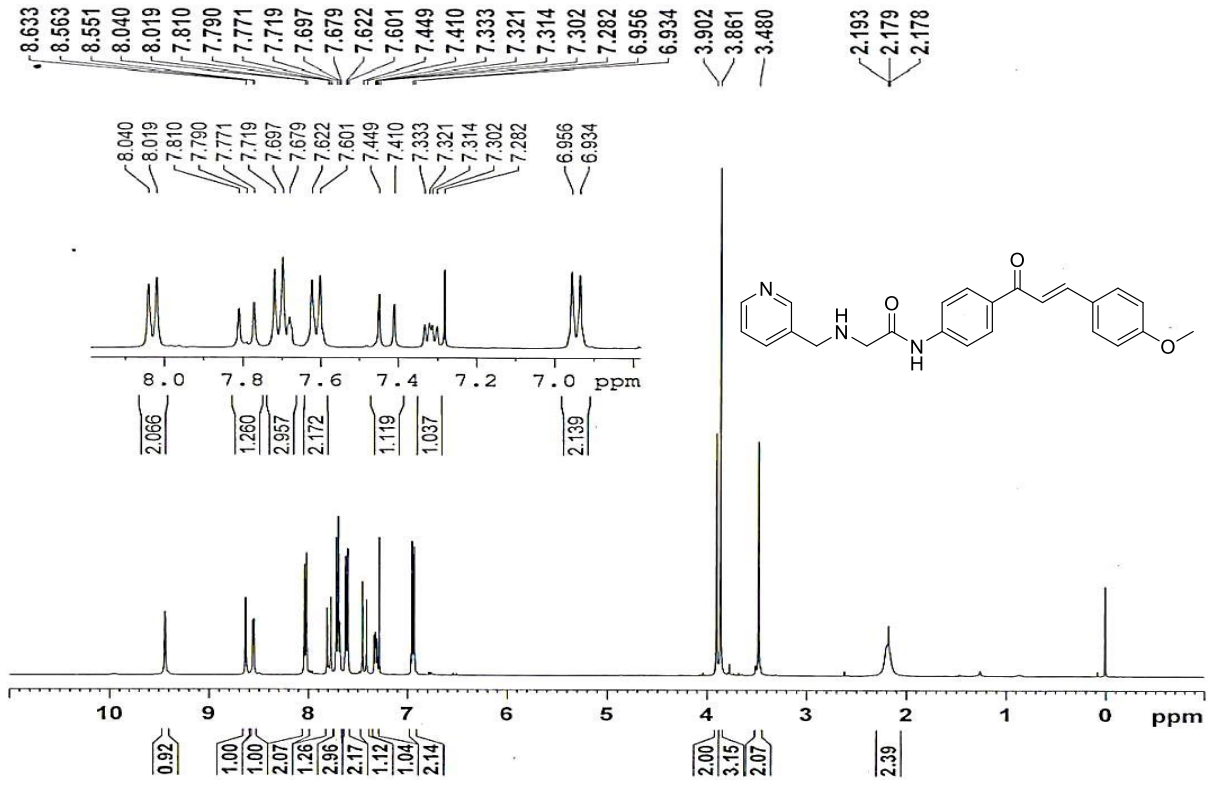

Figure-3b.7.3 ^{13}C-NMR spectrum of N-{4-[(2E)-3-(4-Methoxyphenyl)prop-2-enoyl]phenyl}-2-{[(pyridin-3-yl)methyl]amino} acetamide (**9c**) in $CDCl_3$

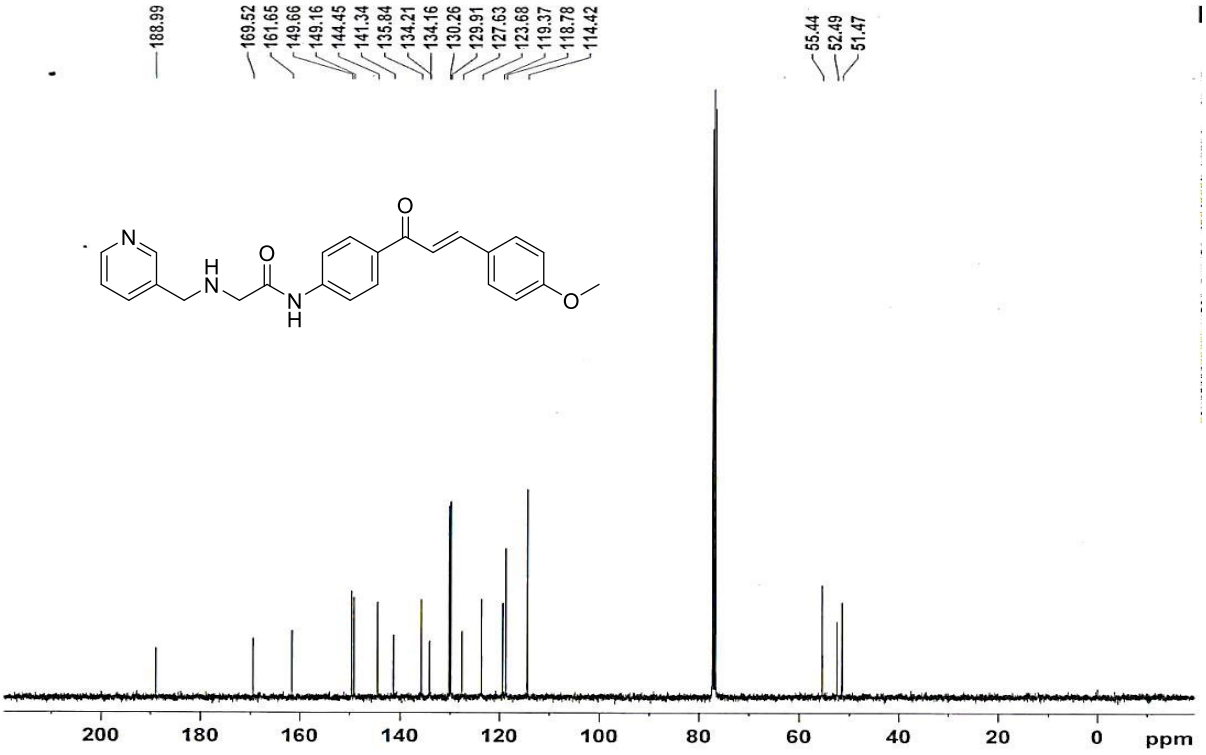

Figure-3b.7.4 ESI-MS spectrum of N-{4-[(2E)-3-(4-Methoxyphenyl)prop-2-enoyl]phenyl}-2-{[(pyridin-3-yl)methyl]amino} acetamide (**9c**) M-H peak at 400.15

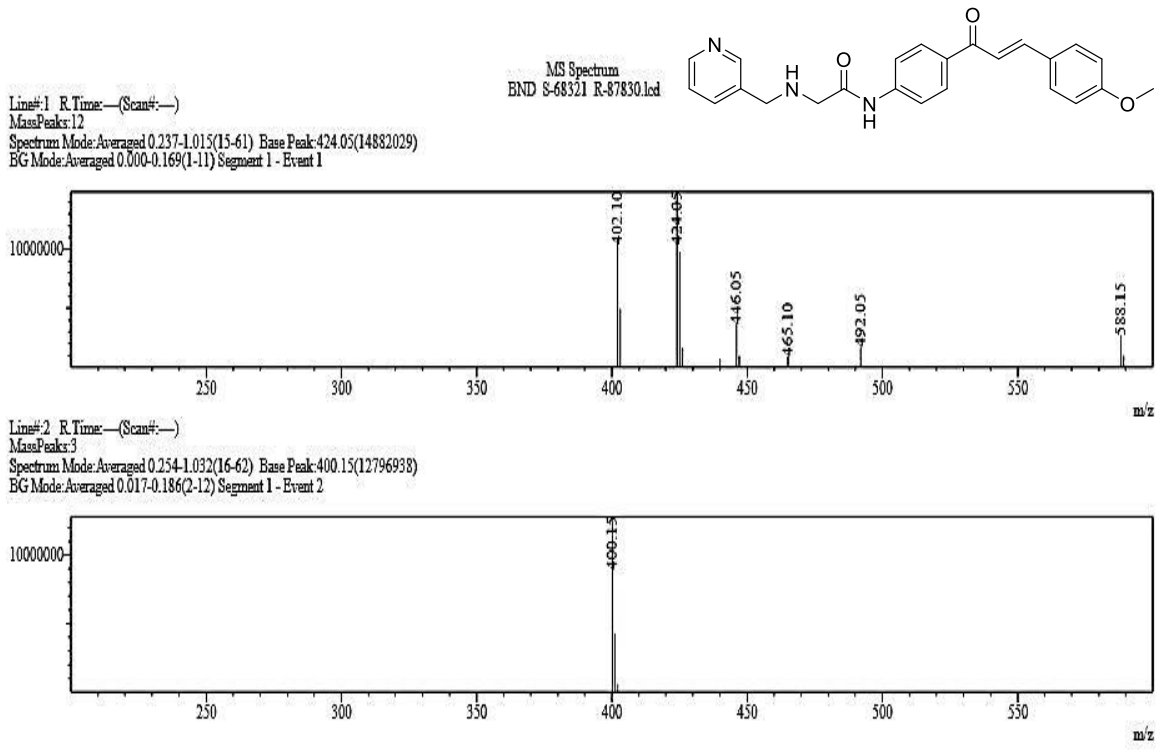

Figure-3b.8.1 IR spectrum of N-{4-[(2E)-3-(4-Fluorophenyl)prop-2-enoyl]phenyl}-2-{[(pyridin-3-yl)methyl]amino} acetamide (**9d**)

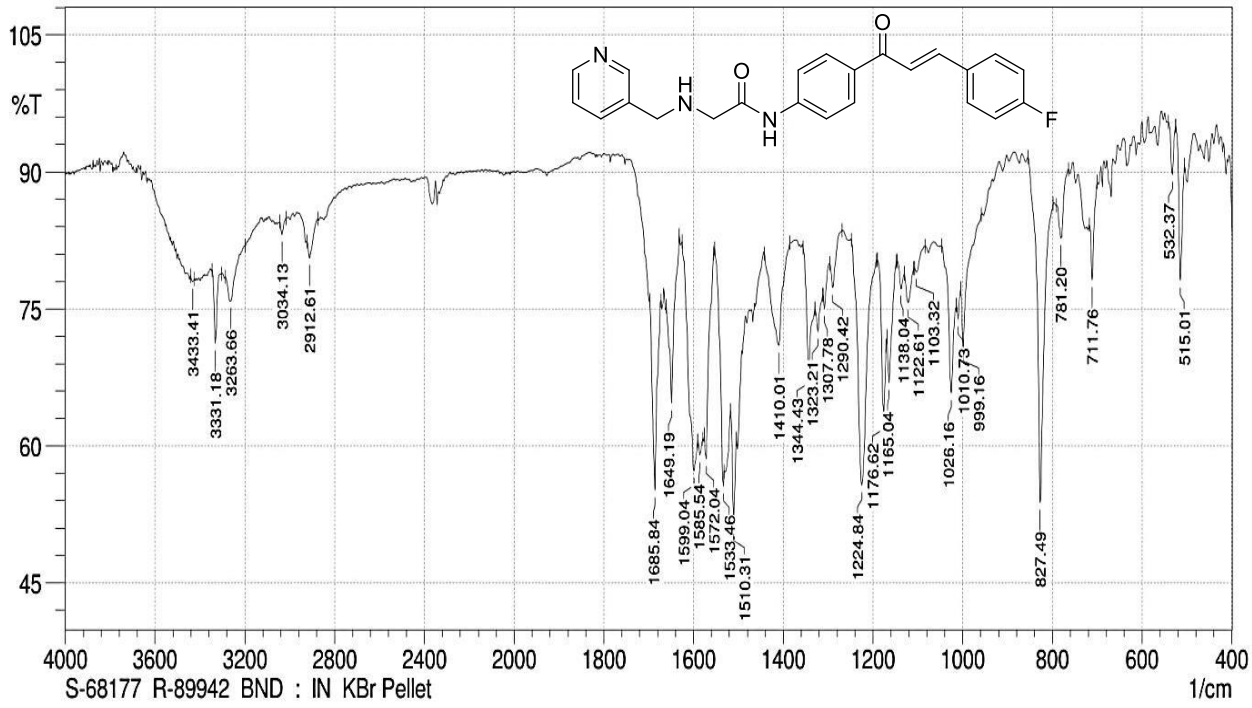

Figure-3b.8.2 ^{1}H-NMR spectrum of N-{4-[(2E)-3-(4-Fluorophenyl)prop-2-enoyl]phenyl}-2-{[(pyridin-3-yl)methyl]amino} acetamide (**9d**) in $CDCl_3$

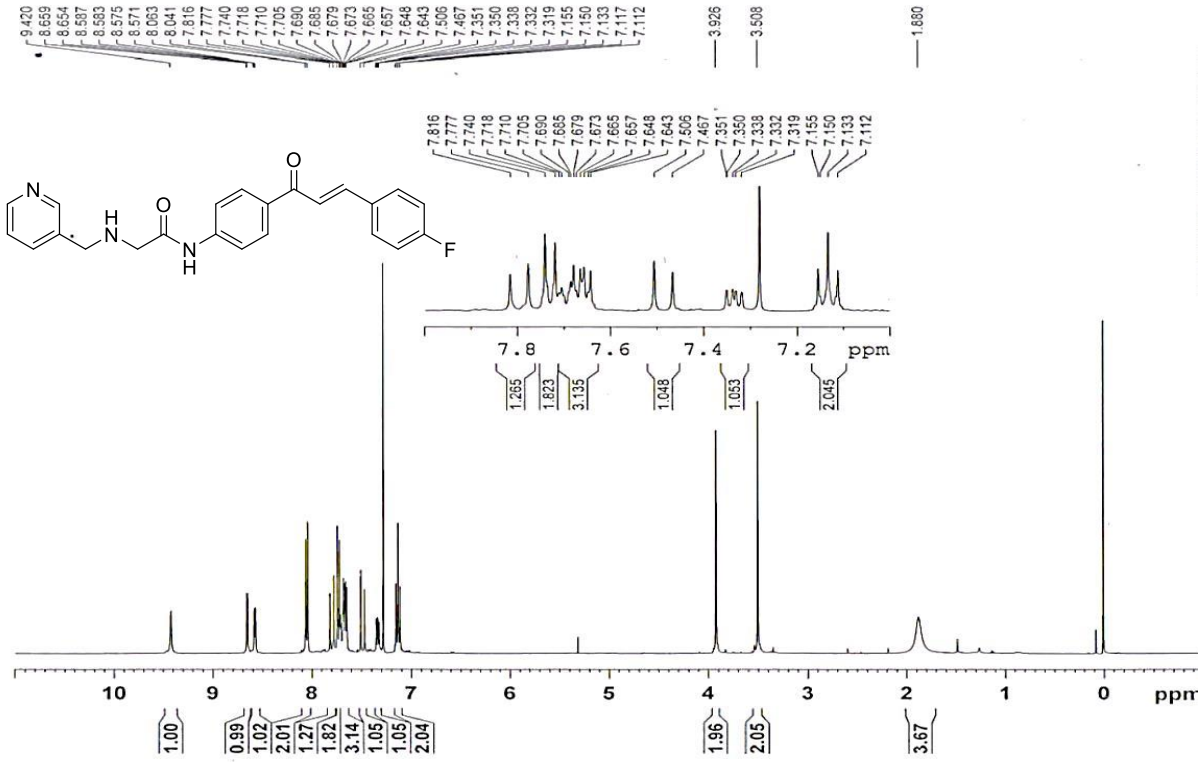

Figure-3b.8.3 ^{13}C-NMR spectrum of N-{4-[(2E)-3-(4-Fluorophenyl)prop-2-enoyl]phenyl}-2-{[(pyridin-3-yl)methyl]amino} acetamide (**9d**) in $CDCl_3$

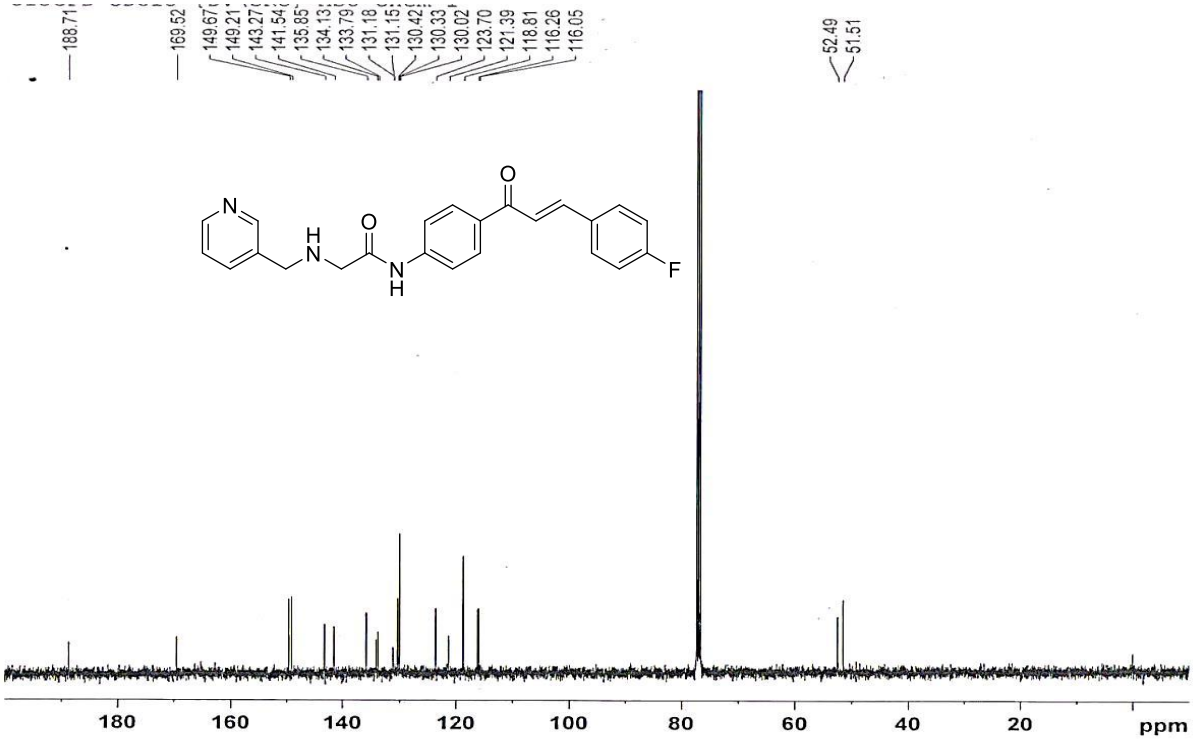

Figure-3b.8.4 ESI-MS spectrum of N-{4-[(2E)-3-(4-Fluorophenyl)prop-2-enoyl]phenyl}-2-{[(pyridin-3-yl)methyl]amino} acetamide (**9d**) M+H peak at 390.10

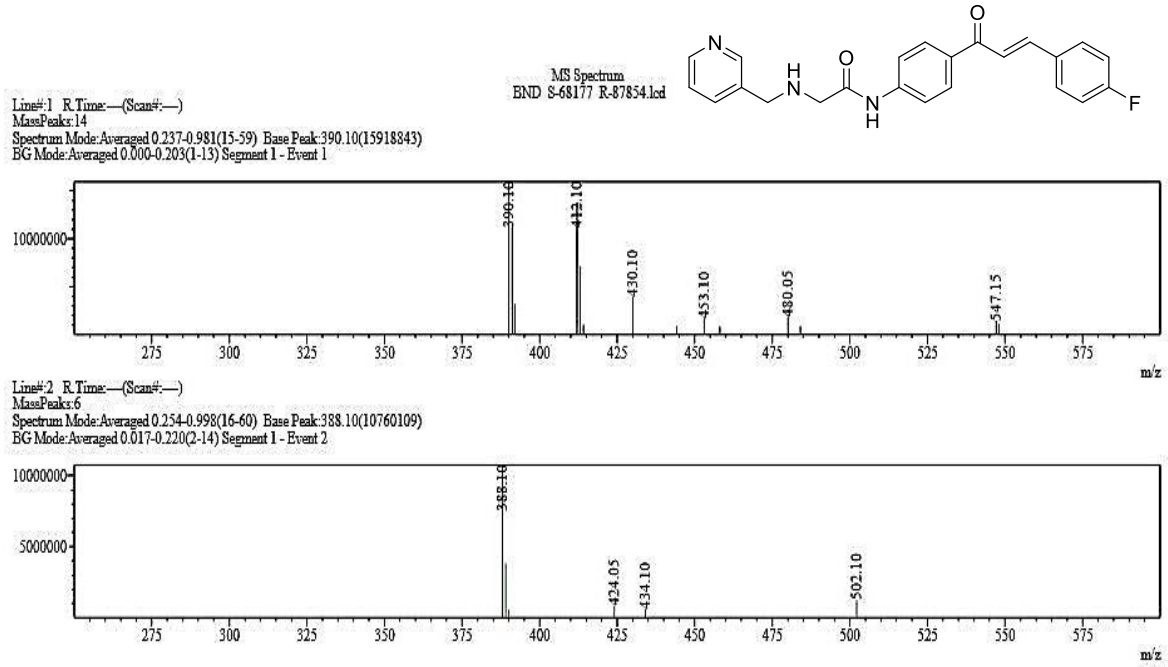

Figure-3b.9.1 IR spectrum of N-{4-[(2E)-3-(4-Chlorophenyl)prop-2-enoyl]phenyl}-2-{[(pyridin-3-yl)methyl]amino} acetamide (**9e**)

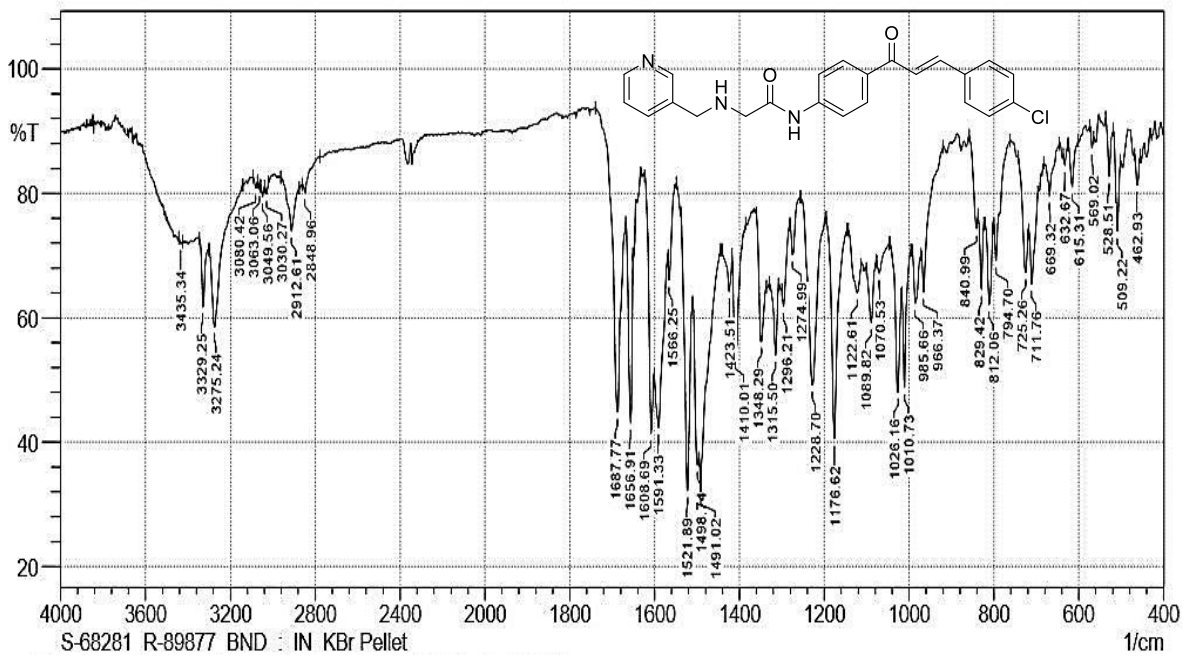

Figure-3b.9.2 ^{1}H-NMR spectrum of N-{4-[(2E)-3-(4-Chlorophenyl)prop-2-enoyl]phenyl}-2-{[(pyridin-3-yl)methyl]amino} acetamide (**9e**) in $CDCl_3$

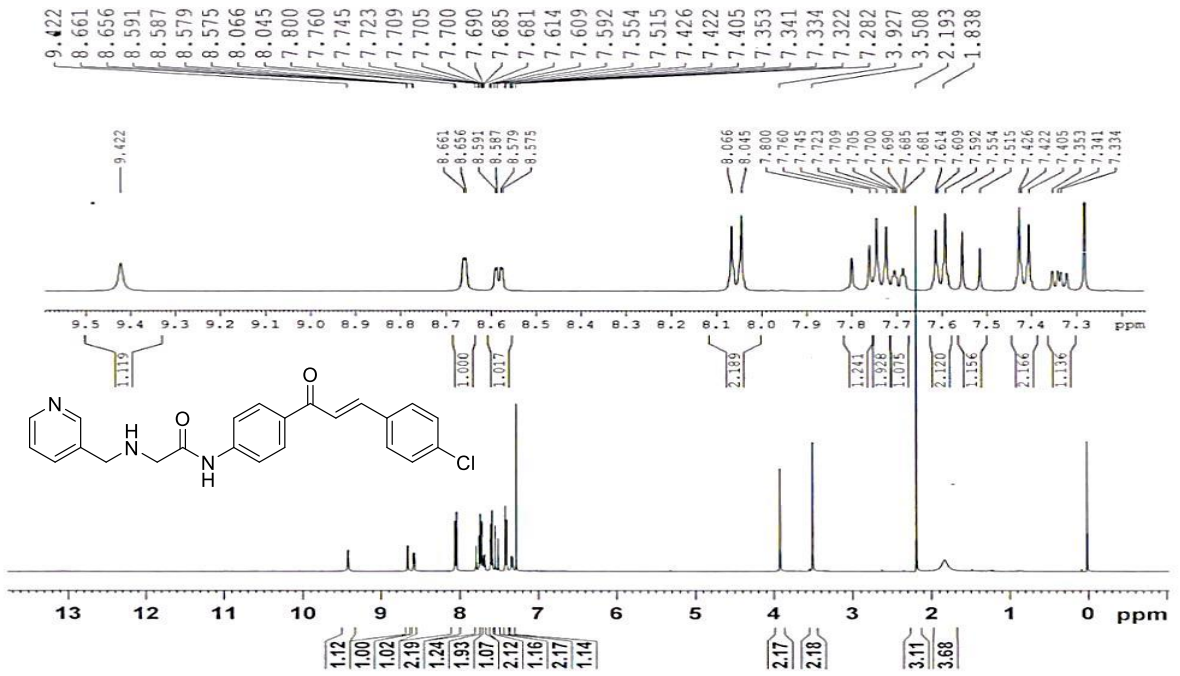

Figure-3b.9.3 ^{13}C-NMR spectrum of N-{4-[(2E)-3-(4-Chlorophenyl)prop-2-enoyl]phenyl}-2-{[(pyridin-3-yl)methyl]amino} acetamide (**9e**) in $CDCl_3$

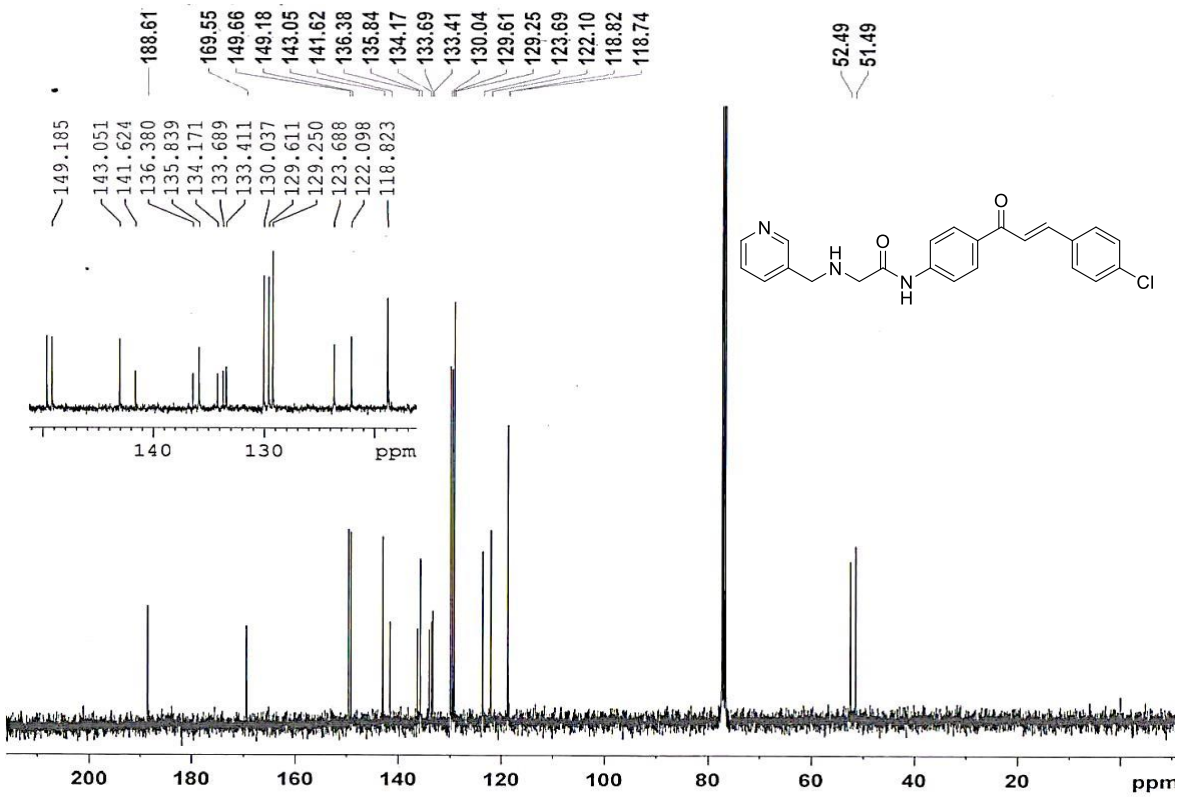

Figure-3b.9.4 ESI-MS spectrum of N-{4-[(2E)-3-(4-Chlorophenyl)prop-2-enoyl]phenyl}-2-{[(pyridin-3-yl)methyl]amino} acetamide (**9e**) M+H peak at 404.10

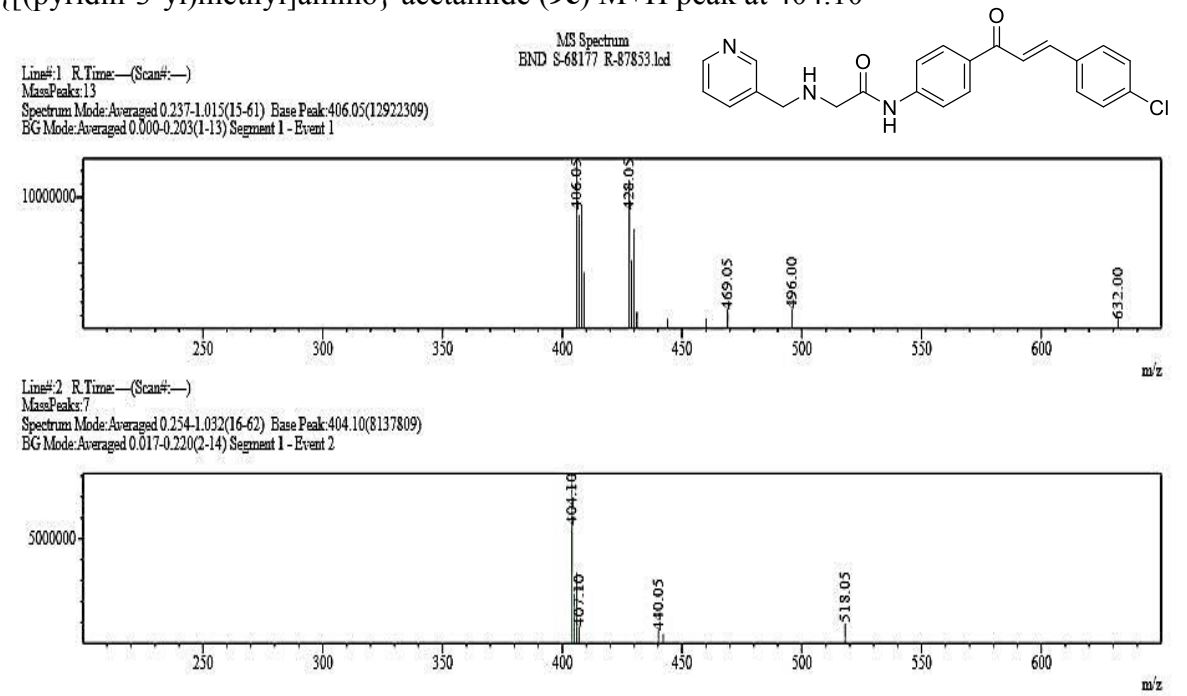

Figure-3b.10.1 IR spectrum of N-{4-[(2E)-3-(4-Nitrophenyl)prop-2-enoyl]phenyl}-2-{[(pyridin-3-yl)methyl]amino} acetamide (**9f**)

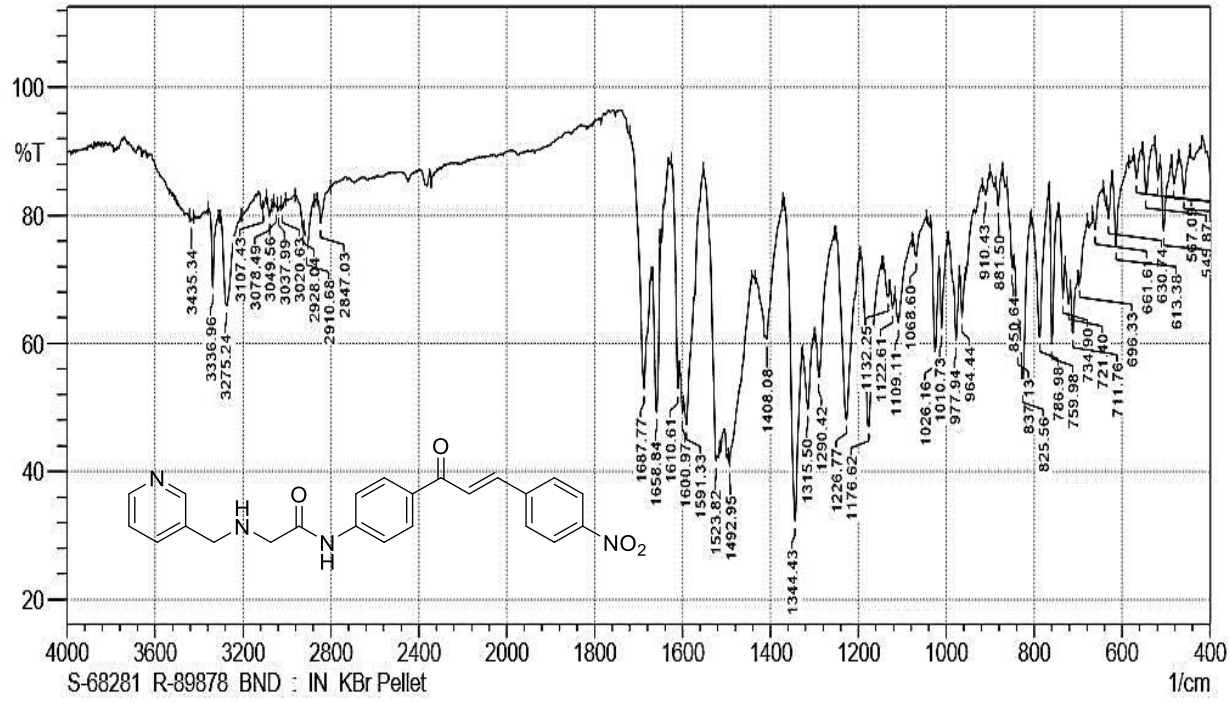

Figure-3b.10.2 ^{1}H-NMR spectrum of N-{4-[(2E)-3-(4-Nitrophenyl)prop-2-enoyl] phenyl}-2-{[(pyridin-3-yl)methyl]amino} acetamide (**9f**) in $CDCl_3$

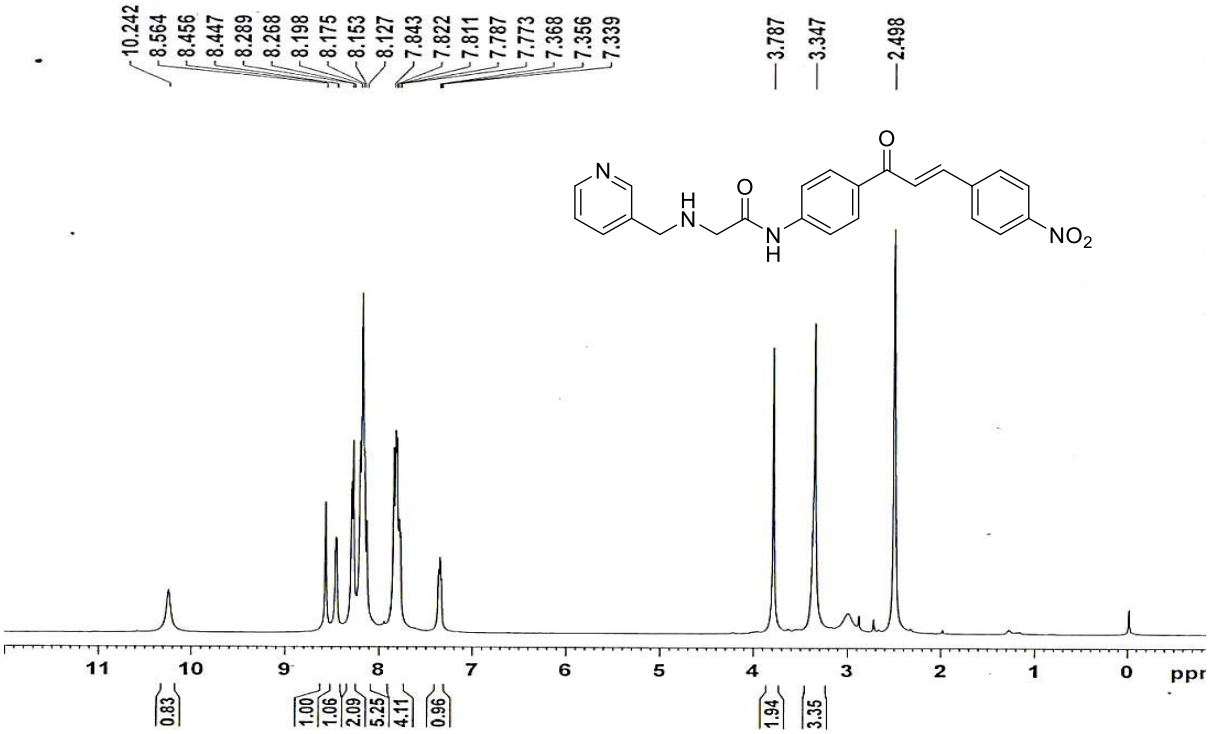

Figure-3b.10.3 ^{13}C-NMR spectrum of N-{4-[(2E)-3-(4-Nitrophenyl)prop-2-enoyl] phenyl}-2-{[(pyridin-3-yl)methyl]amino} acetamide (**9f**) in $CDCl_3$

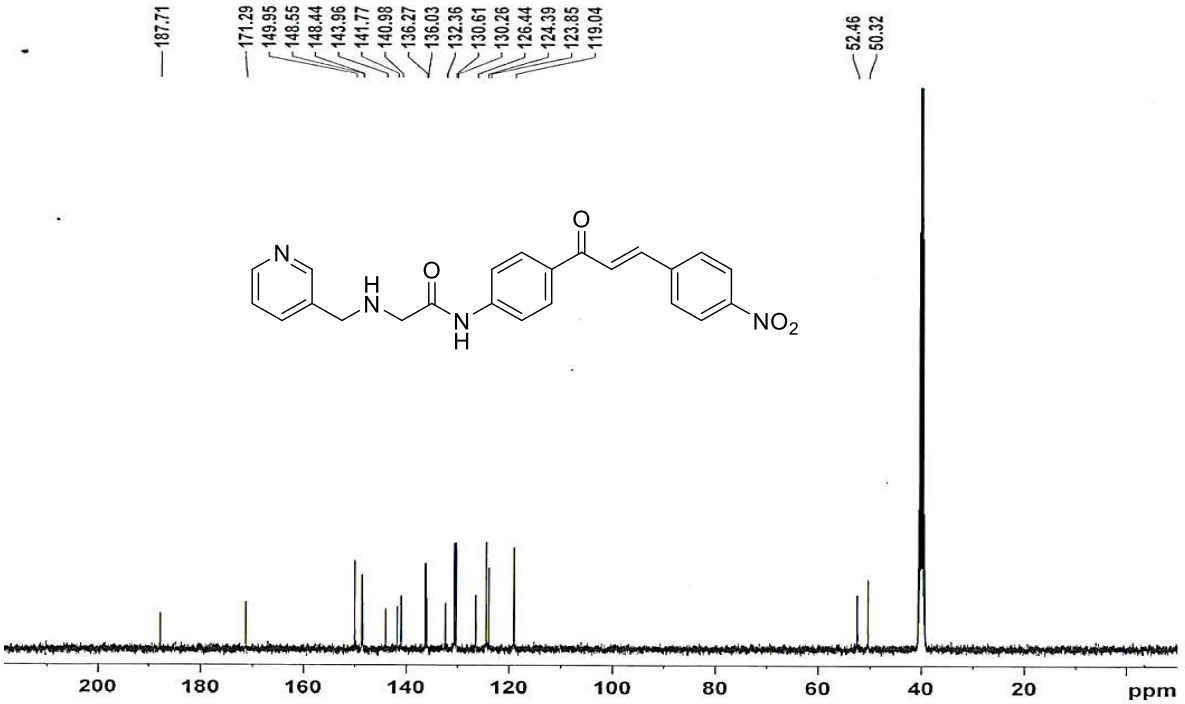

Figure-3b.10.4 ESI-MS spectrum of N-{4-[(2E)-3-(4-Nitrophenyl)prop-2-enoyl] phenyl}-2-{[(pyridin-3-yl)methyl]amino} acetamide (**9f**) M-H peak at =415.10

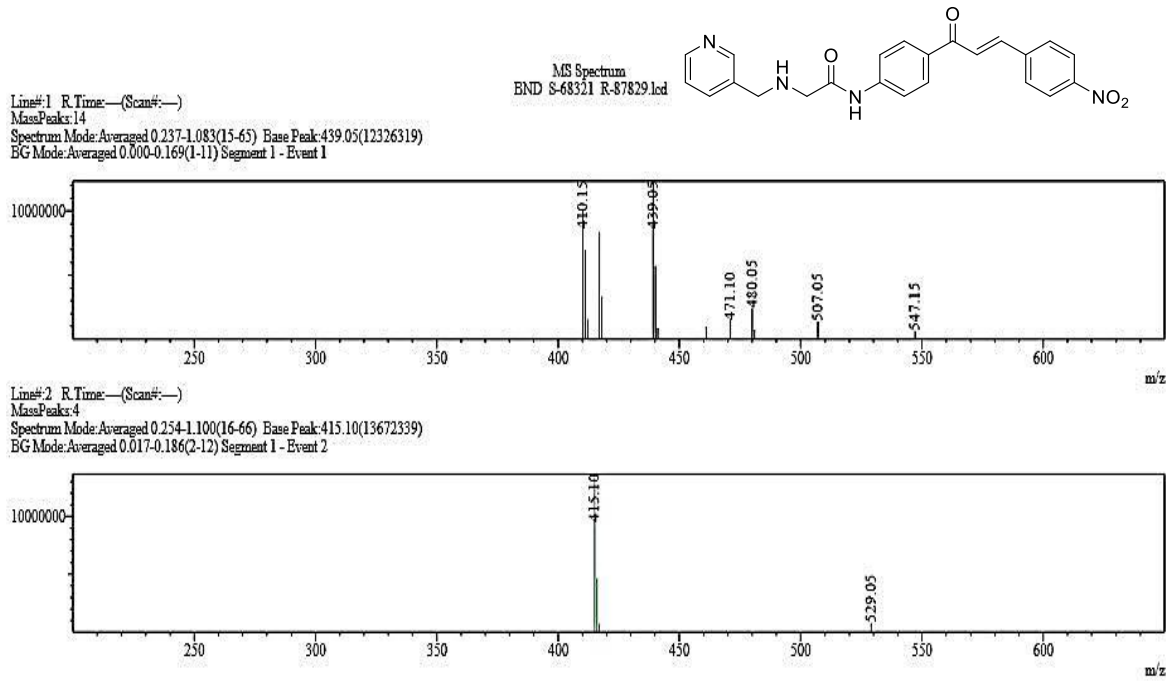

Figure-3b.11.1 IR spectrum of N-{4-[(2E)-3-(3-Methoxyphenyl)prop-2-enoyl] phenyl}-2-{[(pyridin-3-yl)methyl]amino} acetamide (**9g**)

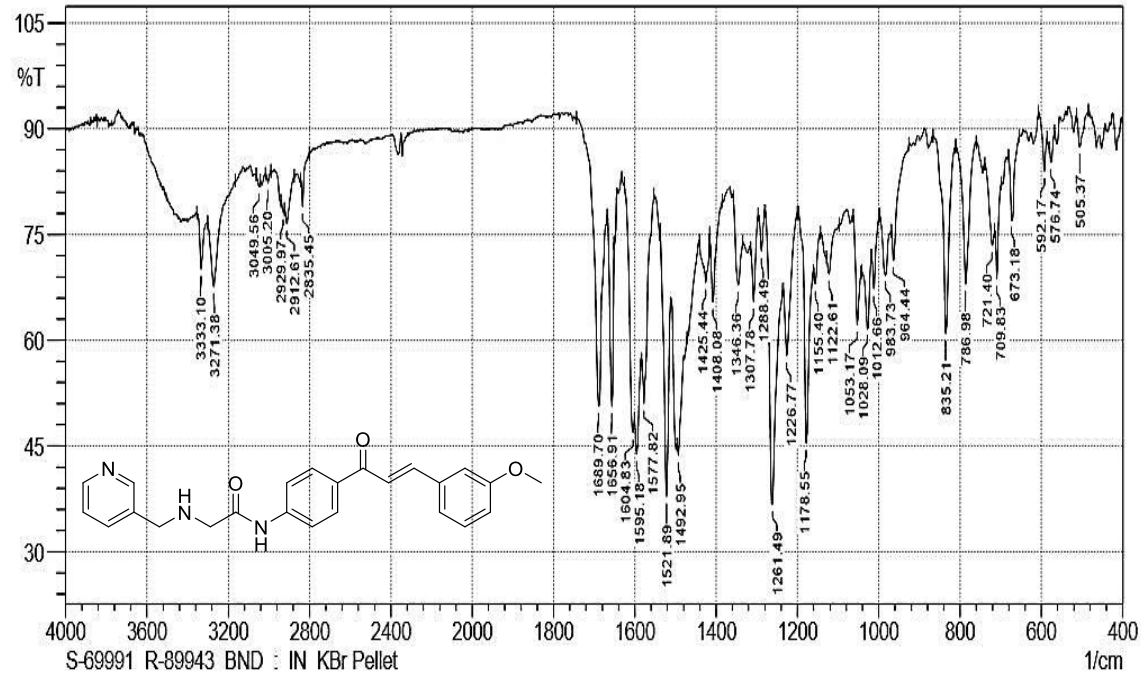

Figure-3b.11.2 ^{1}H-NMR spectrum of N-{4-[(2E)-3-(3-Methoxyphenyl)prop-2-enoyl]phenyl}-2-{[(pyridin-3-yl)methyl]amino} acetamide (**9g**) in $CDCl_3$

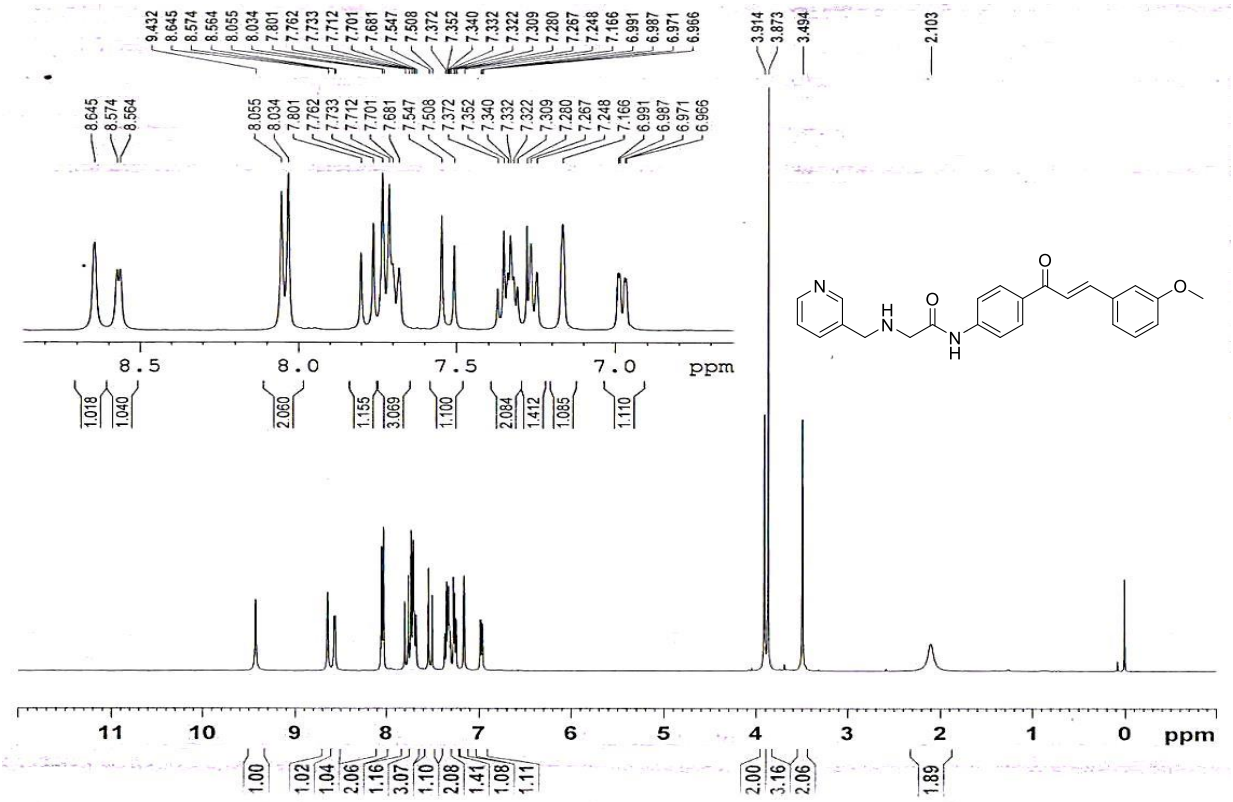

Figure-3b.11.3 ^{13}C-NMR spectrum of N-{4-[(2E)-3-(3-Methoxyphenyl)prop-2-enoyl] phenyl}-2-{[(pyridin-3-yl)methyl]amino} acetamide (**9g**) in $CDCl_3$

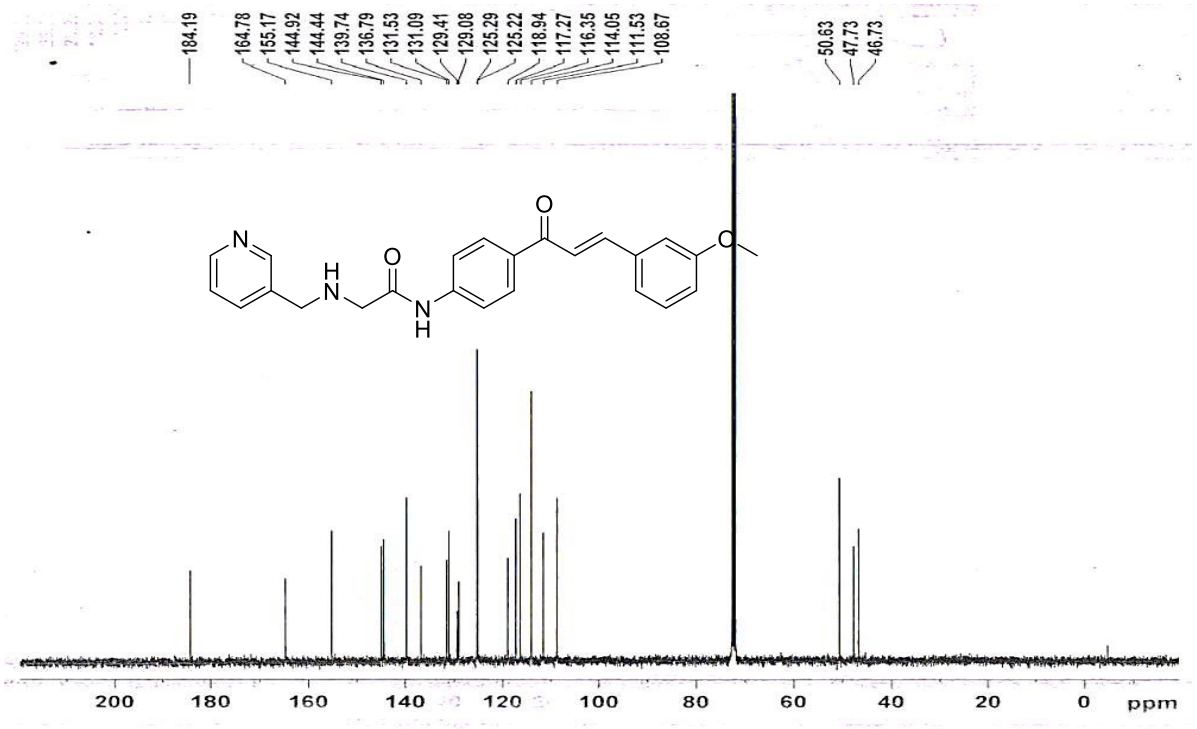

Figure-3b.11.4 ESI-MS spectrum of N-{4-[(2E)-3-(3-Methoxyphenyl)prop-2-enoyl]phenyl}-2-{[(pyridin-3-yl)methyl]amino} acetamide (**9g**) M+H peak at 402.15

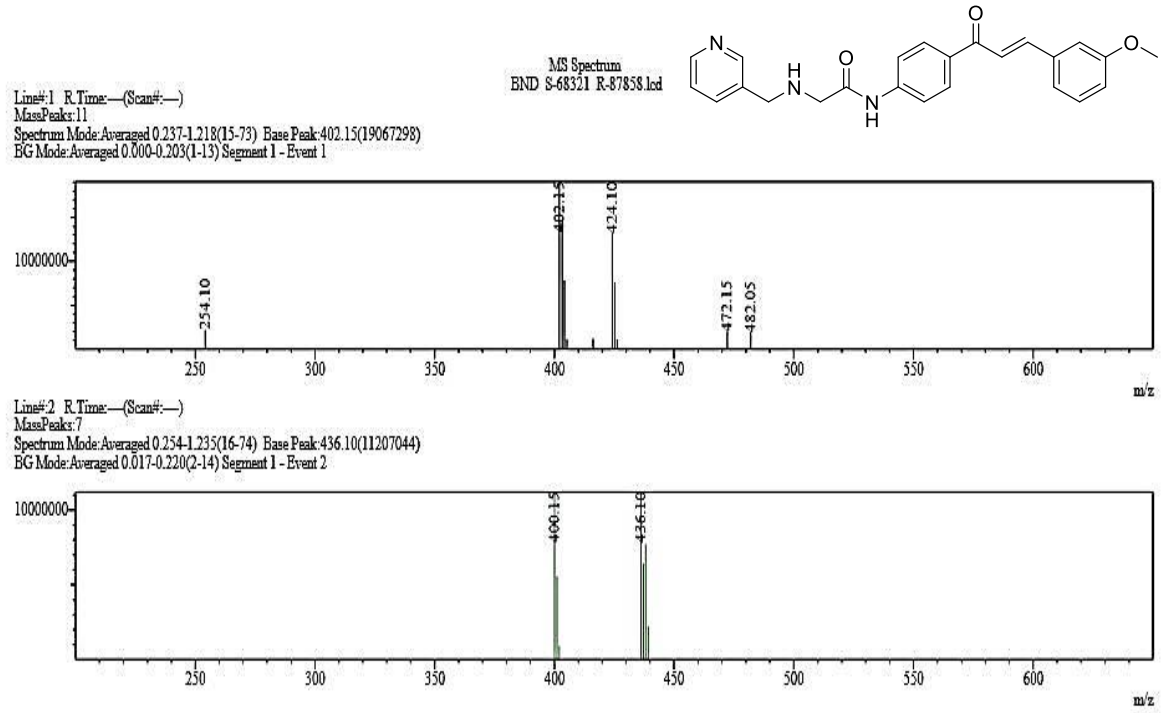

Figure-3b.12.1 IR spectrum of N-{4-[(2E)-3-(2-Chlorophenyl)prop-2-enoyl]phenyl}-2-{[(pyridin-3-yl)methyl]amino} acetamide (**9h**)

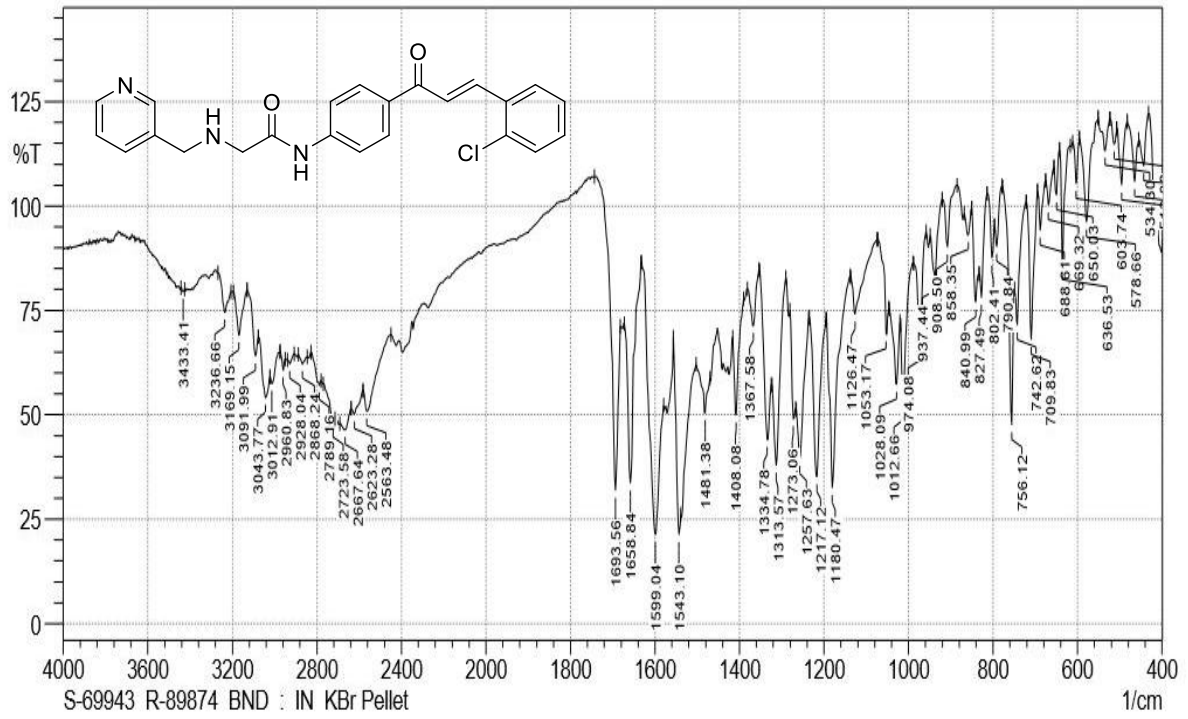

Figure-3b.12.2 ^{1}H-NMR spectrum of N-{4-[(2E)-3-(2-Chlorophenyl)prop-2-enoyl] phenyl}-2-{[(pyridin-3-yl)methyl]amino} acetamide (**9h**) in $CDCl_3$

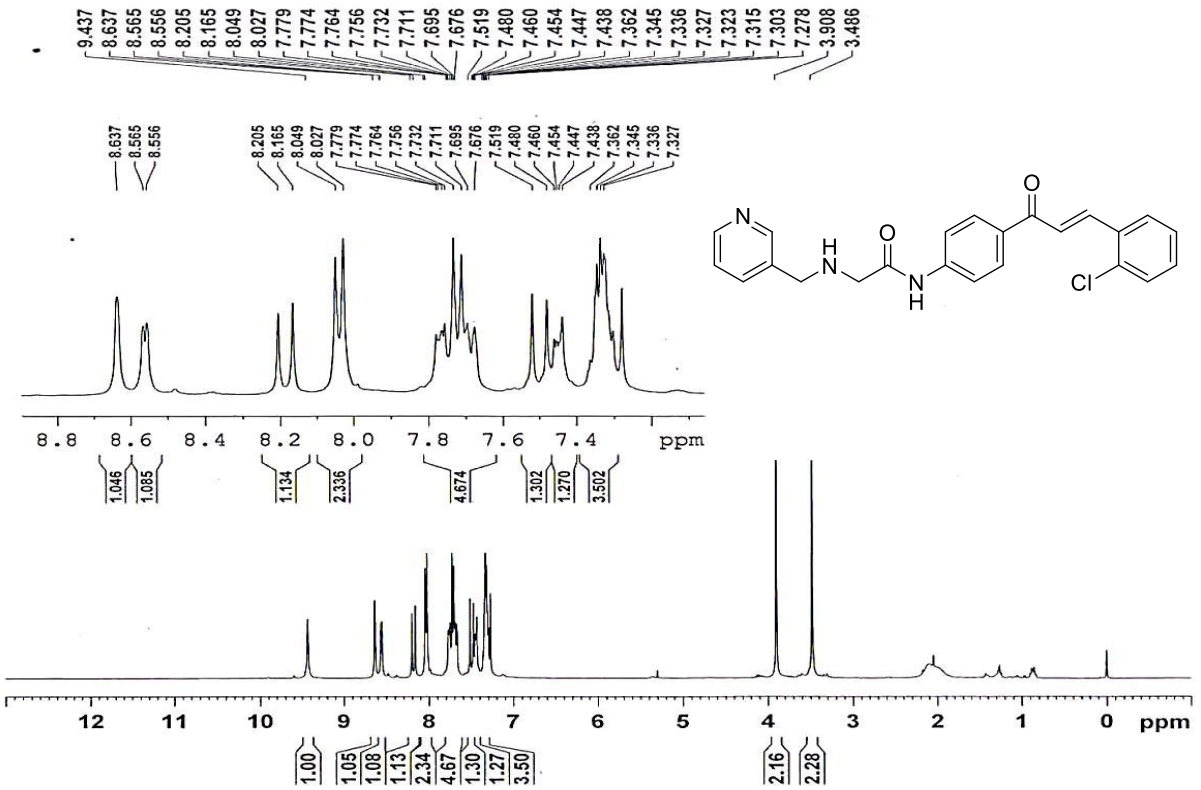

Figure-3b.12.3 ^{13}C-NMR spectrum of N-{4-[(2E)-3-(2-Chlorophenyl)prop-2-enoyl]phenyl}-2-{[(pyridin-3-yl)methyl]amino} acetamide (**9h**) in $CDCl_3$

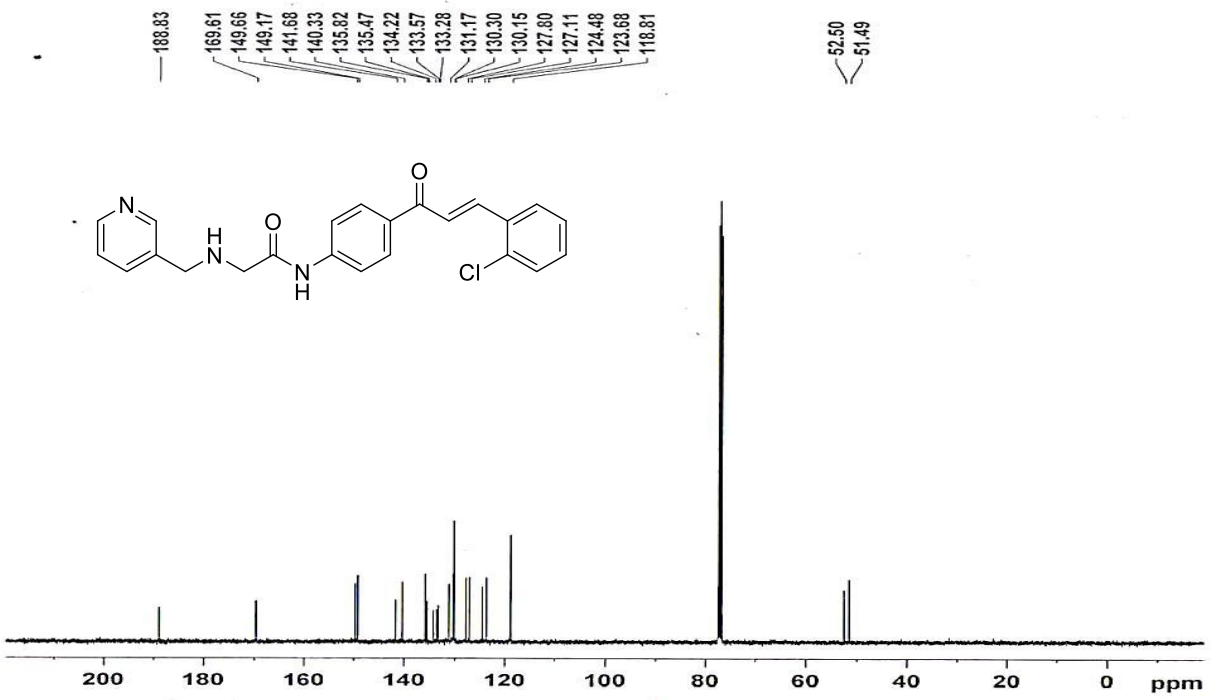

Figure-3b.12.4 ESI-MS spectrum of N-{4-[(2E)-3-(2-Chlorophenyl)prop-2-enoyl]phenyl}-2-{[(pyridin-3-yl)methyl]amino} acetamide (**9h**) M+H peak at 406.05

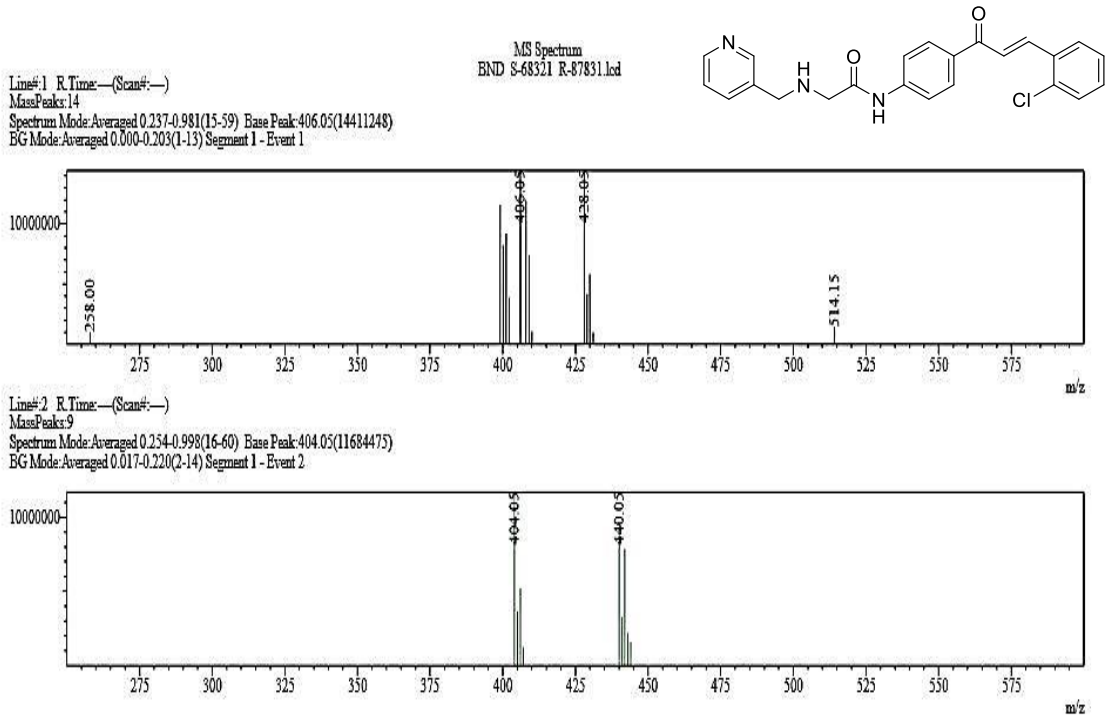

Figure-3b.13.1 IR spectrum of N-{4-[(2E)-3-(3-Chlorophenyl)prop-2-enoyl]phenyl}-2-{[(pyridin-3-yl)methyl]amino} acetamide (**9i**)

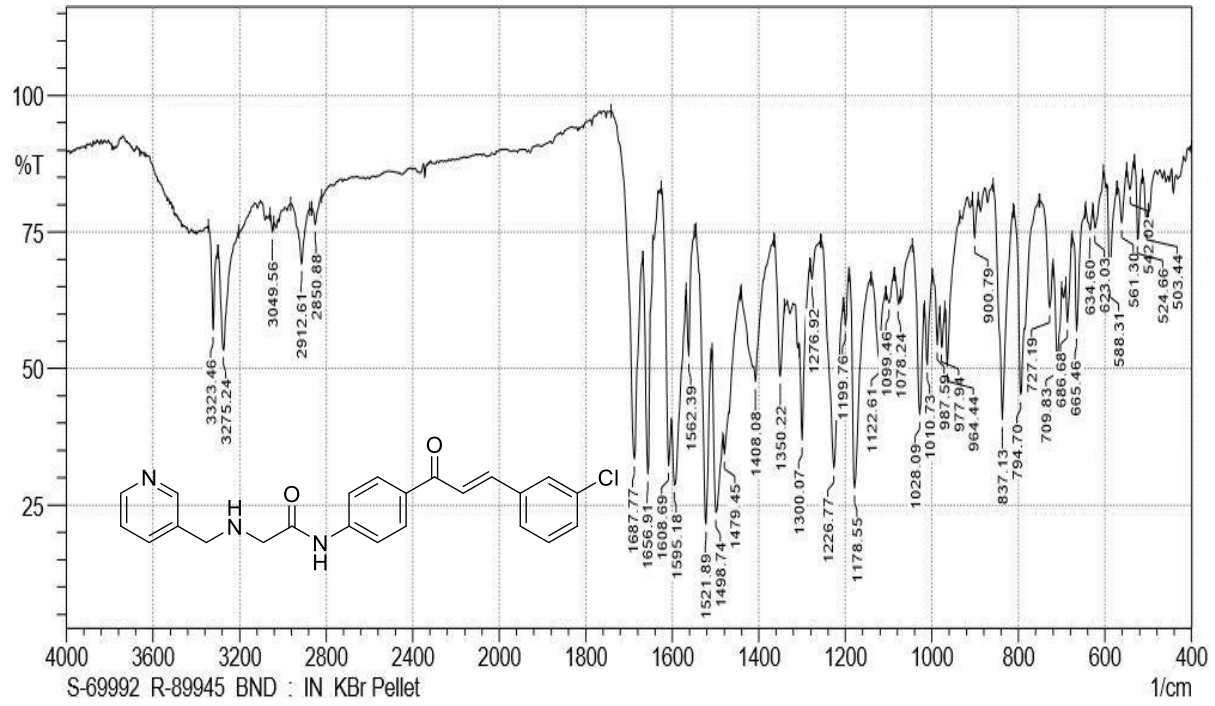

Figure-3b.13.2 ^{1}H-NMR spectrum of N-{4-[(2E)-3-(3-Chlorophenyl)prop-2-enoyl]phenyl}-2-{[(pyridin-3-yl)methyl]amino} acetamide (**9i**) in $CDCl_3$

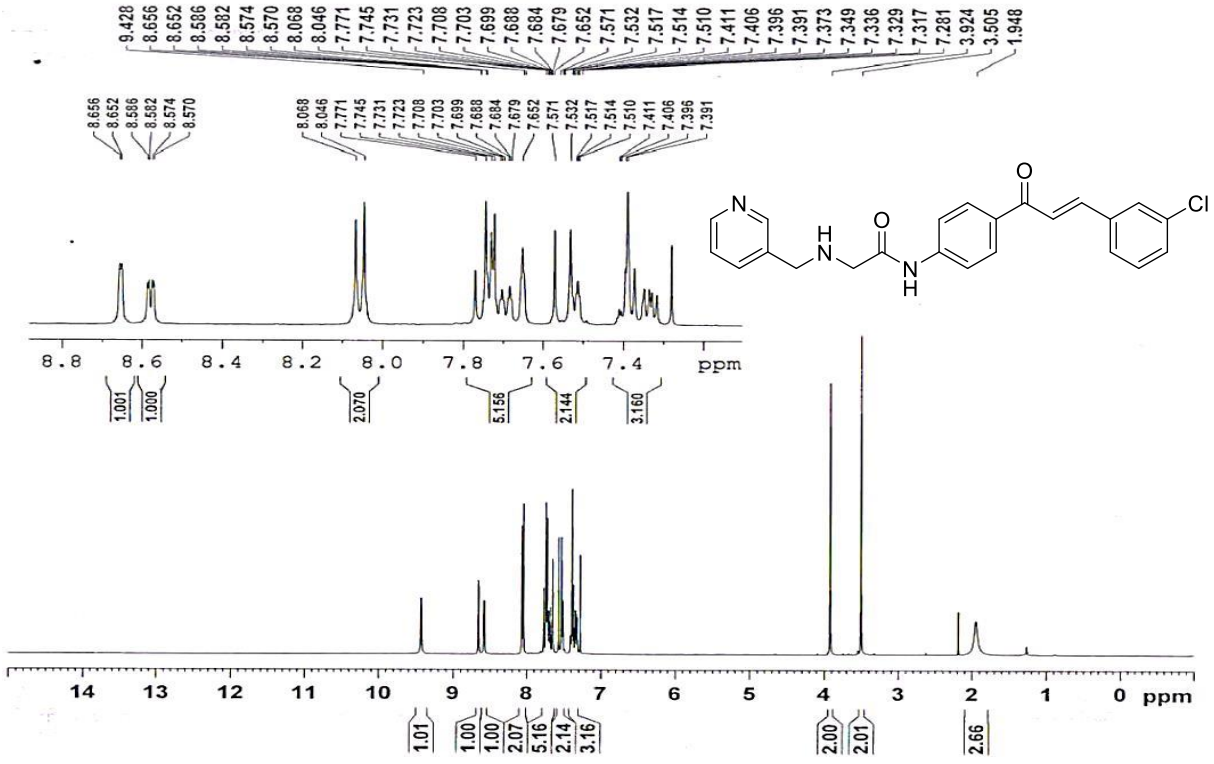

Figure-3b.13.3 ^{13}C-NMR spectrum of N-{4-[(2E)-3-(3-Chlorophenyl)prop-2-enoyl]phenyl}-2-{[(pyridin-3-yl)methyl]amino} acetamide (**9i**) in $CDCl_3$

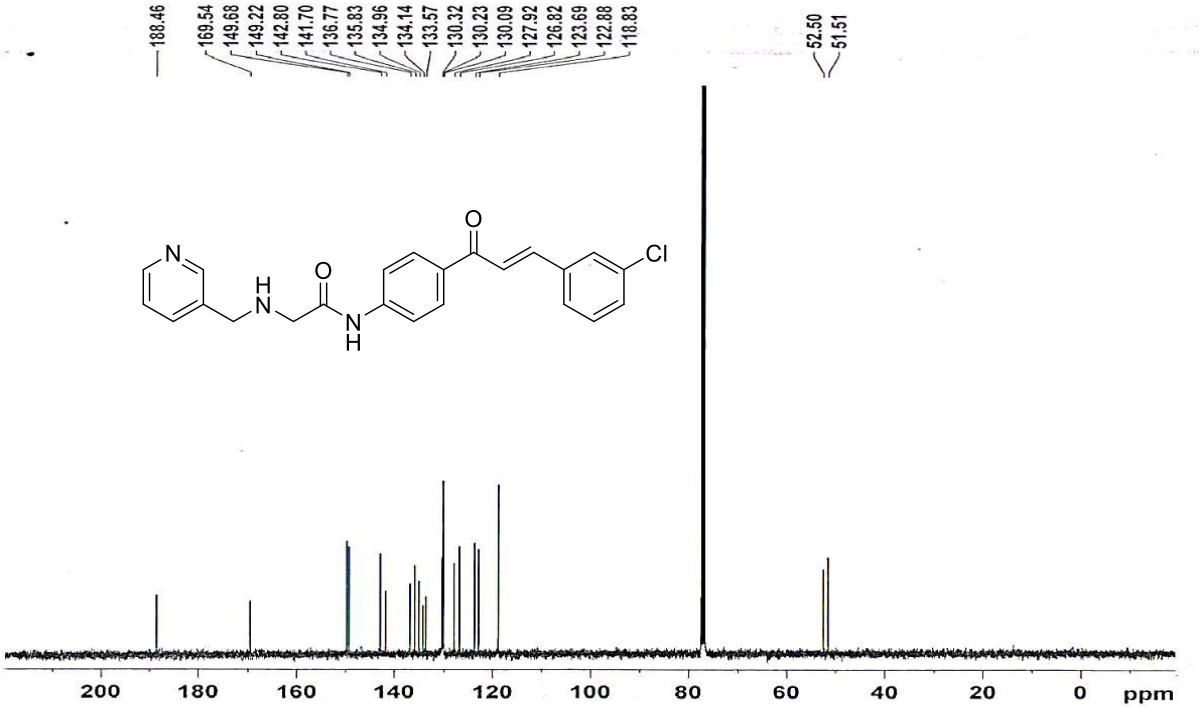

Figure-3b.13.4 ESI-MS spectrum of N-{4-[(2E)-3-(3-Chlorophenyl)prop-2-enoyl]phenyl}-2-{[(pyridin-3-yl)methyl]amino} acetamide (**9i**) M+H peak at 406.10

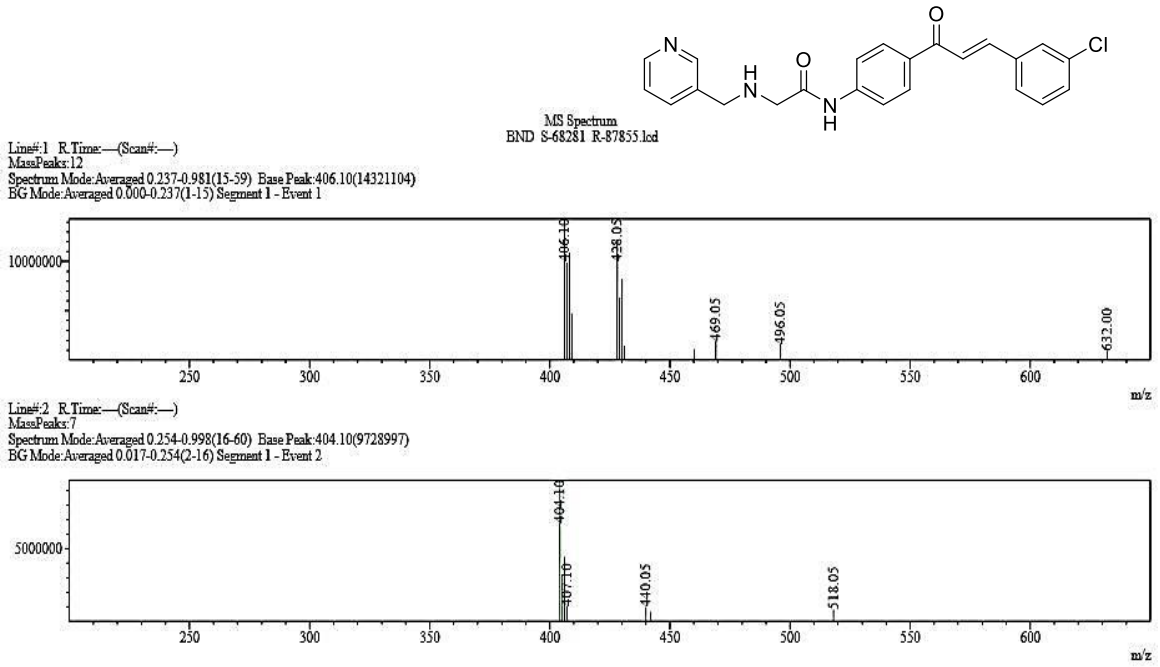

Figure-3b.14.1 IR spectrum of N-{4-[(2E)-3-(2,4-Dichlorophenyl)prop-2-enoyl]phenyl}-2-{[(pyridin-3-yl)methyl]amino} acetamide (**9j**)

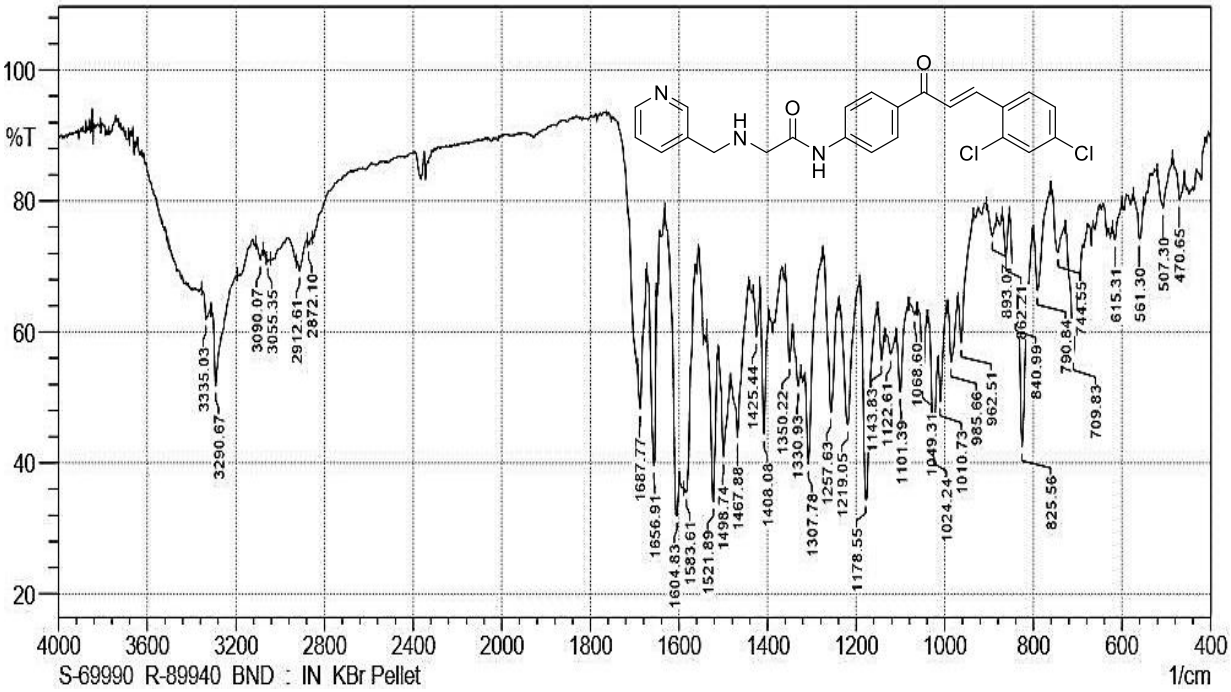

Figure-3b.14.2 ^{1}H-NMR spectrum of N-{4-[(2E)-3-(2,4-Dichlorophenyl)prop-2-enoyl]phenyl}-2-{[(pyridin-3-yl)methyl]amino} acetamide (**9j**) in $CDCl_3$

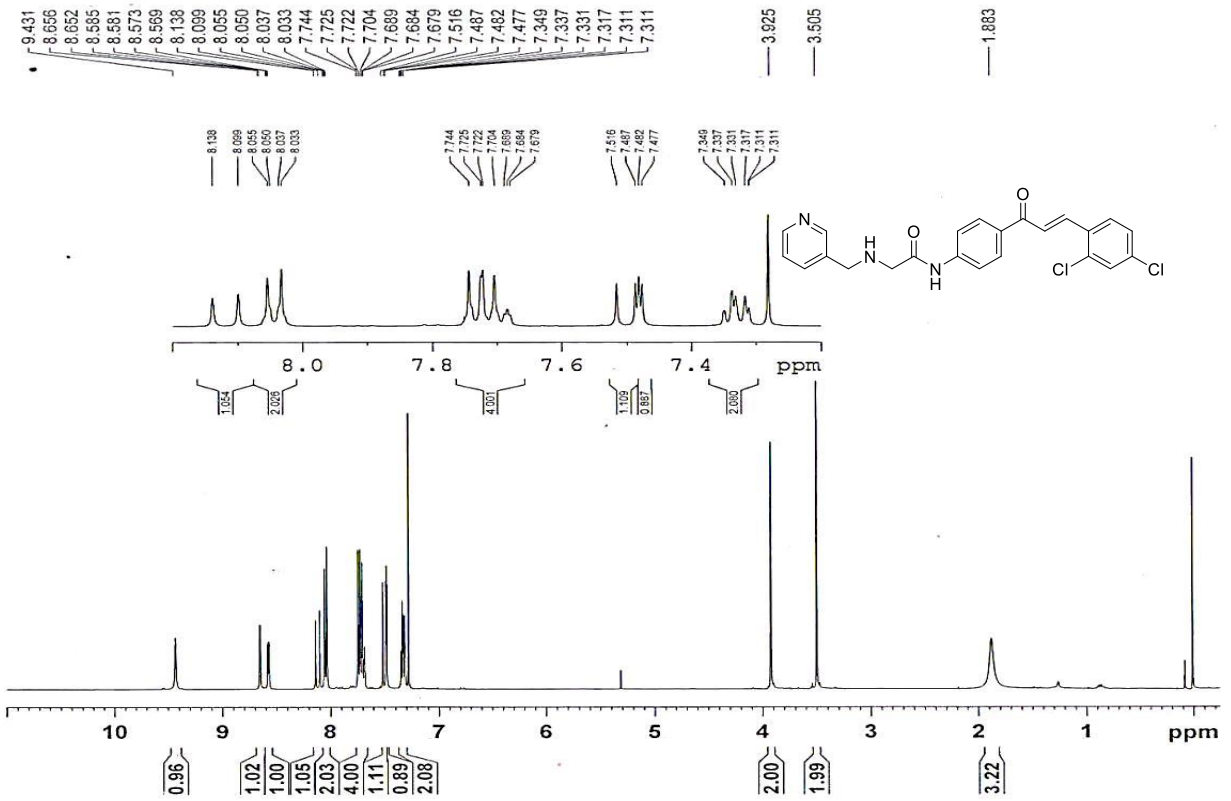

Figure-3b.14.3 ^{13}C-NMR spectrum of N-{4-[(2E)-3-(2,4-Dichlorophenyl)prop-2-enoyl]phenyl}-2-{[(pyridin-3-yl)methyl]amino} acetamide (**9j**) in $CDCl_3$

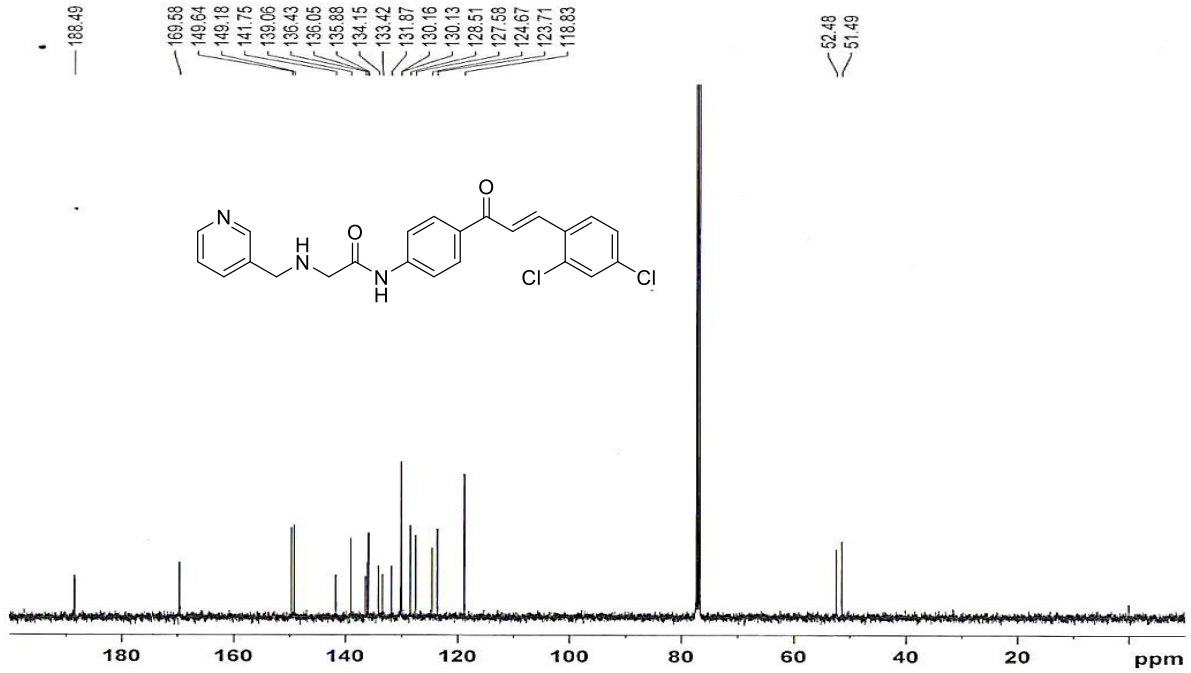

Figure-3b.14.4 ESI-MS spectrum of N-{4-[(2E)-3-(2,4-Dichlorophenyl)prop-2-enoyl]phenyl}-2-{[(pyridin-3-yl)methyl]amino} acetamide (**9j**) M+H peak at 440

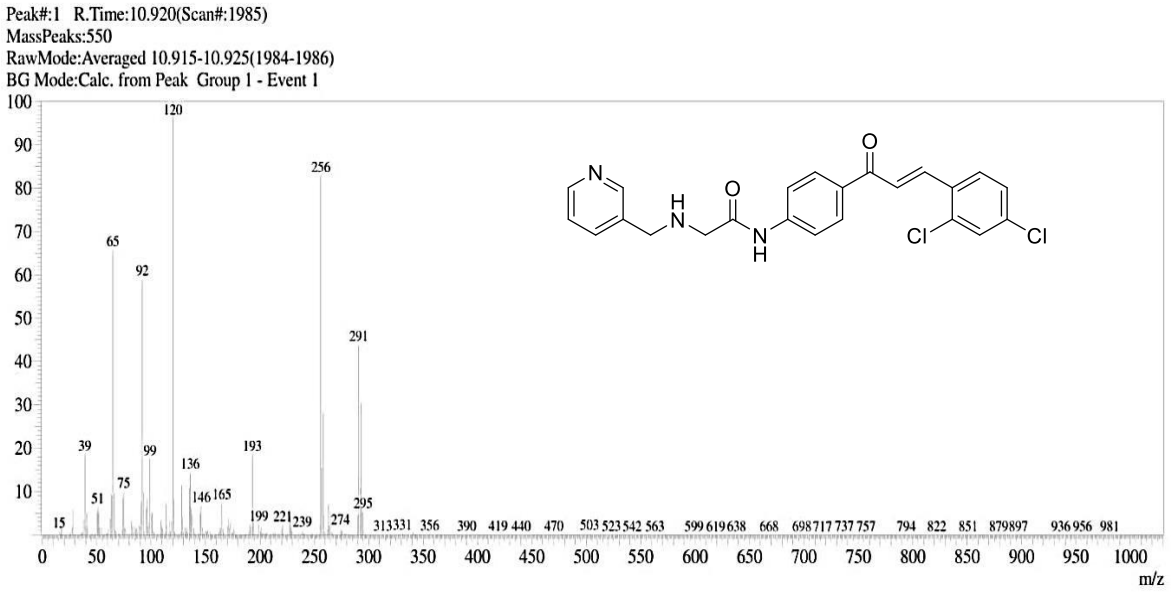

Figure-3b.15.1 IR Spectrum of (E)-N-(4-(3-(4-methoxyphenyl)acryloyl)phenyl)-2-((pyridin-2-yl methyl)amino)acetamide (**10c**)

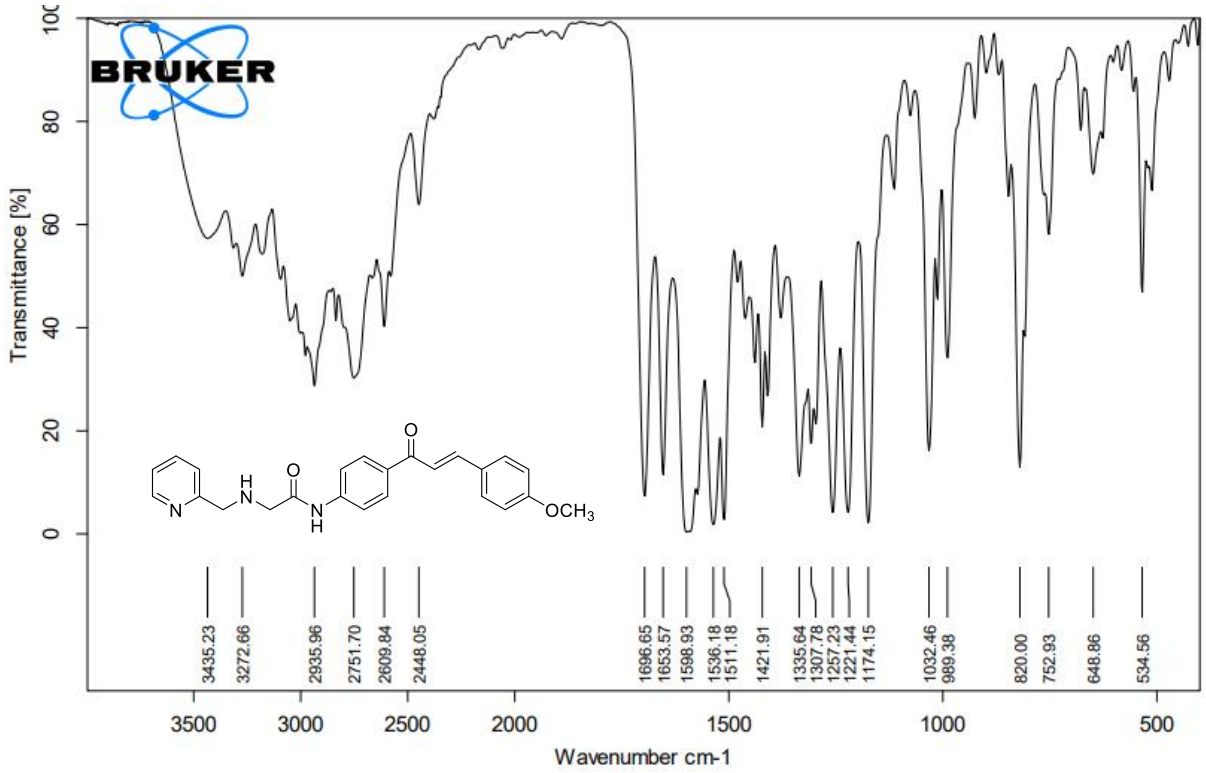

Figure-3b.15.2 ^{1}H-NMR Spectrum of (E)-N-(4-(3-(4-methoxyphenyl)acryloyl) phenyl)-2-((pyridin-2-yl methyl)amino)acetamide (**10c**) in $CDCl_3$

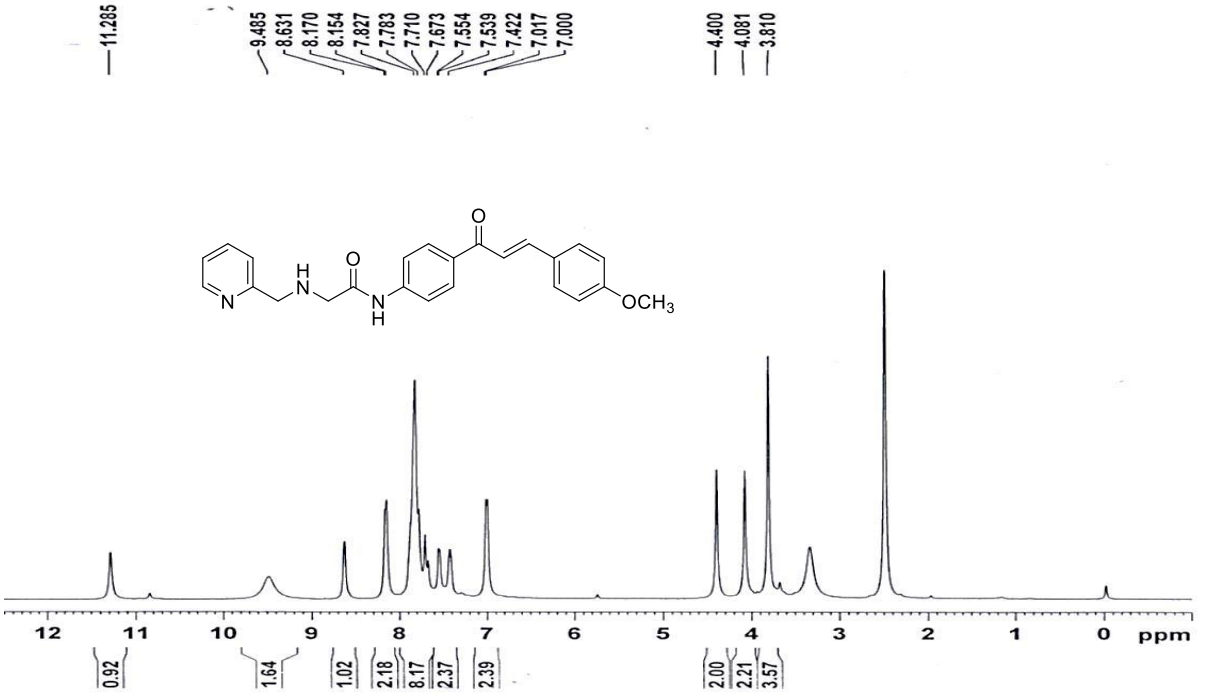

Figure-3b.15.3 ^{13}C-NMR Spectrum of (E)-N-(4-(3-(4-methoxyphenyl)acryloyl) phenyl)-2-((pyridin-2-yl methyl)amino)acetamide (**10c**) in $CDCl_3$

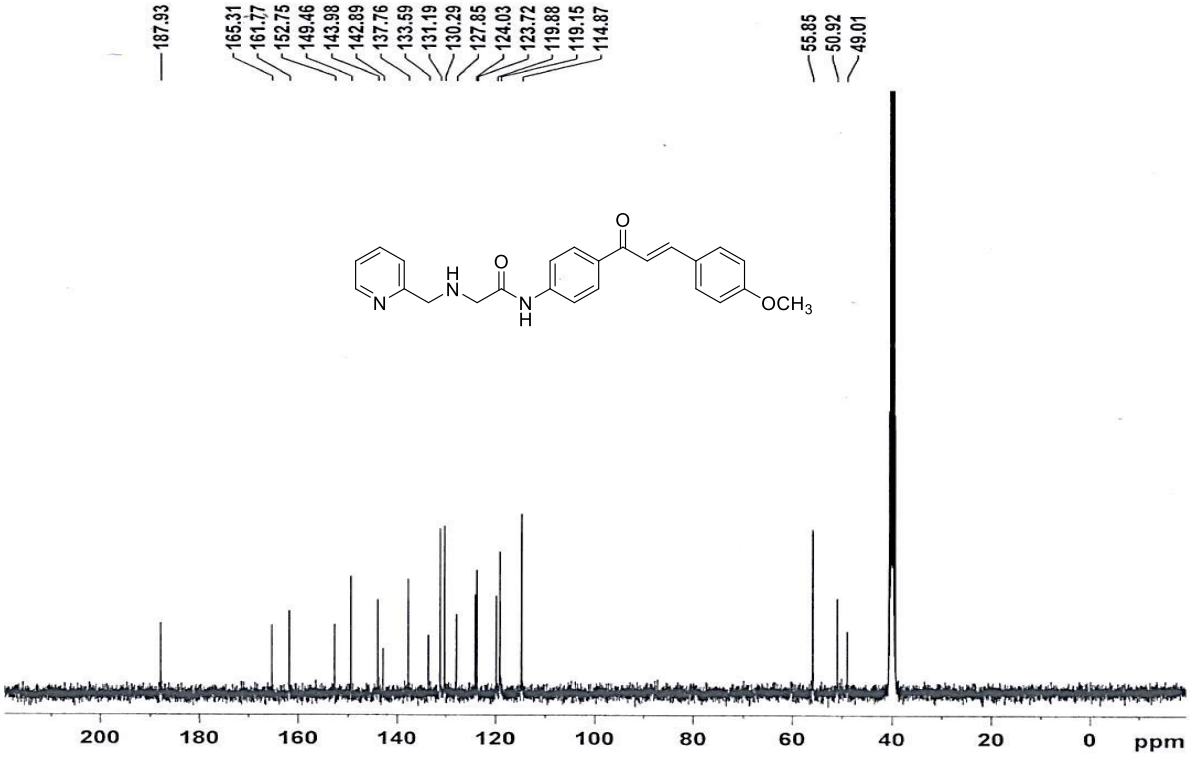

Figure-3b.16.1 IR spectrum of (E)-N-(4-(3-(3-chlorophenyl)acryloyl)phenyl)-2-((pyridin-2-yl methyl)amino)acetamide (**10i**)

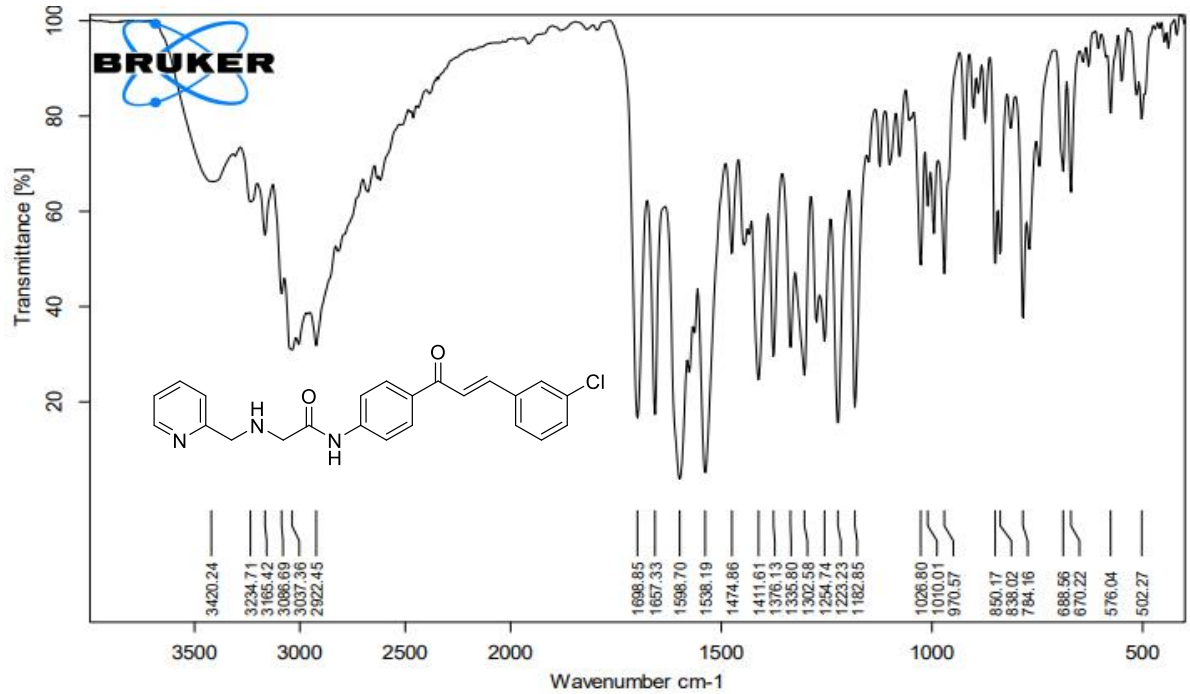

Figure-3b.16.2 ^{1}H-NMR spectrum of (E)-N-(4-(3-(3-chlorophenyl)acryloyl)phenyl)-2-((pyridin-2-yl methyl)amino)acetamide (**10i**) in $CDCl_3$

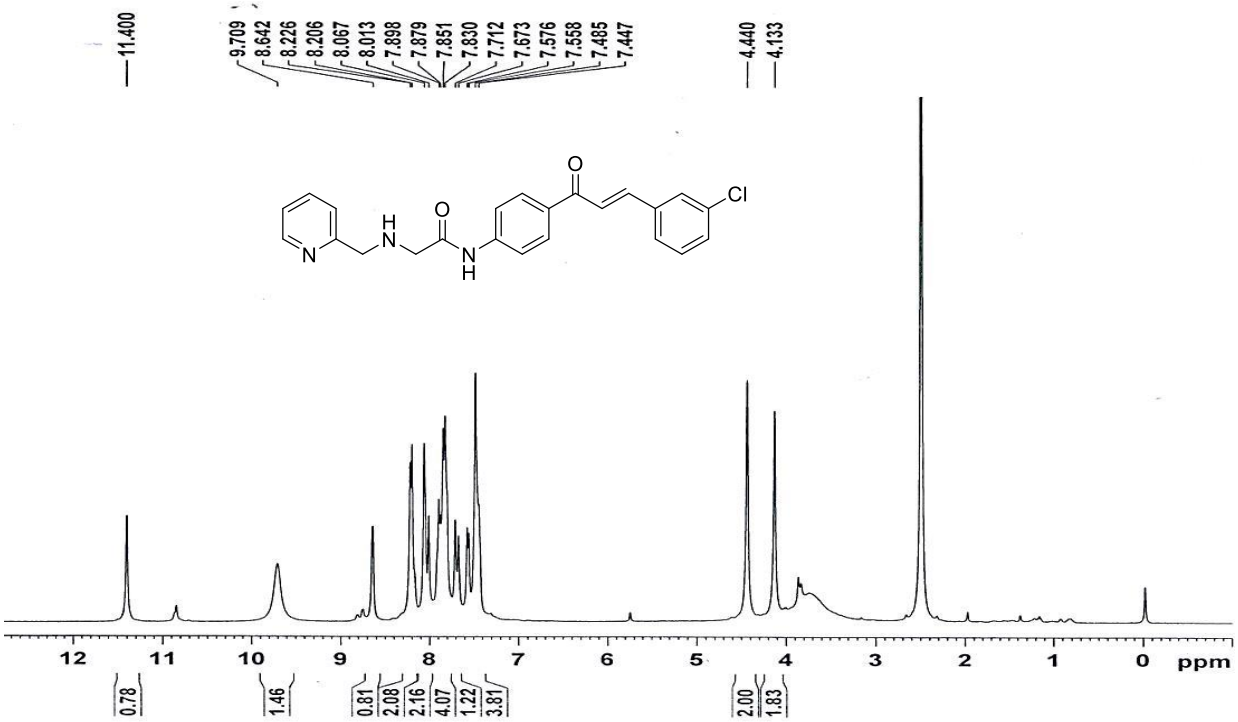

Figure-3b.16.3 ^{13}C-NMR spectrum of (E)-N-(4-(3-(3-chlorophenyl)acryloyl)phenyl)-2-((pyridin-2-yl methyl)amino)acetamide (**10i**) in $CDCl_3$

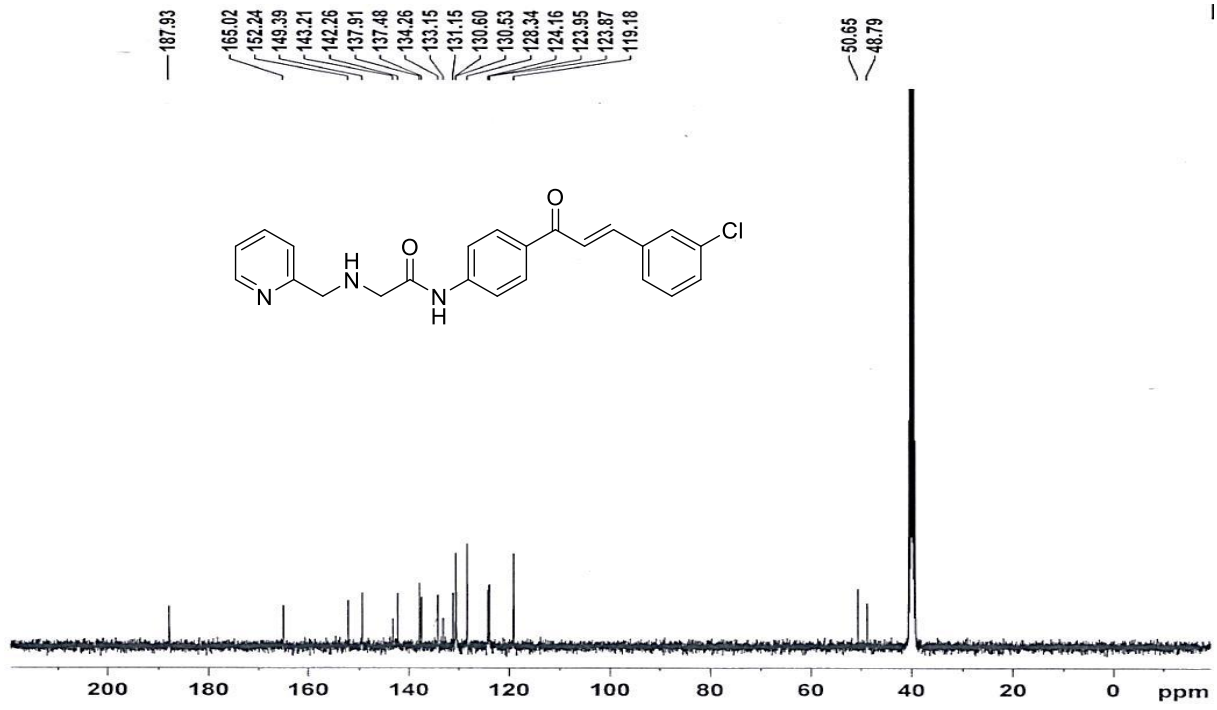

3b.2.2 Biological Evaluation

3b.2.2.1 Anticancer activity

3-Aminomethyl pyridine derivatives **6a-b, 9a-j** and **10c,i** were screened for their anticancer activity against A549 (Lungs cancer cell line), and MCF-7 (Breast cancer cell line) cell lines using MTT assay and compared the results with that of standard drug Fluorouracil (**Table-3b.1**) [13].

Structure activity relationship (SAR) for anticancer activity

Compound **6a** with 7-amino 4-methyl chromen-2-one and **6b** with 3-amino chromen-2-one showed very poor anticancer activity against lung cancer A549 and breast cancer MCF7 cell lines. 3-Aminomethyl pyridine linked to 4-amino chalcones showed very good activity profile for anticancer activity in MTT assay against tested cell lines (**Table-3b.2**). Compounds **9g-j** showed good activity against MCF-7 cell line as compared to A549 cell line. Compound **9a** showed very good activity against A549 cell line with IC_{50} 6.18 ± 0.11 μM, but showed poor activity in MCF-7 cell line. On placing methyl group at para position of benzene ring of chalcone in compound **9b** resulted in loss of activity against both tested cell lines.

Table-3b.1: Anticancer activity against A549 (Lungs cancer cell line), MCF-7 (Breast cancer cell line) for compounds **6a,b**.

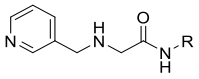

Compound no	R	IC_{50} in μM[a] A549	MCF-7
6a	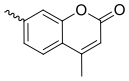	177.10 ± 18.2	377.8 ± 29.32
6b	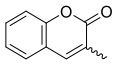	69.1 ± 8.2	298.9 ± 21.2
fluorouracil		11.13 ±0.083	45.04 ±1.02

[a]IC_{50} values were determined based on MTT assay using GraphPadPrism software. NA = Not active

Compound **9c** with methoxy group on 4th position showed very good activity against A549 cell line with IC_{50} 0.269 ± 0.0089 μM, but it was inactive against MCF-7 cell line. When nitro group is at para position for compound **9f**, showed poor activity against A549 cell line, while remained inactive against MCF-7 cell line. Compound **9e** having chloro at 4th position, showed very good activity with IC_{50} 5.14 ± 1.07 μM against A549 cell line. Further position change of methoxy group from 4th position in compound **9c** to 3rd position in compound **9g**, resulted in decrease in activity against A549 cell line, however this variation showed excellent activity against MCF-7 cell line with IC_{50} 0.174 ± 0.0076 μM (**Table-3b.2**).

Table-3b.2: Anticancer activity against A549 (Lungs cancer cell line), MCF-7 (Breast cancer cell line) compounds **9a-j, 10c,i**.

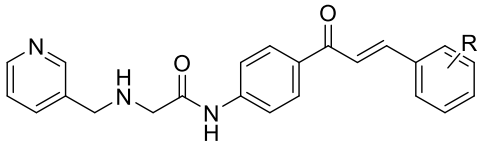

Compound no	Ar	IC_{50} in μM[a]	
		A549	**MCF-7**
9a	-H	6.18 ± 0.11	53.27 ± 3.56
9b	4-CH_3	132.00 ± 9.86	90.61 ± 5.96
9c	4-OCH_3	0.269 ± 0.0089	n/a
9d	4-F	16.04 ± 3.43	n/a
9e	4-Cl	5.14 ± 1.07	n/a
9f	4-NO_2	28.19 ± 1.19	n/a
9g	3-OCH_3	32.42 ± 2.08	0.174 ± 0.0076
9h	2-Cl	46.89 ± 6.08	71.72 ± 5.32
9i	3Cl	0.245 ± 0.011	0.0067 ± 0.0002
9j	2,4-Cl	62.26 ± 5.9	92.21 ± 7.21
10c	4-OCH_3	36.25±0.952	13.07±1.438
10i	3-Cl	10.32±0.082	16.25±2.013
fluorouracil		11.13 ±0.083	45.04 ±1.02

[a]IC_{50} values were were determined based on MTT assay using GraphPad Prism software. NA = Not active

On replacement of chloro from 4th to 2nd position in compound **9h** showed loss of activity against both tested cell lines. Interestingly, compound **9i** with chloro on 3rd position showed very good activity against A549 cell line and excellent activity against MCF-7 cell line. Compound **9j** containing 2,4-dichloro showed moderate activity against tested cell lines. Compound **10c** having 2-amino methylpyridine with methoxy on 4th position of chalcone showed poor activity in A549 cell line and moderate activity in MCF7 cell line. Compound **10i** with chloro on meta position showed moderate activity on both the tested cell lines.

Out of all screened compounds **6a,b** (**Table-3b.1**) and **9a-j, 10c,i** (**Table-3b.2**), compounds **9g** and **9i** showed excellent activity with IC_{50} 0.174 ± 0.0076 μM and 0.0067 ± 0.0002 μM respectively, as compared to standard drug Fluorouracil against MCF-7 cell line in MTT assay. Hence Compounds **9g** and **9i** were selected for DNA binding studies.

3b.2.2.2 DNA binding studies

From the results of MTT assay compound **9g** and **9i** were selected for DNA-binding studies as they showed excellent activity against MCF7 cancer cell lines. To explore mode of interaction of compounds **9g** and **9i** with DNA in cell, DNA binding UV based DNA titration and fluorescence emission study against DNA-EtBr complex were carried out (**Fig-3b.17**) [14]. The fixed concentration of compounds **9g** and **9i** was titrated against the known concentration of CT-DNA solution with tris-HCl buffer (pH 7.2). The strength of binding to CT-DNA was determined through the calculation of intrinsic binding constant K_b which is obtained by monitoring the changes in the absorbance of the compounds with increasing concentration of CT-DNA. Plot of [DNA]/ (ε_A-ε_f) *versus* [DNA] (equation 1) is used to find out K_b (**Fig-3b.17**).

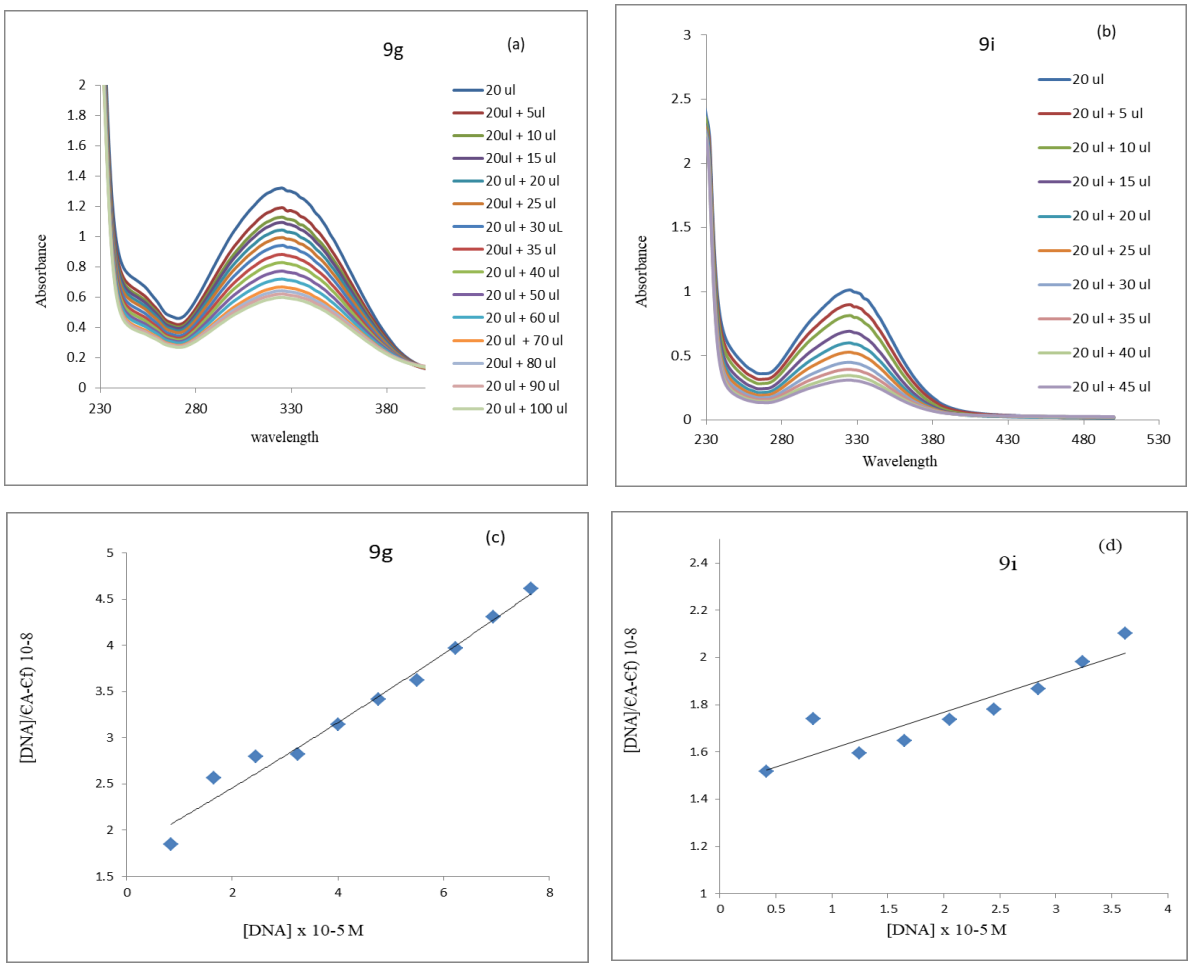

Figure-3b.17: Titration plot of compounds **9g** and **9i** with DNA. Plot of Absorbance *versus* Wavelength (nm) (a) for compound **9g** and (b) compound **9i**; Plot of [DNA]/(ε_A-ε_f) versus [DNA] (c) for compound **9g** and (d) for compound **9i.**

Compound **9g** and **9i** showed the hypochromic shift with the intrinsic binding (k_b) values 2.12 x 10^4 M^{-1} and 1.06 x 10^4 M^{-1} respectively in UV based DNA titrations indicated intercalative mode of binding (λ_{max} = 325 nm) (**Fig-3b.17** & **Table-3b.3**).

$$[DNA]/ (\varepsilon_A-\varepsilon_f) = [DNA]/ (\varepsilon_b-\varepsilon_f) + 1/K_b(\varepsilon_b-\varepsilon_f) \quad \text{(eq 1)}$$

Table-3b.3 K_b and K_{SV} values for compound **9g** and **9i** .

Compound no	λ_{max} nm	UV based assay K_b (M^{-1})	Emission λ_{max} nm	Fluorescence assay K_{SV} (M^{-1})
9g	325	2.12 x 10^4	610	5.21 x 10^3
9i	325	1.06 x 10^4	608	5.85 x 10^3

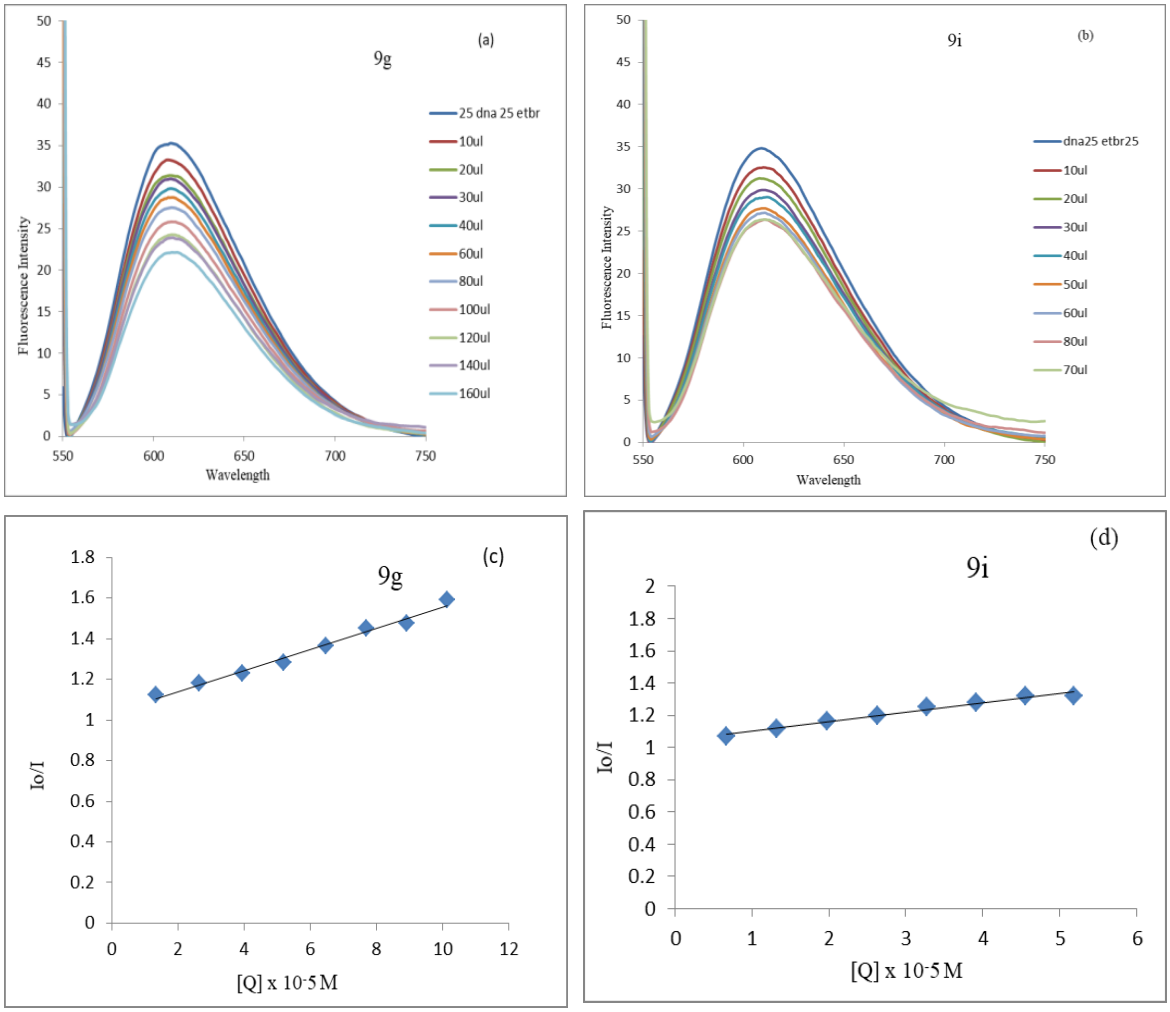

Figure-3b.18 Plot of Fluorescence emission intensity I *versus* Wavelength (nm) for DNA-EtBr complex at different concentrations (a) for compound **9g** and (b) for compound **9i.** Stem-Volmer quenching plot of DNA-EtBr (c) for compound **9g** and (d) compound **9i**.

Fluorescence emmission based Ethidium bromide (EtBr) displacement assay was also performed with compound **9g** and **9i**. The emission spectra of DNA-EtBr (λ_{ex} = 546 nm) in the absence and presence of increasing amount of compound **9g** and **9i** were recorded at emission λ_{max} 608 nm**.** (**Fig-3b.18**). The data were plotted according to the Stern-Volmer equation (eqation 2). Quenching of fluoroscence intensity was observed for compound **9g** and **9i** with K_{sv} values 5.21 x 10^3 M^{-1} and 5.85 x 10^3 M^{-1} respectively (**Table-3b.3**), which supports the DNA intercalating property of these compounds (**Figure-3b.18**).

$$I_0/I = 1 + K_{SV}[Q] \qquad \text{(eq 2)}$$

3b.2.2.3 Cytotoxic studies

Compound **9i** induced cytotoxic studies in A549, MCF-7 cancer cell lines and NIH/3T3 non cancer cell lines were performed. The cytotoxicity of compound **9i** was estimated using MTT assay and IC_{50} conc. of compound **9i** was measured in both the cancer cell line as well as in non-cancer cell line. Mechanism of cytotoxicity was evaluated by Trypan blue and LDH assay in cancer cell lines. LDH assay is based on the release of cytosolic enzyme into culture medium due to the damage of cell membrane which is a hallmark of necrosis, while MTT assay is based on the activity of mitochondrial dehydrogenase enzyme activity and represent the metabolic rate or percentage viability of cell [15-17] (**Fig-3b.19).**

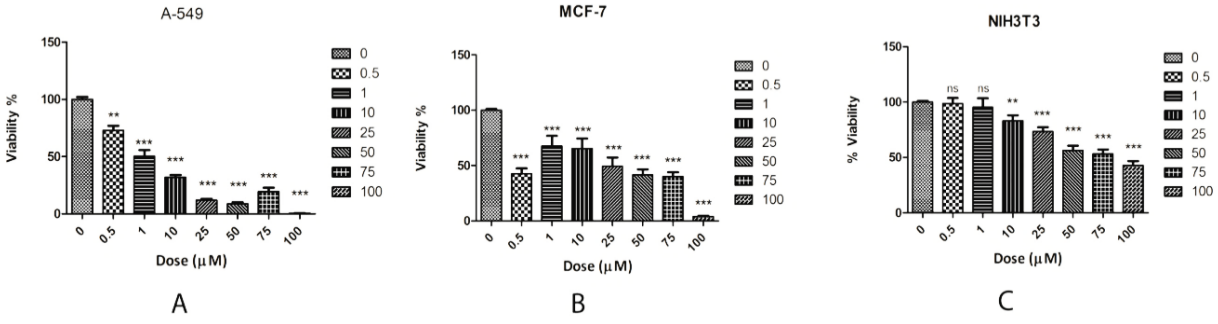

Figure-3b.19: The cytotoxicity of compound **9i** against A549 (A), MCF-7 (B) and NIH/3T3 (C) cell line. **In MTT assay (A-C)** cells were treated with 0.5, 1, 10, 25, 50, 75, 100 µM concentrations of compound **9i** graph was plotted against % viability v/s dose. Data were represented as mean ± SD from three independent experiments. ***P<0.001

In MTT assay, the percentage viability of cell line was decreased with increased concentration of compound **9i**. IC_{50} concentration of compound **9i** was estimated using Graphpad Prism 5

software viz. 0.245 ± 0.011, and 0.0067 ± 0.0002 µM in A549 and MCF-7 cell line respectively (**Fig-3b.19** (A) and **Fig-3b.19** (B)). Compound **9i** showed IC_{50} 79.31 ± 0.08 µM (**Fig-3b.19** (C)) for non-cancer mouse fibroblast cell line (NIH/3T3), which was significantly high compare to IC_{50} values against cancer cell lines A549 and MCF-7. These results prove beyond doubt that when cancer cell will be treated at such lower concentration of compound **9i**, will not be cytotoxic to nearby normal cells, hence, compound **9i** was very specific toward cancer cells. Therefore, it was taken further for the study of mechanism in cancer cell lines against A549 and MCF-7 cell line.

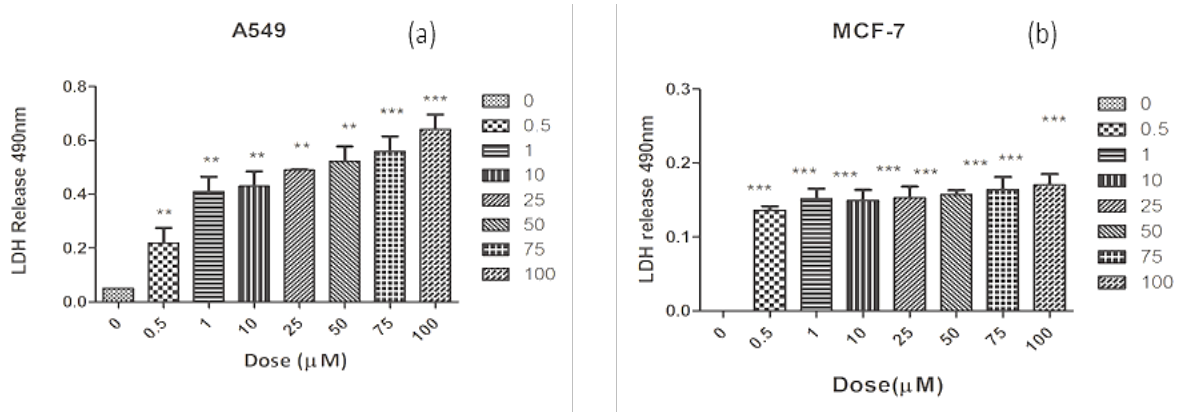

Figure-3b.20 In LDH assay (a-b): Representation of cytosolic enzyme LDH (a) activity of LDH in A549 cell line (b) activity of LDH in MCF-7 cell line. Cells were treated with 0.5, 1, 10, 25, 50, 75, 100 µM concentrations of compound **9i**. Graph was plotted against LDH release versus dose. (***P ≤ 0.001, **p < 0.01) significance one-way ANOVA (Tukey–Kramer). ANOVA, analysis of variance; LDH, lactic dehydrogenase

There are several mechanisms by which an anticancer compound exerts its effect on cancer cell *in vitro*. Apoptosis and necrosis are the most preferred mechanisms. To understand the mode of cytotoxicity of compound **9i** for cancer cell lines, LDH Assay was performed in both cancer cell lines (**Fig-3b.20**). At lower concentration of compound **9i**, the LDH release was very low which revealed that at lower concentration the prevalent mechanism of cytotoxicity was apoptosis but with increased concentration of compound **9i** LDH release increases significantly therefore, at higher concentration treated cells changed its fate towards the necrosis from apoptosis. As IC_{50} value of compound **9i** is very low for both cell lines therefore, it can be deduced that preferred mechanism of cytotoxicity for compound **9i** can be apoptosis (**Fig-3b.20** (a)-(b)).

To confirm, that loss of percentage viability was either due to cell death or due to cell proliferation inhibition effect of compound **9i**, Trypan blue assay was performed in both A549

and MCF-7 cell lines. The percentage cell death at IC_{50} concentration of compound **9i** was approx. 36% ± 3% in A549 cell line and 45% ± 2.68% in MCF-7 cell line (**Fig-3b.21**), from this it can be construed that compound **9i** is cytotoxic towards the MCF-7 whereas it might be cytotoxic or cytostatic toward A549 cell line, further experimental confirmation is required to explain the effect of compound **9i** on cancer cell lines.

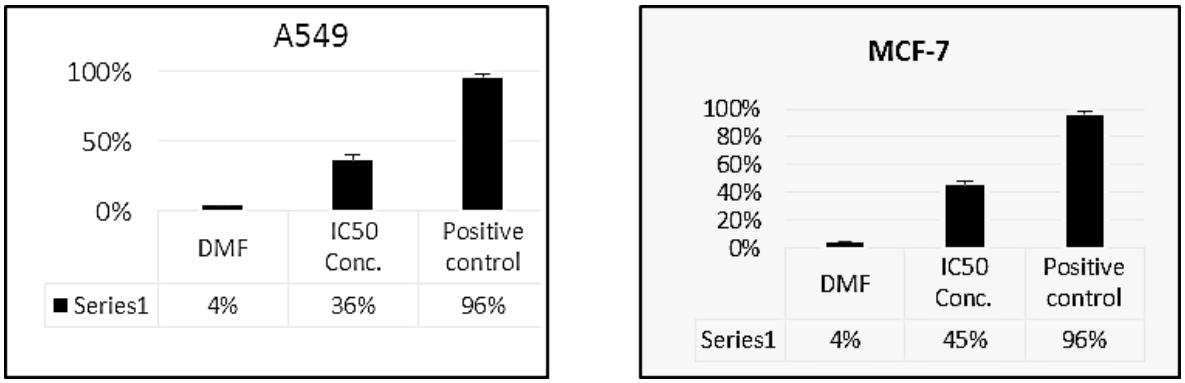

Figure-3b.21 Trypan blue assay- The percentages cell death of A549 and MCF-7 cell line treated with DMF, with IC_{50} concentration of compound **9i** and with positive control was plotted. Data was represented as mean ± SD from three independent experiments.

In order to reaffirm the findings of LDH assay, the EtBr/AO staining assay was performed with compound **9i**. Acridine orange is a vital dye that stains both live and dead cells however, ethidium bromide stains only the cells that have lost their membrane integrity. EtBr/AO dye stains, necrotic cells red, live cells green, early apoptotic cell's nuclei green but with visible condensation whereas, late apoptotic cell's nuclei Orange with condensation and fragmentation.

Cells were treated with IC_{50} concentration of compound **9i** and it was found that most of the cells of A549 cell line (**Fig-3b.22** a,b,c) were under late apoptosis, there were no cells under necrosis whereas, in MCF-7 cell line (**Fig-3b.22** d,e,f) most of the cells were under early apoptosis with few under necrosis. Number of the cells under apoptosis and necrosis were negligible in control cell lines; which confirmed the LDH assay finding that compound **9i** exhibits cytotoxic activity in both cell lines *via* apoptosis. To confirm the possible interaction of compound with DNA, compound **9i** was studied for DNA binding activity.

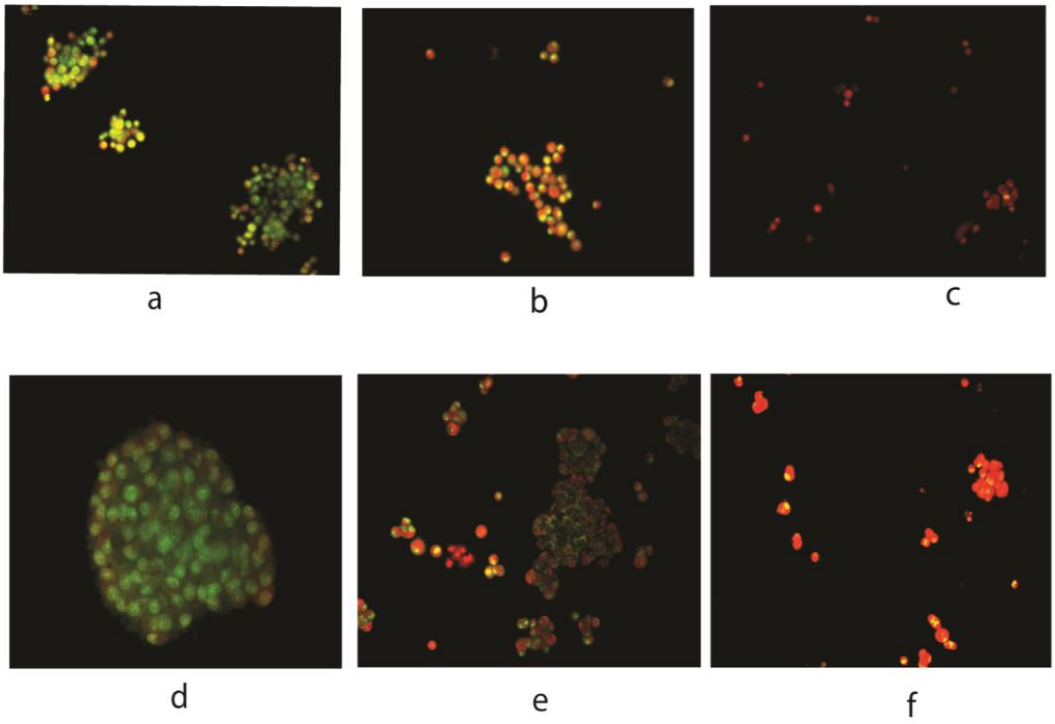

Figure-3b.22 EtBr/AO assay: EtBr/AO assay was performened with A549 cell line (a,b,c) and MCF-7 (d,e,f). (a,b,c) images represent control, IC_{50} conc. compound **9i** treated and positive control in A549 cell line. (d,e,f) images represent control, IC_{50} conc. compound **9i** treated and positive coontrol in MCF-7 cell line.

3b.3 Conclusion

In conclusion, a series of chalcones of 3-aminomethyl pyridine derivatives were synthesized and evaluated for their anticancer activity against A549 and MCF-7 cell lines. Based on MTT assay, compound 6a,b were inactive in both lungs and breast cancer cell lines. One of the compounds **9i** has shown very good selectivity for MCF-7 cancer cell line as compared to NIH/3T3 normal cell line (non-cancer mouse fibroblast cell line). DNA binding studies of compound **9i** indicated intercalation mode of binding with CT-DNA. The cytotoxic studies of compound **9i** have shown the apoptosis in MCF-7 cell line using LDH assay and the EtBr/AO assay. From K_b binding values it is observed that **9g** has two fold higher affinity for CT-DNA binding than **9i** but **9i** has more selectivity than **9g**. compounds **10c** and **10i** with 2-amino methylpyridine chalcone derivatives showed moderate activity as compared to active compound **9i** and

3b.4 Experimental

3b.4.1 Chemistry

Reagent grade chemicals and solvents were purchased from commercial supplier and used after purification. TLC was performed on silica gel F254 plates (Merck). Acme's silica gel (60-120 mesh) was used for column chromatographic purification. All reactions were carried out in nitrogen atmosphere. Melting points are uncorrected and were measured in open capillary tubes, using a Rolex melting point apparatus. IR spectra were recorded as KBr pellets on Perkin Elmer RX 1 spectrometer. ^{1}H NMR and ^{13}C NMR spectral data were recorded on Advance Bruker 400 spectrometer (400 MHz) with $CDCl_3$ or DMSO-d_6 as solvent and TMS as internal standard. *J* values are in Hz. Mass spectra were determined by ESI-MS, using a Shimadzu LCMS 2020 apparatus (Shimadzu Scientific Instruments, Inc., USA). Elemental analyses were recorded on Thermo Finnigan Flash 11-12 series EA. All reactions were carried out under nitrogen atmosphere. 7-amino-4-methyl chromen-2-one, 3-amino chromen-2-one and chalcones were prepared as reported in literature [19-21].

Preparation of N-substituted bromoacetamide derivatives (4, 5, 8)

To an ice-cold solution of substituted amines (10.0 mmol) in dichloromethane (DCM) (25 mL) was added triethylamine (TEA) (15.0 mmol) and stirred for 5-10 min. To this bromoacetyl bromide (12.0 mmol) was added dropwise over a period of 10 min under cooling. The resulting solution was stirred at 0-5 ^{o}C for 30 min and at room temperature for 24 hrs. The reaction mixture was diluted with water and extracted with DCM (2 x 30 mL). The organic layers were combined, washed with 0.5N HCl solution (15 mL), dried over anhydrous Na_2SO_4, filtered and evaporated on a rotavapor to give compounds **4**, **5** and **8**. The substituted bromoacetamide **4**, **5** and **8** were directly used for next step without any purification

General procedure for the preparation of compounds 6a-b, 9a-j and 10c,i.

To a cold solution of substituted bromoacetamide **4, 5**/**8** (1.0 eq) in DMF (20 mL) was added of 3-aminomethyl pyridine (0.5 g, 1.730 mmol) along with base triethylamine (1.5 eq) and stirred for 30 min. The resulting mixture was stirred at room temperature for 14-16 h. The completion of reaction was checked by TLC using DCM:MeOH (9:1). The reaction mixture was poured into ice-cold water. The aqueous layer was extracted using ethyl acetate or dichoromethane (3 x 25 mL). The organic layers were combined, dried over anhy. Na_2SO_4, filtered and concentrated on a rotavapor to give crude product. The crude compound was purified by column chromatography using DCM:MeOH (95:5). Compounds **6a-b, 9a-j** and

10c,i were obtained as a solid after column purification.

N-(4-Methyl-2-oxo-2H-1-benzopyran-7-yl)-2-{[(pyridin-3-yl)methyl]amino}acetamide (6a)

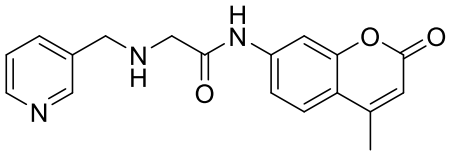

Pale yellow solid, Yield: 78 %; M.P: 138-140 °C; IR (KBr) 3294, 3286, 2895, 1685, 1620, 1587, 1535, 1419, 1386, 1230, 866, 752, 713 cm^{-1}; ^1H NMR (400 MHz, $CDCl_3$): δ 2.41 (s, 3H), 3.49 (s, 2H), 3.91(s, 2H), 6.19 (s, 1H), 7.28-7.33 (m, 1H), 7.53-7.57 (m, 2H), 7.65-7.78 (m, 2H), 8.55 (s, 1H), 8.62 (s, 1H), 9.48 (s, 1H), ^{13}C NMR (100 MHz, $CDCl_3$): δ ppm 18.64, 51.41, 52.41, 106.86, 113.39, 115.37, 116.18, 123.70, 125.33, 134.28, 135.90, 140.78, 149.11, 149.64, 152.36, 154.24, 161.12, 169.77; Anal. Calc. for $C_{18}H_{17}N_3O_3$; C, 66.86; H, 5.30; N, 13.00; found: C, 66.83; H, 5.26; N, 12.96 %; ESI-MS: 323.0 $[M-H]^+$.

N-(2-Oxo-2H-1-benzopyran-3-yl)-2-{[(pyridin-3-yl)methyl]amino}acetamide (6b)

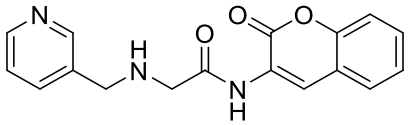

Pale yellow solid, Yield: 66 %; M.P: 170-172 °C; IR (KBr) 3059, 2836, 1712, 1691, 1624, 1508, 1483, 1361, 1220, 900, 800, 756, 715 cm^{-1}; ^1H NMR (400 MHz, $CDCl_3$): δ 3.51 (s, 2H), 3.89 (s, 2H), 7.28-7.35(m, 3H), 7.43-7.45 (m, 1H), 7.51 (d *J*=7.6 Hz, 1H), 7.89 (d, *J*=8.0 Hz, 1H), 8.55 (d *J*=4.0 Hz, 1H), 8.60 (s, 1H), 8.68 (s, 1H), 10.03 (s, 1H), ^{13}C NMR (100 MHz, $CDCl_3$): δ ppm 51.41, 52.46, 116.40, 119.77, 123.28, 123.62, 123.80, 125.13, 127.77, 129.71, 134.14, 136.32, 149.20, 149.61, 150.14, 158.63, 170.88; Anal. Calc. for $C_{17}H_{15}N_3O_3$; C, 66.01; H, 4.89; N, 13.58; found: C, 66.04; H, 4.92; N, 13.62 %; ESI-MS: 309.0 $[M-H]^+$.

N-{4-[(2E)-3-Phenylprop-2-enoyl]phenyl}-2-{[(pyridin-3-yl)methyl]amino}acetamide (9a)

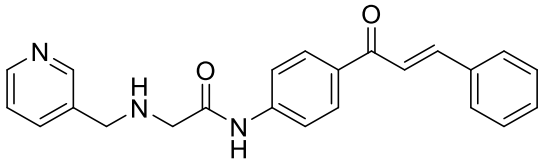

Pale yellow solid, Yield: 35 %; M.P: 148-150 °C; IR (KBr): 3327, 3267, 3055, 2912, 1685, 1649, 1604, 1587, 1529, 1344, 1174, 833, 765, 734, 711, 690 cm^{-1}; ^1H NMR(400 MHz, $CDCl_3$): δ 2.20 (br s, 1H), 3.48 (s, 2H), 3.94 (s, 2H), 7.30-7.33 (m, 1H), 7.42-7.43 (m, 3H), 7.55 (d, *J*=15.6 Hz, 1H), 7.64-7.67 (m, 3H), 7.20 (d, *J*=8.8 Hz, 2H), 7.81 (d, *J*=15.6 Hz, 1H), 8.04 (d, *J*=8.8 Hz, 2H), 8.56 (d, *J*=3.6 Hz, 1H), 8.63 (s, 1H), 9.5 (s, 1H); ^{13}C NMR (100 MHz, $CDCl_3$): δ ppm 51.39, 52.44, 118.83, 121.68, 123.70, 128.47, 128.98, 130.00, 130.56, 133.79,

134.27, 134.86, 135.91, 141.62, 144.57, 149.07, 149.61, 169.65, 188.95; Anal. Calc.for $C_{23}H_{21}N_3O_2$; C, 74.37; H, 5.70; N, 11.31; found: C, 74.40; H, 5.72; N, 11.36 %; ESI-MS: 372.10 $[M+H]^+$.

N-{4-[(2E)-3-(4-Methylphenyl)prop-2-enoyl]phenyl}-2-{[(pyridin-3-yl)methyl]amino} acetamide (9b)

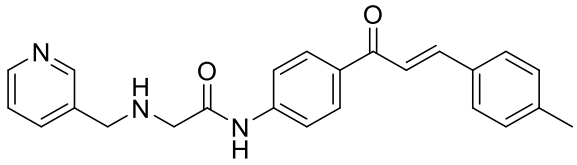

Pale yellow solid, Yield: 64 %; M.P: 172-174 °C; IR (KBr) 3327, 3275, 2912, 1687, 1656, 1604, 1593, 1500, 1228, 1176, 1026, 808, 709 cm^{-1}; ^1H NMR (400 MHz, $CDCl_3$): δ 2.30 (s, 3H), 3.48 (s, 2H), 3.91 (s, 2H), 7.24 (d, *J*= 7.6 Hz, 2H), 7.30-7.34 (m, 1H), 7.51 (d, *J*=15.6 Hz, 1H), 7.56 (d *J*=8.0 Hz, 2H), 7.68-7.72 (m, 3H), 7.80 (d, *J*=15.6 Hz, 1H), 8.04 (d, *J*=8.8 Hz, 2H), 8.56 (d, *J*=3.6 Hz, 1H), 8.64 (s, 1H), 9.42 (s, 1H), ^{13}C NMR (100 MHz, $CDCl_3$): δ ppm 21.57, 51.48, 52.50, 118.78, 120.70, 123.67, 128.50, 129.72, 129.97, 132.17, 134.01, 134.22, 135.81, 141.08, 141.44, 144.67, 149.17, 149.67, 169.55, 189.04; Anal. Calc. for $C_{24}H_{23}N_3O_2$; C, 74.78; H, 6.01; N, 10.90; found: C, 74.81; H, 6.05; N, 10.94 %; ESI-MS: 386.10 $[M+H]^+$.

N-{4-[(2E)-3-(4-Methoxyphenyl)prop-2-enoyl]phenyl}-2-{[(pyridin-3-yl)methyl]amino} acetamide (9c)

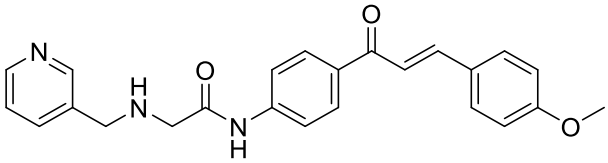

Pale yellow solid, Yield: 62 %; M.P: 150-160 °C; IR (KBr) 3325, 3269, 2910, 2833, 1687, 1654, 1602, 1591, 1523, 1512, 1500, 1226, 1170, 1028, 821, 721 cm^{-1}; ^1H NMR (400 MHz, $CDCl_3$): δ 3.48 (s, 2H), 3.86 (s, 3H), 3.90 (s, 2H), 6.94 (d, *J*= 8.8 Hz, 2H), 7.30-7.33 (m, 1H) 7.43 (d *J*=15.6 Hz, 1H), 7.61 (d *J*=8.4 Hz, 2H), 7.68-7.72 (m, 3H), 7.79 (d *J*=15.6 Hz, 1H), 8.03 (d *J*=8.4 Hz, 2H), 8.55 (d, *J*=4.8 Hz, 1H), 8.63 (s, 1H), 9.45 (s, 1H), ^{13}C NMR (100 MHz, $CDCl_3$): δ ppm 51.47, 52.49, 55.44, 114.42, 118.78, 119.37, 123.68, 127.63, 129.91, 130.26, 134.16, 134.21, 135.84, 141.34, 144.45, 149.16, 149.66, 161.65, 169.52, 188.99; Anal. Calc. for $C_{24}H_{23}N_3O_3$; C, 71.80; H, 5.77; N, 10.47; found: C, 71.83; H, 5.81; N, 10.51 %; ESI-MS: 402.10 $[M+H]^+$.

N-{4-[(2E)-3-(4-Fluorophenyl)prop-2-enoyl]phenyl}-2-{[(pyridin-3-yl)methyl]amino} acetamide (9d)

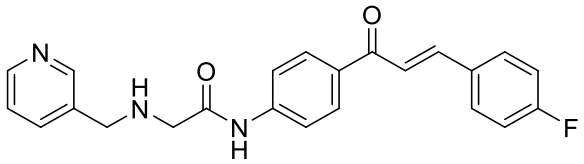

Pale yellow solid, Yield: 50 %; M.P: 150-152 °C; IR (KBr) 3331, 3263, 2912, 1685, 1649, 1599, 1533, 1510, 1224, 1176, 1026, 827, 711 cm^{-1}; ^1H NMR (400 MHz, $CDCl_3$): δ 3.51 (s, 2H), 3.93 (s, 2H), 7.11-7.15(m, 2H), 7.32-7.35 (m, 1H), 7.49 (d *J*=15.6 Hz, 1H), 7.64-7.74 (m, 5H), 7.80 (d *J*=15.6 Hz, 1H), 8.05 (d, *J*=15.6 Hz, 2H), 8.57 (dd *J*=4.8, 1.6 Hz, 1H), 8.65 (d, *J*=2.0 Hz, 1H), 9.42 (s, 1H), ^{13}C NMR (100 MHz, $CDCl_3$): δ ppm 51.51, 52.49, 116.05, 116.26, 118.81, 121.39, 123.70, 130.02, 130.33, 130.42, 131.15, 133.79, 135.85, 141.54, 143.27, 149.21, 149.67, 169.52, 188.71; Anal. Calc. for $C_{23}H_{20}N_3O_2$; C, 70.94; H, 5.18; N, 10.79; found: C, 70.97; H, 5.20; N, 10.82 %; ESI-MS: 390.10 $[M+H]^+$.

N-{4-[(2E)-3-(4-Chlorophenyl)prop-2-enoyl]phenyl}-2-{[(pyridin-3-yl)methyl]amino} acetamide (9e)

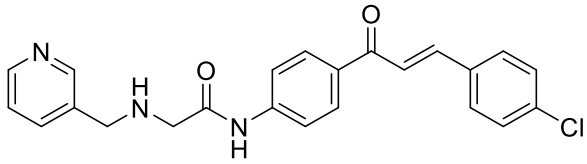

Pale yellow solid, Yield: 37 %; M.P: 190-192 °C; IR (KBr): 3435, 3329, 3275, 2912, 1687, 1656, 1608, 1591, 1521, 1491, 1228, 1176, 829, 812, 794, 725, 711 cm^{-1}; ^1H NMR (400 MHz, $CDCl_3$): δ 3.50 (s, 2H), 3.92 (s, 2H), 7.33-7.35 (m, 1H), 7.41 (d, *J*= 8.8 Hz, 2H), 7.53 (d, *J*=15.6 Hz, 1H), 7.60 (d *J*=8.4 Hz, 2H), 7.67-7.70 (m, 1H), 7.73 (d *J*=8.4 Hz, 2H), 7.77 (d *J*=15.6 Hz, 1H), 8.05 (d, *J*=8.8 Hz, 2H), 8.57 (dd *J*=4.8, 1.2 Hz, 1H) 8.65 (s, 1H), 9.51 (s, 1H); ^{13}C NMR (100 MHz, $CDCl_3$): δ ppm 51.49, 52.49, 118.82, 122.10, 123.69, 129.25, 129.61, 130.04, 133.41, 133.69, 134.17, 135.84, 136.38, 141.62, 143.05, 149.18, 149.66, 169.55, 188.61; Anal. Calc. for $C_{23}H_{20}ClN_3O_2$; C, 68.06; H, 4.97; N, 10.35; found: C, 68.09; H, 4.99; N, 10.37 %; ESI-MS: 406.10 $[M+H]^+$.

N-{4-[(2E)-3-(4-Nitrophenyl)prop-2-enoyl]phenyl}-2-{[(pyridin-3-yl)methyl]amino} acetamide (9f)

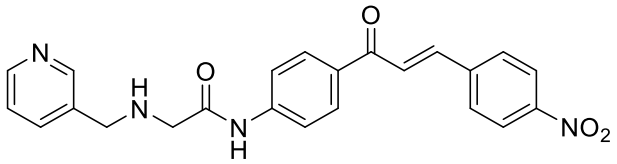

Pale yellow solid, Yield: 34 %; M.P: 182-184 °C; IR (KBr) 3336, 3275, 2910, 2847, 1687, 1658, 1610, 1591, 1523, 1492, 1344, 1226, 1176, 1026, 837, 825, 786 cm^{-1}; ^1H NMR (400 MHz, $CDCl_3$): δ 3.35 (s, 2H), 3.79 (s, 2H), 7.34-7.37 (m, 1H), 7.77-7.84 (m, 4H), 8.13-8.20 (m, 5H), 8.28 (d *J*=8.4 Hz, 2H), 8.45 (d, *J*=3.6 Hz, 1H), 8.56 (s, 1H), 10.24 (s, 1H), ^{13}C NMR (100 MHz, $CDCl_3$): δ ppm 50.32, 52.46, 119.04, 123.85, 124.35, 126.44, 130.26, 130.61, 132.36, 136.03, 136.27, 140.98, 141.77, 143.96, 148.44, 148.55, 149.95, 171.29, 187.71; Anal. Calc. for $C_{23}H_{20}N_4O_4$; C, 66.34; H, 4.84; N, 13.45; found: C, 66.31; H, 4.81; N, 13.44 %; ESI-MS: 439.05 $[M+Na]^+$.

N-{4-[(2E)-3-(3-Methoxyphenyl)prop-2-enoyl]phenyl}-2-{[(pyridin-3-yl)methyl]amino}acetamide (9g)

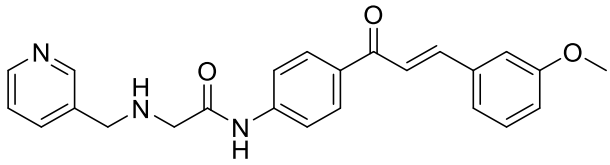

Pale yellow solid, Yield: 55 %; M.P: 142-144 °C; IR (KBr): 3333, 3271, 2929, 2912, 2835, 1689, 1656, 1604, 1595, 1521, 1261, 1178, 835, 786, 721, 709 cm^{-1}; ^1H NMR (400 MHz, $CDCl_3$): δ 3.49 (s, 2H), 3.87 (s, 3H), 3.91 (s, 2H), 6.98 (dd, *J*= 8.0, 1.6 Hz, 1H), 7.16 (s, 1H), 7.25 (d, *J*=7.6 Hz, 1H), 7.30-7.37 (m, 2H), 7.52 (d, *J*=15.6 Hz, 1H), 7.68-7.73 (m, 3H), 7.78 (d, *J*=15.6 Hz 1H), 8.04 (d, *J*=8.4 Hz, 2H), 8.57 (d, *J*=4.0 Hz, 1H), 8.64 (s, 1H), 9.43 (s, 1H) ^{13}C NMR (100 MHz, $CDCl_3$): 46.73, 47.73, 50.63, 108.67, 111.53, 114.50, 116.35, 117.27, 118.94, 125.22, 125.29, 129.08, 129.41, 131.09, 131.53, 136.79, 139.74, 144.44, 144.92, 155.17, 164.78, 184.19 δ ppm ; Anal. Calc. for $C_{24}H_{23}N_3O_3$; C, 71.80; H, 5.77; N, 10.47; found: C, 71.77; H, 5.74; N, 10.45 %; ESI-MS: 402.15 $[M+H]^+$.

N-{4-[(2E)-3-(2-Chlorophenyl)prop-2-enoyl]phenyl}-2-{[(pyridin-3-yl)methyl]amino}acetamide (9h)

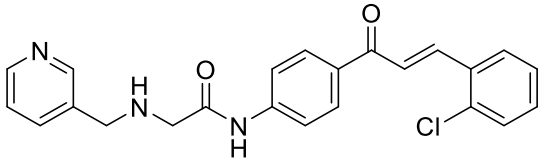

Pale yellow solid, Yield: 76 %; M.P: 218-220 °C; IR (KBr) 3236, 3169, 3043, 1693, 1658, 1591, 1543, 1312, 1217, 1180, 1028, 827, 756, 742, 709 cm^{-1}; ^1H NMR (400 MHz, $CDCl_3$): δ 3.49 (s, 2H), 3.91 (s, 2H), 7.32-7.36 (m, 3H), 7.44-7.46 (m, 1H), 7.50 (d, *J*=15.8 Hz, 1H), 7.68-7.78 (m, 4H), 8.04 (d, *J*=8.8 Hz, 2H) 8.18 (d, *J*=15.8 Hz, 1H), 8.56 (d, *J*=3.6 Hz, 1H), 8.64 (s, 1H), 9.44 (s, 1H), ^{13}C NMR (100 MHz, $CDCl_3$): δ ppm 51.49, 52.50, 118.81, 123.68,

124.48, 127.11, 127.80, 130.15, 130.30, 131.17, 133.28, 133.57, 134.22, 135.47, 135.82, 140.33, 141.68, 149.17, 149.66, 169.61, 188.83; Anal. Calc. for $C_{23}H_{20}ClN_3O_2$; C, 68.06; H, 4.97; N, 10.35; found: C, 68.03; H, 4.98; N, 10.37 %; ESI-MS: 406.05 $[M+H]^+$.

N-{4-[(2E)-3-(3-Chlorophenyl)prop-2-enoyl]phenyl}-2-{[(pyridin-3-yl)methyl]amino}acetamide (9i)

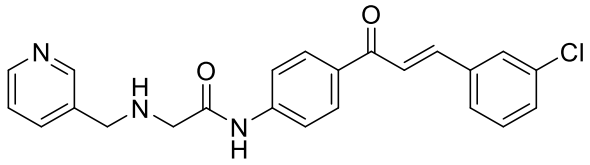

Pale yellow solid, Yield: 57 %; M.P: 158-160 °C; IR (KBr): 3323, 3275, 2912, 2850,1687, 1656, 1608, 1595, 1521, 1498, 1300, 1226, 1178, 1028, 837, 794, 727 cm^{-1}; ^1H NMR (400 MHz, $CDCl_3$): δ 3.50 (s, 2H), 3.92 (s, 2H), 7.32-7.41 (m, 3H), 7.51-7.53 (m, 1H), 7.55 (d, *J*= 15.6 Hz, 1H), 7.65-7.77 (m, 5H), 8.06 (d *J*=7.8 Hz, 2H), 8.58 (dd, *J*=4.4, 1.2 Hz, 1H), 8.65 (d, *J*=1.6 Hz, 1H), 9.43 (s, 1H); ^{13}C NMR (100 MHz, $CDCl_3$): δ ppm 51.49, 52.51, 118.86, 122.92, 123.69, 128.81, 127.94, 130.08, 130.23, 130.32, 133.57, 134.22, 134.97, 136.72, 136.79, 141.77, 142.78, 149.17, 149.67, 169.60, 188.47; Anal. Calc. for $C_{23}H_{20}ClN_3O_2$; C, 68.06; H, 4.97; N, 10.35; found: C, 68.10; H, 4.95; N, 10.37 %; ESI-MS: 406.10 $[M+H]^+$.

N-{4-[(2E)-3-(2,4-Dichlorophenyl)prop-2-enoyl]phenyl}-2-{[(pyridin-3-yl)methyl]amino} acetamide (9j)

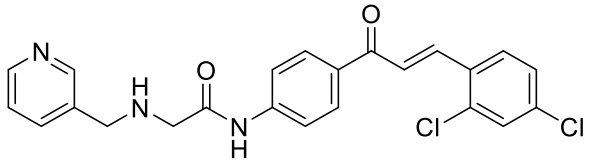

Pale yellow solid, Yield: 61 %; M.P: 158-160 °C; IR (KBr) 3335, 3290, 2912, 1687, 1656, 1604, 1583, 1521, 1307, 1178, 1024, 825, 790, 709 cm^{-1}; ^1H NMR (400 MHz, $CDCl_3$): δ 3.50 (s, 2H), 3.92 (s, 2H), 7.31-7.35 (m, 2H), 7.48 (t, *J*= 2.0 Hz, 1H), 7.52 (s, 1H), 7.68-7.74 (m, 4H), 8.04 (d *J*=8.8 Hz, 2H), 8.12 (d, *J*=15.6 Hz, 1H), 8.57 (d, *J*=4.8 Hz, 1H), 8.65 (s, 1H), 9.43 (s, 1H), ^{13}C NMR (100 MHz, $CDCl_3$): δ ppm 51.49, 52.48, 118.83, 123.71, 124.67, 127.58, 128.51, 130.13, 130.16, 131.87, 133.42, 134.15, 135.88, 136.05, 136.42, 139.06, 141.75, 149.18, 149.64, 169.58, 188.49; Anal. Calc.for $C_{23}H_{19}Cl_2N_3O_2$; C, 62.74; H, 4.35; N, 9.54; found: C, 62.71; H, 4.33; N, 9.57 %; ESI-MS: 440.0 $[M+H]^+$.

(E)-N-(4-(3-(4-methoxyphenyl)acryloyl)phenyl)-2-((pyridin-2-ylmethyl)amino) acetamide (10c)

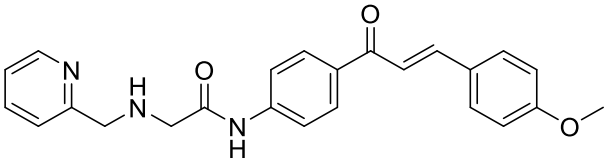

Pale yellow solid, Yield: 71 %; M.P: 240-242 °C; IR (KBr) 3272, 2935, 2751, 2609, 1696, 1653, 1598, 1536, 1511, 1421, 1307, 1257, 1221, 1174, 1032, 989, 820, 752, 684 cm^{-1}; ^1H NMR (400 MHz, $CDCl_3$): δ 3.80 (s, 3H), 4.08 (s, 2H), 4.40 (s, 2H), 7.01 (s, 2H), 7.42 (s, 1H), 7.54 (d, *J*= 6.00 Hz, 1H), 7.67-7.83 (br, m, 8H), 8.16 (d, *J*=6.4 Hz, 2H), 8.63 (s, 1H), 9.48 (br, s, 1H), 11.28 (s, 1H), ^{13}C NMR (100 MHz, $CDCl_3$): δ ppm 49.01, 50.92, 55.85, 114.87, 119.15, 119.88, 123.72, 124.03, 127.85, 130.29, 131.19, 133.59, 137.76, 142.89, 143.98, 149.46, 152.75, 161.77, 165.31, 187.93.

(E)-N-(4-(3-(3-chlorophenyl)acryloyl)phenyl)-2-((pyridin-2-ylmethyl)amino) acetamide (10i)

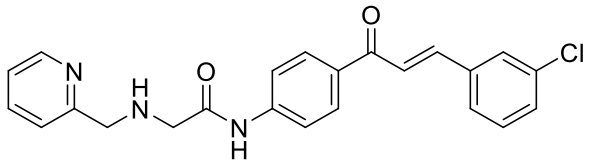

Pale yellow solid, Yield: 65 %; M.P: 228-230 °C; IR (KBr) 3234, 3165, 3086, 3037, 2922, 1698, 1657, 1598, 1474, 1411, 1376, 1335, 1302, 1254, 1223, 1026, 1010, 970, 850, 784, 670, 576 cm^{-1}; ^1H NMR (400 MHz, $CDCl_3$): δ 4.13 (s, 2H), 4.40 (s, 2H), 7.56 (d, *J*= 7.2 Hz, 2H), 7.69 (d, *J*= 15.6 Hz, 1H), 7.83-7.90 (m, 4H), 8.04 (d, 2H), 8.21 (d, *J*=8.00 Hz, 2H), 8.64 (s, 1H), 9.71 (s, 1H), 11.40 (s, 1H), ^{13}C NMR (100 MHz, $CDCl_3$): δ ppm 48.79, 50.65, 119.18, 123.87, 123.95, 124.16, 128.34, 130.53, 130.60, 131.15, 133.15, 134.26, 137.48, 137.91, 142.26, 143.21, 149.39, 152.24, 165.02, 187.93.

3b.4.2 Materials and methods for biological assays

3b.4.2.1 Reagent and cell culture

MTT, LDH assay kit (Pierce LDH Cytotoxicity Assay), *N*,*N*-dimethylformamide (DMF), EtBr and Acridine Orange, were purchased from Sigma-Aldrich, India. DMEM, Fetal Bovine Serum (FBS) and trypsin were sourced from (Gibco USA). Human lung carcinoma cell line A549 and human breast cancer cell line MCF-7 were purchased from NCCS, Pune, India. Cell line was maintained in Dulbecco's modified eagles medium (DMEM) supplemented with 2 mM l-glutamine and 10% fetal bovine serum (GIBCO, USA). Penicillin and streptomycin

(100 IU/100g) were adjusted to 1 mL/L. The cells were maintained at 37 ^{o}C with 5% CO_2 in a humidified CO_2 incubator.

Stock solutions of derivatives were prepared in DMF and were diluted with PBS (Phosphate-buffered saline) to achieve working concentration. However, care was taken to maintain the final concentration of DMF not exceed more than 0.5% in any case.

3b.4.2.2 MTT assay

The half minimal inhibitory concentration was evaluated using MTT [3-(4,5-dimethylthiazol-2-yl)-2,5-diphenyltetrazolium bromide] assay as per standard protocol. Cells were plated in a 96-well plate (1 x 10^4 cells/well) and incubated overnight in 100 µl DMEM media supplemented with 10% FBS. Each compound was added in 0.5, 1, 10, 25, 50, 75, 100 µM conc. and incubated further for 48h. 20 µl of MTT solution (5 mg/mL in PBS) was added and further plate was incubated for 4h. Supernatant solution was removed and the blue formazan was dissolved in 100µl of acidified isopropanol. The absorbance was measured using microplate reader at 570 nm (Metertech Σ960)

Cell viability (%) = (average absorbance of treated groups/average absorbance of control group) × 100%. IC_{50} values were calculated using GraphPad Prism. Each experiment was performed in triplicates.

3b.4.2.3 UV-Based Assay

PerkinElmer Lambda- 35 dual beam UV–Vis spectrophotometer was used for absorption spectral studies. Solution of calf thymus DNA (CT DNA) was prepared in water. The UV absorbance at 260 was found to 0.277 which is used to calculate the DNA concentrations (Ɛ = 6600 M^{-1}) and was expressed in terms of base molarity. UV absorption titrations were carried out by keeping the concentration of compounds **9g** and **9i** (dissolved in DMSO) fixed and by adding a known concentration of CT DNA solution in both the cuvettes in increasing amount until hypochromism saturation was observed. Absorbance values were recorded after each successive addition of DNA solution and equilibration.

3b.4.2.4 Ethidium Bromide Displacement Assay

DNA (100 µL, 8.4 x 10^{-4} M), EtBr (100 µL, 4.2 x 10^{-4} M), and Tris-HCl buffer pH 7.2 was used to make a total volume of 3 mL, EtBr displacement fluorescence assay was employed to find DNA intercalation. Fluoroscence emission spectra (λmax= 600 nm, excitation wavelength 546nm, slit width 10nm, 1cm path length) were obtained at 30^{o}C on a JASCO FP-6300 fluorescence spectrophotometer. The assays were performed by using different concentrations of compounds **9g** and **9i** in buffer solution (3 mL). I_0/I are plotted along with y

axis against the concentration of compound, where in I and I_0 are the fluorescence intensities of the DNA-EtBr complex in the presence of and in the absence of compounds, respectively.

3b.4.2.5 Trypan blue

5×10^5 cells per well were seeded in 12 well plate and kept overnight for attachment. Next day cells were treated with IC_{50} conc. of compound **9i**, DMF and TritonX-100 and were incubated for 48 h. DMF treated cells were taken as vehicle control and TritonX-100 as positive control. Following incubation, the supernatant pool was collected and adherent cells were trypsinized and collected. Cell viability was performed by the dye exclusion test with 0.5% trypan blue using a hemocytometer. Each experiment was performed in triplicates.

3b.4.2.6 LDH assay

Lactate dehydrogenase enzyme remains in cytoplasm, however during necrosis due to plasma membrane damage it leaches out. Cells were plated on 96 well plate (1×10^4 cells/well) for 24 h in DMEM media without phenol red, then derivatives were added in the 0.5, 1, 10, 25, 50, 75, 100 µM concentration range. Subsequently, they were incubated for 48 h. Assay was performed according to the manufacture's instruction (Pierce LDH Cytotoxicity Assay, Thermo Scientific, USA). Absorbance was measured at 490 nm in a microplate reader and percentage cytotoxicity was calculated.

3b.4.2.7 Ethidium Bromide/Acridine Orange staining assay

Morphological changes due to apoptosis and necrosis were visualized using EtBr/AO staining technique [18]. Cells were treated with IC_{50} concentration of compound **9i**. For positive control cell were treated with Triton-X 100 and incubated for 48h. Cells were washed with Phosphate-buffered saline (PBS) and stained with 1 µl of 1:1 ratio of EtBr and AO (100 µg/ml). Cell to stain ratio was maintained as 1:25 µl. 10 µl of cell suspension was placed on microscopic slide and images were taken using Leica DM 2500 fluorescence microscope fitted with Leica EZ camera.

3b.5 References

[1] D. D. Jandial, C. A. Blaie, S. Zhang,L. S. Krill,Y. B. Zhang, X. Zi, *Curr Cancer Drug Targets*, **2014**, *14*, 181.

[2] P. Hinnen, F. A. Eskens, *Br. J. Cancer,* **2007**, *96*, 1159.

[3] H. Kumar, A Chattopadhyay, R. Prasath, V. Devaraji, R. Joshi, P. Bhavana, P. Saini, S. K. Ghosh, *J. Phys. Chem. B*, **2014**, *118* ,7257.

[4] L. D. Via, O. Gia, G. Chiarelotto, M. G. Ferlin, *Eur. J. Med. Chem.*, **2009**, *44*, 2854.

[5] V. Markovic, N. Debeljak, T. Stanojkovic, B. Kolundzija, D. Stadic, M. Vujcic, B. Janovic, N. Tanic, M. Perovic, V. Tesic, J. Antic, M. D. Joksovic, *Eur. J. Med. Chem.*, **2015**, *89*, 401.

[6] A. K. Singh, G. Saxena, S. Dixit, Hamidullah, S. K Singh, S.K. Singh, M. Arshad, R. Konwar, *J. Mol. Str.*, **2016**, *1111*, 90-99.

[7] X. Yang, G. L. Shen, R. Q. Yu, *Microchem. J.*, **1999**, *62*, 394.

[8] T. Suzuki, T. Ando, K. Tsuchiya, N. Fukazawa, A. Saito, Y. Mariko, T. Yamashita, O. Nakanishi, *J. Med. Chem.*, **1999**, *42*, 3001.

[9] S. Bilginer, H. I. Gul, E. Mete, U. Das, H. Sakagami, N. Umemura, J. R. Dimmock, *J. Enzyme. Inhib. Med. Chem.*, **2013**, *28*, 974.

[10] T. Lu, A. W. Goh, M. Yu, J. Adams, F. Lam, T. Teo, P. Li, B. Noll, L. Zhong, S. Diab, O. Chahrour, A. Hu, A. Y. Abbas, X. Liu, S. Huang, C. J. Sumby, R. Milne, C. Midgley, S. Wang, *J. Med. Chem.*, **2014**, *57*, 2275.

[11] R. Soni, S. Umar, N. Shah, B. Suresh, S. S. Soman, *J. Heterocyclic Chem.*, **2017**, *54*, 2501.

[12] S. Durgapal, R. Soni, S. Umar, B. Suresh, S. S. Soman, *ChemistrySelect*, **2017**, *2*, 147.

[13] T. Mosmann, *J. Immunol. Methods*,**1983**, *65*, 55.

[14] C. V. Kumar, E. H. Asunsion, *J. Am. Chem. Soc.*, **1993**, *115*, 8547.

[15] M. Balduzzi, M. Diociaiuti, B. De Berardis, S. Paradisi, L. Paoletti, *Environ. Res.*, **2004**, *96*, 62.

[16] C. M. Sayes, A. M. Gobin, K. D. Ausman, J. Mendez, J. L. West, V. L. Colvin, *Biomaterials*, **2005**, *26*, 7587.

[17] G. Fotakis, J. A. Timbrell, *Toxicol. Lett.* ,**2006**, *160*, 171.

[18] S. Kasibhatla, G. P. Amarante-Mendes, D. Finucane, T. Brunner, E. Bossy-Wetzel, D. R. Green, *CSH Protocols*, **2006**, 1, pdb.prot4429.

[19] R. L. Atkins, D. E. Bliss, *J. Org. Chem.*, **1978**, *43*, 1975.

[20] Y. D. Kulkarni, D. Srivastava, D. A. Bishnoi, P. R. Dua, *J. Indian Chem. Soc.*, **1996**, *73*, 173.

[21] L. J. Simons, B. W. Caprathe, M. Callahan, J. M. Graham, T. Kimura, Y. Lai, H. LeVine III, W. Lipinski, A. T. Sakkab, Y. Tasaki, L. C. Walker, T. Yasunaga, Y. Ye, N. Zhuang, C. E. Augelli-Szafran, *Bioorg. Med. Chem. Lett.*, **2009**, *19*, 654.